Fatigue Life Assessment of Roadway Bridges based on Actual Traffic Loads

THÈSE N^{O} 5575 (2013)

PRÉSENTÉE LE 12 AVRIL 2013

À LA FACULTÉ DE L'ENVIRONNEMENT NATUREL, ARCHITECTURAL ET CONSTRUIT
LABORATOIRE DE LA CONSTRUCTION MÉTALLIQUE
PROGRAMME DOCTORAL EN STRUCTURES

ÉCOLE POLYTECHNIQUE FÉDÉRALE DE LAUSANNE

POUR L'OBTENTION DU GRADE DE DOCTEUR ÈS SCIENCES

PAR

Nariman MADDAH

acceptée sur proposition du jury:

Prof. A. Muttoni, président du jury
Prof. A. Nussbaumer, Prof. J.-P. Lebet, directeurs de thèse
Dr M. Alvarez, rapporteur
Prof. A.-G. Dumont, rapporteur
Prof. G. Marquis, rapporteur

ÉCOLE POLYTECHNIQUE
FÉDÉRALE DE LAUSANNE

Suisse
2013

درخت تو گر بار دانش بگیرد بزیر آوري چرخ نیلوفري را

— ناصر خسرو

If your life tree fruits knowledge you can shape your own destiny

— Naser Khosrow

To my wife, my family,
and
my deceased father . . .

Acknowledgements

This work has been carried out under the supervision of Professor Alain Nussbaumer and I would like to thank him for all his help and encouragement. His professionalism, intellectual rigour, high standards and attention to detail have been challenging and stimulating, and I hope the work presented here is an adequate reflection of that. I would like to thank Professor Jean-Paul Lebet, director of ICOM, for granting me the opportunity to work in an outstanding research environment and for his support and advice.

I would like also to acknowledge the support of the Federal Roads Office (FEDRO) that funded my projects (AGB2002/005 and AGB2007/004). I wish to express my gratitude to the members of the AGB committee for their periodic advice, guidance and valuable ideas. This committee consisted of H. Figi, Dr. A. Fürst, Prof. A. Muttoni, Dr. D. Somaini, Dr. H. Ganz and Dr. M. Alvarez. The valuable comments received have improved considerably the quality of this document.

I would like to thanks the member of examination jury for the time spent reading and commenting on this thesis: Prof. Gary Marquis (Aalto University, School of Science and Technology, Helsinhki, Finland), Dr. Manuel Alvarez (Federal Roads Office), Prof. André-Gilles Dumont, Prof. Aurelio Muttoni, the president of the jury, Prof. Alain Nussbaumer director of thesis and Prof. Jean-Paul Lebet co-director of thesis.

I would like to specially mention the efforts of Thierry Meystre during the development of the traffic simulation program (WinQSIM). He patiently taught me the WinQSIM program and how to perform traffic data processing and traffic simulations. I highly appreciated his valuable help. I wish to also express my special thanks to Dr. Gary Prinz for proofreading my english and for his kind advices.

I am thankful to Esther von Arx for her valuable help with administrative issues. I wish to express my gratitude to the competent team of the structural laboratory, Sylvain Demierre and Gérald Rouge. Their competence, assistance and humour made the time spent in the laboratory and on-site quite pleasant.

My time at ICOM has been memorable thanks to my colleagues. A great thanks to all the ICOM team, especially to Maria Lindqvist, Dimitrios Papastergiou, Claire Acevedo, Claudio Leonardi, Michel Crisinel, Gustavo Cortes, Luis Borges, Farshid Zamiri, Raphaël Thiébaud, Luca D'Angelo, Manuel Santarsiero, Christian Louter, Valentin Gavillet ... for the good times we spent at work and out of work. I am also greatly indebted to colleagues and friends from IMAC, MCS, I-BETON, CCLAB, EESD laboratories, and especially to James Goulet, Mark Treacy and Romain Pasquier for our collaborations, discussions and their help.

Acknowledgements

Finally, my gratitude goes to my family for their love, understanding, and encouragement. Last but not least, I would like to thank my wife, Hamideh, for her infinite patience, kindness and support over the last four years while I have been working on this research, and indeed over the last seven years that we have been together.

Lausanne, 12 November 2012 Nariman Maddah

Abstract

Fatigue is an important consideration in the design of bridges, especially those made of steel. Cycles resulting from the passage of a truck over a bridge depend essentially on bridge type, detail location, span length and vehicles axles configuration. To address the complex limit state of fatigue, *damage equivalence factors* (λ-factors) are given in the SIA codes and the Eurocodes. However, the λ-factors given in the codes are not valid for all bridge influence lines. Another issue in the application of damage equivalence factors is that the *fatigue equivalent length* is defined for limited cases in the codes. Moreover, the λ-factors are determined with very simplified load models of real traffic that entirely neglect simultaneous presence of multiple heavy vehicles.

The main objective of this research is to study the relationship linking influence line and damage, to find the effect of main parameters on damage equivalence factors for roadway bridges with actual loads and improve them. As far as accurate traffic simulations need actual traffic data, it is also necessary to study real traffic flow.

The first two chapters introduce the thesis objectives and give a literature review in the various directly related research fields. In the next chapter, a series of simplified traffic models (the same models applied in the codes) are used in order to evaluate the accuracy of the damage equivalence factors as defined in the code for different bridge types. Initial traffic simulations are also performed to compare the output with the damage equivalence factors given in the codes.

Then, the author profoundly investigates the relationship between bridge influence lines, loads geometry and fatigue damage sum. Some modifications for improving the damage equivalence factors, which are developed through a step-by-step analytical approach, are proposed. The proposed modifications aim not only to improve the accuracy of the damage equivalence factors for continuous traffic flow, but also enhance their applications to various bridge types and traffic conditions. A partial factor, λ_5, dedicated for influence lines that have repetition is also defined. In addition, the λ_4-factor for double lane traffic is updated in order to take into account the effect of crossing.

Before final traffic simulations, the most important parameters needed to express realistic traffic model and their range of variation are determined by analysing the available traffic data from measurement stations in Switzerland. Finally, the accuracy of the proposed modifications for damage equivalence factors are assessed by comparing them with the final simulation results obtained for different traffic conditions. It shows that the proposed fatigue load model and fatigue equivalent length can properly represent damage equivalence factors for any

influence line. In addition, for several double lane traffic conditions, the crossing ratios are determined.

Keywords: bridge; fatigue design; damage equivalence factor; fatigue load model; influence line; traffic model; Monte-Carlo simulation; heavy vehicle; traffic flow; crossing effect.

Résumé

La fatigue représente un aspect important dans la conception et le dimensionnement des ponts, en particulier ceux en acier. Les cycles générés par le passage d'un camion sur un pont dépendent principalement du type de ce dernier, de l'emplacement du détail de fatigue considéré, de la portée et de la configuration des essieux des véhicules. Pour traiter le cas complexe de l'état limite de fatigue, *les facteurs de correction des charges* (λ-facteurs) sont donnés dans les normes SIA et Eurocodes. Toutefois, ces facteurs λ ne sont pas valables pour tous les cas de lignes d'influence relatives aux ponts. Un autre problème lié à l'application des facteurs λ réside dans la *longueur équivalente de fatigue*, qui n'est définie dans les normes que pour un nombre limité de cas. En outre, les facteurs λ des normes sont déterminés avec des modèles simplifiés des charges réelles de trafic qui négligent complètement la présence simultanée de plusieurs véhicules lourds.

L'objectif principal de cette recherche est d'étudier le relation qui lie ligne d'influence et endommagement, d'en déduire l'effet des principaux paramètres sur les facteurs de correction des charges pour les ponts routiers avec des charges actualisées et de les améliorer. Puisque des simulations de trafic précises nécessitent des données actualisées, ces dernières requièrent une étude des flux de trafics réels.

Les deux premiers chapitres introduisent les objectifs de la thèse et donnent un état de l'art des différents domaines de recherche associés. Ainsi, dans le chapitre qui suit, une série de modèles simplifiés de trafic (identiques à ceux appliqués dans la norme SIA) est utilisée afin d'évaluer l'exactitude des facteurs de correction des charges définis dans les des normes pour différents types de ponts. Une première série de simulations de trafic est également effectuée pour comparer les résultats obtenus avec les facteurs λ fournis par les normes.

Ensuite, l'auteur étudie de manière approfondie la relation entre les lignes d'influence de pont, le géométrie des charges et la somme du dommage de fatigue. Des modifications pour améliorer les facteurs de correction des charges développées grâce à une approche analytique par étapes successives sont proposées. Ces modifications n'ont pas seulement pour but d'améliorer l'exactitude des facteurs λ pour des flux de trafic continus, mais également d'élargir l'application de ceux-ci à différents types de ponts et conditions de trafic. Un facteur partiel, λ_5, lié aux lignes d'influence qui ont des répétition, est également défini. De plus, le facteur λ_4, relatif aux ponts avec deux voies de circulation, est mis à jour pour tenir compte de l'effet des croisements.

Avant les simulations finales de trafic, les paramètres les plus importants nécessaires pour formuler un modèle de traffic réaliste et leur étendue de variation sont déterminés en analysant

les données de trafic disponibles à partir des stations de mesures en Suisse. Finalement, la précision des modifications proposées pour les facteurs de correction des charges est évaluée par comparaison avec les résultats des simulations finales obtenues pour différentes conditions de trafic. Il est vérifié que le modèle de charge ainsi que la longueur de fatigue équivalente proposés représentent correctement les facteurs λ pour n'importe quelle ligne d'influence. De surcroît, les proportions de croisement correspondants à plusieurs conditions de trafic sur ponts à double voie de circulation sont déterminées.

Mots-clés : pont, dimensionnement en fatigue, facteurs de correction des charges, modèles de charge de fatigue, ligne d'influence, modèle de trafic, simulation Monte-Carlo, poids lourds, flux de trafic, effet de croisement

Contents

List of Figures

List of Tables

1 Introduction

1.1 Background

An increasing part of work on the roadway infrastructures concerns the assessment and maintenance of existing structures. OFROU[1] being directly affected by these issues, the agency finances research projects to improve methods of assessment of existing structures. In previous projects (see VSS 515 [10], VSS 530 [8], VSS 556 [41] and VSS 594 [59]), essentially ultimate limit states to verify structural safety of Type 2 (SIA 260 [78]) was considered. As for railway bridges [37], the application of SIA codes for verification of structural safety of Type 4 (corresponding to fatigue) and for maintenance of structures (SIA 269) has raised questions. Indeed, their strict application sometimes leads to lives greatly underestimated, thus high maintenance costs.

In the engineering office, the fatigue verification of a structure according to SIA code or Eurocode is performed using a simplified load model applying the concept of equivalent damage, represented by the *damage equivalence factor*, λ. Although this concept is not new, fatigue verification by damage equivalence factor has become much more demanding with the introduction of European traffic load models. The fatigue verification is an important step for both states of design of new structures and evaluation of existing structures. Therefore, some simplifying assumptions made in the development of structural design codes, i.e. Eurocode and SIA, require to be re-evaluated for both road and rail bridges.

In the latest research AGB 2002/005 [59], a traffic simulation program (WinQSIM) which provides a flexible configuration was developed. This program allows determining the maximum values of the internal forces by simulating various traffic load model on several types of two-lane bridge (bidirectional traffic) as well as two-lane highway bridges (unidirectional traffic). The current research project reuses the simulation program and extends its capabilities by developing specific modules for the determination of spectra and histograms of the internal forces as well as cumulative damage. Extending the program to determine the damage equiv-

[1] Office Fédéral des Routes (OFROU) or Federal Roads Office (FEDRO) in English

alence factor allows us to eliminate a number of conservative and simplifying assumptions while improving the accuracy of fatigue verification of bridges.

The current study is a part of a more general framework which is the review of the fatigue sections of structural design codes, concerning both roadway and railway bridges for both new and existing structures. The current study also enable improvements of the concept of the damage equivalence factor within the European project of 2^{nd} generation of the Eurocodes (2012-2015).

1.2 Motivation

Fatigue evaluation is an important task in design of bridges because the metallic members of bridges are subjected to variable amplitude loading due to passage of traffic on bridge. For fatigue evaluation, stress ranges and number of cycles should be determined as accurately as possible. However, they are highly dependent of different parameters like bridge type, detail location, span length and vehicles axles configuration. For example, considering the negative moment at the mid support of a two-span continuous bridge and assuming large spans for simplicity, two cycles occur due to passage of one truck. Also, the problem becomes more complicated, assuming presence of more than one truck over the bridge. Some of these parameters are known while some are not studied or studied very poorly, which is the case for multi-lane traffic or traffic direction effects. The cycles (in number and magnitude) in different details of the same bridge can also differ by an order of magnitude.

Design of bridges under the *Constant Amplitude Fatigue Limit* (CAFL) also does not address the issue properly, because the maximum "frequent" stress range (defined with the average return period of one week) due to traffic actions highly depends on the probability of occurrence of several trucks on bridges. Besides, design of bridges under CAFL is not economical. Based on these requirements, several attempts are made to address the issues for fatigue design of bridges. As a result, *damage equivalence factors* are proposed by the SIA code and implemented in a similar approach in Eurocode.

Damage equivalence factors effectively express the traffic actions by *equivalent stress range* at two million cycles. However, the damage equivalence factor given in the codes is not valid for all bridge types such as arch bridges or truss bridges. Another issue in the application of damage equivalence factors, is that the *fatigue equivalent length* is defined for limited cases in the SIA code as well as Eurocode; therefore, it is unknown for some bridge types or elements.

Moreover, the damage equivalence factors in the SIA code are determined with a very simplified traffic load model, composed of only three truck types passing on the bridge one by one. This simplified model cause a different response spectrum in comparison with a continuous traffic flow. The traffic load model applied for the determination of the damage equivalence factors of Eurocode, is somewhat improved by applying the Weigh-In-Motion (WIM) measurements of the Auxerre highway in France. However, Eurocode assumes that the vehicles pass

on a bridge one by one with, as a result, that the effect of occurrence of several trucks on the bridge is neglected.

In addition to steel members of bridges, the fatigue evaluation of concrete rebars under the axle loads of trucks is an increasing concern in the design of bridges slabs. The current codes attempt to address this issue through the damage equivalence factors; however, the damage equivalence factors given in the codes are limited to the defined cases which are mostly steel girders.

1.3 Objectives

The main objective of this research is to study main parameters in the fatigue damage analysis of bridges under actual traffic loads, concentrating on action effects modelling. Thus, the main goals of this research are addressed through the definition of the following:

1. to model single lane and double lane traffic conditions on bridges for determining internal forces and damage sum for various traffic conditions,
2. to evaluate the SIA code as well as the Eurocode fatigue design rules for various traffic conditions and bridge types, by comparing the damage equivalence factors of the codes with the results obtained from the traffic simulations,
3. to clarify the rules for the determination of the fatigue equivalent length in order to have a unique method based on the influence line, resulting in a wider range of validity of damage equivalence factor,
4. to define a proper fatigue load model in order to have a coherent fatigue verification for any influence line,
5. to determine the damage equivalence factors based on the proposed modifications, for different traffic conditions as well as bridge types,
6. to quantify the effect of more than one traffic lane and traffic direction on damage equivalence factor.

As far as accurate traffic simulations need actual traffic data, it is necessary to study real traffic flows in order to distinguish the main traffic parameters. The actual traffic parameters are based on the available database from the measurement stations in Switzerland [54].

1.4 Scope

The possible applications of the current thesis theoretical developments are very wide. However, for practical purpose, the scope of this thesis report is limited to the study of:

- roadway bridges with span lengths up to 200 m,
- single lane and double lane traffic conditions,
- unidirectional and bidirectional traffic conditions,
- highway and main road traffic flows,
- steel members of bridges as well as reinforcements of concrete bridge decks or slabs.

The goal of this study is not to evaluate the accuracy of different damage accumulation rules. Therefore, in the determination of damage equivalence factors, linear damage accumulation rule (Miner rule) is applied. In addition, this study does not aim to investigate the fatigue resistance of details, thus the shape of fatigue resistance curves i.e. slope coefficient and knee points as defined in the SIA code (similar to Eurocode) can be applied for the determination of damage equivalence factors.

A traffic simulation program was developed in the AGB2002/05 project with the goal of modelling ultimate loads on bridges. In the current study, the assumptions made in the definition and the determination of the statistical parameters for traffic models remain the same. Nevertheless, the capabilities of the program are extended by adding some modules for free-flow traffic simulations. The statistical parameters of the traffic simulations are obtained from the traffic measurements in Switzerland.

In addition, one goal of single lane and double lane traffic simulations is to study the effect of occurrence of several trucks on bridges. However, the determination of actual frequencies of these situations is not part of this study.

1.5 Personal contributions

In the framework of this study, the following personal contributions are made:

- Comparing SIA code and Eurocode and determining practical deficiencies and limitations of code-base damage equivalence factor.
- Proposing fatigue equivalence length and fatigue load model through an analytical approach, demonstrated the general validity of the propositions by traffic simulations for several bridge cases and different traffic conditions.
- Proposing an analytical formulation in order to quantify the effect of repetition in influence lines.
- Developing an analytical formulation which allows taking into account the effect of crossing and overtaking on damage equivalence factors, and quantifying the effect of crossing and overtaking for different traffic conditions.

- Identifying traffic features which allow precise modelling of traffic actions, and quantifying them based on the Swiss traffic measurements.
- Parametric study is performed in order to highlight the effect of different variables on damage equivalence factor and proposing practical approaches to account for the effect of each variable.
- Quantifying the effect of S-N curve shape (for shear stresses, concrete rebars and shear studs) upon damage equivalence factors and proposing a simplified approach to be used for codes specifications.

1.6 Structure of the thesis

This thesis is divided into seven chapters including the current chapter. Chapter 2 is a review of the current state-of-the-art in the various directly related research fields that includes the following sections: fatigue damage theories, fatigue resistance curves, cycle counting methods, traffic actions, cycle per truck passage, multiple presences of trucks on bridge and Dynamic Amplification Factor (DAF). A concluding paragraph at the end of each section points out how that section contributes to this thesis.

Chapter 3 includes evaluation of the current fatigue design rules for bridges using the damage equivalence factors based on the SIA codes and the Eurocodes. In Chapter 3, different elements involved in the fatigue verification using the damage equivalence factors are described, and shortcomings that might be the source of inaccuracy are researched. Then, a series of simplified traffic models (same as the model applied in the SIA code) are used in order to evaluate the accuracy of the damage equivalence factors for different bridge types according to code definition. Initial traffic simulations are also performed to compare the damage equivalence factors given in the codes with the simulations output. When simulating the initial traffic conditions on different bridge types, the effective parameters in the damage equivalence factors are distinguished for the detailed studies in the next chapters.

Chapter 4 includes analytical approaches that aim to improve the accuracy of the damage equivalence factors. Through an step-by-step analytical approach, a suitable fatigue effective length and fatigue load models are defined. As a result, some modifications for improving the damage equivalence factors are proposed. The proposed modifications not only improve the accuracy of the damage equivalence factors for continuous traffic flow, but also enhance their applications to various bridge types and traffic conditions.

Chapter 5 discusses the most important parameters needed to model the traffic by analysing the available traffic data from measurements in Switzerland. These parameters are applied to the final traffic simulations in the next chapter. The most important parameters are: Hourly Heavy Vehicle Traffic Variations (HHVTV), Hourly Traffic Variations (HTV), Hourly Variations of Heavy Vehicles Proportion in Traffic (HVHVPT), proportion of heavy vehicles in traffic (P_{HV}), heavy vehicle traffic distribution by lane, and GVW distribution.

In Chapter 6, the detailed results of damage equivalence factors are presented for various cases. In addition, the proposed modifications for damage equivalence factors from Chapter 4 are assessed in Chapter 6 by comparing them with the simulation results obtained for different bridge types. The effect of various traffic conditions, described in Chapter 5, is also discussed in Chapter 6.

Chapter 7 presents a summary merging the results from the different preceding chapters. Finally, the main conclusions of the thesis are presented, along with a list of future work propositions.

2 Literature review

2.1 Fatigue damage theories

Fatigue life Prediction for a structural detail subjected to a variable loading conditions is an complex issue. The simplest damage accumulation model is linear damage rule or Miner rule [62]. This model has been widely used due to its simplicity. Miner suggested its damage law as: $D = \sum(n_i / N_i)$ where D is the total damage, and n_i, and N_i, are respectively the applied cycles and the total cycles to failure for i-th constant amplitude loading level. Schilling et al. [75], for example, investigated accuracy of the Miner rule for steel bridge members under variable amplitude loadings and noticed that root-mean-square has slightly better agreement with tests; however, Miner rule is conservative. This disagreement might be due to the fact that the Miner rule does not take into account the load sequence effects. Hashin and Rotem [38] also through experiments mentioned that load sequence can significantly affect the lifetime of a specimen under fatigue variable amplitude loading.

In agreement with an opinion that the errors in life predictions based on Miner rule are due to the assumption of damage rate, Leipholz [50] suggested to use modified S-N curve for fatigue life prediction. Figure 2.1 shows a schematic example how the modified S-N curve replace to the original curve at a loading levels. However, this method can mostly provide accurate predictions for fatigue lives under repeated block loading, which is not the case for bridges.

Some methods attempts to calculate fatigue damage due to variable amplitude loading by keeping the simplicity of the Miner rule and in the same time include the load sequence effect. Since several empirical fatigue damage theories were expressed based on the observation that fatigue fracture involves a crack initiation stage and a crack propagation stage, Manson and Halford [55, 56] proposed the well-known Double Linear Damage Rule (DLDR). The DLDR has been viewed as a credible alternative to Miner's rule. Some scientists also attempted to find other parameters, in addition to stress range and cycles, that influence fatigue damage of steel members; mean stress or stress ratio [12, 22, 43, 86] are such parameters. However, it is found that the applied mean stress is of secondary importance in compare with load sequence effect for variable amplitude loading.

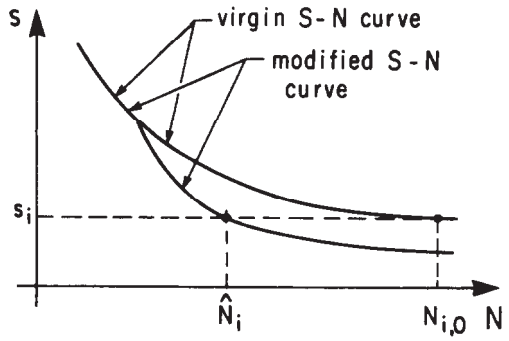

Figure 2.1: Schematic representation of the modified S-N curve according to the Leipholz approach [50]

Numerous studies have been carried out until now to determine a reliable measure or indication of fatigue damage sum under variable amplitude loading. Fatemi and Yang [29] provided a comprehensive review of cumulative fatigue damage theories for metals and their alloys emphasizing the approaches developed between the early 1970s to early 1990s. They separated cumulative fatigue damage modelling in six major categories:

- linear damage evolution and linear summation;
- nonlinear damage curve and two-stage linearization approaches;
- S-N curve modifications to account for load interactions;
- approaches based on crack growth concept;
- models based on continuum damage mechanics;
- energy-based methods.

Though many damage models have been developed, unfortunately, none of them enjoys universal acceptance. Each damage model can only account for one or several phenomenological factors, such as multiple damage stages, nonlinear damage evolution, load sequence, overload effects, spectrum shape, small amplitude cycles below fatigue limit, and mean stress. The conclusion is that due to the complexity of the problem, none of the existing predictive models can encompass all of these factors; the applicability of each model varies from case to case and can be complex to use in design. Consequently, due to its simplicity, the Palmgren-Miner linear damage accumulation is still dominantly used in design, in spite of its major shortcomings.

2.2 Fatigue resistance curves

Wöhler [88], for the first time, conducted series of tests to determine fatigue resistance of specimens due to constant amplitude fatigue load at different stress levels. The S-N curve

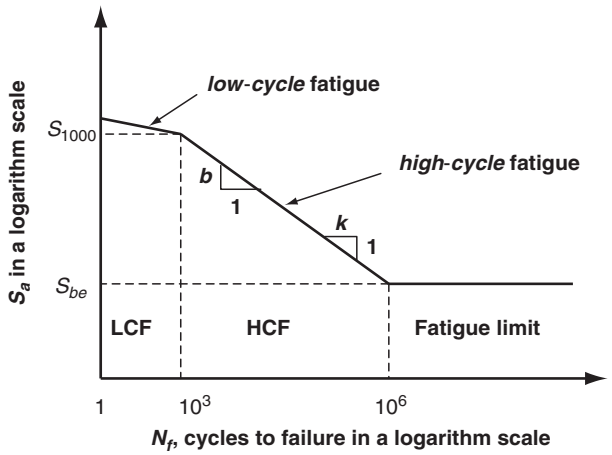

Figure 2.2: A schematic S-N curve for steel [49]

as illustrated in Figure 2.2 is divided in two main parts: 1) Low-cycle fatigue with number of cycle between 1 and 1'000 or even 10'000, which is occurring under earthquake or possibly silos, 2) High cycle fatigue with number of cycles more than 10'000, which can be the case for bridges. At low stress levels (S_{be}) fatigue life is infinite as represented in Figure 2.2 and it is called Constant Amplitude Fatigue Limit (CAFL). Typically, there is a knee point in the S-N curve at CAFL and, for C-Mn steel, it becomes horizontal after this point. CAFL is well documented for small specimens; however, for large scale specimens, only a few test results have been done to verify long-life fatigue behaviour (typically over 10^7 cycles) because of limitations in time and budget.

In general, three cases of variable amplitude stress spectrum might occur, as shown in Figure 2.3. Case 1 occurs when all cycles in the spectrum are above the constant amplitude fatigue limit. The general approach for these cases is applying Miner summation rule to find the equivalent stress range. When some, but not all, stress ranges are below the CAFL, the

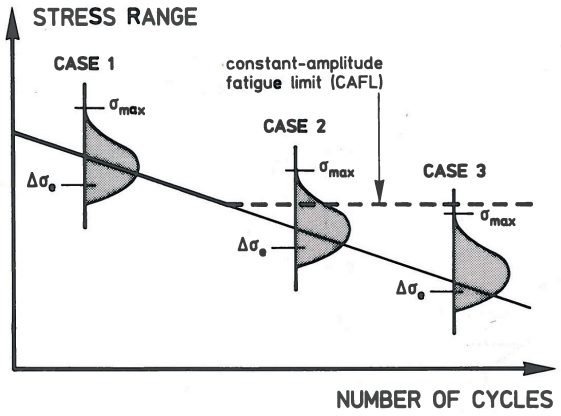

Figure 2.3: Three cases of variable amplitude stress spectrums [83]

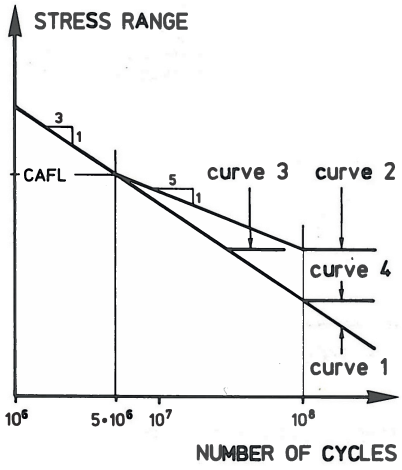

Figure 2.4: The different fatigue S-N curves examined by Smith et al. [83]

stress spectrum is Case 2 which is a rather typical case in bridge details and it is discussed more in the next paragraphs. In Case 3 spectrum, all stress ranges are below the CAFL, then no fatigue crack is expected.

Schilling et al. [75] conducted fatigue tests on welded steel members under variable amplitude corresponding to stress spectrums and ranges typically for bridge members. They concluded that the root mean square of stress ranges can transform variable amplitude stress ranges into constant amplitude tests, and Miner's rule is overestimating damage. However, Schilling et al. [75] did not describe their assumptions about the elimination of low amplitude stresses. Fisher et al. [30] expanded Schilling et al. [75] experiments to long life fatigue loading and found that the existence of a fatigue limit below which no fatigue crack propagation occurs is assured only if none of the stress ranges (not even as few as one per ten thousand cycles) exceeds the CAFL.

Therefore, the CAFL is applicable for the variable amplitude loading provided that all stress ranges remain below CAFL. In the other words, the stress ranges which are below CAFL does not provoke damage at the beginning of the fatigue life, but the same stress ranges may causes damage after some cycles above CAFL that initiate cracking. That is the main reason that the S-N curve of most steel details are proposed to be extended below the CAFL with a shallower slope [34–36]. Although, defining the characteristic value of CAFL is still a point of debate.

Smith et al. [83] investigated on long life fatigue under variable amplitude loading and compared the fatigue recommendations proposed by the European Convention for Constructional Steelwork (ECCS [24]) with tests results. Figure 2.4 illustrates four different variations for S-N curve, with different slopes and cut-off limit after CAFL, that Smith et al. [83] examined for computing damage sum and compared with the tests results. They summarized that a double slope S-N curve (Curve 2), can improve the accuracy of fatigue assessments, but not in all types of structural elements.

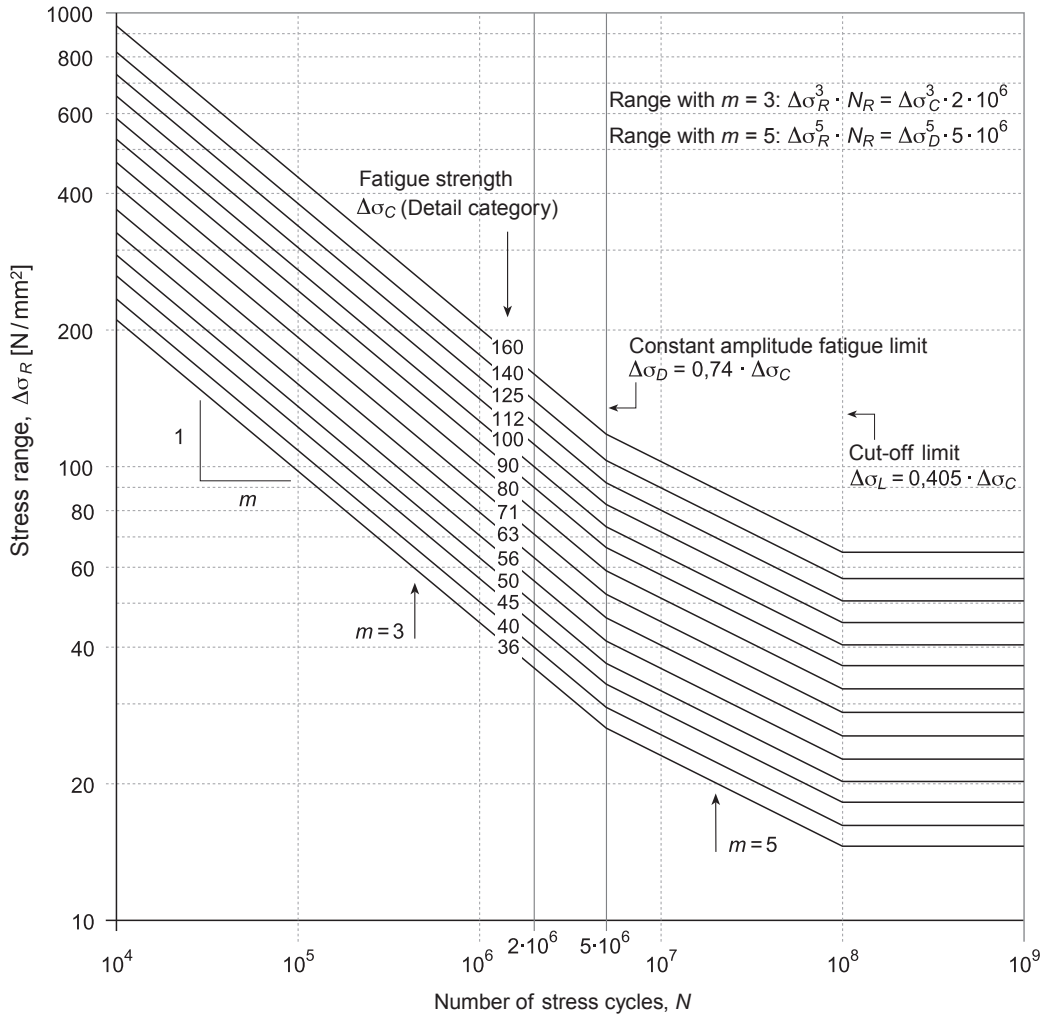

Figure 2.5: Fatigue resistance and CAFL for different detail categories based on SIA263 [80]

The SIA263 [80] follows the ECCS [24] recommendations and propose a double slope curve for fatigue strength and damage sum computations, with parallel lines for different detail categories as presented in Figure 2.5. Stress ranges inferior to the cut-off limit may be completely neglected in damage accumulation. The EN1993-1-9 [26] also apply the same a double-slope curves for steel details under direct stresses.

In the other extreme, the American AASHTO[1] bridge rule gives a constant slope S-N curve ($m = 3$) with CAFL at 2×10^6 to 2×10^7. To apply this theoretically infinite fatigue life, AASHTO requires that the maximum cycles due to the passage of the factored fatigue load model to be lower than the half of the CAFL [2].

Since the current study concentrates on the action effect, the fatigue resistance curves (S-N curves) as given in the SIA263 [80] and the EN1993-1-9 [26] will be applied in order to be in

[1] American Association of State Highways and Transportation Officials

accordance with the codes. For steel details under direct stress, S-N curve has slope of 3 for cycles with stress range higher than CAFL, and slope of 5 for cycles lower than CAFL, also cycles lower than cut-off limit are dismissed. For steel details under shear stresses S-N curve has a single slope of 5, and a cut-off limit at 10^8 cycles. In addition, some analysis is performed for shear studs which has the S-N curve with slope of 8 without any CAFL or cut-off limit.

2.3 Cycle counting methods

The fatigue life can be obtained from fatigue resistance curves generated under constant amplitude loading. In service life of structural components, the components are subjected to cyclic loading which can be either constant amplitudes or time dependent amplitudes. For cases that are subjected to constant amplitude loading, determination of amplitude and number of cycles is straightforward. However, if amplitude of load changes with time it is more difficult to determine what contribute to damage within the cycles and the corresponding amplitude of that cycle.

Lee et al. [49] classified the proposed cycle counting methods in two main groups of one-parameter and two-parameter cycle counting methods. The one-parameter cycle counting methods includes: peak-valley, level crossing and range counting. These methods, however, are not satisfying for the purpose of connecting a loading cycle to the local stress-strain hysteresis which has a strong influence on fatigue failure. In the contrary, two-parameter cycle counting methods such as the Rainflow and Reservoir cycle counting can appropriately represent variable-amplitude cyclic loading. The Rainflow counting method is generally regarded as the main method for predictions of fatigue life. For a given stress history Rainflow and Reservoir cycle counting methods lead to the same results.

Downing and Socie [23] proposed two computer base algorithms to extract cycles by applying the Rainflow method. However, most Rainflow algorithms require that the entire stress history to be known before start of cycle counting. Glinka and Kam [32] presented a procedure which allow performing the Rainflow counting without knowing entire stress history. Most cycle counting methods are disable to keep load sequence information. Anthes [4] proposed an algorithm for performing Rainflow cycle counting that provides information about the load sequence.

Generally, two Rainflow algorithms have been used for computer programming since 1960s. These two algorithms have three-point and four-point basis and both are still currently in popular use. McInnes and Meehan [58] showed both three-point and four-point algorithms gives the same hysteresis loops and the only difference between their outcomes is the order in which the hysteresis loops are listed in the output.

On the order hand, the Reservoir method is a quite convenient and easy to apply since it is more visual. In this method, the diagram of a given stress history assume to be the cross-section of a reservoir which is drained successively from the lowest point until the water is

fully drained. Each draining step counts one cycle with the magnitude corresponding to the depth of the water drained [34].

Sometimes, it is necessary to reconstruct a load-time history from the results of cycle counting and apply it as an input for fatigue testing or simulation [3, 42]. The procedure for reconstruction is the reverse process of the four-point cycle extraction. The original and the reconstructed loading sequences result in the same cycles, though they have a different loading sequence [49].

The Rainflow method, specifically, the Rainflow four-point algorithm is chosen and implemented in the simulation program (WinQSIM) due to its simplicity for programming. In Chapter 4, a method for cycle counting of influence line is also required (assuming that influence line is a stress history). The Reservoir counting method would be more convenient for this purpose since it is easier to understand for practical engineers.

2.4 Traffic actions

Traffic represents external actions to consider for fatigue limit state analysis of bridges. However, the actual value of traffic load on bridges is very difficult to be modelled accurately because of its high randomness nature. None of the traffic load models is thorough. Each model covers a range of span length and/or limit state of design depending on its assumptions. In fact, a few models are valid for both short spans and long spans bridges as far as it is valid for both ultimate limit state and fatigue limit state. Crespo-Minguillon and Casas [19] divided the methods to address the issue into three groups: 1) methods based on theoretical models, such as the theory of stochastic processes and the convolution or integration approach; 2) methods based on the simulation of static configurations of traffic; and 3) methods based on the simulation of real traffic flow.

Several theoretical-based models have been proposed by researchers such as Tung [85], Larrabee [46] and Ghosn and Moses [31]. It can be also found some theoretical-based models for the study of the fatigue due to traffic on bridges [53]. Also, Ditlevsen [21] proposed to use white-noise as traffic load model on bridge but a lot of simplifications in this method make it uninteresting for short span bridges.

For the methods based on the simulation of static configurations of traffic, Nowak [65] and Bez [9] can be found. In these models, two traffic condition of congested and free-flow are analysed separately. The statistical parameters in these models (gross vehicle weight, vehicles geometry, distance between vehicles) are based on the recorded traffic data. Then the model extrapolates the results to obtain the maximum effects for a given service life [19].

The third group, which are the methods simulating real traffic flows on bridges, contains the most comprehensive approach for traffic load evaluations. The methods developed by Gorse [33] and Miki et al. [61] are within this group. These methods are the more accurate that then

other ones and can applied to the analysis of the both serviceability and ultimate limit states without less limitation of span length; however, they need complicated simulation process that needs time-consuming computer calculation.

Accuracy of traffic flow simulations is highly depending on real traffic statistical data such as gross vehicle weight, vehicle geometry, axle's load, contribution of each vehicle type in total traffic, average daily traffic, percentage of trucks in traffic flow and etc. If the statistical variation of all these parameters are determined properly, traffic actions can then be modelled accurately. Nowak [65] mentions that uncertainties involved are due to limitations and biases in the surveys. Also, the available data base is small in compare with the actual number of heavy vehicles in a 75 year lifetime. Finally, a considerable degree of uncertainty is due to unpredictability of the future traffic trends.

One important improvement in heavy vehicles loading knowledge has been achieved by application of Weigh-in-motion (WIM). WIM devices are designed to capture and record truck axle weights and gross vehicle weights as they drive over a sensor. Unlike older static weigh stations, current WIM systems do not require the trucks to stop, making them much more efficient and representative. The first WIM measurement and data collected in mid 1980's were not reliable, with estimated error 30-40% [65]. But nowadays by advances in the technology of these devices, the estimated error is much lower.

The COST323 [18] [2] defines seven levels of accuracy class for each types of measurements including Gross Vehicle Weight (GVW), axle's load, vehicle speed, inter-axle distance and total flow. For example, the tolerance of the accuracy for the GVW in the class A is lower than 5% and it is more that 25% for the class E. The current WIM devices in Switzerland are of good quality; for instance, the Götthard WIM station in Switzerland is tested [18] and the accuracy of GVW, axle's load and spacing between axles are respectively obtained 5%, 10% and 5%.

Recently most traffic simulations are based on WIM measurements. Laman and Nowak [45] used Weigh-in-Motion to determine damage due to fatigue loading on steel girders of road bridges, assuming one-by-one passage of trucks over bridge though. O'Connor and O'Brien [69] also assess the sensitivity of extreme loads to two method of prediction: generalized codified loading models and the models based on WIM. Miao and Chan [60] studied how to analyse the obtained WIM data statistically and use results to calculate extreme daily bending moments. Chotickai and Bowman [17] used traffic data from WIM sites to evaluate the safety level of the fatigue truck of the AASHTO [2] for simple span and two-span continuous bridges with different span lengths.

For many years, the Swiss Federal Roads Authority has been carrying out permanent automatic traffic counts and measurements, as well as periodical manual traffic counts, within the scope of the on-going statistical surveys conducted by the federal government. These measurements include Swiss Automatic Road traffic counts (SARTC), Swiss Road Traffic Census (SRTC), Weigh-

[2] COST 323 is one of the actions supported by the COST Transport part of the European Commission's Transport Directorate, DG VII.

in-Motion (WIM) and traffic development. Two Weigh-In-Motion (WIM) stations of Götthard and Mattstetten started working in 1994, and from 2003 six more WIM stations were installed. These WIM installations can record the Gross Vehicle Weight (GVW), axles load and distance, vehicle class, speed, vehicle length and time intervals for trucks weighting over 35 kN.

In this thesis, traffic actions are modelled by simulating the real traffic flow with the WinQSIM program, which is developed and applied for this purpose (see Appendix B). The parameters of traffic flow and heavy vehicles properties are derived from the measurements in Switzerland as explained in Chapter 5.

2.5 Cycles per truck passage

Passage of one vehicle over a bridge does not necessarily results in one cycle in a detail of a bridge. The number and amplitude of cycles resulting from the passage depend on the bridge length, the number of spans, the detail location and the vehicle geometry. Schilling [74] investigated the stress cycles resulting from individual passage of HS truck of AASHTO [3] for longitudinal members of different bridge types. He introduced equivalent number of simple cycles, by applying Miner rule and single-slope of S-N curve. The equivalent cycles per truck passage is representative of complex cycles due to passage of AASHTO (1983) truck as shown in Figure 2.6 for different bridge types and span lengths. For a simple span bridge as an example, Schilling [74] suggests one equivalent cycle for span length above 12 m and two equivalent cycles for span length below 12 m.

[3]The HS truck of AASHTO consists of three axles in which the distances between the first-second and the second-third axles are respectively equal to 4.2 m and 9.1 m. HS gross weight is 222.4 kN of which the first axle has 11.2% propostion and the second and third axles has 44.4% proportion equally.

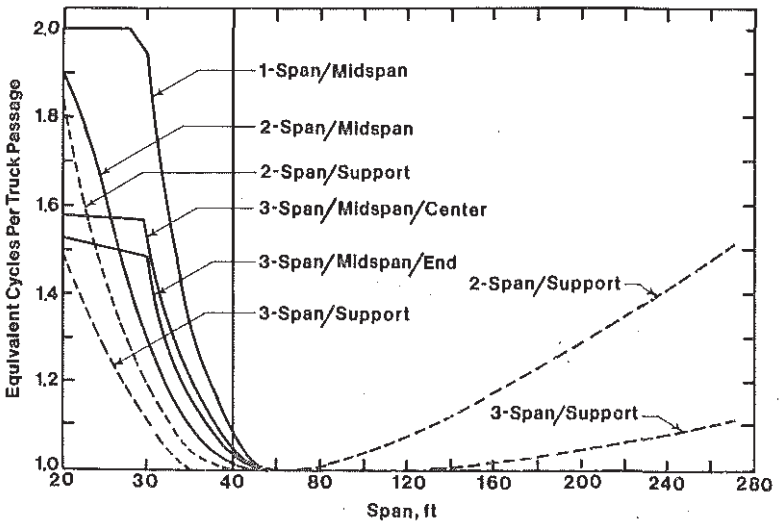

Figure 2.6: Equivalent cycles per truck passage as a function of span (1 ft = 30.5 cm) [74]

The real traffic, however, is composed of various types of vehicles passing on bridges. Among other, Mori et al. [64] studied the fatigue of bridges with simulation of traffic and showed that the fatigue life decreases as the span length decreases and that steel bridges made out of steel with higher yield stress are more vulnerable to fatigue. Mori et al. [64] also introduced a parameter for arranging the fatigue life of the main girder of short and medium span bridges, which tries to represents the effect of Average Daily Truck Traffic (ADTT) and influence surface.

In this study, the number of cycles per truck passage is not investigated specifically, except a few arguments stated in Chapter 4. Nevertheless, the effect of the number of cycles per truck passage is included in the damage equivalence factors or equivalent force ranges obtained for different bridge types.

2.6 Multiple presences of trucks on bridge

Several studies have been carried out about the distance between vehicles (any vehicles, or just truck neglecting cars) for different traffic flow conditions. Since, the traffic flow condition is indispensable in determination of distance between vehicles and accordingly probability of multiple presences of vehicles on bridges, the principal characteristics of traffic flow conditions should firstly be described.

The basic traffic flow diagrams assuming a linear speed-density relationship are shown in Figure 2.7. Basically, flow can be defined as the number of vehicles passing a specific point in a given period of time in each lane. The maximum feasible flow is called capacity (v_m). Speed can be defined as the average speed of vehicles. The speed has two unique parameters:

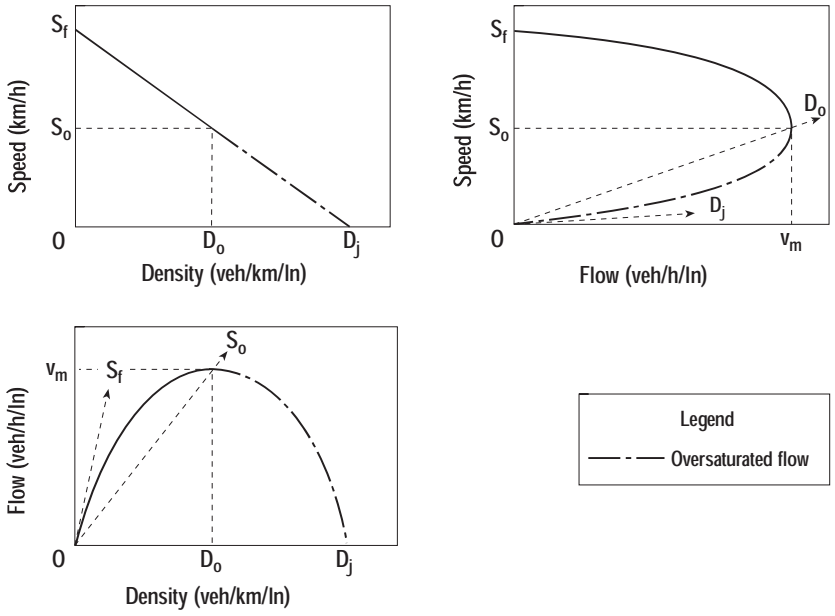

Figure 2.7: General relationships among speed, density and flow rate [39]

free-flow speed (S_f) and optimum speed (S_o). Free-flow speed occurs as flows approach zero under free-flow conditions, and the optimum speed occurs under maximum flow conditions. Density can be defined as the number of vehicles in a section of roadway in each lane. The density has two unique parameters: jam density (D_j) and optimum density (D_o). The jam density occurs when both flow and speed approach zero, and the optimum density occurs under maximum flow conditions. In Figure 2.7, the free-flow corresponds to the upper part of the speed-flow curve and the congested or oversaturated flow regime corresponds to the lower part of the speed-flow curve [57].

The free-flow speed (S_f) is an important parameter for determining capacity. The factors influencing S_f include number of lanes, lane width, lateral clearance and interchange density or spacing. The freeways may have capacities as high as 2400 (veh/h/lane); this capacity is typically archived on freeways with S_f of 120 km/h. However, the capacity of basic freeway segment with S_f of 90 (km/h) is expected to be about 2250 (veh/h/lane). The average speed at flow rate that represent capacity is expected to range from 86 (km/h) for a section with S_f of 120 (km/h) to 80 (km/h) for a section with a S_f of 90 (km/h) [39].

For free flow traffic regime, which is the most interesting traffic condition for fatigue analysis, the non-queuing traffic is commonly modelled as a Poisson process. The inter-vehicle times are thus theoretically represented by an exponential distribution which varies as a function of the volume of traffic flow. This distribution may be shifted to the right to allow for a minimum distance between vehicles and is known as the shifted exponential distribution [7]. Figure 2.8 shows an example of shifted exponential distribution for free-flow traffic condition. The shifted exponential distribution is a function of flow rate which allows obtaining the distribution of distance for any flow rate. However, this relationship remains valid only until the capacity of

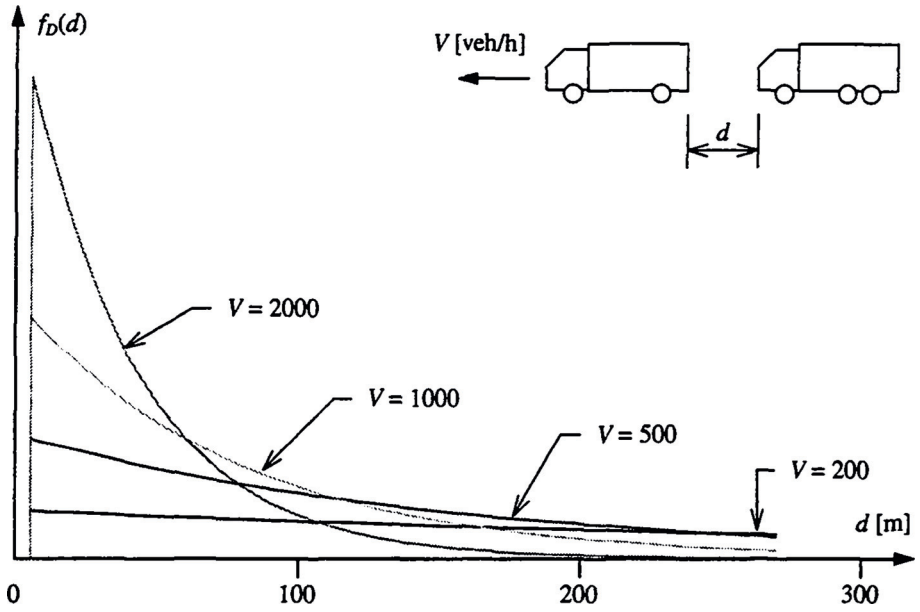

Figure 2.8: Distance between vehicles in free-moving traffic [7]

the highway is reached.

Time interval between vehicles, instead of accurate distance between vehicles, has been also investigated in some researches. Crespo-Minguillon and Casas [19] observed that the time interval between vehicles depends on flow rate (Fig 2.9a). Rather than fitting individual distributions for each flow, Crespo-Minguillon and Casas [19] proposed a non-dimensional distribution (Fig 2.9b) defined as the normalized time intervals divided by the average time intervals for a given flow rate. The vertical scale in Figure 2.9 corresponds to the inverse of the standard normal distribution.

The determination of distance between trucks (instead of all vehicle types) is more interesting for both fatigue and ultimate limit states, although the time intervals or distance between vehicles is also useful for accurate traffic modelling. O'Brien and Caprani [67] applied five days of Weigh-In-Motion (WIM) data of A6 motorway near Auxerre in France to obtain the time intervals (in second, between the front axles of two successive trucks). They observed that for time intervals of less than 1.5 seconds, the correlation between hourly flow of trucks and time intervals is weak; because for small time intervals, driver perception of safe distance rather than traffic flow determines the time intervals. On the other hand, O'Brien and Caprani [67] described, for time intervals between 1.5 and 4 seconds, there is a correlation between time intervals and truck traffic flow. At each various truck traffic flow intervals, Enright [28] fitted a set of quadratic curves to the gap distribution functions for gaps below 2.6 second; Enright [28] assumed that the negative exponential distribution, which also had applied in the former studies, for intervals above 2.6 second is accurate enough. The fitted gap distribution functions of Enright [28] for two traffic flows of 200 and 400 trucks per hour as well as the observed values are shown in Figure 2.10.

In addition to trucks time intervals, some researches carried out on frequency of multiple

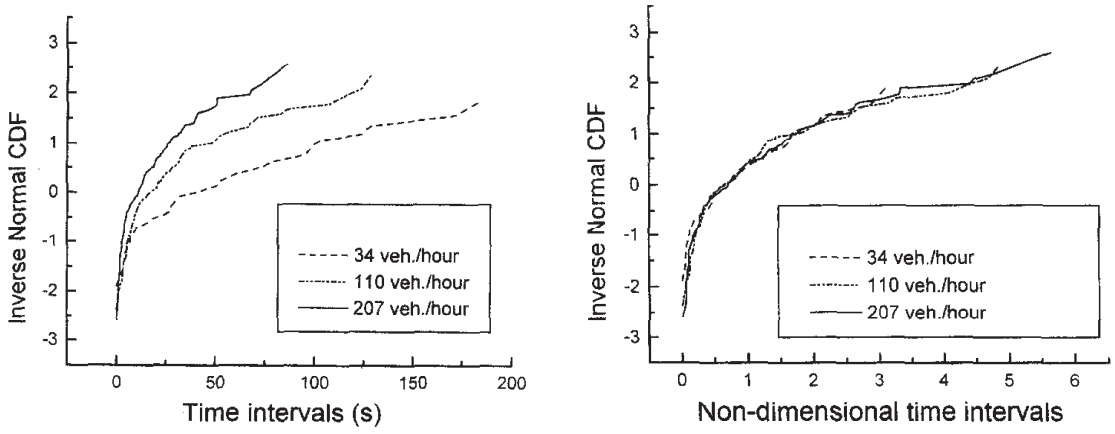

(a) CDF of time intervals

(b) CDF of non-dimensional time intervals

Figure 2.9: Time intervals for different traffic flows [19]

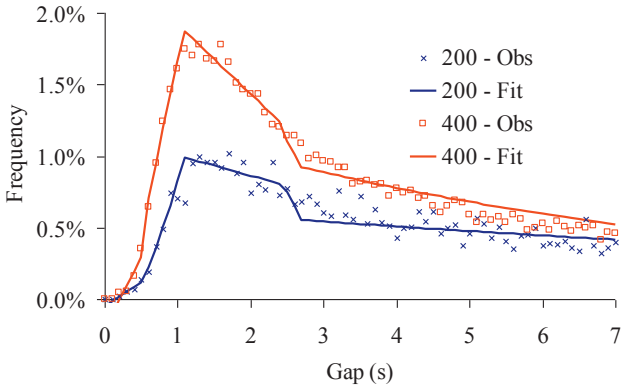

Figure 2.10: Trucks time intervals distributions at two flow rates [28]

presences of trucks on bridges in the same lane (following) or inter-lane (side-by-side or staggered). For bridges of different length, O'Brien and Enright [68] studied the frequency of occurrence of two trucks on double-lane and unidirectional traffic also applying WIM data. In Figure 2.11, the frequency of occurrence of the two-truck event (both side-by-side and staggered), with one truck in each lane, is shown for two European sites and an US site (the US site curve is based on the study of Sivakumar et al. [82]). The Average Daily Truck Traffic (ADTT) for the Netherlands (NL) and Czech Republic (CZ) sites are respectively 6545 and 4490 and ADTT of the US site is between 2500 and 5000.

Sivakumar et al. [82] also studied the occurrence of multiple trucks for a given span length applying the WIM measurements of US sites. Their research also indicates that probability of occurrence of multiple trucks on a bridge depends on factors such as truck traffic volume and the bridge span length. The multiple-presence for four loading patterns including single (only one truck on the bridge), following (two trucks in the same lane on the bridge), side by side (two trucks in adjacent lanes with an overlap of more than one-half of the first truck), and staggered (two trucks in adjacent lanes with an overlap of less than one-half of the first truck) presented in Figure 2.12. Based on Sivakumar et al. [82] studies, for each day, the number of multiple-presence events is counted and recorded as a percentage of the total truck traffic of that day. The average multiple-presence percentage is then calculated for all days with the

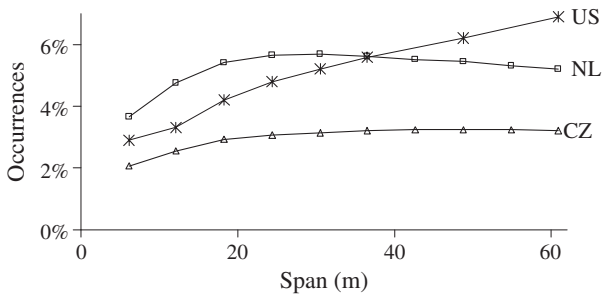

Figure 2.11: Multiple presences of trucks with one truck in each lane [68]

same range of ADTT, including days with light truck volume (ADTT ≤ 1000 trucks per day per direction), average truck volume (1000 ≤ ADTT ≤ 2500), heavy truck volume (2500 ≤ ADTT ≤ 5000) respectively.

The WIM measurement devices in Switzerland only record the "timestamp" with a precision of a second for each truck passage. Therefore, in the current study, the distribution of distance between vehicles is modelled with the shifted exponential distribution for the free-flow regime, in spite of its inaccuracy for short intervals (less than about 1.5 s as mentioned above). In addition, the aim of this study is not to quantify the actual frequencies of multiple trucks presence on bridges. Nevertheless, the effect of simultaneous presence of trucks is included in the simulations carried out in the thesis, except in some special cases which are clearly mentioned.

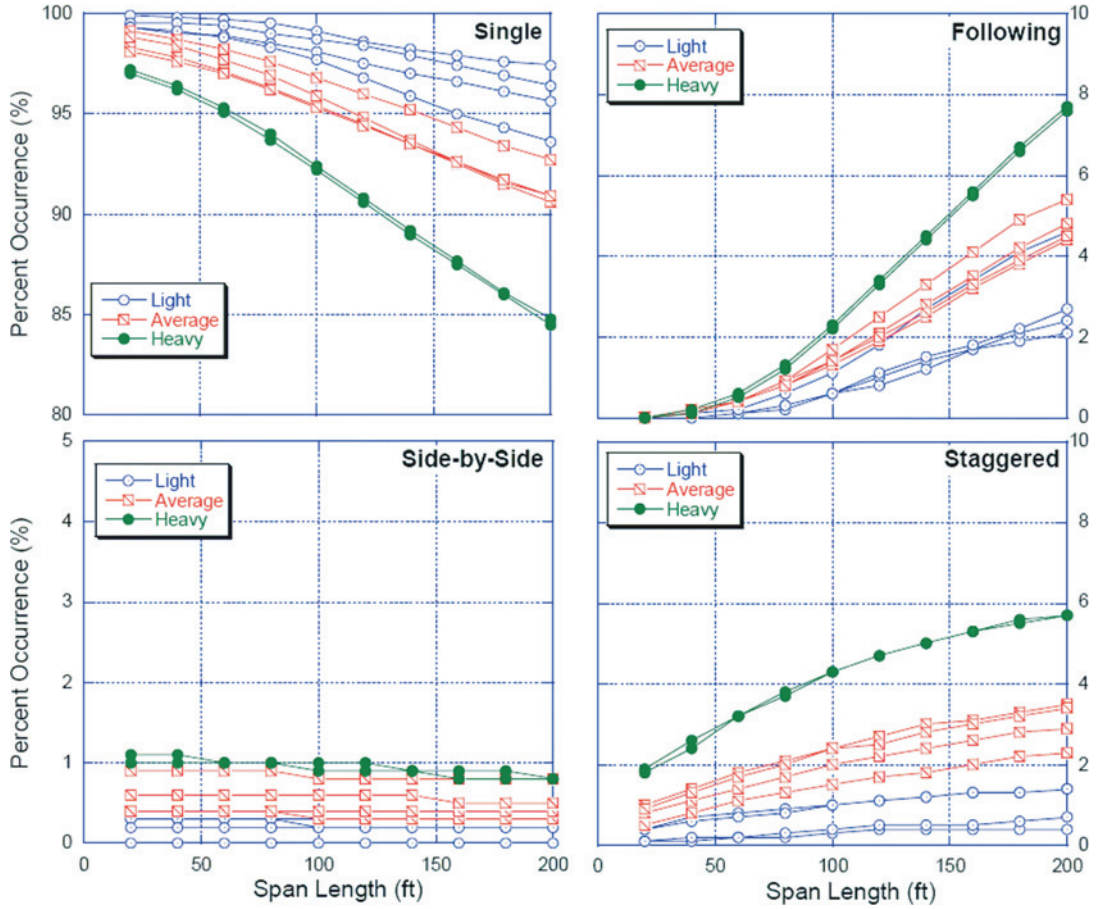

Figure 2.12: Multiple presences frequencies for four loading patterns (1 ft = 30.5 cm) [82]

2.7 Dynamic Amplification Factor (DAF)

In practice, a moving static load is often used to model the vehicle loads on bridges. The static vehicle loads or their effects are then increased by a dynamic amplification factor (DAF) which takes into account the dynamic effects from the vehicle vibration and interaction between the vehicle and bridge. This simplified approach prevents from performing dynamic response analysis of vehicle-bridge interaction.

In reality, the dynamic response from the vehicle-bridge interaction is a complex problem and is function of many parameters such as vehicle position, vehicle weight, vehicle suspension, vehicle speed, number of loading lanes, girder spacing, road surface condition, road roughness, and dynamic properties of both vehicle and bridge. Among these parameters, three main parameters can be identified: span length, vehicle speed and road surface condition [20].

Hwang and Nowak [40] performed a parametric study using the Monte Carlo method by generating road surface profiles from a power spectral density function (PSD). They found that the DAF always decreases as the gross vehicle weight (GVW) increases, but it varies with speed depending on GVW. Wang et al. [87] and later Deng and Cai [20] carried out a parametric study with major focus on effect of surface roughness using H20-44 and HS20-44 AASHTO trucks. They reported that DAF is affected slightly with vehicle speeds for both “very good” and “good” surface profiles; however, the vehicle speeds influence DAF significantly for “average” and “poor” surface profiles. This is explained by the fact that the vehicles circulating at low speed over a “very poor” road surface experience excitations at frequencies close to the vehicles natural frequencies, which cause large dynamic responses [47].

Some studies reported that DAF can be as high as 2.30 [16, 70], especially for short span lengths. In Switzerland, Cantieni [14] reported dynamic response of 226 instrumented bridges which were tested through passages of a two-axle truck with a gross vehicle weight near the legal limit. The pavement quality of the tested bridges are classified as ranging between

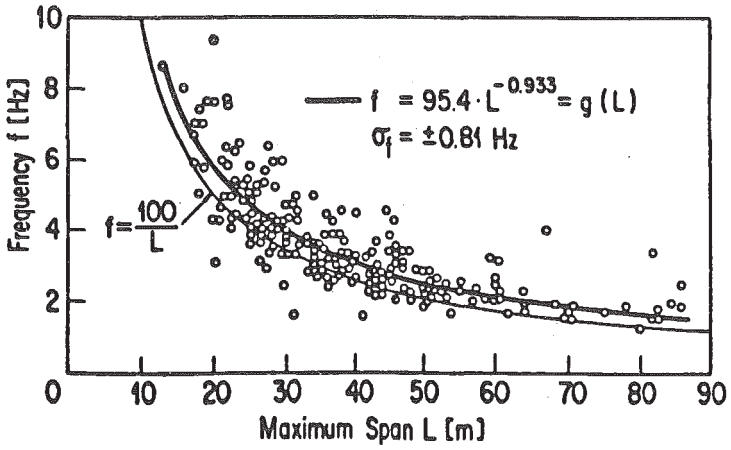

Figure 2.13: Natural frequency versus span length, taken from Cantieni [14]

"good surface", "medium" and "poor". Based on the measurements from different bridge types (including prestressed concrete, reinforced concrete, composite steel/concrete and prestressed lightweight concrete), Cantieni [14] proposed a DAF as a function of the natural frequency of the bridge. In order to facilitate the practical application of the proposition, he also provided an empirical relation between natural frequency of bridge (f) and maximum span length (L), as shown in Figure 2.13.

Unlike the large DAF values mentioned above, several studies have shown that the value of DAF decreases when two or more heavy vehicles traverse the bridge simultaneously [11, 40, 52]. Since the extreme traffic loads are typically obtained from multiple presence of heavy vehicles, it is logical to expect a reduced DAF for characteristic maximum loading [15]. In addition, in most researches, the dynamic deflection is compared to static deflection to determine DAF. However, the DAF resulting from deflection measurements on medium or long span bridges may very well be decreased by 10 to 20% [52]. For these reasons, the DAF given in the codes is lower than the extreme measured values.

In codes, the dynamic amplification factor is often defined as the ratio of total dynamic response to maximum static response of a given bridge. In some codes, the term *dynamic amplification factor* (DAF) is replaced by *dynamic load allowance* (DLA) which is basically equal to DAF - 1. Many codes, including AASHTO [1], specify the DLA as a function of span. However, some codes such as the Ontario Highway Bridge Design Code [71] or Australia's National Road Authority [5], define the DLA as a function of the first flexural frequency of the bridge. In some codes such as the EN1991-2 [25] and SIA261 [79], for highway bridges, dynamic amplification is included in the specified design loads. Moghimi and Ronagh [63] compared DLAs of all of the aforementioned codes together, as shown in Figure 2.14. As can be seen, there is a large variety of models, a general trend being a reduction with increasing

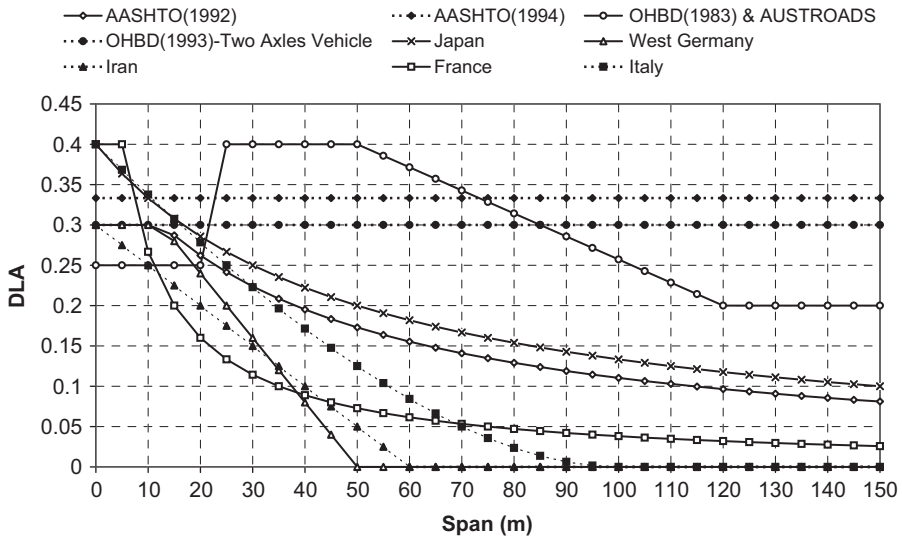

Figure 2.14: Dynamic load allowance based on various design codes [63]

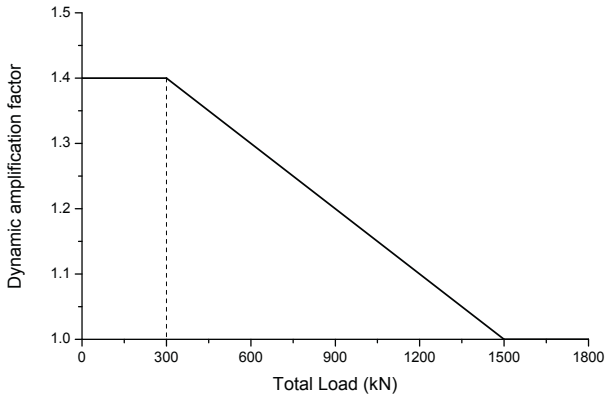

Figure 2.15: Dynamic amplification factor in function of total load [51]

span.

A few studies were carried out to provide DAF regarding specifically fatigue loading. The recommended DLA for the fatigue limit state in the AASHTO LRFD [2] is 50% of the value for the ultimate limit state or the serviceability limit state [48]. In the EN1991-2 [25] and SIA codes [79, 80], the given fatigue load model and damage equivalence factors include dynamic effect resulting from bridge-vehicle interaction (since given in function of span length) for roads with good surface quality.

Ludescher and Brühwiler [51] proposed a simplified relationship between DAF and total load on a bridge for fatigue analysis of bridges, as shown in Figure 2.15. This is interesting for traffic simulations for fatigue analysis because of the following reasons. First, the Ludescher and Brühwiler [51] DAF reduces linearly from 300 kN over and equals to one when total load on bridge is 1500 kN. This reduction can be either due to large GVW of trucks which is found in several studies [40, 70] or due to multiple presence of trucks as expressed in many researches [11, 15, 40, 52]. Second, the proposed DAF is not function of vehicles speed. The previous studies [20, 87] have shown that the effect of vehicles speed is negligible for roadways with “good” and “very good” surface quality. Therefore, in the current study, the Ludescher and Brühwiler [51] DAF for fatigue is used for traffic simulations and is implemented in the WinQSIM program.

3 Evaluation of the current fatigue design rules

In this chapter, the current fatigue design rules for roadway bridges using the damage equivalence factors as given in the SIA code as well as the Eurocode are evaluated. First, the different elements constituting the damage equivalence factors for fatigue verification of bridges are presented. Besides, the advantages and difficulties in application of damage equivalence factors are described. A series of simplified traffic models (one-by-one truck passage) are then used in order to evaluate the accuracy of the damage equivalence factors for different bridge types. So-called "initial traffic simulations" (as opposed to traffic simulations in Chapter 6) assuming a basic traffic flow are performed to compare the damage equivalence factors given in the SIA code and the Eurocode with results of the traffic flow simulations. As a result, the elements that may cause inaccuracy in fatigue verification using the damage equivalence factors are distinguished. In addition, by simulating the initial traffic conditions on different bridge types, a first estimate of different parameters effects on damage equivalence factors can be obtained. This will be useful for further studies in the next chapters.

3.1 Background of fatigue design rules for roadway bridges

3.1.1 Swiss Codes

The fatigue verification of bridges subjected to a variable load history is complex and requires knowledge of the imposed loads on the structure during its entire life. Even assuming that the imposed loads are known, the engineers still requires to deal with the tedious work of damage accumulation procedure, although it is impossible to know truck and traffic trend. Hence, it is necessary to simplify this complicated procedure, which permits engineers to be able to perform fatigue verification for typical bridges and traffic cases.

Thus, the concept of the damage equivalence factor was proposed to eliminate the tedious calculation procedure of damage accumulation. Thanks to this method, which is presented in Figure 3.1, the computation of the usual cases is performed once for all during development of the code. The left side of Figure 3.1 illustrates different elements involved in fatigue verification

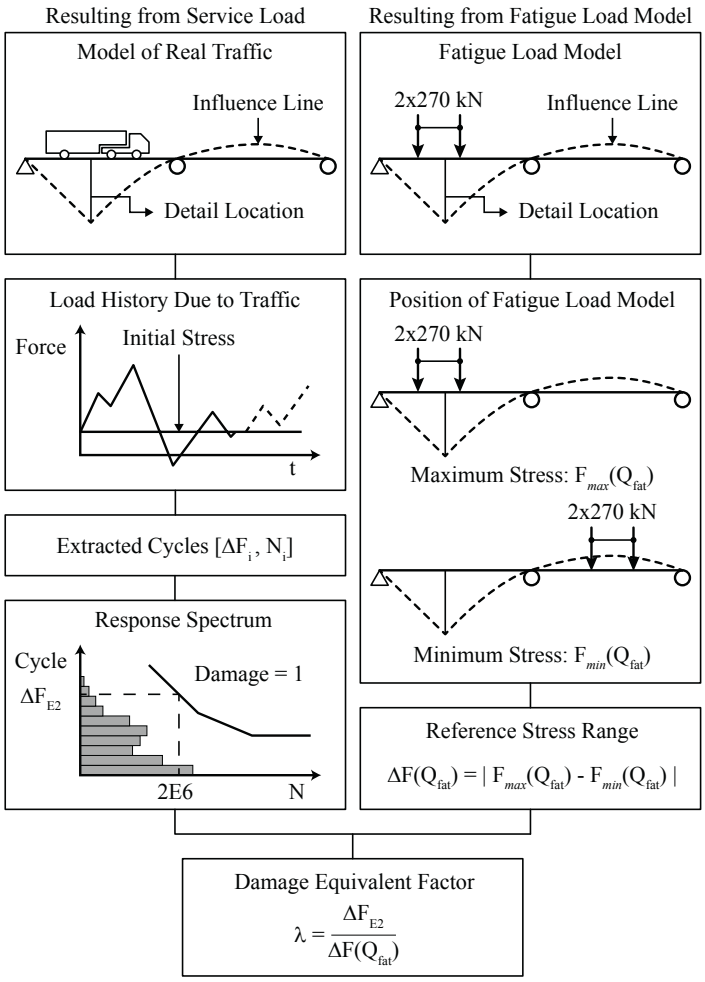

Figure 3.1: Concept of damage equivalence factor

using damage accumulation which includes the following steps:

- a model of real traffic
- the load history due to the traffic model including dynamic effects,
- the extracted cycles and calculation of equivalent force range (ΔF_{E2}).

The model of real traffic should be as close as reality; besides, it should comprise the different traffic types for design states. More description and discussions about the selection of real traffic flow is provided in Chapter 5. The load history including the dynamic amplification due to traffic model should be determined for different bridge static systems. The cycles can be extracted from the load history with the Rainflow method. Finally, the equivalent force range corresponding to 2×10^6 can be determined by iteration on the vertical position of the fatigue resistance curve as long as the total damage sum bears about one. It should be noted that the

force denotes the internal forces that can be moment, reaction or shear. Obviously during the development of the code, the bridge dimensions are unknown, thus the transformation from the internal forces to stresses is not applicable. Also, both sides of the diagram (Fig. 3.1) are of the same response type and unit, thus knowing the section properties is not necessary.

The right side of Figure 3.1 shows the application of the fatigue load model to obtain maximum response, $F_{max}(Q_{fat})$, and minimum response $F_{min}(Q_{fat})$, by placing the fatigue load model at the most severe positions. To obtain the same value as the equivalent force range, ΔF_{E2}, which takes into account the damage accumulation, the value of $\Delta F(Q_{fat})$ should be corrected by damage equivalence factor, λ.

The engineers then can carry out the fatigue assessment of bridges with λ as follows [80]:

$$\lambda \Delta\sigma(Q_{fat}) \leq \frac{\Delta\sigma_c}{\gamma_{Mf}} \tag{3.1}$$

where $\Delta\sigma(Q_{fat})$[1] is the stress range due to the passage of fatigue load model on the bridge, $\Delta\sigma_c$ is the reference value of fatigue strength at 2 million cycles corresponding the detail under consideration, and γ_{Mf} is the partial safety factor for fatigue strength.

The damage equivalence factor, λ, based on the SIA263 [80] can be obtained from:

$$\lambda = \lambda_1 \times \lambda_3 \times \lambda_4, \quad however \lambda \leq \lambda_{max} \tag{3.2}$$

where λ_1 is a partial factor for damage effect of traffic depending on influence length L_Φ, λ_3 is a partial factor for modification of the bridge design life, λ_4 is a partial factor which adds up the effect of traffic on the other lanes to the first lane, and λ_{max} is the maximum value of damage equivalence factor which takes into account the Constant Amplitude Fatigue Limit (CAFL). It worthy of note that λ_2, as defined in the EN1993-2 [27], is not exist in the SIA263 [80], and λ_1 is given for different traffic volumes.

In the SIA263 [80], the factor λ_1 is originally determined for various bridge types with span lengths ranging from 1 m to 100 m, by applying Q_{fat} as the fatigue load model. The λ_1-factors are then represented, for different traffic volumes with a dynamic amplification factor 1.2, in function of the influence length as shown in Figure 3.2.

The geometry of the SIA fatigue load model (Q_{fat}) [79], which is in accordance with damage equivalence factors, includes two axles with distance 1.2 m each weighting 270 kN and in total 540 kN. It is also important to mention, the influence length (L_Φ) is not clearly defined in the SIA codes [79, 80]. It can be taken as the dynamic factor length, which seems not to be very reasonable, and creates a confusion associating dynamic and fatigue phenomena.

[1] the Eurocodes use $\Delta\sigma_{FLM}$ denotation rather than $\Delta\sigma(Q_{fat})$

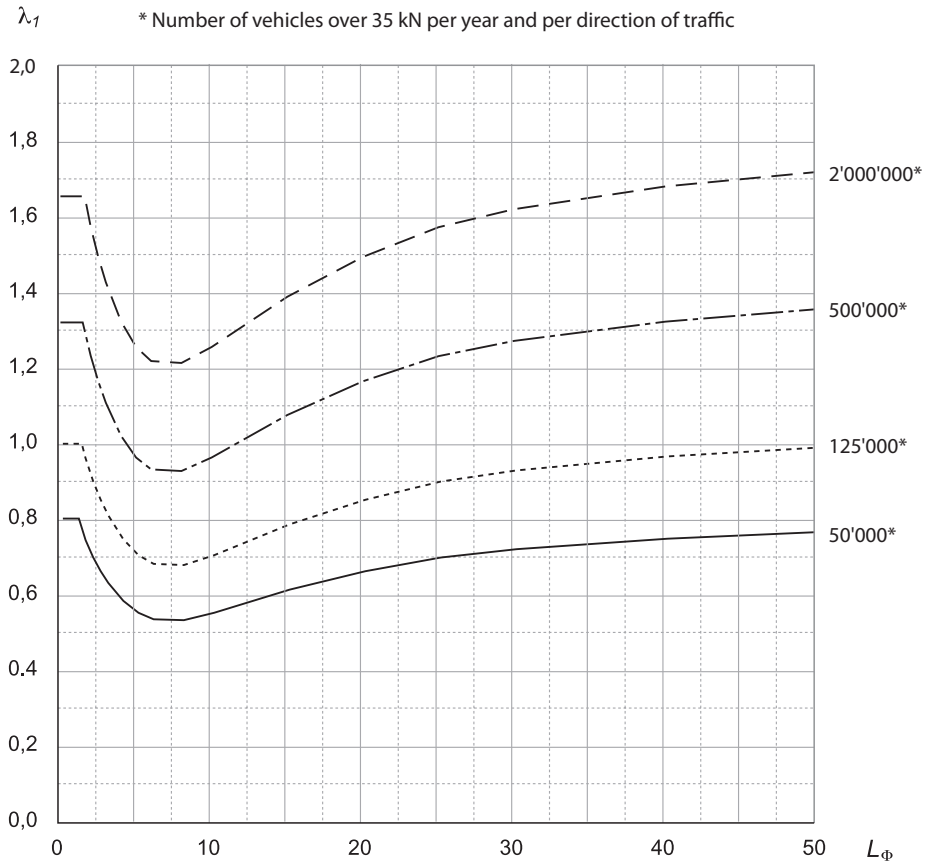

Figure 3.2: λ_1 for roadway bridge with different traffic volumes, taken and modified from the SIA261 [79]

The influence length can be also taken as the maximum distance between the null points of influence line. For instance, in the case of mid support reaction of a two-span continuous bridge (spans with equal length), influence length (L_Φ) which corresponds to the dynamic factor length gives 1.2 times of the span length, while the distance between null points is 2 times of span length. Such a large difference in determination of L_Φ cause confusions in application of damage equivalence factors for engineers; it may also be a source of inaccuracy in fatigue verification using damage equivalence factors especially for the cases defined by the distance between null points.

The partial factor, λ_3, is intended for modification of bridge design life. The basis fatigue design life of roadway bridges in the code is 70 years (Paragraph 10.4.3.1 of the SIA261 [79]). In other words, in determining the partial damage equivalence factor λ_1, and particularly $\Delta\sigma_{E2}$, the total damage sum corresponds to 70 years of traffic. This service life is somewhat an average between 50 and 100 years of service life, and a simplification due to the difficulties in predicting traffic so far in future. For modification of service life the factor λ_3, as follows, can

be applied:

$$\lambda_3 = \left(\frac{t_{Ld}}{70}\right)^{(1/5)} \tag{3.3}$$

where t_{Ld} is the design life of the bridge in years. The multi-lane traffic effect can be calculated by applying the λ_4-factor. This factor adds up traffic volume of other lanes to the first lane, as follows:

$$\lambda_4 = \left[\sum_{j=1}^{n}\left(\frac{\lambda_{1,j} \times \Delta\sigma_j}{\lambda_{1,1} \times \Delta\sigma_1}\right)^m\right]^{1/m} \tag{3.4}$$

Where $m = 3$ if the number of cycles during the service life remains inferior to 5 million and for conservative calculations, or $m = 5$ if the number of cycles during the service life exceeds 5 million. $\Delta\sigma_1$ is stress range caused by the traffic on the first lane and $\Delta\sigma_j$ is stress range caused by traffic on the j_{th} lane. $\lambda_{1,1}$ is partial damage equivalence factor for traffic on the first traffic lane and $\lambda_{1,j}$ is partial damage equivalence factor for traffic on the j_{th} lane.

In order to exemplify the different parameters of λ_4 in the SIA263 [80], assume a two-lane unidirectional highway with 2'000'000 annual truck traffic per direction[2] which passes over a simple span bridge with 20 m length. The cross section and the lateral loads position of the

[2]For different roadway types, the annual truck traffics in the SIA261 [79] are defined per direction, while in the Eurocodes, the annual truck traffics are defined per slow lane.

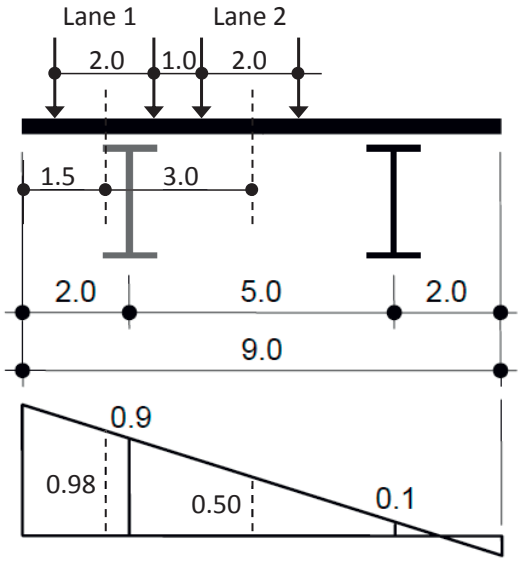

Figure 3.3: Example of transverse distribution of two-girder bridge cross section in function of lateral load positions

bridge is shown in Figure 3.3. If 75% of annual truck traffic circulates in Lane 1, the different parameters of λ_4 can be obtained as follows:

- first, the truck traffic on each lane should be determined as $N_1 = 0.75 \times 2'000'000 = 1'500'000$ and $N_2 = 0.25 \times 2'000'000 = 500'000$;
- then, $\Delta\sigma_1 = 0.98$ corresponds to stress range due to passage of fatigue load model on Lane 1 and $\Delta\sigma_2 = 0.50$ corresponds to stress range due to passage of fatigue load mode on Lane 2, as shown in Figure 3.3 can be obtained;
- the $\lambda_{1,1}$ factor and the $\lambda_{1,2}$ factor can be interpolated from Figure 3.2 for $N_1 = 1'500'000$ and $N_2 = 500'000$ depending on the influence length of the bridge;
- finally, the λ_4-factor can be calculated using Equation 3.4, and equals to 1.002.

It must be noted that in multi-lane traffics, for determining λ_1, the first lane (Lane 1) is the one for which the fatigue load model cause the largest stress range on the detail under consideration. The $\Delta\sigma(Q_{fat})$ is accordingly due to passage of fatigue load model on the first lane. Besides, in determination of λ_1 the truck traffic of the first lane should be considered instead of the whole truck traffic on bridges. In the current example, where $N_1 = 1'500'000$, and $L_\Phi = 20$ m, then λ_1 equals 1.39 from Figure 3.2 by interpolation.

When, for a particular case, all cycles due to the passage of the truck traffic are lower than the constant amplitude fatigue limit (CAFL), fatigue life is theoretically unlimited. Accordingly, the λ_{max}-factor is given to control the fatigue limit. Figure 3.4 illustrates the maximum damage equivalence factor for roadway bridges as given in the SIA263 [80], based on the Eurocode.

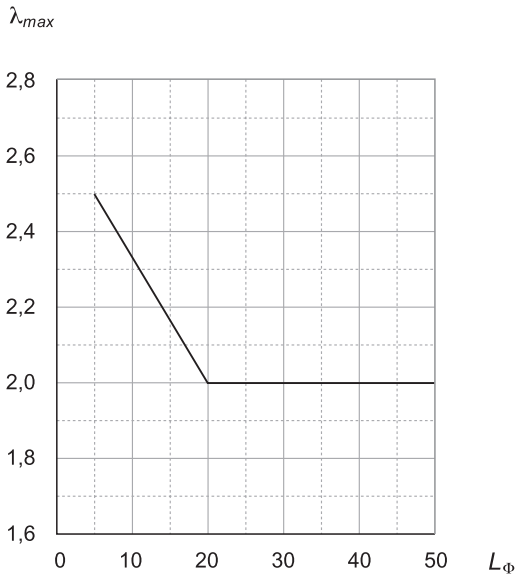

Figure 3.4: λ_{max} for roadway bridges based on SIA263 [80]

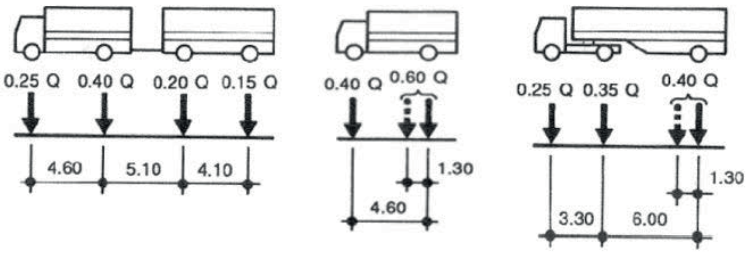

Figure 3.5: Three truck types applied in development of the SIA codes [44]

The damage equivalence factors given in the SIA263 [80], however, are accompanied with shortcomings. First, for determining λ_1, it is assumed that a continuous[3] traffic flow can be simplified and modelled with one-by-one passage of trucks on bridge. In other words, it is neglected to have more than one truck on bridges in the same lane. For multi-lane traffic, similarly, it is neglected to have several trucks on different lanes on bridges. Occurrence of several trucks simultaneously on bridges, either in the same lane or in the other lanes, cause a large cycle instead of two smaller cycles, and it results in higher damage equivalence factors and damage sum.

Moreover, the damage equivalence factors in the SIA263 [80] were developed by applying only three vehicle types passing over bridges one by one. Figure 3.5 shows schematically the three different truck types applied in development of the SIA codes. Although the weights distribution of each truck type is adapted with the real traffic measurements, the three truck types cannot represent the complication of real traffics on bridges.

To figure out the accuracy of the damage equivalence factors given in the SIA263 [80], same analysis is redone with the same assumptions applying the three truck types. The fatigue resistance curve of steel is considered with slope of 3 for cycles with stress range higher than constant amplitude fatigue limit (CAFL), and slope of 5 for cycles lower than CAFL; also, cycles lower than cut-off limit are dismissed. Damage equivalence factor for following bridge types and detail locations are calculated:

- simple span bridges, mid span moment (1SS-MM) and support reaction (1SS-SR),
- two-span continuous bridges, second support negative moment (2CS-2SM) and reaction (2CS-2SR),
- five-span continuous bridges, mid moment at third span (5CS-MM) and third support reaction (5CS-3SR).

Based on the aforementioned simplified assumptions, the damage equivalence factors are obtained for the bridges static systems with highway traffic, as shown in Figure 3.6, along

[3] Continuous traffic is denoted as opposite of one-by-one truck passage. In some references the term of following traffic is used as a synonym of continuous traffic.

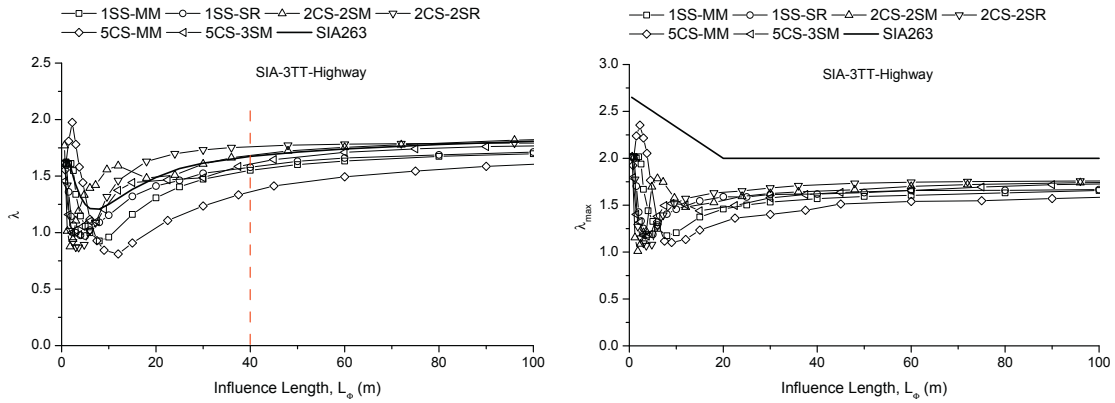

(a) λ (b) λ_{max}

Figure 3.6: Comparison of damage equivalence factors obtained from three truck types with SIA263 [80]

with the curve given in the SIA263 [80]. The same analysis is performed for the other traffic conditions and reported in Appendix A.1. According to the aforementioned assumptions, current damage equivalence factors are consistent with different bridge types and detail locations while its span is longer than 40 m. However, for the different bridge cases with spans length lower than 40 m results are scattered and it is inaccurate to assign same damage equivalence factor for all bridge types. The SIA λ-curve (Fig. 3.6a) follows the average of the values obtained for the different bridge cases for short L_Φ and is an upper bound for long L_Φ ; however, the code curve of λ_{max} is conservatively above the values obtained for the different bridge cases.

3.1.2 Eurocodes

The EN1991-2 [25] defines five load models for fatigue verification denoted FLM1 to FLM5. These models correspond, in principle, to various applications. Fatigue Load Model 1 (FLM1) derives from Load Model 1 (LM1) with only 70% of the characteristic values of axle loads and 30% of the characteristic values of uniformly distributed loads [13]. Fatigue Load Model 2 (FLM2) consists of a set of five lorries[4]. Both FLM1 and FLM2 were intended to be used to check whether the fatigue lifetime of steel bridges can be considered as unlimited by reference to S-N curves that have a constant amplitude fatigue limit.

The EN1993-2 [27] also applies the concept of damage equivalence factor for fatigue verification of road bridges, but with some differences comparing to the SIA263 [80]. The Fatigue Load Model 3 (FLM3), instead of Q_{fat} in the SIA codes, is intended for use with the damage

[4]Eurocode applies both words of lorry and heavy vehicle for the same meaning instead of trucks which is applied in the SIA261 [79]. The main difference between heavy vehicle (or lorry) and truck, as specified in the EN1991-2 [25], is that the gross vehicle weight of heavy vehicle is over 100 kN while the gross vehicle weight of trucks is over 35 kN. In Chapter 5, this issue is discussed thoroughly.

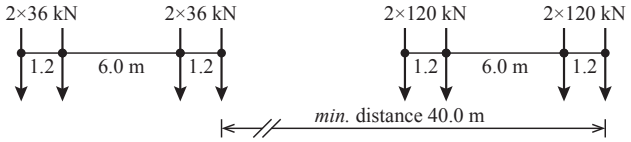

Figure 3.7: Geometry of the fatigue load model (FLM3) taken from the EN1991-2 [25]

equivalence factors in the EN1993-2 [27]. It consists of 4 axles, as shown in Figure 3.7, where the weight of each axle is 120 kN. For bridges with total length more than 40 m, a second set of axles in the same lane should be taken into account. The distance between axles of the second set is similar to the first set, whereas the weight of each axle is equal to 36 kN (instead of 120 kN). The minimum distance between two vehicles measured from centre to centre of vehicles is at least 40 m. Due to the differences between the fatigue load model of the Eurocode (FLM3) and the SIA code (Q_{fat}) the damage equivalence factors of the EN1993-2 [27] are not comparable to the ones in the SIA261 [79].

The basic idea for definition of Fatigue Load Model 3 (FLM3) was originally to select a fatigue *single vehicle* so that assuming a conventional number of crossings on a bridge by this vehicle (e.g. 2×10^6), and after a numerical adaptation with appropriate factors, it led to the same damage as the real traffic during the intended lifetime of the bridge [13].

Table 3.1: Set of equivalent lorries (FLM4) - Taken from the EN1991-2 [25]

Vehicle geometry			Traffic contribution (%)		
Lorry	Axle spacing (m)	Equivalent axle loads (kN)	Long dist.	Medium dis.	Local traffic
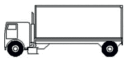	4.5	70 130	20.0	40.0	80.0
	4.2 1.3	70 120 120	5.0	10.0	5.0
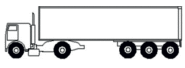	3.2 5.2 1.3 1.3	70 150 90 90 90	50.0	30.0	5.0
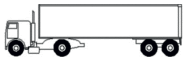	3.4 6.0 1.8	70 140 90 90	15.0	15.0	5.0
	4.8 3.6 4.4 1.3	70 130 90 80 80	10.0	5.0	5.0

Fatigue Load Models 4 and 5 are intended to be used for accurate verifications based on damage calculations using Miner's rule. FLM4 consists of a set of five lorries, as shown in Table 3.1, from which it is possible to simulate the traffic by adjusting the proportion of each one in the global traffic. FLM5 is based on the direct use of recorded traffic, and it is the most accurate and complicated approach.

The damage equivalence factor, λ, based on the EN1993-2 [27] which is in accordance with FLM3 can be obtained from:

$$\lambda = \lambda_1 \times \lambda_2 \times \lambda_3 \times \lambda_4, \quad however \lambda \leq \lambda max \tag{3.5}$$

where λ_1 is a partial factor for damage effect of traffic depending on critical length of influence line, λ_2 is a partial factor for modification of traffic volume, λ_3 is a partial factor for modification of the bridge design life, λ_4 is a partial factor which adds up the effect of traffic on the other lanes to the first lane, and λ_{max} is the maximum value of damage equivalence factor which takes into account the Constant Amplitude Fatigue Limit (CAFL).

In the EN1993-2 [27], the λ_1-factor is originally determined for different bridge types with span lengths ranging from 10 m to 80 m by applying the FLM3. The λ_1 is then separately represented for mid span and support sections as a function of the critical length as shown in Figure 3.8. The λ_1-factor includes dynamic load amplification, because the recorded axle loads from the Auxerre traffic already contain a dynamic impact from "good" surface quality.

It is important to mention that the critical span length is defined in the EN1993-2 [27] on a

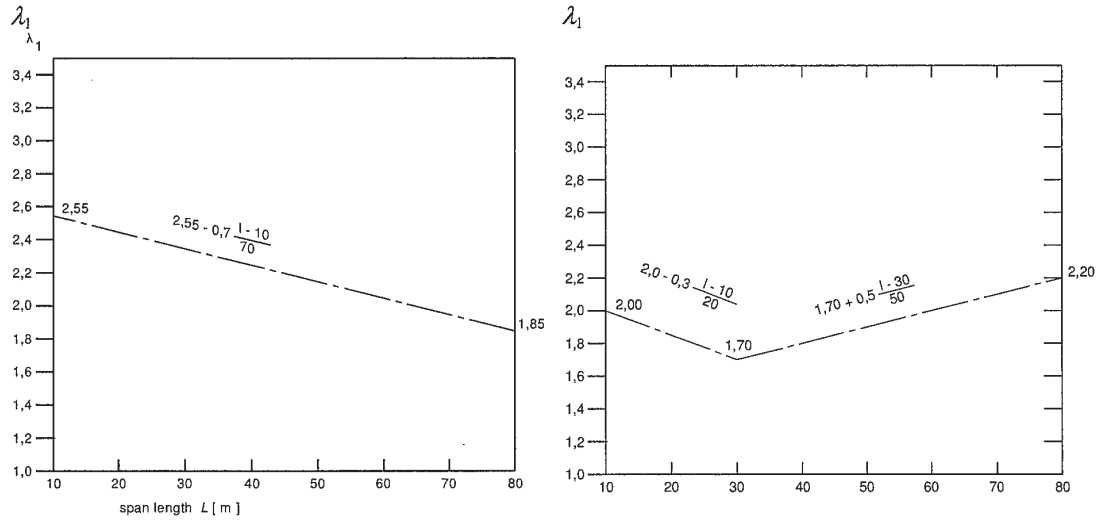

span length L [m] at midspan

span length L [m] at support

Figure 3.8: λ_1 for roadway bridges based on EN1993-2 [27]

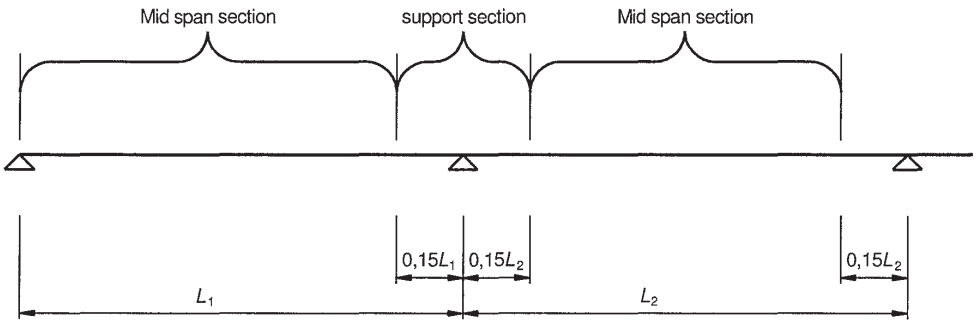

Figure 3.9: Eurocode definition for location of mid span and support section zones [27]

case-by-case basis; consequently, the critical span length is unknown for undefined cases. Some of the defined critical lengths are:

- for a single-span bridge, equal to span length,
- in support sections (as defined in Fig. 3.9) of a continuous-span bridge, the mean of the two spans adjacent to that support,
- for reaction of intermediate supports of a continuous-span bridge, the sum of two adjacent spans.

Whereas the λ_1-factor is given only for one traffic type (main road) in Eurocode, the factor λ_2 is given to adapt the traffic volume passing over a bridge, and it can be calculated as:

$$\lambda_2 = \frac{Q_{m1}}{Q_0} \times \left(\frac{N_{obs}}{N_0}\right)^{1/5} \tag{3.6}$$

where Q_{m1} is the average gross weight of the trucks in the slow lane with power of 5 as follows:

$$Q_{m1} = \left(\frac{\sum N_i \times Q_i^5}{\sum N_i}\right)^{1/5} \tag{3.7}$$

where N_{obs} is the annual number of heavy vehicles in slow lane, Q_0 and N_0 are the base values in determination of λ_1. In fact, the factor curve given for the partial factor λ_1 is representing a traffic with average gross weight $Q_0 = 480\ kN$ and annual truck traffic $N_0 = 500'000$.

Similar to the SIA263 [80], the partial factor λ_3 is also for modification of bridge design life. Unlike the SIA code, the basis bridge design life in the EN1993-2 [27] is 100 years, meaning the partial damage equivalence factor, λ_1, is determined for 100 years of traffic. For modification of service life the λ_3-factor can be applied as follows:

$$\lambda_3 = \left(\frac{t_{Ld}}{100}\right)^{(1/5)} \tag{3.8}$$

where t_{Ld} is the intended bridge design life.

Similar to the SIA263 [80], the multi-lane traffic effect can be calculated applying the factor λ_4. This factor adds up traffic volume of other lanes to the slow lane, as follows:

$$\lambda_4 = \left[1 + \frac{N_2}{N_1}\left(\frac{\eta_2 Q_{m2}}{\eta_1 Q_{m1}}\right)^5 + \frac{N_3}{N_1}\left(\frac{\eta_3 Q_{m3}}{\eta_1 Q_{m1}}\right)^5 + \ldots + \frac{N_k}{N_1}\left(\frac{\eta_k Q_{mk}}{\eta_1 Q_{m1}}\right)^5\right]^{(1/5)} \tag{3.9}$$

where k is the number of lanes with heavy vehicle traffic, N_j is the number of heavy vehicles per year in lane j, Q_{mj} is the average gross weight of heavy vehicles in lane j, and η_j is the value of the influence line for internal forces that produces the stress range in the middle of lane j and should be inserted with positive sign.

Although the λ_4-factor seems to be different from the one given in the SIA263 [80], its general concept is comparable. In Eurocode, the damage accumulation power is constant and equal to 5, but in the SIA263 [80] it can be 3 or 5. The ratio of $\Delta\sigma_j/\Delta\sigma_1$ of the SIA code can also be replaced by η_k/η_1. Indeed, the factor λ_4 in Eurocode adds the traffic volume of other lanes applying the N_j and Q_{mj} to the first lane, rather than calculating separate partial factors for each lane which is the case in the SIA code ($\lambda_{1,j}$). As a result, Eurocode λ_4 [27] allows calibrating the damage due to traffic volume of each additional lane by two parameters: average gross weight and annual heavy vehicle traffic. It must be noted that in multi-lane traffics, the factor η_k is always positive, because the negative stress ranges are assumed to cause the same damage as positive stress ranges.

When, for a particular case, all cycles due to the passage of the truck traffic are lower than the constant amplitude fatigue limit (CAFL), fatigue life is unlimited. Accordingly, the factor λ_{max} is given to make a check respect to the fatigue limit. Figure 3.10 illustrates the maximum damage equivalence factor for roadway bridges based on the EN1993-2 [27].

The damage equivalence factor based on the Eurocodes [25, 27] is also accompanying with some shortcomings, although it is developed by applying Auxerre WIM measurements [76]. First for determination of λ_1, it is assumed that a real continuous traffic flow can be simplified and modelled with one-by-one passage of trucks on bridge. In other word, it is neglected to have more that one truck on a bridge in the same lane. For multi-lane traffic it is similarly neglected to have several trucks on different lanes on bridge.

Since the Auxerre traffic applied in determination of the damage equivalence factors is not available, performing the same analysis for different bridge types is not possible. To still try to do such a comparison, in spite of differences in definition of the Fatigue Load Model 3 and Fatigue Load Model 4, the obtained results are compared here. To this end, first, the five lorries intended for Fatigue Load Model 4 (As shown in Table 3.1) are applied as the “artificial real traffic” load for determining damage equivalence factor. The five lorries of Fatigue Load Model 4 as well as Fatigue Load Model 3 include identic dynamic load amplification appropriate for pavements of good quality, hence it is not needed to consider any impact factor.

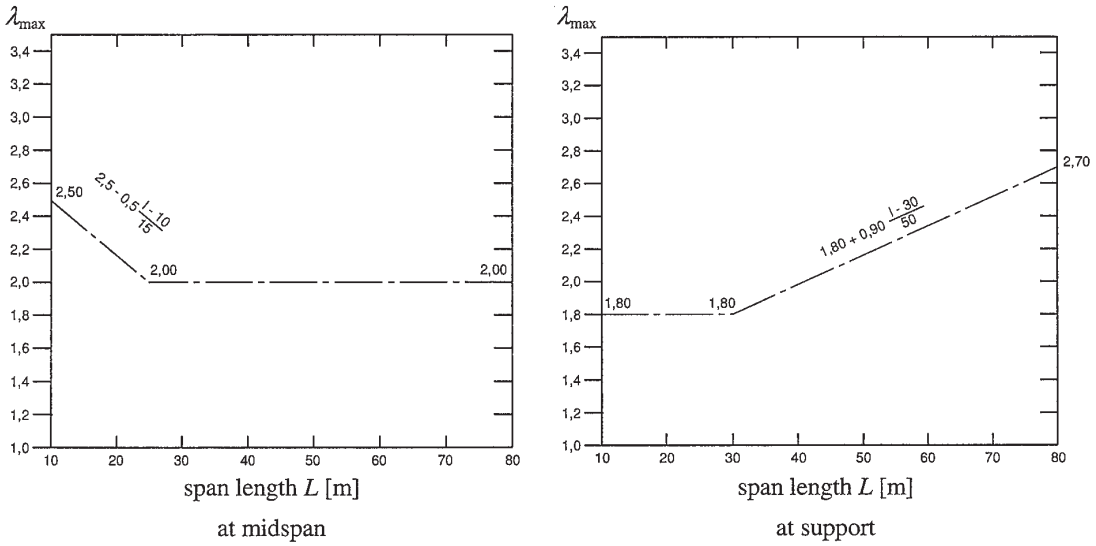

Figure 3.10: λ_{max} for roadway bridges based on EN1993-2 [27]

The fatigue resistance curve of steel under direct stress is considered, same as the EN1993-1-9 [26] with double slope (3 and 5) and cut-off limit. The analysis is performed for the same bridge cases, as the ones applied in the previous section.

Based on the aforementioned simplified assumptions, the damage equivalence factors are obtained for three traffic conditions at mid span and support sections. Figure 3.11 illustrates the λ-factors for long distance traffic in comparison with the EN1993-2 [27]. The results of the other traffic conditions are provided in Appendix A.2. Although the critical span length of damage equivalence factor in the EN1993-2 [27] is limited between 10 m and 80 m, it is broaden from 0 m to 100 m for comparison purpose. The obtained results are determined for $N_{obs} = 500'000$ and design life of 100 years, which are the base values intended for calculation of damage equivalence factor in the EN1993-2 [27]. Depending on the traffic type of FLM4, however, the average gross weight of heavy vehicles (Q_{m1}) is different, i.e. 445 kN, 407 and 317 for long distance, medium distance and local traffics respectively. Therefore, the damage equivalence factor, λ, is calculated as the multiplication of $\lambda 1$ and $\lambda 2$. In Figure 3.11, the value of Q_{m1} corresponding to each traffic is also printed. In Figure 3.11, the curves given in the EN1993-2 [27] do not follow the curves obtained for different bridge types at both mid span and support sections. For very short critical lengths, results are scattered, and for longer critical lengths, the decreasing λ value in the mid span zone is not observed in the simulations. Whereas FLM4 is considered as the "artificial real traffic", the inconsistency in Figure 3.11 indicates FLM3 and FLM4 are not coordinated; therefore, the bridges designed with FLM3 have a different safety margin compared to the bridges designed with FLM4. FLM4 tends to provide a more precise fatigue design by involving the damage accumulation procedure, though this procedure is more tedious. From Figure 3.11 it can be concluded that the FLM3 does not necessarily lead to a more conservative value, and in some cases, it underestimates the results.

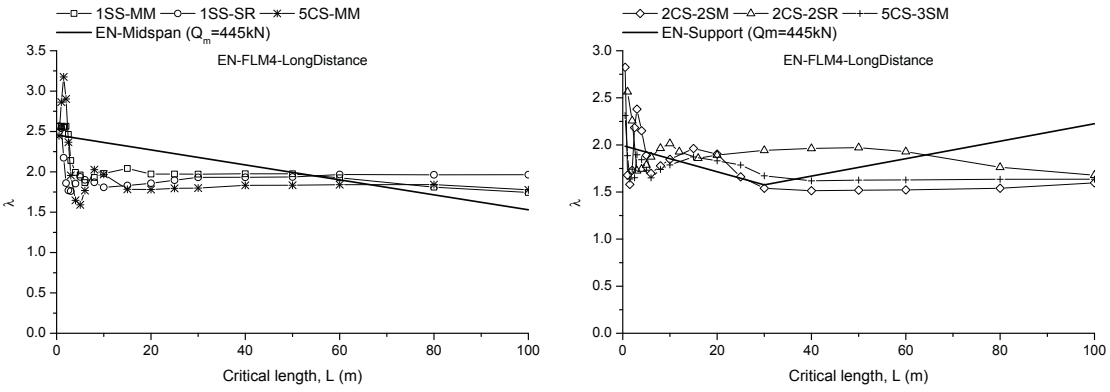

(a) At mid span (b) At support

Figure 3.11: Comparison of Eurocode damage equivalence factor with FLM4 for long distance traffic

3.2 Initial traffic simulations, hypotheses and scenarios

In order to evaluate the current damage equivalence factors of the codes, traffic simulations are executed with les simplified hypothesis as above. These traffic simulations are performed by WinQSIM program which was initially developed on Microsoft C# during the research project AGB2005/005 [59]. This program is adapted for the purpose of fatigue analysis in order to perform continuous flow of traffic and extract cycles from bridge responses. Further description on the WinQSIM program is provided in Appendix B.

Statistical parameters of actual traffic are based on Weigh-In-Motion (WIM) measurements of Mattstetten on the highway of Bern-Solothurn in 2003. Further studies in the next chapters are done using more recent WIM measurements. These statistical parameters include: proportion of different vehicle types in traffic, geometry of the vehicle types, gross vehicle weight distribution of the vehicle types, and correlation between the axle loads of the vehicle types. The program randomly chooses each vehicle properties from a database which is in accordance with the actual traffic. Such a simulation is able to model fluid traffic as well as congested traffic close to reality. Also, it allows having several trucks over bridges simultaneously. Detailed descriptions of the traffic simulation method applied here are provided in Appendix B.

The daily variation of truck traffic flow can be defined with different scenarios. In fact, the traffic flow depends on many parameters e.g. location, roadway type, annual traffic. In the initial traffic simulation, however, a simplified hypothesis for the daily variation of truck traffic flow is considered. Nevertheless, more accurate traffic simulations considering different traffic flows based on the measurements are performed in Chapter 6.

In the initial traffic simulation, the traffic is always fluid and trucks circulate on weekdays (255 days per year 2003). Figure 3.12 shows the weekday truck traffic distribution of Mattstetten in 2003 which is adapted to highway traffic with 2'000'000 trucks per year and per direction. Two

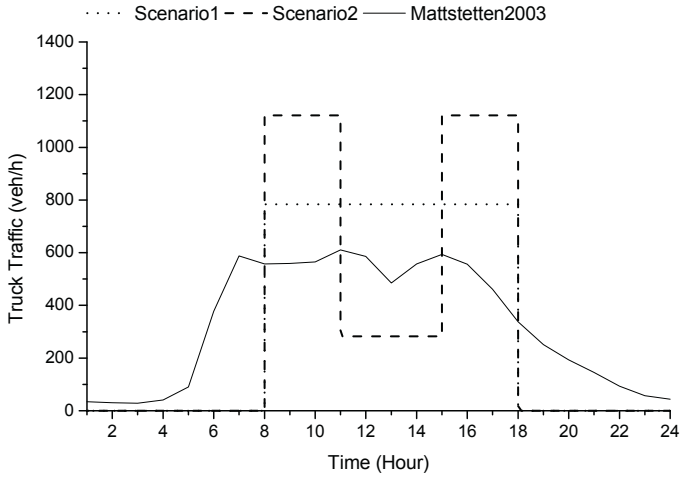

Figure 3.12: Weekday truck traffic distribution of Mattstetten (2003), adapted to 2×10^6 trucks/year/direction and two considered scenarios

unfavourable traffic scenarios compared to the real traffic distribution are considered for the initial traffic simulations as shown in Figure 3.12: 1) flat distribution of traffic over 10 hours of each day, and 2) two traffic peaks of 3 hours per day. All add up to daily truck traffic of 7843 trucks per direction.

A program (FDABridge) is also developed to calculate damage summation using Miner linear damage sum rule as well as damage equivalence factor by applying the code defined fatigue load model and S-N curve parameters. Specification of FDABridge program is given in Appendix B. Whereas the simulation of traffic is done with the Monte-Carlo method that has a time-consuming process to run, performing the simulations for the whole design life is hardly feasible. Thus, it is needed to find an efficient period of simulations that ensures a stable result. To this end, the traffic simulations are performed for 1 year and 10 years, then the number of cycles is increased by a factor to achieve a response spectrum for 70 years (fatigue design life based on the SIA261 [79]). The number of simulated trucks is 2'000'000 per year per direction, which corresponds to highway traffic.

The traffic simulations for the following bridge types and detail locations are executed:

- simple-span bridges, mid moment (1SS-MM);
- two-span continuous bridges with equal spans length, second support negative moment (2CS-2SM), second support reaction (2CS-2SR), mid span moment of first span (2CS-1MM), and moment at 4/5 of first span length (2CS-0.8LM);
- three-span continuous bridges with equal spans length, second span mid moment (3CS-MM), second support moment (3CS-2SM), first and second supports reaction (3CS-1SR and 3CS-2SR).

The bridges span length ranges from 1 m to 80 m. In addition, the fatigue resistance curve of steel under direct stress is considered, as defined in the EN1993-1-9 [26] (the same as the SIA263 [80]). In addition, in the traffic simulations, a simple dynamic amplification factor 1.2 is applied to all simulated vehicles, for all bridge types and lengths. More accurate analyses are performed using a dynamic amplification factor depending on total traffic load on the bridge for the final traffic simulations as described in Chapter 6.

3.3 Evaluation of the SIA Codes

3.3.1 Single lane traffic

For the first comparison of different traffic scenarios, the traffic simulations are performed for mid moment of simple-span bridges and second support moment of two-span continuous bridges. Figure 3.13 shows the comparison of damage equivalence factors, λ, resulting from two described scenarios (S1 and S2) as well as for 1 year and 10 years (1Y and 10Y) of traffic simulation (in both cases the cycles are multiplied to get the service life of 70 years). In order to compare the continuous traffic flow with one-by-one flow, the traffic simulations are also done with prevention of having more than one truck over bridge (VbV). In Figure 3.13, the damage equivalence factors obtained from three truck types (3TT), which are originally applied in development of the SIA263 [80] code as well as the curve of the code are also printed.

Figure 3.13 shows that there are slight differences between the damage equivalence factors obtained for Scenario 1 and Scenario 2. However, it clears up that the effect of continuous traffic on bridge is indispensable. Since the damage equivalence factors resulting from simulation of traffic for 1 year and 10 years were similar, the 1 year traffic simulation is reliable and consistent. In the case of second support moment of two-span continuous bridges, as shown in Figure 3.13b, the curve of the λ-factor obtained from continuous traffic simulations (S1 and S2) overtakes the curve of the code at influence lengths of about 40 m, indicating the

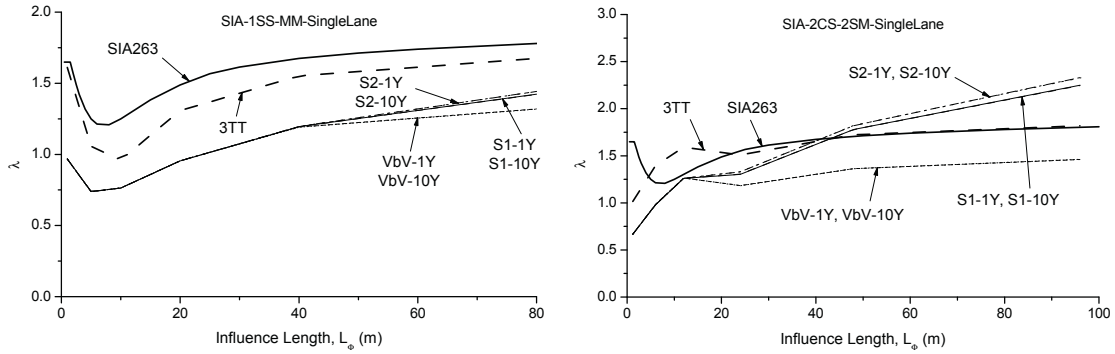

(a) Mid moment of simple-span bridges

(b) Second support moment of two-span continuous bridges

Figure 3.13: λ for different single lane scenarios in comparison with SIA263 [80]

Table 3.2: Swiss WIM measurements in 2005

Station	Annual Average Daily Traffic (AADT)	Average Daily Truck Traffic (ADTT)	Annul proportion of truck in traffic (%)
Mattstetten	73637	6671	9.1
Götthard	16069	2944	18.3
Plazzas	14768	1065	7.2
Denges	80591	3210	4.0
Trübbach	30985	2210	7.1
Ceneri	37179	4141	11.1
Oberbüren	48489	3831	7.9

code may give an underestimating value for some bridges in the case of continuous traffic.

For existing bridges, the safety of fatigue details near support areas might be lower than expectations if the fatigue verifications are performed with the current code. However, the heaviest traffic according to the SIA261 [79] is studied here. A sample of Swiss daily traffic flows measured in WIM stations is given in Table 3.2. In Mattstetten, the busiest highway, the average daily truck traffic per direction is 6671 / 2 = 3335 (trucks per day) in 2005. The simulated traffic is 7843 × 255/365 = 5480 (trucks per day), which is much higher than the average daily truck traffic of Mattstetten (per direction) and therefore anywhere in Switzerland.

The maximum damage equivalence factors, λ_{max}, resulting from two described scenarios (S1 and S2) for 1 year and 10 years (1Y and 10Y) of traffic simulation are also illustrated in Figure 3.14. Similar to the λ-factors, the traffic simulations are also performed once by preventing having more than one truck over bridge (VbV). In Figure 3.14, the λ_{max}-factors obtained for three truck types (3TT) as well as the curve of the code are also printed. Figure 3.14 represents that there are slight differences between the damage equivalence factors obtained for Scenario 1 and Scenario 2; however, it clears up that effect of continuous traffic on the λ_{max}-factors is also important. In the case of second support moment of two-span continuous bridge as shown in Figure 3.14b, the curve of λ_{max} obtained from continuous traffic simulations

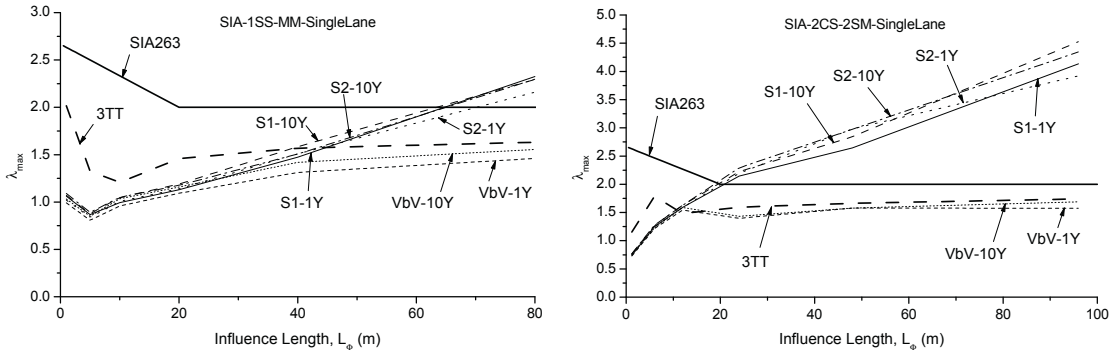

(a) Simple-span bridge - mid moment

(b) two-span continuous bridge - second support moment

Figure 3.14: λ_{max} for different dingle lane scenarios in comparison with SIA263 [80]

(S1 and S2) passes the code curve at the influence lengths about 20 m, and by increasing the length their difference increases, which means that the λ_{max} based on the SIA263 [80] may be unsafe for some bridges, specially, with long spans.

The λ_{max}-factors obtained for 10 years are slightly larger than 1 years of traffic simulations, in Figure 3.14. It can be explained by the fact that the maximum cycle due to 10 years traffic simulation is greater than the 1 year (since the traffic simulations are performed by Monte-Carlo process). It is important to note that FDABridge program calculates the λ_{max}-factor assuming all cycles remained below CAFL. However, a few cycles, as few as 0.01 percent during the life of structures, might be allowed to stand above CAFL. Such a tolerance in determining λ_{max} allows overlooking the differences in λ_{max} obtained for 10 years and 1 year simulations. Nevertheless, this subject is dealt with in more detail in Chapter 4.

Further analyses are done for different bridges types and detail locations. Due to the fact that Scenario 2 is the worst case, all results are presented for Scenario 2 with 10 years traffic simulations, as shown in Figure 3.15. It must be mentioned that L_Φ is equal to decisive length to determine dynamic factor which is equal to 1.2 times of span length for two-span continuous bridges and 1.3 times of span length for three-span continuous bridges. In Figure 3.15, in order to show the results of traffic simulation for the three-span continuous bridges, the maximum illustrated L_Φ is extended to 110 m. The resulting λ and λ_{max} are widespread for different bridges types and detail locations; the code gives in some cases an underestimating value. Indeed, the safety margin of the code damage equivalence factor depends on span length, bridge type and detail location, which is not desirable.

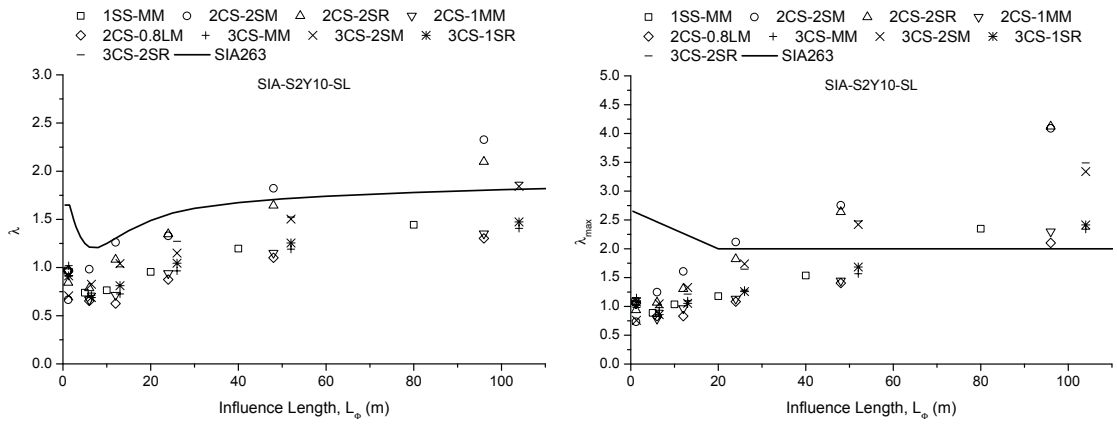

(a) λ (b) λ_{max}

Figure 3.15: λ and λ_{max} for different bridge cases in comparison with SIA263 [80]

3.3.2 Double lane traffic

In order to determine the effect of multi-lane traffic on damage equivalence factors, the same bridge types and detail locations are used. In the initial traffic simulations, the multi-lane bridges are limited to two cases: a bidirectional and a unidirectional traffic condition. In the case of bidirectional, the repartition of traffic by direction is 50-50 percent, considering the same amount of trucks in each direction. For second double lane traffic condition, unidirectional, the repartition of truck traffic in each lane is 80-20 percent. For both traffic conditions the total number of trucks in both lanes is 2'000'000 per year. Whereas the traffic simulations are performed by the Monte-Carlo method, simulations of traffic are performed for 1 year and 10 years, which demonstrates the stability of the results for double lane traffic.

The main objective of the double lane traffic simulations is to know the influence of the trucks crossing or overtaking on damage equivalence factors. The transverse distribution of the loads has an important effect in the multi-lane traffic studies. In the case of a box section, the most unfavourable one, there is not any transverse distribution and the box section can uniformly be charged when either of the lanes loaded. Similarly, considering a box section permits neglecting the lateral position of the axles in each lanes and lateral distance between the vehicles wheels. This assumption also allows us neglect the dimension of section. Nevertheless, the effect of different cross sections on damage equivalence factors is studied in Chapter 6.

Initially, the simulations are performed for mid moment of simple-span bridges and second support moment of two-span continuous bridges in order to compare different traffic scenarios. The damage equivalence factor values obtained for the box section (with the maximum effect of second lane) are illustrated in Figure 3.16 for bidirectional (BD) and unidirectional (UD) as well as single lane traffics (SL). Only the results of traffic simulations for 10 years are

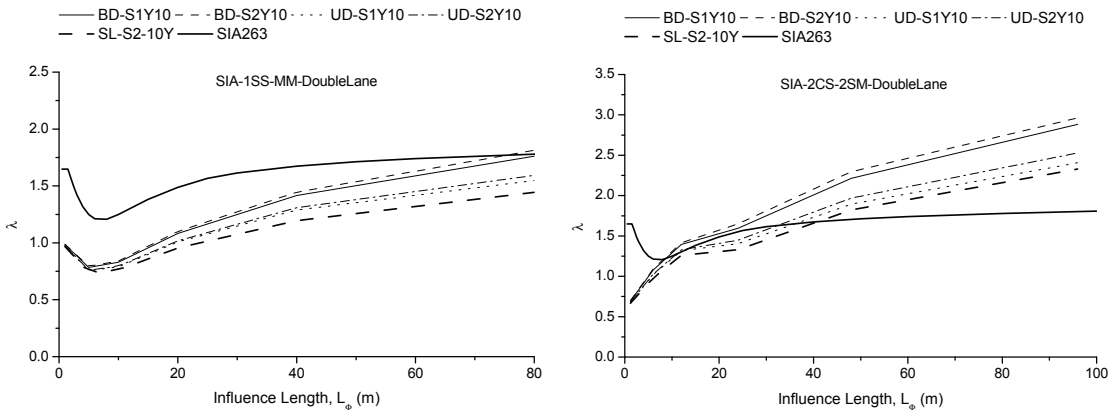

(a) Mid moment of simple-span bridges

(b) Second support moment of two-span continuous bridges

Figure 3.16: λ, for different double lane scenarios in comparison with SIA263 [80]

printed here to prevent illegibility, though the 1 year traffic simulations bears the same results. Figure 3.16 shows the effect of having two truck traffic lanes comparing with one lane is rather significant. It is worthy of note that the total traffic volume for the three curves (single lane, unidirectional and bidirectional traffic) is equal. From Figure 3.16, it can concluded that the probability of simultaneity of several trucks on bridge (crossing or overtaking) exists, this effect also increases with span length. In addition, the curve obtained for the bidirectional traffic stands above the unidirectional traffic because the probability of having several trucks on the bridge is logically higher in the 50-50 percent traffic repartition.

A slight difference between the two scenarios of traffic simulations in Figure 3.16 is also observed; Scenario 2 leads to the higher damage equivalence factors. It can be explained by the fact that the Scenario 2 with two traffic picks causes more crossing or overtaking on bridges. It is important to explain that when two trucks are crossing or overtaking on bridge, e.g. a long simple-span bridge, instead of two independent cycles due to passage of each truck, one in the first lane and another in the second lane, one cycle larger than the two independent cycles occurs. Due to the negative slope of fatigue resistance curve in the logarithmic scale, m equals to 3 or 5 for steel details, the damage increases by $2^5 = 32$ assuming the stress range doubles; however, if the number of cycles doubles, the damage follows linearly and doubles. Accordingly, the increase of damage equivalence factors is considerable for double lane traffic conditions and it should be taken into account.

The maximum damage equivalence factor, λ_{max}, is also represented in Figure 3.17 for bidirectional (BD) and unidirectional (UD) as well as single lane (SL) traffics. Figure 3.17 shows the effect of having several trucks in double lane traffic condition is also important in λ_{max}. Generally, a larger stress range may occur when two or several trucks pass on a bridge. Therefore, the maximum damage equivalence factor, which correspond to the maximum cycle, raises considerably in the case of double lane traffic. As shown in Figure 3.17, the λ_{max}-factor

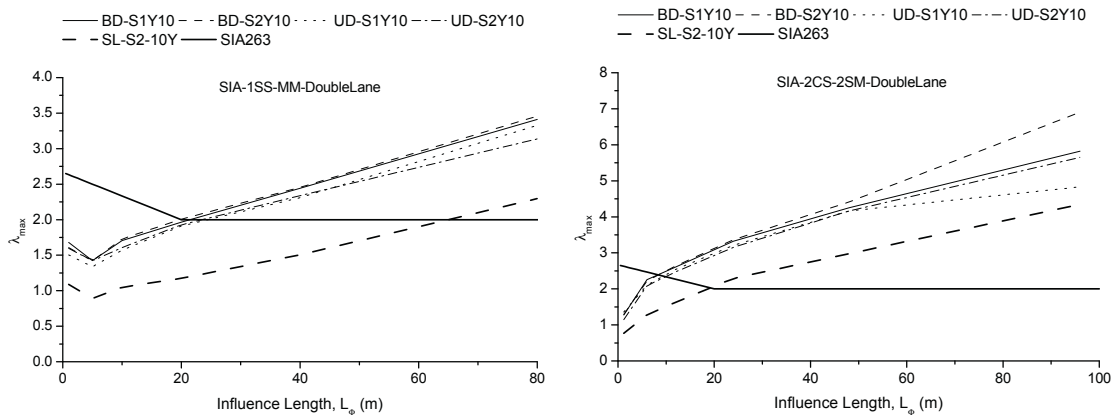

(a) Simple-span bridge - mid moment

(b) two-span continuous bridge - second support moment

Figure 3.17: λ_{max} for different double lane scenarios in comparison with SIA263 [80]

obtained for bidirectional traffic case is rather higher than unidirectional traffic because the probability of standing two heavy trucks side by side on a bridge in the case of 50-50 percent distribution is higher than 80-20 percent. In addition, it can be observed λ_{max} resulting from the Scenario 2 is slightly higher than Scenario 1, indicating the probability of simultaneity is higher in the case of Scenario 2 with two traffic peaks.

In addition, it is important to recall that λ_{max} is calculated assuming all cycles remain below CAFL. However, a tolerance of a few cycles above CAFL in determining λ_{max} may change the results for double lane traffic. This subject is discussed in more detail in Chapter 4.

The λ_4-factor for each bridge static system based on the SIA263 [80] hypothesis is calculated and illustrated in Figure 3.18 for unidirectional and bidirectional traffic. Whereas the traffic on first lane (slow lane) is less than single lane traffic (80% for unidirectional and 50% for bidirectional), the λ_2-factor (as given in the EN1993-2 [27]) is applied to modify the volume of traffic on the first lane. In Figure 3.18, the factor λ_4 obtained from Equation 3.4 is also presented. The λ_4-factor obtained for unidirectional traffic as well as bidirectional traffic is rather larger than the λ_4-factor given in the SIA263 [80] because the probability of multiple presences of trucks on a bridge exists. For both bidirectional and unidirectional traffic, this effect should be considered and it is more significant than the traffic volume, solely, on the second lane.

Herein, a uniform lateral load distribution, which is only true for a box section, was assumed. The effect of multi-lane presence of trucks on damage equivalence factors might be lower in the case of I-girder bridges where the lateral load distribution in not uniform. For such a cases, the λ and λ_{max} curves will be between the curves given for single lane and double lane traffics.

In addition, in the case of the bidirectional traffic, the annual truck traffic taken as 1'000'000 per direction, while the bridges designed for a bidirectional traffic has typically the main road traffic volume. On such roads there are theoretically 500'000 trucks per direction (base on the

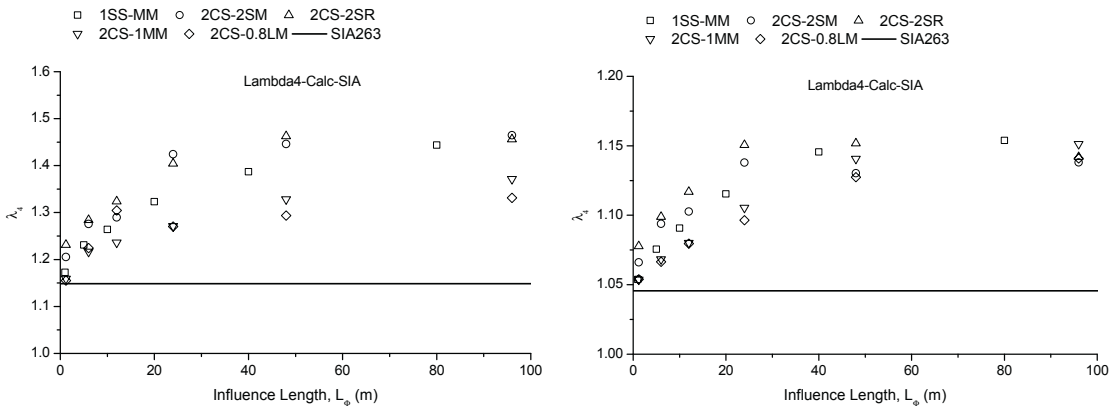

(a) Bidirectional traffic 50-50 percent

(b) Unidirectional traffic 20-80 percent

Figure 3.18: λ_4 for different bridge cases in comparison with SIA263 [80]

SIA261 [79]), resulting in lower probability of multiple presences of trucks and lower equivalent stress range. Nevertheless, such a traffic flow conditions may occur on highly loaded roadways, and the design codes should consider the probability of simultaneous presence of trucks for condition of multi-lane traffic.

3.4 Evaluation of the Eurocodes

3.4.1 Single lane traffic

The same analysis is done to evaluate the Eurocode damage equivalence factors by applying the Fatigue Load Model 3 (FLM3) and the critical span length. Whereas the results for damage equivalence factors for the SIA code are discussed in Section 3.3, here the results are only described briefly, as the main conclusions are the same for both codes. Since Scenario 2 with 10 years traffic simulation bears slightly more conservative results, thus the analysis is done only with this hypothesis (S2-10Y).

Figure 3.19 illustrates the damage equivalence factor, λ, obtained from the simulations comparing with the EN1993-2 [27]. The critical span length in determination of λ_1 in the code ranges from 10 m to 80 m; however in Figure 3.19 for comparison purpose, the critical span length starts from 0, where the corresponding values of λ_1 are extrapolated.

The average gross weight of trucks, Q_m, at the station of Mattstetten (2003) which is applied for the traffic simulations is 255 kN, and the simulated annual truck traffic is 2'000'000; therefore, the partial damage equivalence factor, λ_2, is used to adapt the Eurocode λ-factor. Also, because the response spectrum of 70 years of traffic is used for determining the λ-factors, the partial damage equivalence factor, $\lambda_3 = (70/100)^{1/5}$ is multiplied to the code curve, though the original λ_1 is also plotted. Figure 3.19 shows that the damage equivalence factors for

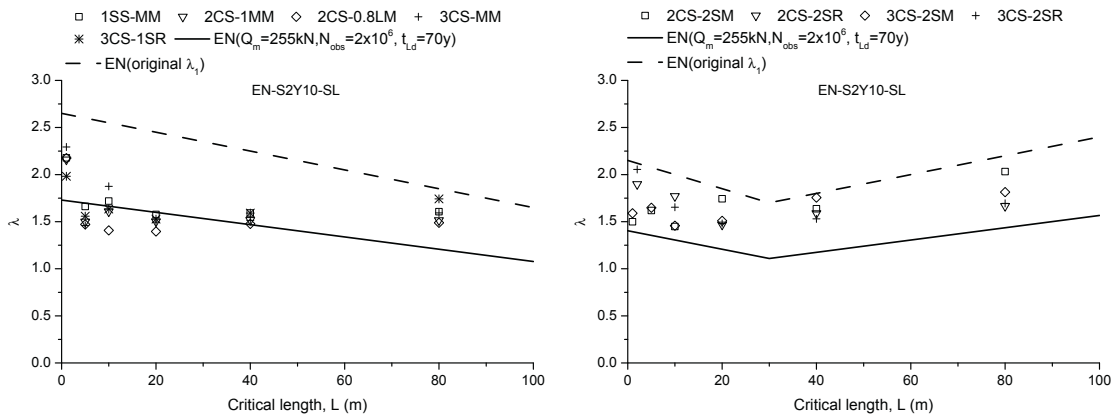

(a) Mid span section (b) Support section

Figure 3.19: λ for different bridge cases in comparison with EN1993-2 [27]

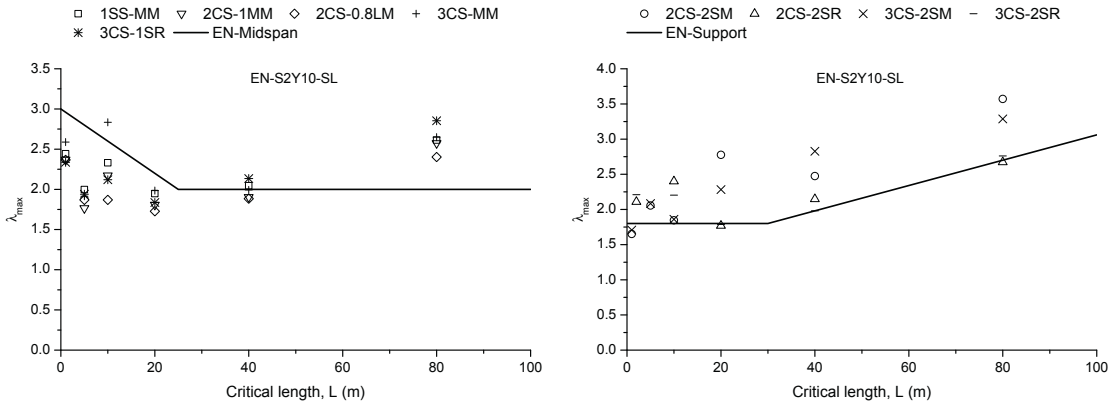

(a) Mid span section (b) Support section

Figure 3.20: λ_{max} for different bridge cases in comparison with EN1993-2 [27]

most bridge cases are above the Eurocode curve (the one adapted with λ_2 and λ_3 for the corresponding traffic), although all values are below the original λ_1.

The traffic volume of different stations in Switzerland in 2005 is presented in Table 3.2. The stations are all located in the highway. The corresponding N_{obs} value in the code is 2'000'000 which is absolutely higher than the measured daily traffic in Switzerland. Moreover, the average gross weight of trucks in Switzerland ranges between 240 and 305 which is much lower than the base average gross weight given in the EN1993-2 [27] with Q_m = 480 kN. However, with λ_2, included in the presented simulations, results to take into account different traffic volume in the EN1993-2 [27], one sees that it may lead to non-conservative design.

The maximum damage equivalence factor, λ_{max}, is also presented in Figure 3.20 for different bridge types and detail locations. The λ_{max}-factor based on the code is also printed in Figure 3.20 for both mid span and support sections. The curves obtained from simulations, especially at support sections, are above the Eurocode curve, indicating the Eurocode might be non-conservative.

The Eurocode definition for critical length as well as fatigue load model, in spite of its complexity in comparison with the SIA code definition, still leads to rather scattered λ and λ_{max} for the different bridge cases, which means that safety margine is not uniform for different bridge cases.

3.4.2 Double lane traffic

The multi-lane traffic conditions are like the ones applied for Section 3.3.2: the bidirectional with 50%-50% of total traffic in each direction (BD5050), and the unidirectional traffic with 80% of total traffic in slow lane and the rest in fast lane (UD 80%-20%). In both traffic conditions the annual number of trucks taken as 2'000'000.

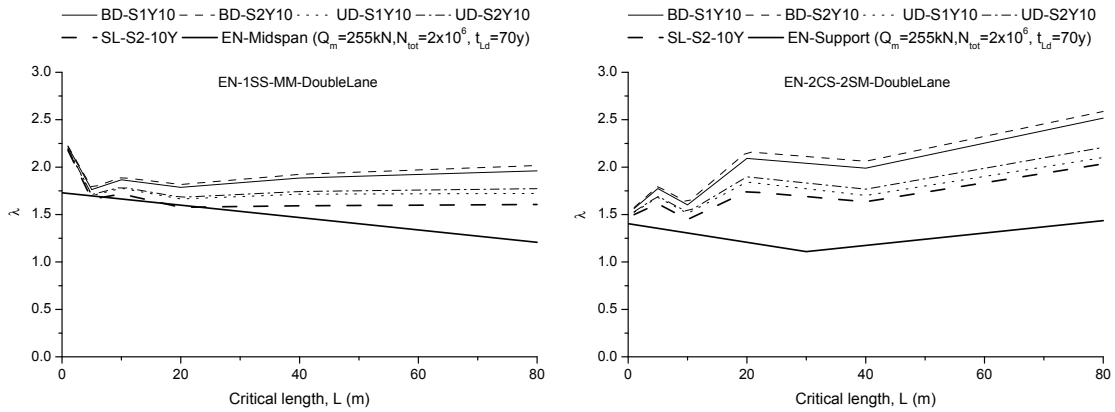

(a) Mid moment of simple-span bridges

(b) Second support moment of two-span continuous bridges

Figure 3.21: λ for different single lane scenarios in comparison with EN1993-2 [27]

The damage equivalence factor obtained for the box section is illustrated in Figure 3.21 for bidirectional (BD) and unidirectional (UD) as well as single lane traffics (SL), along with the λ-factor given in the EN1993-2 [27]. For mid moment of simple-span bridges (Fig. 3.21a), the Eurocode curve is rather close to the single lane traffic curve, considering the code critical length originally ranges from 10 m to 80 m; however, it is lower than curve obtained from double lane traffics, especially, bidirectional traffic. For second support moment of two-span continuous bridges (Fig. 3.21b), the differences between the code curve and the double lane curves are even greater than single lane traffic curve.

The maximum damage equivalence factors, λ_{max}, obtained for bidirectional (BD) and unidirectional (UD) as well as single lane traffics (SL), are presented in Figure 3.22. The λ_{max}

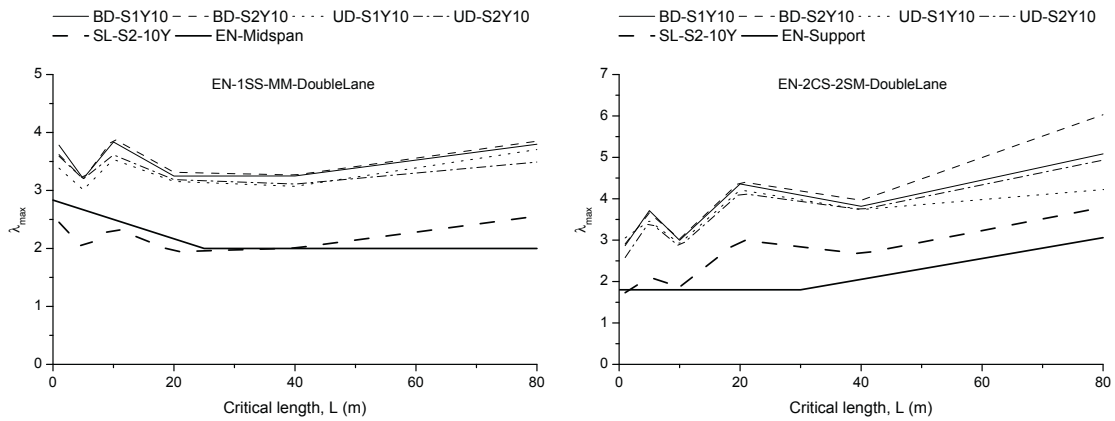

(a) Mid moment of simple-span bridges

(b) Second support moment of two-span continuous bridges

Figure 3.22: λ_{max} for different double lane scenarios in comparison with EN1993-2 [27]

obtained for bidirectional traffic as well as unidirectional traffic are obviously above the curve of single lane traffic and the Eurocode λ_{max} curves, indicating the Eurocode maximum damage equivalence factor might underestimate the effect of double lane traffic due to simultaneous presence of trucks.

However, it must be noted that the analysis is performed for the box cross-section which has the most critical condition for the crossing and overtaking effect. Also, the traffic of highways used for simulations while the bridges with lower traffic unlikely suffer the simultaneity effect.

3.5 Summary

In this chapter, the fatigue design rules for fatigue verification of roadway bridges based on the SIA codes and the Eurocodes are firstly explained. The concept of damage equivalence factors and the different elements involving in their determination are also described.

In the SIA codes [79, 80], the influence length is not univocally defined, where it can be equal to the decisive lengths to determine dynamic factors or the maximum distance between the null points of influence lines. In the EN1993-2 [27], also, the critical span length is defined on a case-by-case basis, consequently the critical span length is unknown for undefined cases. Both Eurocode and SIA code neglect the effect of having several trucks on bridge on both λ_1 and λ_{max}. It is the partial damage equivalence factor, λ_4, which is intended for considering the effects of multi-lane traffics on bridges. Based on the EN1993-2 [27] and the SIA263 [80], λ_4 adds up the damages due to traffic volume of other lanes with the first lane, but it neglects the effect of trucks crossing or overtaking on bridges.

By comparison of the fatigue equivalence factors obtained from the three trucks traffic (that is the traffic used for the development of the SIA code) with the curve of the SIA263 [80], it is found that firstly, there is a rather larger scatter in the obtained results for the bridges with the influence lengths lower than 40 m; secondly, the SIA curve follows the average of the values obtained for the different bridge cases.

The damage equivalence factors based on the Eurocode hypothesis are determined by assuming the fatigue load model 4 (FLM4) as an input traffic. The inconsistency between results is found, indicating the designing based on FLM3 and FLM4 would not provide the same safety level. Also, FLM3 does not always lead to a more conservative value than FLM4, as it is generally expected.

In order to evaluate the damage equivalence factors based on the SIA codes and Eurocodes, a series of so-called “initial traffic simulations” are performed. Two unfavourable scenarios for hourly truck traffic distribution are considered. The traffic simulations are done once for 1 year traffic simulations and once for 10 years in order to determine the stability of Monte-Carlo simulations. Also several bridge types and detail locations are considered for simulations.

The damage equivalence factors obtained from initial traffic simulations were compared with

the SIA codes [79, 80]. In the single lane traffic simulations, the λ-factors obtained for the continuous traffic flow are obviously larger than the one-by-one traffic flow, which justifies recommending to account for the effect of simultaneous occurrence of trucks on bridge. There is a slight difference between the damage equivalence factors that resulted from 1 year and 10 years traffic simulations. Therefore, it can be concluded that 1 year Monte-Carlo traffic simulations provides enough samples that ensure accurate results. Also, in some cases, e.g. mid support moment of two-span continuous bridges, the λ-factor resulting from simulation stands above the SIA λ-factor. Consequently, the SIA code might underestimate the damage equivalence factors in some cases, especially for long-span bridges. Although, it must be noted that the most critical traffic condition (highway) is concerned.

Similar to the λ-factors, the effect of continuous traffic flow on λ_{max} is also tangible, and this effect takes an importance with increasing span length. Generally, the damage equivalence factors, λ as well as λ_{max}, obtained for different bridge types and detail location are widespread, and differences between the curves obtained for the different cases is such large that one curve cannot apply to all of them. The double lane traffic simulations are executed for the same bridge types and detail location, in order to investigate the effect of crossing or overtaking on damage equivalence factors. To this end, two double lane traffic conditions are applied: bidirectional and unidirectional. From the results obtained for double lane traffic simulations, it can be deduced that the probability of crossing and overtaking on bridges exists, and its effect should be taken into account in both λ and λ_{max}, in particular, for bridges with box section. Also, the damage equivalence factors, λ as well as λ_{max}, corresponding to bidirectional traffic bears slightly greater values. However, the SIA λ_4 disregards the effect of crossing and overtaking.

In addition, the results of the same simulations are applied for determining damage equivalence factors based on the Eurocode Fatigue Load Model 3 (FLM3) and critical span length. In general, the FLM3 and λ_1 of Eurocodes provides a wider range of safety for fatigue design of bridges through defining larger average gross weight of truck (Q_m). However, for a given traffic volume (in terms of Q_m and N_{obs}) the λ_2-factor can be applied which may result in unsafe design. The λ_{max}-factor resulting from simulations are also higher than the Eurocode curves for long-span bridges, especially in the case of support sections. Both λ and λ_{max} curves obtained for different bridge types and detail locations are widely scattered.

The following main points are extracted from the background explanations of the damage equivalence factors and the results of the initial traffic simulations described in this chapter:

- the concept of damage equivalence factors provides a simplify method for fatigue verification of bridges by preventing the tedious procedure of damage accumulation calculations (with, as prerequisite, definition of traffic model),
- the definition of “fatigue equivalent length”, based on both Eurocode and SIA code, is so limited that hardly takes in all bridge static systems and detail locations,

- Monte-carlo traffic simulations show stability and one year can be used for the determination of damage equivalence factors,
- the hourly traffic distribution scenarios may have some effects on damage equivalence factors, but a realistic scenario is sufficient for the further traffic simulations,
- the effect of having several trucks on bridges either in the same lane or in several lanes is important and it should be taken into account,
- both Eurocodes and SIA codes neglect the effect of simultaneity (in the same lane or in the other lane) which might result in underestimation of λ as well as λ_{max}, especially for long-span bridges with high traffic volume,
- the damage equivalence factors, λ and λ_{max}, obtained for different bridge influence lines, based on both Eurocodes and SIA codes hypothesis, are widespread, thus attributing one value to all influence lines is not an acceptable approximation.

4 Proposal to improve fatigue equivalence factors

In the current chapter, first the main causes of shortcomings in damage equivalence factors are described; then the possibilities to improve these shortcomings are explained. In order to investigate effect of different characteristics of influence lines, some imaginary bridge influence lines are defined. Then equivalent stress range for each case is analysed. Accordingly, new definitions for fatigue load model and equivalent length are proposed, which can properly represent damage equivalence factors for different bridge types and detail locations. In addition, for double lane traffic conditions, some modifications to damage equivalence factors are proposed which improve their accuracy by taking into account the effect of crossings and overtakings. The maximum damage equivalence factor, λ_{max}, is also investigated in this chapter with respect to the exceedance rate above CAFL (allowing a few cycles above it) for single lane and double lane traffic. Recall that the damage equivalence factor can be obtained as follows [27]:

$$\lambda = \lambda_1 \times \lambda_2 \times \lambda_3 \times \lambda_4, \quad however \lambda \leq \lambda_{max} \tag{4.1}$$

For the purpose of generalizing the propositions given for damage equivalence factors, the fatigue damage of rebars in bridge decks is studied here. As a result, a method is proposed in which fatigue equivalent length is obtained from 3D influence surfaces. In addition, an equation for determining damage equivalence factors for the cases where lateral position of axles might have a large effect is given.

4.1 Main shortcomings in damage equivalence factors

The damage equivalence factors based on the SIA codes [79, 80] and the Eurocodes [25, 27] are accompanying with some shortcomings. As described in Chapter 3, they can be summarized as follows:

- the definition of *fatigue equivalent length*[1] is non-exhaustive, and defined case by case
- the effect of simultaneity in which several trucks stand on a bridge simultaneously either in the same lane or in several lanes is neglected,
- λ and λ_{max} obtained for different bridge influence lines are widespread,
- the safety margin for some bridge cases are over-conservative and for some cases are non-conservative.

Some of these shortcomings are of secondly importance, and can be addressed by some minor modifications. For example, one shortcoming is that the effect of trucks following each other in the same lane on damage equivalence factors is neglected. This problem could be addressed, for instance, by modifying the λ_1 curves using results from more accurate traffic simulations. However, such solutions are not able to properly compensate the principal shortcomings, for example, the dispersion of the curves obtained for different bridges types and detail locations, or non-comprehensive definition of the fatigue equivalent length.

Current study aims to find a solution that firstly respects the main concept of damage equivalence factors, and in the same time, improves the principal shortcomings. Referring the main variables involved at the concept of damage equivalence factors, the modifications are limited to two variables which are fatigue load model and fatigue equivalent length.

The role of the fatigue load model is to calibrate the damage equivalence factors based on the main cycle obtained from the passage of a predefined vehicle on a bridge. The damage equivalence factor equal the equivalent force range (moment, shear or reaction) at two million cycles divided by the force range due to the passage of fatigue load model. However, the force range due to fatigue load model depends on the geometry and the axles weight of fatigue load model. In order to analyse the effect of traffic actions on different bridge types with different lengths, first the equivalent force range is concentrated. To this end, the damage equivalence factors obtained from the single lane traffic simulations in Chapter 3 are multiplied by the corresponding forces due to the fatigue load model. Figure 4.1 shows separately the equivalent moment range and equivalent reaction range separately. The bridge types and detail locations as well as other traffic simulations hypothesis are described in Section 3.2.

In Figure 4.1, equivalent force ranges are increasing for all cases with respect to span length. The damage equivalence factors, based on both EN1993-2 [27] and SIA263 [80], increase with decreasing span length below about 10 m. However, there is no changes in the sign of slope for the equivalent force ranges in short span lengths in Figure 4.1. Usually, an incorrect interpretation is to attribute the large damage equivalence factors for short span lengths to the high number of cycles that normally occurs due to the passages of axles on short span

[1] The SIA code terminology for fatigue equivalent length is decisive length to determine dynamic factor (L_Φ) and Eurocode's terminology is critical span length. Here the fatigue equivalent length terminology is chosen to prevent confusion with codes terminology.

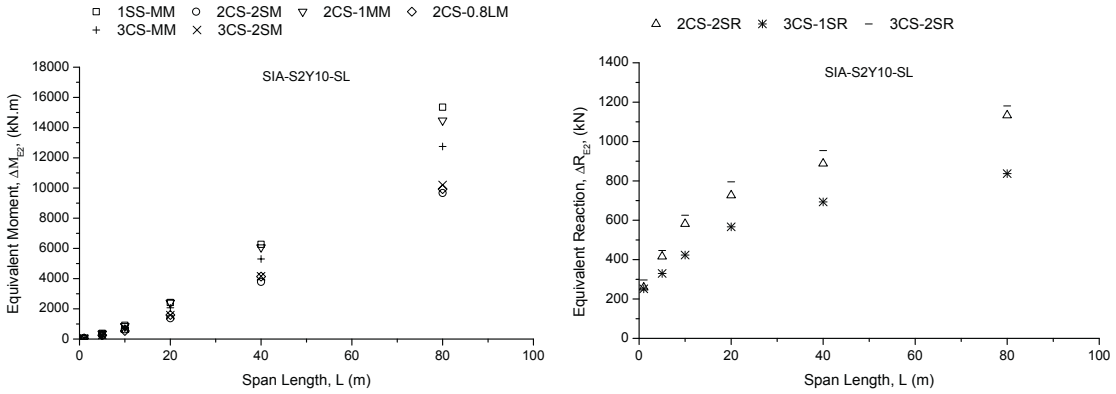

(a) Equivalent moment range

(b) Equivalent reaction range

Figure 4.1: Equivalent force range at two million cycles for different bridge cases

bridges. In fact, the increase of damage equivalence factors in short span lengths is mainly because of higher rate of reduction in the force range due to passage of fatigue load models and then because of increasing in number of cycles. For example, the length of Eurocode fatigue load model (FLM3) is 8.4 m (considering only the first axles' set). In the case of a simple span bridge, for instance, by decreasing the span length, some axles of fatigue load model remains out of the bridge, hence the moment range due to the fatigue load model suddenly reduces, which leads to increase of damage equivalence factors for short span bridges. This condition more or less applies also to the SIA fatigue load model.

As mentioned before, both SIA codes and Eurocodes follow a case-by-case definition method that cannot be applied to all bridge types. What theoretically involves in calculation of damage equivalence factors is influence line. Accordingly, the best definition of fatigue equivalent length is the one directly derived from influence line, which takes into account fatigue characteristics of any influence line such as length, shape, repetitions of shape, difference between maximum and minimums values. All the same, the definition of fatigue equivalent length must be simple to apply, since the main objective of damage equivalence factor method is to simplify the fatigue verification procedure.

4.2 Analytical solution for single lane traffic

4.2.1 Imaginary influence lines

In order to focus on different characteristics of influence lines, six imaginary influence lines are chosen as shown in Figure 4.2. These imaginary cases are not aiming at representing real bridge types; nevertheless, each of them is considered for a special purpose that logically could have an effect on the equivalent force range. The I0 case is the base shape with a triangular shape. The I1 case, with a trapezoidal shape, is intended to study the shape effect. The I2 case is intended to study the effect of sign change in influence lines. The I3 case, with five

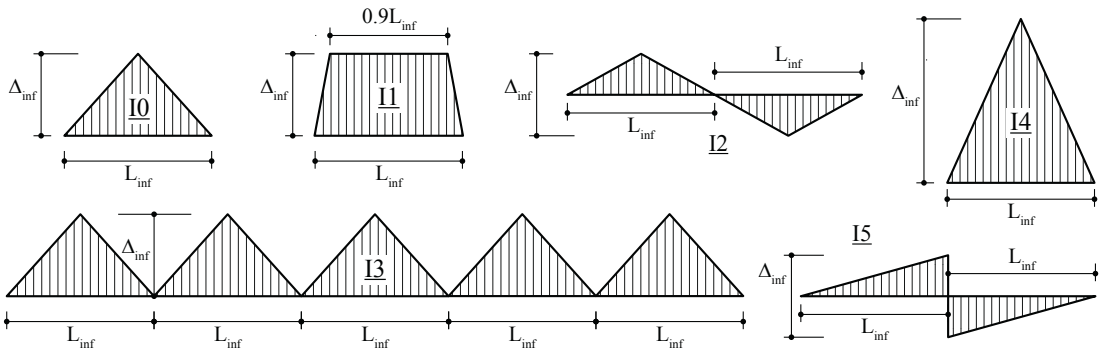

Figure 4.2: Shape of imaginary influence lines

repetitions of the shape I0, is intended to study the repetition effect. The I4 case is intended to study the effect of difference between the minimum and maximum values on the influence line by doubling this range. The I5 case is intended to study discontinuity in influence lines with suddenly changes. The length of each unit (distance between the null points of influence line), L_{inf}, is equal for all cases and it ranges from 1 m to 100 m. For all cases except I4, the difference between the maximum and minimum values on the influence lines is 1 ($\Delta_{inf} = 1$), where by increasing the unit length it remains constant.

Generally, the equivalent force range (it can be for example moment, shear, reaction, stress, etc.) at two million cycles for a given response spectrum (cycles range and number of cycles) by assuming a single slope S-N curve can be calculated as follows:

$$\Delta F_{E2} = \left(\frac{1}{2 \times 10^6} \sum \Delta F_i^m n_i \right)^{1/m} \tag{4.2}$$

where ΔF_{E2} is the equivalent force range, ΔF_i is the i^{th} cycle range of the response spectrum, n_i is the number of the cycles corresponding to ΔF_i.

The WinQSIM program is used to perform the traffic simulations. The actual traffic statistical parameters are based on WIM measurement at the Götthard station in 2009. The detailed description on traffic simulation methodology is provided in Appendix B. To facilitate interpretation of the results, vehicle-by-vehicle traffic simulations are considered, even though the continuous traffic simulations results are of importance and thus will be considered at the end of this chapter. The equivalent force range is calculated by linear damage accumulation with a single slope S-N Curve (m = 5). Total number of simulated vehicles is 8'000'000, composed of 25 percent of heavy vehicles[2]. The impact factor is not considered here, i.e. is taken equal to 1.

The results of equivalent force range, ΔF_{E2} obtained from vehicle-by-vehicle traffic simulations are illustrated in Figure 4.3. The results obtained for I0, I2 and fairly I5 are very close in the

[2]The minimum weight of heavy vehicles is 100 kN.

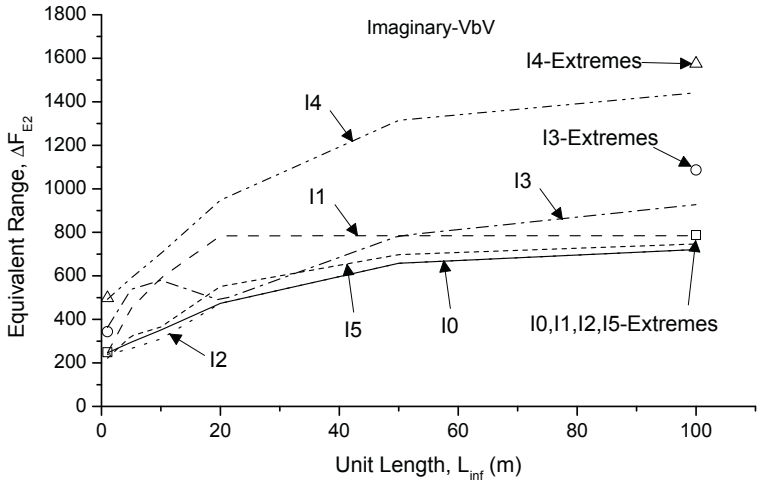

Figure 4.3: Equivalent force range for imaginary influence lines

considered range, indicating the influence lines that have a negative part or sudden change can be treated similarly as long as the difference between the maximum and minimum is similar. However, the results for I1, I3, I4 are different from I0.

In the case of I1, having a trapezoidal influence line shape, the equivalent force range increases sharply up to 20 m length and remains constant from 20 m on. That is because the length of vehicles are rarely higher than 20 m, and all axles (regardless of their positions) cause the same effect when $L_{inf} \geq 20m$. In addition, the equivalent force ranges obtained for I0 and I1 starting from the same point ($L_{inf} = 1\ m$) and converging again by increasing the unit length. These convergences at two ends are described in Section 4.2.2.

The I3 case is representative of repetition in the influence line. The equivalent force ranges obtained for I3 at the two limits (L_{inf} = 1 m and 100 m) are higher than the basic case, I0. In the I3 case, for very short as well as very long lengths, the number of cycles are 5 times more than the I0 case, hence the resulted equivalent force ranges will increase by $5^{(1/5)} = 1.38$ at these points. The mid-range results, however, are highly dependent on the vehicles' geometry.

In the case of I4, the difference between the minimum and maximum values on the influence line is twice of other cases. Thus, the equivalent force range obtained for I4 is almost twice of the I0 case. Nevertheless, the equivalent force range is studied here, and the effect of difference between the minimum and the maximum values of influence lines can be adapted by a suitable fatigue load model, as explained in Section 4.2.6.

4.2.2 Extremes unit lengths

Since determination of equivalent force range for very short and very long span lengths is straightforward, the equivalent force range at these extreme lengths are studied first.

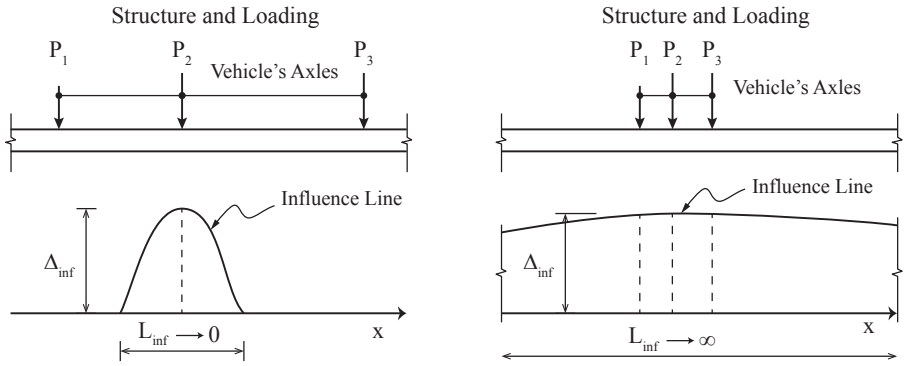

(a) Very short span length

(b) Very long span length

Figure 4.4: Schematic view of loading and influence lines with extreme unit lengths

For very short lengths ($L \to 0$) as shown in Figure 4.4a, passage of each axle over bridge causes one cycle, providing the influence line has one repetition. For influence lines with more than one repetition, the passage of each axle causes N_{inf} cycles. Concerning the imaginary cases, passage of each axle over I0, I1, I2, causes one cycle equal to the axle weight ($\Delta_{inf} = 1$). Therefore, the equivalent force range by assuming a single slope S-N curve can be calculated as follows:

$$\Delta F_{E2,Axle} = \Delta_{inf} \left(\frac{N_{inf}}{2 \times 10^6} \sum q_i^m f_i \right)^{1/m} \tag{4.3}$$

where $\Delta F_{E2,Axle}$ is the equivalent force range calculated for the axles frequency, f_i is the frequency (during the whole design life of a given bridge) corresponds to the axle intensity q_i, N_{inf} is the total number of repetition in the influence line and Δ_{inf} and m are as already defined. It is worthy of note that N_{inf} is a real positive number that can be specified by Reservoir or Rainflow method assuming the influence line is the response of the bridge.

Note the units of an influence line reflect the units of the response function and the unit load. For example, the units for the influence line of support reaction and mid-span moment of a simple span bridge are force per force (kN/kN) and moment per force ($kN \cdot m/kN$) respectively.

The axle load distribution at the Götthard station in 2009 is illustrated in Figure 4.5a. The ΔF_{E2} for I0, I1, I2 and I5 can be calculated by Equation 4.3, and it bears 249.0 kN which is very close to the simulations results for these cases with 1 m length, as shown in Figure 4.3. In addition, in the case of I4, the resulting cycle will be twice of the axle weight ($\Delta_{inf} = 2$), thus the equivalent force range will be twice. In the case of I3, the resulted cycles will be equal to the axle weight but, instead of one cycle, five cycles occur ($N_{inf} = 5$). Hence the equivalent force range will $5^{1/5}$ time more than I0.

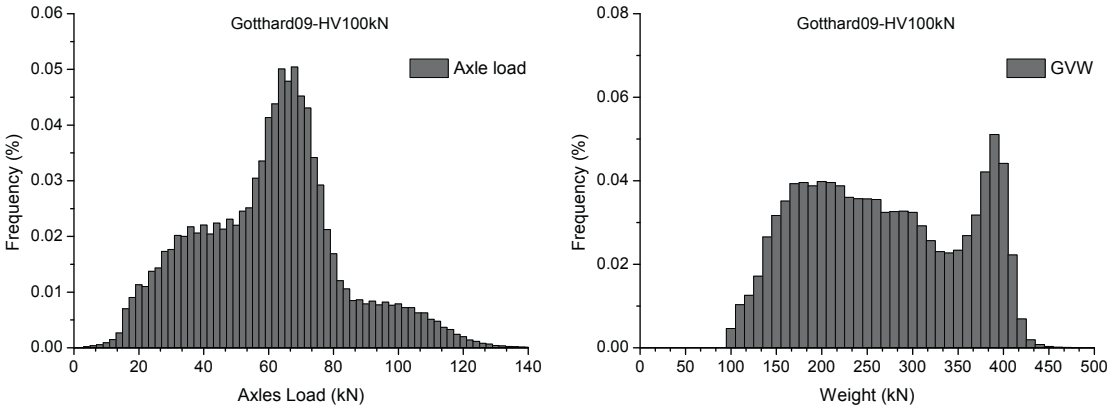

(a) Axle load (b) Gross Vehicle Weight

Figure 4.5: Frequencies for the Götthard traffic measured in 2009

On the other extreme, for very long unit lengths ($L \to \infty$) as shown in Figure 4.4b, due to the passage of each vehicle one cycle occur, providing only one repetition in influence line. Regarding to the imaginary cases, passage of each vehicle over I0, I1, I2 and I5 causes one cycle equal to the gross vehicle weight ($\Delta_{inf} = 1$), since the vehicle length is limited and comparing to the unit length, $L \to \infty$, can be assumed like a concentrated load. Similar to $F_{E2,Axle}$, the equivalent force range can be then determined as follows:

$$\Delta F_{E2,GVW} = \Delta_{inf} \left(\frac{N_{inf}}{2 \times 10^6} \sum Q_i^m f_i \right)^{1/m} \tag{4.4}$$

where $\Delta F_{E2,GVW}$ is the equivalent force range calculated for the GVW frequency, f_i is the frequency (during the whole design life of a given bridge) corresponds to the GVW intensity Q_i; also N_{inf}, Δ_{inf} and m are as already defined.

The GVW distribution of the Götthard station in 2009 is illustrated in Figure 4.5b. The ΔF_{E2} for I0, I1, I2 and I5 can be calculated by Equation 4.4, and it bears 787.7 kN which is very close to the corresponding simulations results for I0, I1, I2 and I5 with 100 m length, as shown in Figure 4.3. For two other cases, I3 and I4, the values of simulation would tend to the values calculated by Equation 4.4, if the unit length went to infinity.

It is important to note that vehicle-by-vehicle traffic simulations are considered here. The flat part of equivalent force range for long unit length (in Fig. 4.3) would not happen if the traffic was continuous in the simulations. In fact, the number of heavy vehicles passing simultaneously on a bridge increases with span length, which causes an increase in the equivalent force range by enlarging the unit length. In addition, the difference between the maximum and minimum, Δ_{inf}, also remains constant by increasing the unit length, which is also another reason why the equivalent force range for very long lengths reaches a fixed value. For many real influence lines (except for reactions) Δ_{inf} increases with span length, and as a

result, the equivalent force range grows with span length. This last issue, nevertheless, can be addressed by a proper fatigue load model.

4.2.3 Mid-range unit lengths

In the previous section, the equivalent force range is calculated using simplifying assumptions that allow neglecting the vehicles geometry. However, in the case of mid-range lengths, the equivalent force range is influenced by the interaction of parameters including: the vehicles' geometry, axles' load, influence line's shape and length. Whereas the vehicles geometries (axles positions and loads) are stochastic, it is not interesting to calculate equivalent force range for every case. An "equivalent vehicle" which represents all vehicle types (heavy vehicles classes) can be proposed to address this issue. The main assumptions for determining the equivalent vehicle are:

1. the total weight of equivalent vehicle is 1,
2. the small cycles due to passage of axles are negligible in total damage sum,
3. for each vehicle, the position of axles are measured from the mass centre of the vehicle,
4. the effect of each vehicle in the equivalent vehicle is equal to the ratio of its gross vehicle weight to total traffic weight,
5. the effect of each vehicle axle load at its corresponding axle position is equal to the ratio of axle load to gross vehicle weight.

Accordingly, the i^{th} axles' effect of j^{th} vehicle in the equivalent vehicle, $R_{i,j}$, is:

$$R_{i,j} = \frac{L_{i,j}}{N_{obs} \times Q_{av}} \tag{4.5}$$

where $L_{i,j}$ is the load intensity of i^{th} axle, and N_{obs} is the total number of vehicles (heavy vehicles) and Q_{av} is the arithmetic mean of gross vehicles weight in the considered traffic. Then, the adjacent axles in certain intervals can be summed up to obtain the axle load of the equivalent vehicle within intervals.

The 3^{rd} item in the definition of equivalent vehicle is now explained further. For finding the maximum or minimum forces, generally, the mass centre of vehicles should be positioned at the maximum or minimum point of the influence line. In this case, the value of the response due to the set of axles can be calculated as:

$$F_R = \sum_{i=1}^{i=n} L_i[I.L.F_R(x_i)] \tag{4.6}$$

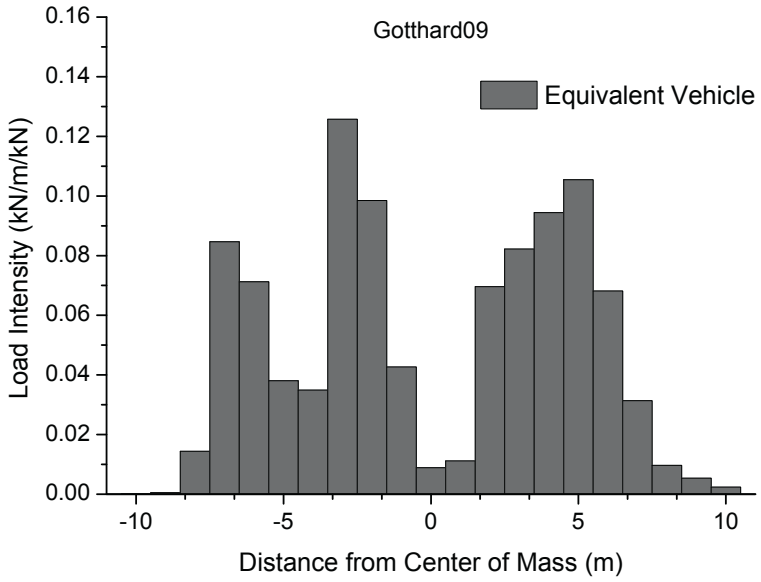

Figure 4.6: Equivalent vehicle determined from the Götthard traffic in 2009

where i is the axle index, n is the total number of axles, L_i is the i^{th} axle load intensity and $[I.L.F_R(x_i)]$ is the influence line ordinates at the abscissas corresponding to the axle position.

However, there are some exceptional conditions for which positioning the mass centre of vehicles at the maximum or minimum will not bear the maximum or minimum responses. For example, when the maximums or minimums are at the start or at the end of influence lines; when the vehicle length (from the first axle to the last axle) is larger than the unit length (L_{inf}); or when influence line is discontinuous or its sign changes suddenly. In the current study, the vehicle mass centre is always considered as the point for determining the equivalent vehicle, despite its limitations for exceptional cases; nevertheless, the accuracy of such an assumption is evaluated in the following paragraphs.

The equivalent vehicle for the Götthard WIM station in 2009 is determined using the mentioned procedure and is illustrated in Figure 4.6, where the adjacent axles are grouped in 1 m intervals. The equivalent force range for the equivalent vehicle can be obtained as follows:

$$\Delta F_{E2,EV} = \Delta F_{R,EV} Q_m \left(\frac{N_{obs} N_{inf}}{2 \times 10^6} \right)^{1/5} \tag{4.7}$$

where $\Delta F_{E2,EV}$ is the equivalent force range obtained for equivalent vehicle, $\Delta F_{R,EV}$ is the force range due to passage of equivalent vehicle on bridge, N_{obs} is the number of trucks passing over the bridge (during the whole design life), Q_m is the power mean (computed with exponent $p = 5$) of gross vehicles weight passing on the bridge and N_{inf} is number of repetition in influence line as already defined. The $\Delta F_{R,EV}$ parameter has the same unit as the influence line since the weight of equivalent vehicle is one and without unit (kN/kN).

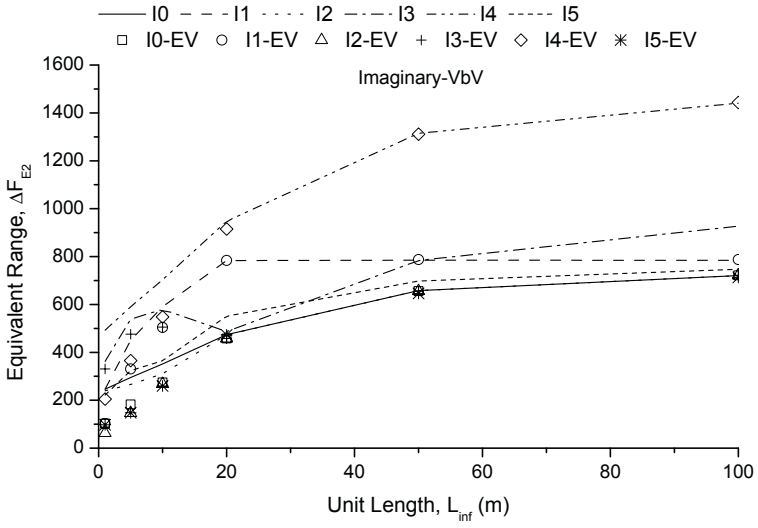

Figure 4.7: Equivalent force range estimated by equivalent vehicle in comparison with simulation results

The equivalent force range calculated by Equation 4.7 is illustrated in Figure 4.7 for the imaginary cases in comparison with the results of vehicle-by-vehicle traffic simulations. Figure 4.7 shows that the results of equivalent force ranges are accurately estimated by Equation 4.7 for unit length $L_{inf} \geq 20m$. However, the precision of equivalent force range resulting from Equation 4.7 reduces as unit length decreases. In fact, the cycles due to passage of axles are becoming more effective by decreasing the unit lengths from 20 m down. Accordingly, the equivalent force range tends towards its minimum value as described in Section 4.2.2.

4.2.4 Uniformly distributed load with defined length

Although the results obtained for the equivalent vehicle are rather satisfying, there are still some limitations, including:

1. the equivalent vehicle is traffic dependant, for instance in the previous section, it is defined for the Götthard traffic in 2009,
2. the continuous traffic is neglected in determining the equivalent vehicle,
3. determination of equivalent vehicle is rather difficult for practicing engineers.

An average equivalent vehicle considering several traffic measurements may address the first issue. To this end, the same method for determining the equivalent vehicle is applied for different available WIM measurements within Switzerland in 2009. Then, the average value of different stations within the intervals is calculated. Figure 4.8 illustrates the average equivalent vehicle obtained for seven different Swiss traffic WIM in 2009 and the standard deviation of

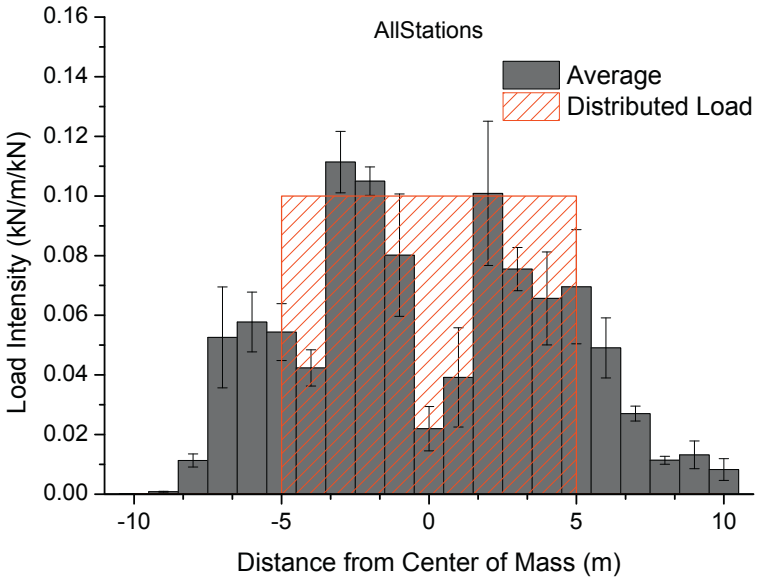

Figure 4.8: Average equivalent vehicle and its standard deviation obtained for Swiss traffic

values within each interval. The load value at each interval partially depends on the traffic station. In order to simplify the equivalent vehicle, at the expense of losing some accuracy, the equivalent vehicle can be modelled with a uniformly distributed load with a defined length.

The length of uniformly distributed load can be equal to average length (axle to axle) of heavy vehicles. The average length of heavy vehicles in Götthard station in 2009, for example, is about 11.7 m, and the average trucks length for all WIM stations in 2009 is about 9.5 m. To evaluate the accuracy of modelling the traffic actions with a distributed load, the uniformly distributed load with 10 m length with load intensity of 0.1 kN/m/kN (it is divided by its total weight to obtain a unit distributed load) is applied, as shown in Figure 4.8. For describing how to obtain the response of bridges subjected to a uniformly distributed load, a bridge and the uniform load with intensity of p is shown in Figure 4.9. Also given in this figure is a segment of an influence line for the response function $[I.L.F_R]$. At section x, an element of the bridge dx in length is taken, and an element load of dP can be taken as a concentrated load at point x. The increment of the response function that results from the load $dP = p\,dx$ as:

$$dF_R = p\,dx\,[I.L.F_R(x)] \tag{4.8}$$

where $[I.L.F_R(x)]$ is the ordinate to the influence line at point x. Integration of Equation 4.8 between A and B gives the total response due to uniformly distributed load $F_{R,Dist}$:

$$F_{R,Dist} = p\int_{x_a}^{x_b}[I.L.F_R(x)]dx \tag{4.9}$$

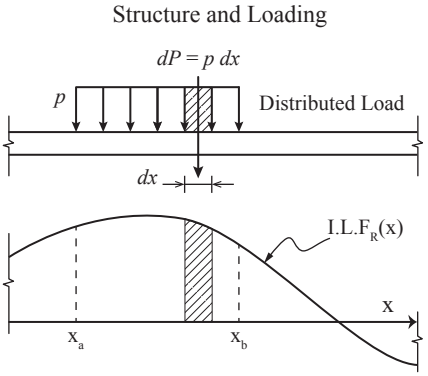

Figure 4.9: Parameters for finding maximum response due to uniformly distributed load

In the above, p has been moved outside the integral since it is a constant. Note that $F_{R,Dist}$ has the same unit as the influence line since p has unit of $kN/m/kN$ and dx has unit of m. In the form of Equation 4.9, it is clear that the integral represent the area under the influence line between the limits of points x_a and x_b. Thus, the force range due to passage of distributed load $\Delta F_{R,Dist}$, as shown in Figure 4.10, is equal to the absolute sum of area under influence line by positioning its centre at the maximum and minimum values of influence line multiply to p, providing the unit length, L_{inf}, be larger than the uniformly distributed load length.

Consequently, the equivalent force at two million cycles using the uniformly distributed load with defined length, $\Delta_{E2,Dist}$ can be determined as:

$$\Delta F_{E2,Dist} = \Delta F_{R,Dist} Q_m \left(\frac{N_{obs} N_{inf}}{2 \times 10^6} \right)^{1/5} \tag{4.10}$$

The equivalent force range obtained from Equation 4.10 is shown in Figure 4.11 for the given imaginary influence lines in comparison with vehicle-by-vehicle equivalent force range result-

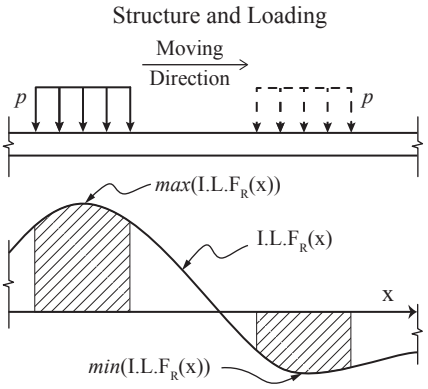

Figure 4.10: Parameters for finding force range due to passage of uniformly distributed load with a defined length

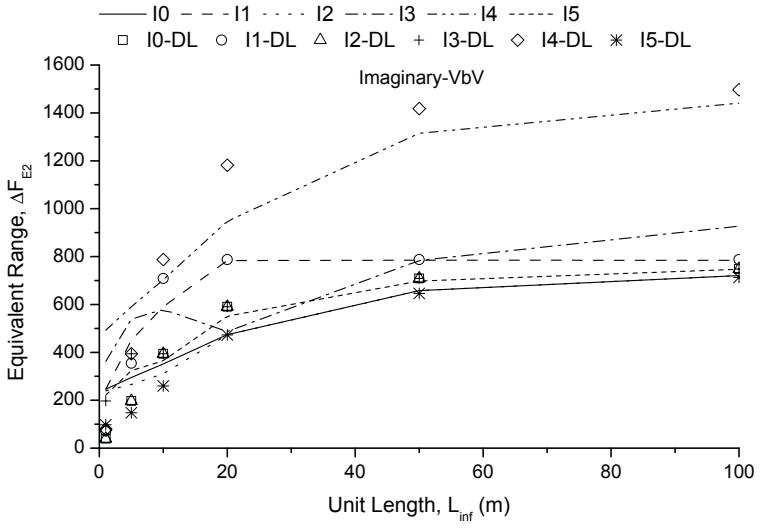

Figure 4.11: Equivalent force range estimated by uniformly distributed load in comparison with simulations

ing from traffic simulation. For the influence lines with unit length, L_{inf}, lower than uniformly distributed load length (10 m), $\Delta F_{R,Dist}$ is also determined by passage of uniformly distributed load on the influence line for the sake of having complete range of results at all unit lengths, although this estimation is not correct. Despite many simplifying assumptions, the estimated equivalent force range by the distributed load is sufficiently precise, except for the unit length lower than 20 m, where the results are mainly influenced by the axles-by-axle passages and the distributed load is not applicable.

It is important to remind that the aim of the equivalent vehicle or the uniformly distributed load with defined length and Equation 4.10 is not to determine the damage equivalent force range. The analytical methods and simplifying solutions are discussed to improve our knowledge about the parameters involving in the determination of equivalent force range and damage equivalence factors.

4.2.5 Continuous traffic

As described in the previous section, the randomness of vehicles can be simplified with a uniformly distributed load with a defined length. However, a vehicle-by-vehicle traffic condition is considered so far, and the results of former traffic simulations have been confirmed that a vehicle-by-vehicle traffic model is not promising. The main difference in a continuous traffic is that the probability of having several trucks on bridges exists.

In order to quantify this probability, the distribution of the intervals between heavy vehicles (GVW over 100 kN) is calculated for the WIM stations of Switzerland in 2009 and illustrated in Figure 4.12. The accuracy of time measurements for each passage in the available databases

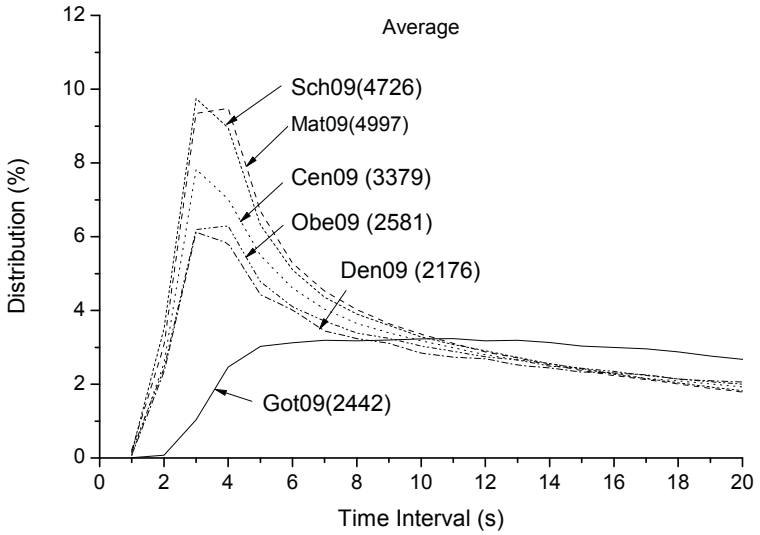

Figure 4.12: Frequency of time intervals between heavy vehicles for different WIM stations of Switzerland in 2009

is the second. Therefore, the minimum possible measured distance between vehicles (head to head) is about 25 m assuming the heavy vehicles are circulating with speed of 90 km/h. Also, the frequency of time intervals are shown up to 20 s, meaning about 500 m between two following heavy vehicle, which is generally not accounted for in simultaneity effect. The values given in the parentheses are the Annual Average Daily Heavy Vehicle Traffic (AADHVT) corresponding to the WIM station. Figure 4.12 confirms that the number of heavy vehicles with small intervals increases with heavy vehicle traffic volume, AADHVT. In Figure 4.12, the shape of distribution functions are similar for different WIM stations except for Götthard station. It can be pointed out that the Götthard station is the only station with one traffic lane in each direction. In this case, the minimum distance between heavy vehicles must be 100 m based on the Swiss traffic regulations, which makes heavy vehicles spacing longer.

The parameters needed for determining the equivalent force range due to continuous traffic are schematically shown in Figure 4.13. For a given bridge type and known traffic, the equivalent force range at two million cycles can be calculated as follows:

$$\begin{aligned}\left(\Delta F_{E2,Follow}\right)^5 &= \frac{N_{inf}}{2\times 10^6}\times\left\{\left(\Delta F_{R,Dist}\times Q_m\right)^5\times\left(N_{obs}-\sum n_i\right)\right.\\ &\quad\left.+\sum\left[\left(\Delta F_{R,Follow,i}\times Q_m\right)^5\times n_i\right]\right\}\end{aligned} \tag{4.11}$$

where, $\Delta F_{E2,Follow}$ is the equivalent force range at two million cycles due to continuous traffic,

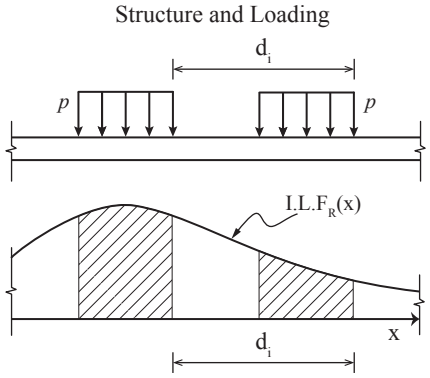

Figure 4.13: Parameters for finding force range due to passage of two following vehicles

n_i is the number of trucks which are following with the distance of d_i and $\Delta F_{R,Follow,i}$ is the stress range due to passage of the two following uniformly distributed load (or the equivalent vehicle) with the distance d_i.

However, such an approach leads to more complications in damage equivalence factors, in spite of providing more precise estimation of damage sum, which contradicts the concept of damage equivalence factors. Therefore, a simplified approach must be considered that can include the effect of continuous traffic within the damage equivalence factors. Such an approach is given in the following section.

4.2.6 Proposition of parameters

The shortcomings of damage equivalence factors, as mentioned in the previous sections, limit the possibilities of modifications to fatigue equivalent length and fatigue load model. The damage equivalence factor for the distributed load with limited length can be obtained by dividing both sides of Equation 4.10 by force range due to the passage of fatigue load model on bridge:

$$\lambda_{Dist} = \frac{\Delta F_{R,Dist}}{\Delta F_{FLM}} \times Q_m \left(\frac{N_{obs} N_{inf}}{2 \times 10^6} \right)^{1/5} \tag{4.12}$$

where ΔF_{FLM} is the bridge response due to a given fatigue load model. Considering the imaginary influence lines, for instance, all cycles due to passage of vehicles over the I3 case is twice of I0 case. In order to have the same damage equivalence factor for both cases, thus the equivalent forces can be simply divided by the difference between the maximum and minimum, Δ_{inf}. Obviously, the response of bridges due to passage of a single axle load with load intensity of P bears $\Delta F_{FLM} = \Delta_{inf} \times P$. Whereas the main purpose of fatigue load model is only to uniform the ordinate of influence lines, a single axle fatigue load model can perform this function. Therefore, a single axle fatigue load model with the weight of 480 kN, same

as total weight of fatigue load model in Eurocode [25], can be proposed. In fact, weight of fatigue load model does not alter equivalent force range, it only moves the curve of damage equivalence factor up and down.

The first part of Equation 4.12 can be rewritten as follows:

$$\frac{\Delta F_{R,Dist}}{\Delta F_{FLM}} = \frac{p \int_{x_a}^{x_b} [I.L.F_R(x)]dx}{\Delta_{inf} \times P} \tag{4.13}$$

The integral part is summation of area parts under influence line. However, a vehicle-by-vehicle traffic is considered in determination of the uniformly distributed load with a defined length. Reading Section 4.2.5 one can notice that indeed the whole area under influence line can be effective since the probability of having several trucks over bridge exists. In addition, the division of the integral part by Δ_{inf} has the unit of length. Since the λ_1-factor is function of length, the parameter of fatigue equivalent length, L_λ, can be proposed as:

$$L_\lambda = \frac{A_{inf}}{\Delta_{inf}} \tag{4.14}$$

Where A_{inf} is the absolute sum of area under influence line and Δ_{inf} is the difference between the maximum and minimum values. The fatigue equivalent length for five different influence lines obtained from Equation 4.14 is shown in Figure 4.14. Also, the critical span length corresponding to the EN1993-2 [27] and the influence length according to the SIA261 [79] are given in Figure 4.14 for comparison.

It must be noted that an equal importance is given to all area sections under influence line in Equation 4.14; however, in reality, the importance of different area sections under influence lines depends on both frequency of the distances between trucks and influence line length and shape. As far as the frequency of distances between trucks vary traffic by traffic, L_λ is traffic dependant. Moreover, for short span bridge lengths as described in Section 4.2.2, the uniformly distributed load is not accurate enough. Nevertheless, a very simple formula is given here for L_λ to make it useful in the framework of damage equivalence factors. The range of validity of the proposed definition as well as the resulting damage equivalence factors must be controlled with several influence lines.

The powered mean of gross vehicles weight, Q_m, and the number of heavy vehicles, N_{obs}, are also important for determining damage equivalence factor. A base value equal to the base value considered in the Eurocodes [25, 27] can be taken for calculation of the λ_1-factor, then in agreement with the Eurocodes, λ_2 can be applied for modification of traffic volume.

The number of repetition in an influence line (N_{inf}) may also have an influence on determining the λ-factor. Establishing any general rule for determining damage equivalence factors regardless of N_{inf} effect cannot be generalized. For the bridges with continuous girders,

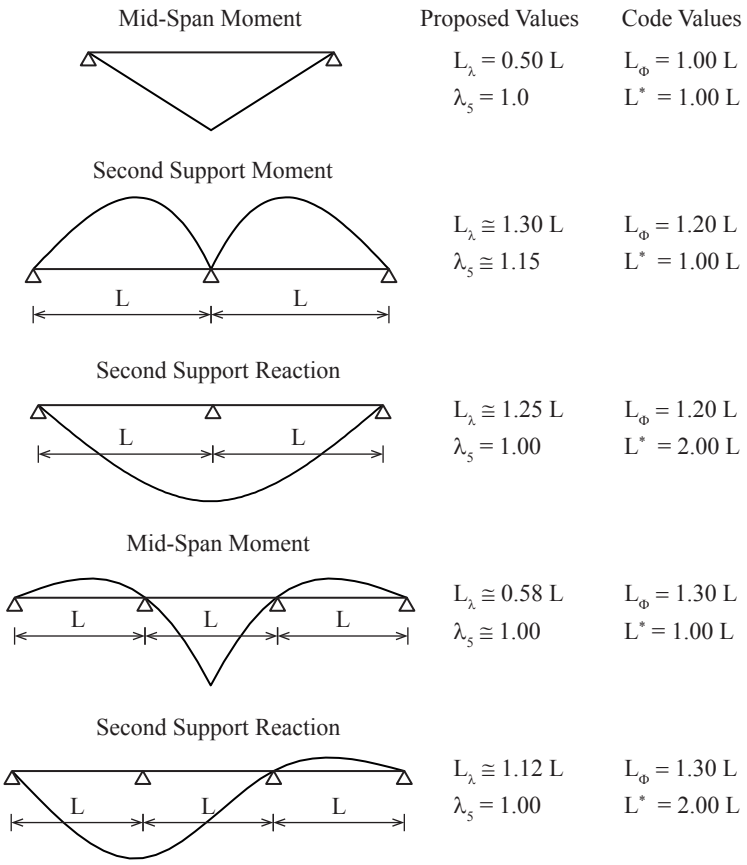

Figure 4.14: Fatigue equivalent length for some sample influence lines

the maximum N_{inf} is likely to be 2 which corresponds to mid-support negative moment of two-span continuous bridges. In these cases, the effect of N_{inf} on damage equivalence factors is $2^{1/5} = 1.15$, assuming effective slope of S-N curve is 5. For taking into account the repetition effect for a given influence line, a new general partial damage equivalence factor can be introduced as follows:

$$\lambda_5 = \frac{1}{\Delta_{inf}} \left(\sum_{i=1}^{N_{inf}} (\Delta_{inf,i})^m \right)^{\frac{1}{m}} \tag{4.15}$$

where $\Delta_{inf,i}$ is the i^{th} cycle range of the influence line that can be extracted by Reservoir method (assuming the influence line is a stress history), Δ_{inf} is the maximum cycle range (or the distance between the maximum and the minimum values) of the influence line m is the effective slope of fatigue resistance curve, which can be taken 5 for steel details under direct stress. The λ_5-factor for five different bridge cases obtained from Equation 4.15 is given in Figure 4.14, though for most cases it is almost equal to 1.0.

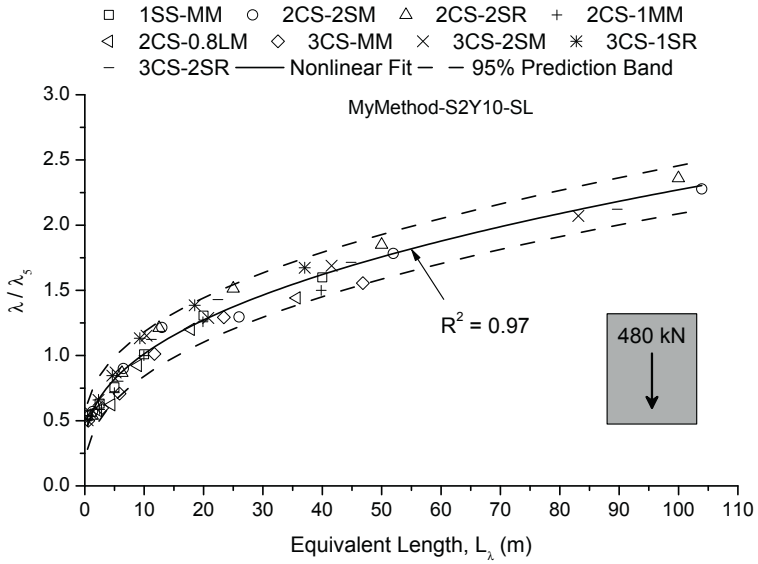

Figure 4.15: λ for different influence lines based on the proposed method

The results of initial traffic condition for single lane traffic are re-employed to test the determination of the damage equivalence factors with the new proposed method. The damage equivalence factor, λ/λ_5, for different influence lines is illustrated in Figure 4.15; the average value nonlinear fit of the results as well as the 95% prediction band are also plotted. The assumed fatigue load model is also illustrated in Figure 4.15 for clarity. The R-square (R^2) is 0.97 and the dispersion of the results is clearly less than the codes, despite the simple definition of the fatigue equivalent length and fatigue load model. Therefore, the proposed fatigue equivalent length is a proper parameter which can represent different influence lines shape and length. Also the proposed fatigue load model does not cause dispersion of the damage equivalence factors in short span lengths region. Nevertheless, to ensure the validity of the propositions, they are evaluated with more traffic conditions in Chapter 6.

4.3 Analytical solution for multi-lane traffic

The λ_4-factor is intended to provide modification of damage equivalence factor corresponding to multi-lane traffic conditions. As described in Chapter 3 the SIA codes and Eurocodes only add up the damages due to each additional lane to first lane. The main throwback of the current λ_4 definition is that it does not embrace the effect of trucks crossing or overtaking on bridges. An updated definition of λ_4 can improve this shortcoming. Let's consider:

$$\Delta\sigma_{code} = \Delta\sigma_1 \tag{4.16}$$

Where $\Delta\sigma_{code}$ is stress range due to passage of fatigue load model and $\Delta\sigma_1$ is stress range due to passage of fatigue load model on first lane. Then, using Miner summation rule and

considering the equivalent stress ranges the following equation can be written:

$$(\Delta\sigma_{E2})^m = \left(\Delta\sigma_{E2,1}\right)^m + \left(\Delta\sigma_{E2,2}\right)^m + \left(\Delta\sigma_{E2,c}\right)^m \tag{4.17}$$

Where $\Delta\sigma_{E2}$ is equivalent stress range at 2 million cycles due to passage of traffic on both lanes including crossings, $\Delta\sigma_{E2,1}$ and $\Delta\sigma_{E2,2}$ are equivalent stress ranges at 2 million cycles due to passage of traffic on lane 1 and lane 2 respectively, $\Delta\sigma_{E2,c}$ is equivalent stress range at 2 million cycles due to crossings only and m is the effective slope of fatigue resistance curve.

The effective slope, m, for steel details under direct stress can be a value between 3 and 5. The SIA263 [80] gives $m = 3$ as a conservative value, and $m = 5$ for the cases that number of cycles during service life exceeds 5 million. The Eurocode [27] takes m equal to 5 for all steel details under direct stresses. For details under shear stresses effective slope, m, can be equal to 5 since the S-N cuve for details subjected to shear stresses has a single slope of 5 with a cut-off limit at 10^8 cycles. In addition, the effective slope for shear studs connection for the same reason is equal to 8. Generally, the effective slope, m, should be determined by considering the number and intensity of applied cycles. However, the precise determination of its value is not the subject of the current study.

Let us define:

$$\lambda_{1-c} = \frac{\Delta\sigma_{E2,1}}{\Delta\sigma_1} \tag{4.18}$$

with number of vehicles equals $N_1 - N_c$,

$$\lambda_{2-c} = \frac{\Delta\sigma_{E2,2}}{\Delta\sigma_2} \tag{4.19}$$

with number of vehicles equals $N_2 - N_c$,

$$\lambda_c = \frac{\Delta\sigma_{E2,c}}{(\Delta\sigma_1 + \Delta\sigma_2)} \tag{4.20}$$

with number of vehicles equals N_c. Also, $\Delta\sigma_{E2}$ can be written as follows:

$$\Delta\sigma_{E2} = \lambda_1 \times \lambda_4 \times (\Delta\sigma_{code}) \tag{4.21}$$

where λ_1 is the partial damage equivalence factor due to the first lane traffic (or slow lane). By substituting the equivalent stress ranges in the Miner summation rule (Eq. 4.17), it results:

$$(\lambda_1 \times \lambda_4 \times \Delta\sigma_{code})^m = (\lambda_{1-c} \times \Delta\sigma_1)^m + (\lambda_{2-c} \times \Delta\sigma_2)^m + (\lambda_c \times \Delta\sigma_{1+2})^m \tag{4.22}$$

where $\Delta\sigma_1$ and $\Delta\sigma_2$ are the stress ranges due to passage of traffic load on first lane and second lane respectively, $\Delta\sigma_{1+2}$ is the stress range due to passage of traffic load on both lanes. If signs of σ_1 and σ_2 are not opposite, then $\Delta\sigma_{1+2} = \Delta\sigma_1 + \Delta\sigma_2$; otherwise the effect of crossing (or overtaking) is favourable and this effect can be conservatively neglected; i.e. $\Delta\sigma_{1+2} = \Delta\sigma_1$;

One can consider two types of proportional bridge response spectra as shown Figure 4.16. In the first type (Fig. 4.16a), for any stress range at the response spectra the number of cycles corresponding to the first response is a constant ratio of number of cycles corresponding to the second response. In this case, the relation of damage equivalence factors can be written as:

$$\left(\frac{\lambda_{1,1}}{\lambda_{1,2}}\right)^m = \left(\frac{N_1}{N_2}\right) \tag{4.23}$$

Where $\lambda_{1,1}$ and $\lambda_{1,2}$ are partial damage equivalence factors due to the first and the second response spectrum respectively. In the second type (Fig. 4.16b), for any number of cycles the stress range corresponding to the first response is a constant ratio of stress range corresponding to the second response. In this case, the damage equivalence factor remains constant, $\lambda_{1,1} = \lambda_{1,2}$. For typical bridges, both proportionalities may happen in the same time, meaning the response spectra are both scaling in number of cycles and stress range together. The Equation 4.23, nevertheless, remain valid for such proportionality.

Assuming the response spectrum due to passage of traffic on lane 1 is proportional to the response spectrum due to passage of traffic on lane 2 as well to the response spectrum due to crossing, then by dividing both sides of Equation 4.22 by λ_1^m and $\Delta\sigma_{code}^m$, the following equation can be obtained:

$$(\lambda_4)^m = \frac{N_1 - N_c}{N_1} + \frac{N_2 - N_c}{N_1}\left(\frac{\Delta\sigma_2}{\Delta\sigma_1}\right)^m + \frac{N_c}{N_1}\left(\frac{\Delta\sigma_1 + \Delta\sigma_2}{\Delta\sigma_1}\right)^m \tag{4.24}$$

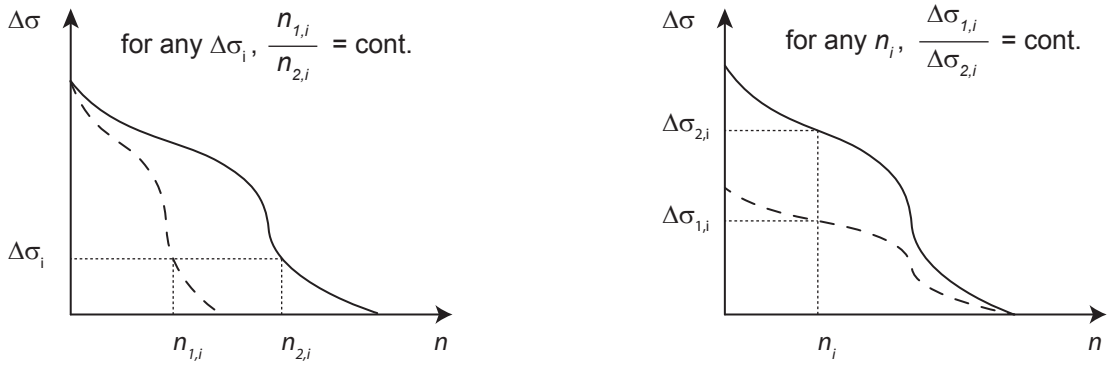

(a) Proportional in number of cycles

(b) Proportional in cycles range

Figure 4.16: Two schematic proportionality types for bridge response spectra

Where N_1, N_2 are the number of trucks passing on lane 1 and lane 2 respectively, and N_c is the number of trucks crossing on bridge (total number of trucks is qual to $N_1 + N_2$). It is then possible to rearrange the equation as follows:

$$\lambda_4 = \sqrt[m]{(1-c) + (n-c)a^m + c(1+a)^m} \tag{4.25}$$

Where:

$$c = \frac{N_c}{N_1}, \quad n = \frac{N_2}{N_1}, \quad a = \frac{\Delta\sigma_2}{\Delta\sigma_1} \tag{4.26}$$

Then, the fatigue verification based on the SIA263 can be done using the following equation:

$$\lambda_1 \times \lambda_4 \times \Delta\sigma_{code} \leq \frac{\Delta\sigma_c}{\gamma_m} \tag{4.27}$$

It is important to recall that the λ_1 based on the SIA code is given for four predetermined annual truck traffic volume per direction (instead of lane). Thus in the case of unidirectional traffic, λ_1 corresponding to the first lane traffic (slow lane) should be calculated. Then the value of λ_4 as defined in Equation 4.25 sums both effect of traffic volume on the second lane and effect of crossing with the λ_1 for the first lane traffic.

The latter point is irrelevant to the Eurocode, because the Eurocode λ_1 is given for slow lane. Through the same procedure and with the same assumptions, Eurocodeλ_4 can be updated as follows:

$$\lambda_4 = \left[(1-c) + \left(\frac{N_2}{N1} - c\right)\left(\frac{\eta_2 Q_{m2}}{\eta_1 Q_{m1}}\right)^5 + c\left(1 + \frac{\eta_2 Q_{m2}}{\eta_1 Q_{m1}}\right)^5\right]^{1/5} \tag{4.28}$$

It worthy of note that, in the proposed equations, it is assumed that the cycles spectrums due to crossing and overtaking are proportional to the cycle response spectrum due traffic action on lane 1 as well as on lane 2. It is partially true, for instance when two trucks pass on bridge side-by-side. However for other cases, for instance when two trucks pass on bridge with a certain distance in different lanes (staggered), this assumption is not correct anymore. In such cases, the response of bridge is function of the trucks geometry, weight, the distance between them, the bridge influence line and the transverse load distribution of the lanes. The frequency of inter-lane distance between the trucks may vary from bridge to bridge and it depends on many parameters like the traffic rules, lane width, trucks speed and traffic volume. Also, as traffic flow increases, all traffic regime change, then overtaking frequency changes.

Therefore, analytical determination of equivalent stress range for such cases is too complicated to be simplified and considered in the framework of damage equivalence factors. The crossing

or overtaking ratio, c, can address the issue to some degree, but it does not correspond to actual frequency of overtaking or crossing. In fact, the c ratio (in Eq. 4.25 as well as Eq. 4.28) is a representative value which takes into account the effect of crossings or overtakings (both side-by-side and staggered), rather than giving the real frequency of crossing or overtaking.

The results of the initial traffic simulations for double lane traffic conditions are re-employed to determine the λ_4-factor based on the proposed fatigue load model and fatigue equivalent length. Figure 4.17 illustrates the λ_4-factors obtained for different influence lines and two traffic conditions of unidirectional (UD10020) and bidirectional (BD5050). The total annual truck traffic in both lanes is 2'000'000 for both traffic conditions. Then, by trial and error, it is found that the c ratios of 3% and 16% for unidirectional and bidirectional traffic respectively can conservatively represent the effect of simultaneity for the defined cases. For comparison purpose, the factor λ_4 with effect of crossing given by SETRA [77] for highways (only bidirectional traffic) is also calculated and presented in Figure 4.17. It is apparent that the proposed ratio underestimates the crossing effect. The intended effective length for determining the crossing ration in SETRA [77] is equal to the bridge length for mid-span sections and sum of two adjacent spans length for support sections. For all influence line cases this effective length, L, is very roughly assumed to be twice of L_λ.

The crossing and overtaking ratio has an important role in calculation of λ_4, and its value is function of traffic volume in each lane and bridge equivalent length. Hence more study on this ratio is necessary in order to figure out the damage equivalence factor due to various multi-lane traffic conditions. The results of several multi-lane traffic conditions are reported in Chapter 6 which helps finding a reasonable c ratio.

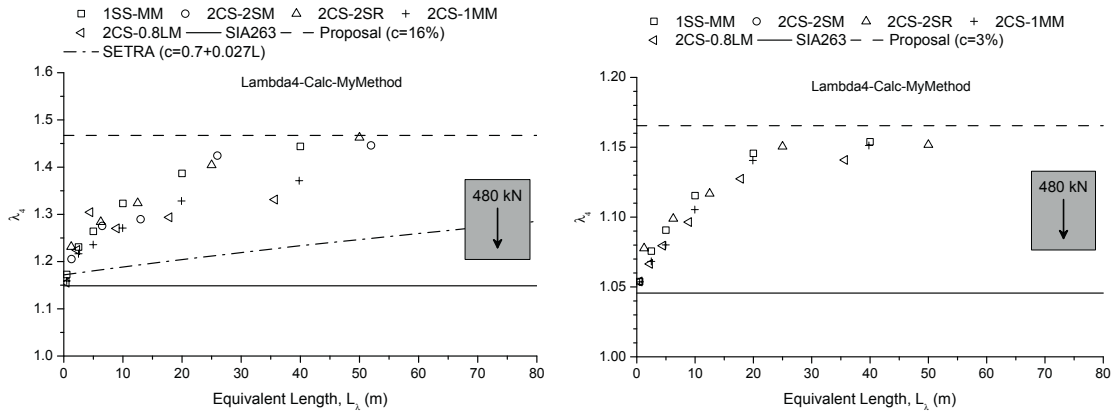

(a) Bidirectional traffic condition

(b) Unidirectional traffic condition

Figure 4.17: λ_4 for the initial traffic simulations and the proposed crossing values

4.4 Maximum damage equivalence factor

The fatigue life of structural details under direct stress tends to be infinite providing all stress cycles remain below constant amplitude fatigue limit:

$$max(\Delta\sigma) \leq \Delta\sigma_D \tag{4.29}$$

where $max(\Delta\sigma)$ is the maximum value of the stress range spectrum and $\Delta\sigma_D$ is the constant amplitude fatigue limit of the considered detail. Knowing $\Delta\sigma_D = 0.74 \times \Delta\sigma_c$ for steel details under direct stresses, the λ_{max}-factor can be calculated as follow:

$$\lambda_{max} = \frac{max(\Delta\sigma)}{0.74 \times \Delta\sigma_{FLM}} \tag{4.30}$$

Then, the general fatigue verification of the Eurocode can be written as:

$$\lambda_{max}\Delta\sigma_{FLM} \leq \frac{\Delta\sigma_c}{\gamma_{Mf}} \tag{4.31}$$

The $max(\Delta\sigma)$ must be well estimated to have a safe verification according to Equation 4.31. Figure 4.18 shows a schematic diagram of bridge response cycles frequency. The characteristic value (ultimate) corresponds to return period of 1000 years or probability of exceedance of 10 percent in 100 years. For constant amplitude fatigue limit (CAFL), the Eurocode accept the exceedance of which would produces a damage contribution of less than 1% of the total damage. This load is interpreted as the “frequent value” for fatigue in Eurocode. The “frequent” values have a mean return period of one week [76], based on typical traffic situations such as flowing traffic and good surface quality of road. The extreme situations applied for the determination of characteristic loads are not considered for “frequent” values.

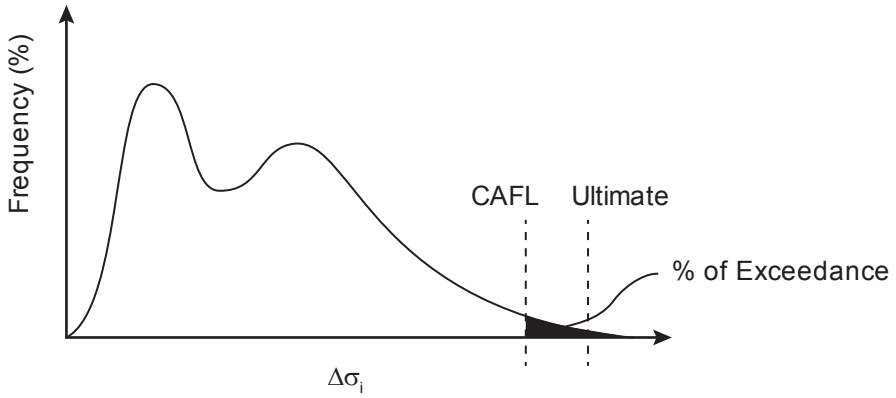

Figure 4.18: Schematic diagram of bridge response cycles frequency due to traffic

In the test results, however, it is observed that occurrence of very few cycles above the CAFL, even one out of ten thousands, may lead to fatigue failure [66]. In fact, it is not the number of cycles above the CAFL that causes a fatigue crack to start, rather the existence of such cycles in a spectrum may cause crack initiation. After the crack initiation, the CAFL threshold decreases and this results in having more cycles over the threshold. By repetition of the same spectrum, the process of decreasing threshold continues which eventually leads to failure.

This point is exemplified in [66] with result of a beam test, as illustrated here in Table 4.1. The test conducted by Fisher et al [30] on a beam subjected to 104 million of variable amplitude cycles. A fatigue crack was found at a transverse stiffener at the end of the test. The damage computations carried out using the detail category C (taken from American code) with CAFL at 86 MPa give $D_{tot} = 4.29$, see Table 4.1. This is way above unity, but it is normal since a test result is considered and damage is computed using the characteristic S-N curve for the detail. Looking at the relative damage according to stress range level, one sees that the higher stress range (the only one above the CAFL) as well as those just below, do account only marginally to the damage sum. It is the median stress ranges that account for most of the damage. The highest stress ranges are not the only ones doing the damage, they usually account for less than 1% of damage in the different tests carried out. The higher stress ranges, however, are the ones responsible for initiating fatigue crack [66]. Therefore, the Eurocode assumption might not always result in a safe design.

The “allowable” percentage of cycles exceeding the CAFL or the corresponding damage percentage would be determined with a probabilistic fracture mechanic approach in which the

Table 4.1: Damage analysis of test result [66] with 0.01% of exceedance

$\Delta\sigma$ (MPa)	Fractile (%)	Damage Total = 4.286	Relative damage (%)	Cumulative damage (%)
32.3	1.70	0.000	0.0	0.0
35.6	13.70	0.111	2.6	2.6
38.8	30.70	0.242	5.7	8.2
42.0	49.70	0.404	9.4	17.7
45.2	65.69	0.493	11.5	29.2
48.5	78.69	0.565	13.2	42.3
51.7	86.69	0.480	11.2	53.5
54.9	92.69	0.710	16.6	70.1
58.2	95.69	0.422	9.8	79.9
61.4	97.69	0.331	7.7	87.7
64.6	98.69	0.193	4.5	92.2
67.9	99.29	0.134	3.1	95.3
71.1	99.69	0.103	2.4	97.7
74.3	99.89	0.059	1.4	99.0
77.6	99.99	0.033	0.8	99.8
103.4	100.00	0.008	0.2	100.0

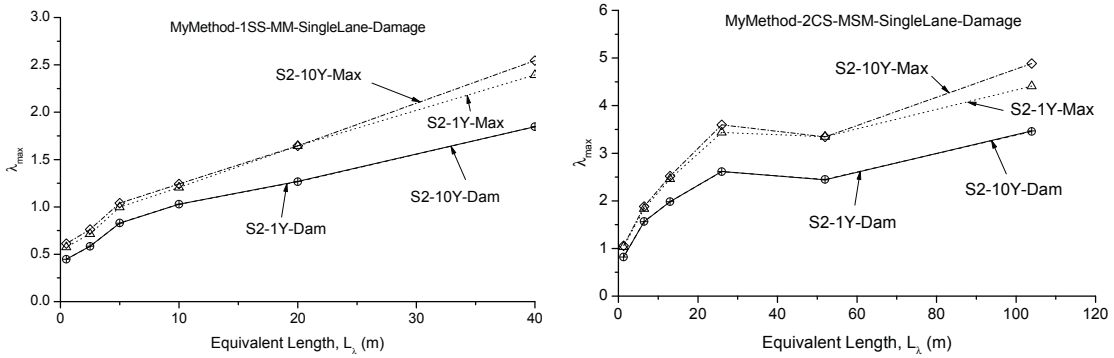

(a) Mid-moment of simple span bridges

(b) Mid-support moment of two-span bridges

Figure 4.19: Effect of diminishing the maximum stress range on λ_{max} for single lane traffic conditions

variation of parameters like initial crack size, stress range spectrum and stress coefficient factors are taken into account; however, such a probabilistic approach is not in the scope of the current study. In order to be in accordance with the Eurocodes, the same hypothesis is applied for the final traffic simulation (Chapter 6) in which the maximum stress range, $max(\Delta\sigma)$, for calculation of maximum damage equivalence factor, λ_{max}, is the value when the superior stress ranges produce less than 1% of total damage. The total damage can be determined with the main slope of S-N curve, i.e. $m = 3$ for steel details under direct stress.

The initial simulations for single lane traffic are re-employed to determine the maximum damage equivalence factors, λ_{max}, with the assumptions given above. The λ_{max}-factor for two cases of mid-moment of simple bridge and mid-support moment of two-span continuous bridge are shown in Figure 4.19. The traffic simulation parameters are similar to the ones described in Chapter 3. In Figure 4.19, the difference between 1 year and 10 years traffic simulations (S2-1Y-Max and S2-10Y-Max) is more perceptible when the absolute maximum stress range of spectrum considered for calculation of λ_{max}. However, considering 1%-damage-threshold as the maximum stress range, both 1 year and 10 years traffic simulations (S2-1Y-Dam and S2-10Y-Dam) give the same maximum damage equivalence factor, λ_{max}.

The maximum damage equivalence factor, λ_{max}, is also determined for double lane traffic conditions by applying the initial traffic simulations. The description of initial traffic simulation parameters for double traffic conditions are provided in Chapter 3. Figure 4.20 shows the results obtained for two cases of mid-moment of simple-span bridge and mid-support reaction of two-span continuous bridge. In Figure 4.20, considering 1%-damage-threshold for determining the maximum stress range leads to reduction of the λ_{max}-factor for both cases of unidirectional and bidirectional traffic (UD2080-Dam and BD5050-Dam) as expected. However, the effect of crossing and overtaking on bridges still causes having larger λ_{max} in comparison with the single lane traffic case (S2-10Y-SL-Dam). This point indicates even

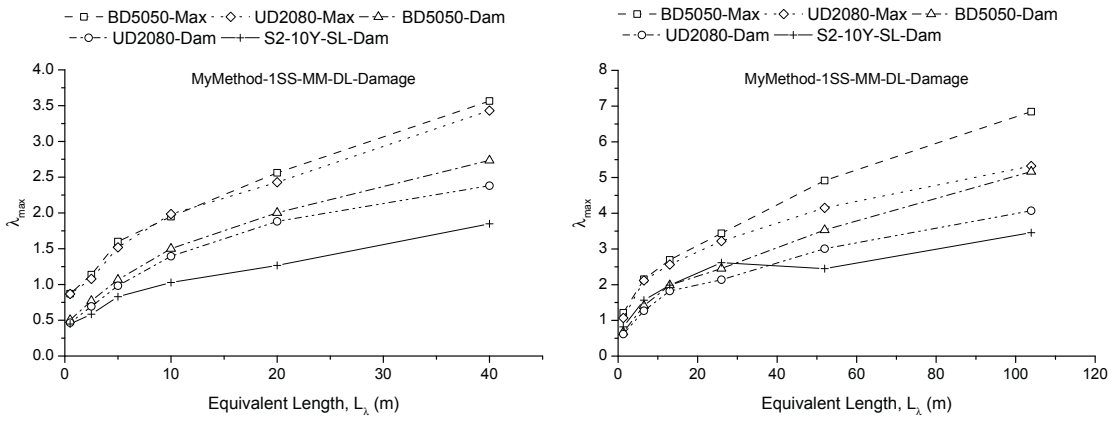

(a) Mid-moment of simple span bridges

(b) Mid-support moment of two-span bridges

Figure 4.20: Effect of diminishing the maximum stress range on λ_{max} for double lane traffic conditions

considering 1%-damage-threshold does not allow us to neglect the effect of crossing and overtaking on λ_{max}. In order to take into account the effect of double lane traffic on maximum damage equivalence factors, λ_{max} can be given separately for the double lane traffic conditions. This is explained in more detail in Chapter 6.

4.5 Damage equivalence factor for rebars in bridge decks

A bridge deck is subjected to internal forces due to traffic actions, where for the fatigue evaluation of their steel rebars, comparing to steel girders, arise two major issues. First, the fatigue resistance curve of the steel rebars is different from a steel detail. This issue is addressed in Chapter 6. Second, the internal forces in a rebar of a bridge deck are rather local and highly depend on the transverse location of vehicles' axle. The internal forces of slabs are typically represented by influence surface rather than influence line by positioning the unit load in two directions: along and across the slab.

For fatigue evaluation of rebars in a bridge deck, a general method for determining fatigue equivalent length from influence surface should be proposed. This method may also be

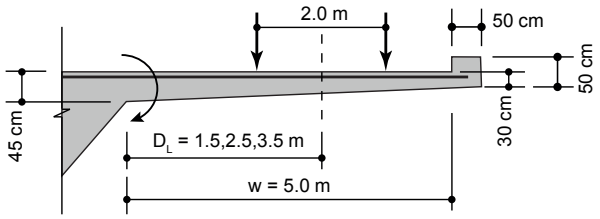

Figure 4.21: Dimensions of studied cantilever slab and traffic lane position

applied to all bridge elements in a general manner; the cross-beams or elements of orthotropic decks are other examples that can be given for its applications.

In order to explain how to determine fatigue equivalent length for any influence surface, the negative moment at the supporting edge of a cantilever slab is studied here as an example, though the similar approach can be applied for other cases. Figure 4.21 illustrates the example of the bridge deck with its superior rebar located in the slab. The cantilever length is 5 m and the slab thickness varies from 45 cm at the supporting edge to 30 cm near external edge. Also in some cases, a curb (with for example size of 50 by 50 cm) is existing at the external edge of the slab. It is assumed that traffic lanes are located at distance of 1.5, 2.5 and 3.5 m measure from cantilever support. The bridge comprises one simple span whose length varies from 5 m to 80 m.

For determining the negative moment at the cantilever support (about longitudinal direction of bridge) locating at the mid-span of the bridges, the bridges are analysed with finite element

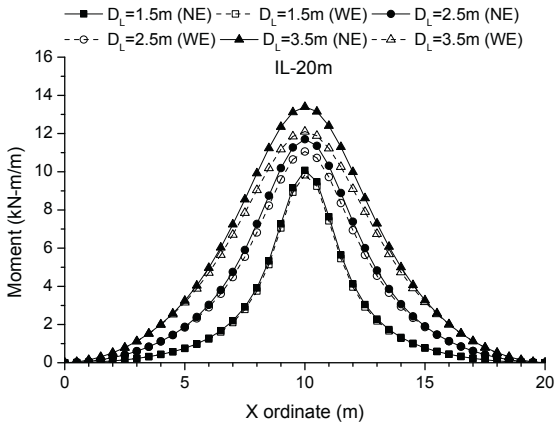

(a) Span length equal to 20 m

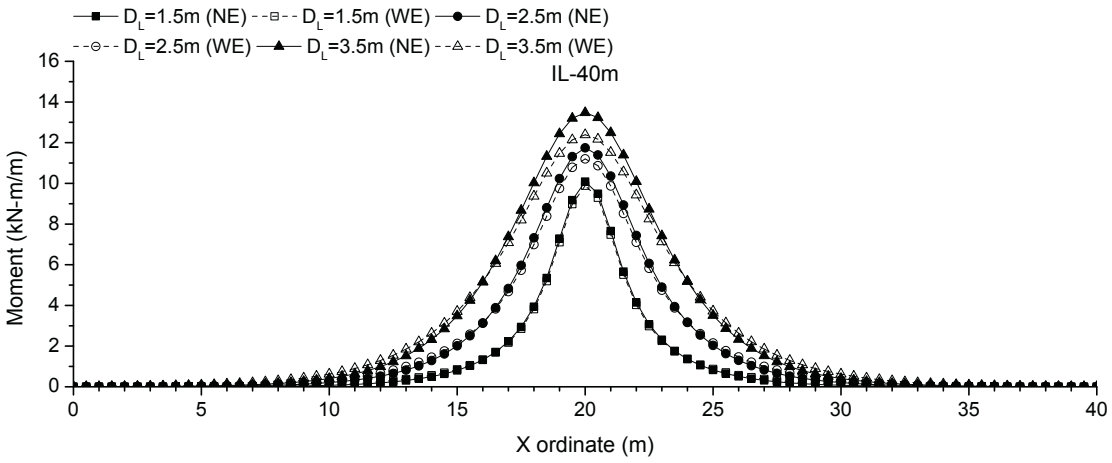

(b) Span length equal to 40 m

Figure 4.22: Transversal moment of cantilever slab according to lane position

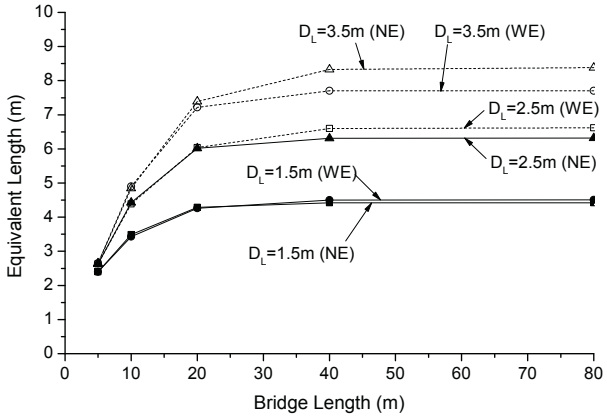

Figure 4.23: Relation between fatigue equivalent length and bridge length

models. The corresponding influence surfaces at this position are obtained from the analyses of all bridge cases. The main step in calculation of fatigue equivalent length is to separate the influence surfaces into group of influence lines for each traffic lane position, as shown in Figure 4.22 for two bridge cases with 20 m and 40 m bridge length. In Figure 4.22, as lane position approaches to the external edge, the maximum value of the response increases; also it can be observed that the stiffness of the edge element (curb) causes a slight reduction of the influence lines maximum value. Comparing the two cases of 20 m and 40 m span length, the maximum value of the influence line as well as the shape of all influence lines remain about the same with increasing span length.

The fatigue equivalent length for the bridge cases is determined trying to use the proposition given in Equation 4.14. Figure 4.23 illustrates the relation between bridge length and L_λ for three lateral lane positions, D_L, and separately for two external edge conditions, with edge (WE) and without edge (NE). The definition of L_λ is sound because of the following three reasons. Firstly, the L_λ values calculated for different bridge cases is small (between about 3.5 m to 8.5 m). This is reasonably in line with expectation that the fatigue damage of rebars is mostly due to local actions, i.e. axle loads. Secondly, the fatigue equivalent length increases with bridge length up to about 20 m, and it remains constant for larger lengths from 20 m. And thirdly, it can be observed that the distribution of influence line along length is getting wider as the distance of the lane to the support (D_L) increases. This means that the L_λ should also grow with increasing of D_L as it happens in the obtained values (see Fig. 4.23).

Based on the EN1991-2 [25], when the transverse location of vehicles has an important effect on internal forces, a statistical distribution of the transverse location should be taken into account in accordance with Figure 4.24. In this case, the damage equivalence factor, λ_1, can be calculated as follows:

$$\lambda_1 = \left[\sum_{i=1}^{n} \frac{f_i}{100} \times \left(\frac{\lambda_{1,i} \times \Delta\sigma_i}{\lambda_{1,1} \times \Delta\sigma_1} \right)^m \right]^{1/m} \tag{4.32}$$

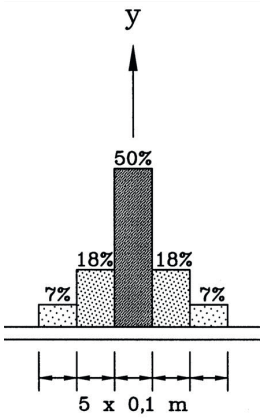

Figure 4.24: Frequency distribution of transverse location of vehicles based on EN1991-2 [25]

where $\Delta\sigma_i$ is the stress range due to traffic on the i^{th} transverse location, $\lambda_{1,i}$ is the partial damage equivalence factor (should be determined like λ_1 for each transverse location), f_i is the frequency corresponding to the transverse location (according to the values given in Figure 4.24) and m is the effective slope of S-N curve which is a value between 4 and 7 for steel rebars. For determining $\lambda_{1,i}$ the fatigue equivalent length can be obtained from Equation 4.14 using the influence line corresponding to the transverse location i, and total number of heavy vehicles in the lane (i.e. 100 percent) should be considered. Although Equation 4.32 is provided for slabs, it can be applied for other cases like cross beams or elements of orthotropic decks. In these cases, the effective slope of S-N curve is a value between 3 and 5 (for steel details under direct stress).

4.6 Summary

In the current chapter, the main shortcomings of damage equivalence factors are firstly summarized. Then the main limitations to improve these shortcomings are explained. In order to come up with a proper solution for improving the accuracy of damage equivalence factors, an analytical approach is considered.

First, the equivalent force at two million cycles is determined for some imaginary influence lines, each of them representing a characteristic feature of real influence lines. Then, using vehicle-by-vehicle traffic simulations, the equivalent force range is determined by damage accumulation. The results of the imaginary cases are interpreted in the three domains corresponding to very short span lengths, very long span lengths and mid-range span lengths. It is justified how the equivalent force range for very short span lengths can be obtained by damage summation from each axle response. Also, for very long span lengths, it is observed that the damage summation from gross vehicle weight response bears the equivalent force range assuming the number of repetitions in influence line is 1.

For mid-span lengths, an *equivalent vehicle* which causes the same effect as passage of all

heavy vehicle traffic is defined. This equivalent vehicle is simplified as a uniformly distributed load over a defined length (found to be about 10 m). The equivalent force range at two million cycles is estimated by the equivalent vehicle as well as by the uniformly distributed load with a defined length and the results compared with the equivalent force range obtained from simulations. For the unit lengths larger than 20 m, it is found that the equivalent vehicle is representative of all heavy vehicles, since it provides a good approximation of the equivalent force range. With a slight degree of inaccuracy, the latter point also applies to the uniformly distributed load.

According to the analytical solutions, a new fatigue equivalent length definition as well as fatigue load model is proposed. The proposed fatigue equivalent length can be defined uniquely and simply for any influence line. For a given influence line, the fatigue equivalent length equals the area under the influence line divided by the difference between the maximum and minimum values of the influence line. The proposed fatigue load model comprises a single axle weighting 480 kN. Using these propositions, the initial traffic simulations are re-employed and the damage equivalence factors determined. The results show that the proposed parameters reduce the scatter in the damage equivalence factors for different influence lines (R^2 is improved up to 0.97). In order to generalize the application of proposed fatigue equivalent length and the corresponding damage equivalence factor, a new partial damage equivalence factor, λ_5, is also defined for taking into account the effect of repetition in influence line. Although λ_5 is very close to unity in typical cases, it is important to consider it for the influence lines that have more than one repetition, and thus ensure the general reliability of the new definition proposed.

The current code λ_4 neglects the effect of simultaneous passage of trucks on bridges. Based on the side-by-side position of trucks, a modification to the λ_4-factor for the SIA codes as well as the Eurocodes is proposed. Then, for the different influence lines, λ_4 is obtained from initial simulations, based on the proposed modifications for fatigue equivalent length and fatigue load model. The results allows the crossing (or overtaking) ratio, c, to be conservatively determined as 3% and 16% respectively for the simulated unidirectional and bidirectional traffic conditions.

For maximum damage equivalence factor, Eurocode allows a few stress ranges above CAFL as long as these stress ranges produce less than 1% of total damage (i.e. this is the definition of the “frequent” load). Although this assumption is not always safe when compared to the experimental test results, it is accepted in the current study in order to have the same safety level as the Eurocodes. Applying the 1%-damage-threshold for determining the maximum stress range, it is observed that λ_{max} diminishes for both single lane and double lane traffic conditions. However, the λ_{max}-factors obtained for double lane traffic conditions are still larger than single lane traffic, indicating the effect of crossing and overtaking should be accounted in λ_{max} as well.

In order to exemplify determination of the fatigue equivalent length for 3D influence surfaces

rather than influence line, the internal forces in transverse rebars at support of a cantilever slab are also studied. Several bridge cases with span length ranging from 5 to 80 m are analysed with FE models and the influence surfaces for each case is obtained. The new definition of fatigue equivalent length is applied to these cases and the general validity of the proposition is shown. An equation for determining λ_1 is also proposed for the cases that statistical distribution of the transverse location of vehicles is important, e.g. rebars of slabs and elements of orthotropic decks.

5 Traffic simulation parameters

In the current chapter, the most important parameters needed for modelling traffics are specified by analysing the available traffic data mostly from measurements in Switzerland. A thorough study on these parameters is carried out by Maddah et al. [54], and in the current chapter, the main results of that study are briefly provided. For more detailed description, refer to the original report.

5.1 Traffic measurement methods in Switzerland

For many years, the Swiss Federal Roads Authority has been carrying out permanent automatic traffic counts and measurements, as well as periodical manual traffic counts, within the scope of the on-going statistical surveys conducted by the federal government. These traffic counts are the responsibility of the Traffic Monitoring section of the Road Networks division. These measurements include Swiss automatic road traffic counts (SARTC), Swiss road traffic census (SRTC), Weigh-in-Motion (WIM) and traffic development. However, only Swiss road traffic census (SRTC) and Weigh-in-Motion (WIM) can identify and record the traffics separately by vehicle category. Therefore, the determination of traffic simulation parameters are limited to analyse of these two measurement method.

Swiss Road Traffic Census (SRTC) counts traffic by category which has been carried out since 1955 every five years in line with the recommendation of the UN European Domestic Transport Committee. Today, traffic censuses are carried out in around thirty countries on the basis of uniform guidelines and criteria. The network for the 2005 Swiss Road Traffic Census includes 453 counting stations. Electronic counting devices from the Automatic Traffic Census network are to be used at 175 of these stations, and these are now programmed to allocate each vehicle to the corresponding category [81]. This measurement records neither vehicle's weight, nor axles' properties; nevertheless, it has been done in many locations, which allows us to determine some parameters like daily traffic distribution of vehicles and trucks as well as annual truck traffic ratio for different road types. The results of these measurements are in accordance with the WIM measurement of 2005 in the common locations. Figure 5.1 shows

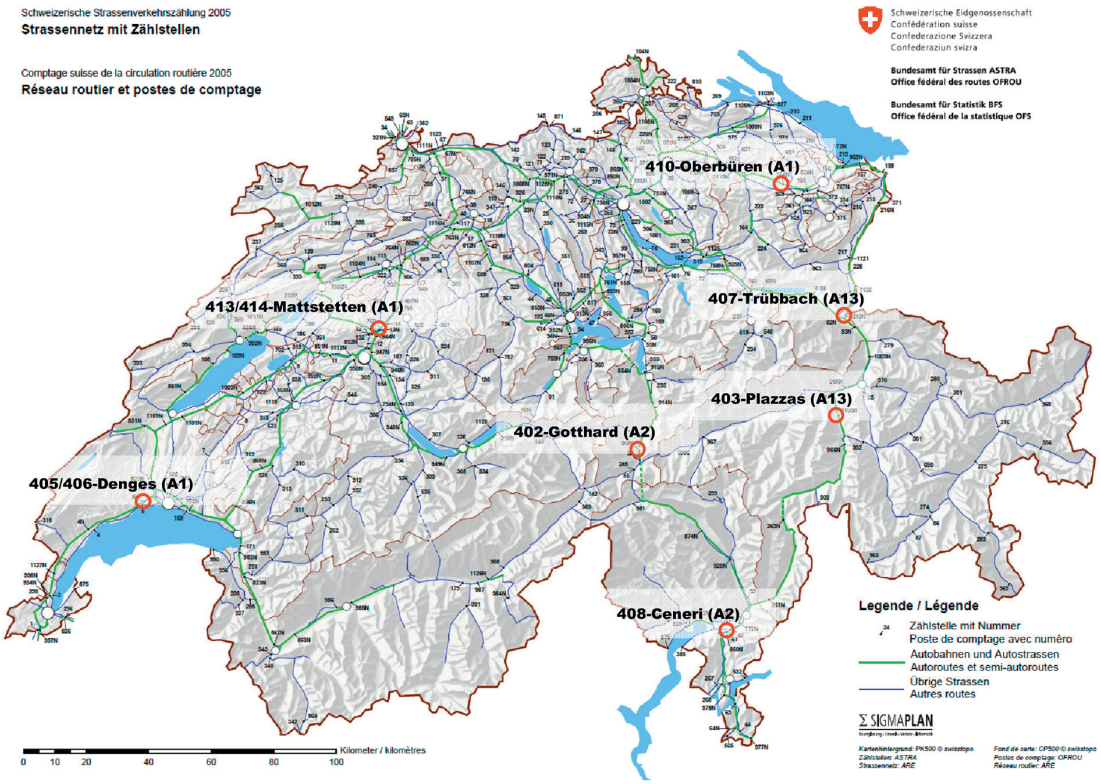

Figure 5.1: Map of Swiss Weight-In-Motion (WIM) stations in 2005 [6]

the map of the WIM stations in 2005.

5.2 Main traffic parameters

The main parameters required for modelling of traffic can be divided in three groups: traffic flow, future traffic development and heavy vehicles properties. The traffic flow parameters are: Hourly Truck Traffic Variations (HTTV), Hourly Traffic Variations (HTV), average proportion of trucks in traffic (P_T), truck traffic distribution by lane and GVW distribution. Average Daily Truck Traffic (ADTT) and Average Gross Weight of Trucks (AGWT) are also important parameters of the traffic flow; however, ADTT is given by the codes and it is considered as an input, and AGWT is a function of GVW distribution. Nevertheless, variation of both parameters are evaluated particularly with respect to the future traffic development.

For the future traffic, hypothetically, the development of each traffic parameter should be estimated for the whole fatigue design life of bridges which is typically 100 years. Whereas the traffic development can be influenced by many factors and such estimation is unjustified. Therefore, all traffic simulation parameters are assumed to remain constant for the whole period. In the future traffic development part, a simplified estimation of future trend for two main aspects of the traffic flow, i.e. ADTT and AGWT, are compared with the given values in

the codes.

The model of traffic stream is composed of light vehicles (cars) and heavy vehicles passing over a bridge. The heavy vehicles are classified based on the number of axles and geometry. The principal heavy vehicles' properties of each class are: geometry, contribution in traffic, axles weight and distance.

It is important to mention, there is a contradiction in the definition of trucks. On the one hand, the SIA261 [79] takes any vehicle with weight over 35 kN as truck. In fact, this definition might mislead that some overweighed cars counted as truck. On the other hand, in the EN1991-2 [25], the minimum weight of trucks (denoted as heavy vehicles) is 100 kN. Moreover, Meystre and Hirt [59] assume the minimum truck weight is based on the number of axles where the minimum weight can be obtained from $(n+4) \times 10$, where n is the number of axles. For example, the minimum weight of a 4-axle truck is taken as 80 kN.

In general, the trucks with lower weight would have a very slight effect in the fatigue damage sum since the stress cycles due to passage of these "light-weight" trucks over bridge is expected to be lower than cut-off limit. However, the different definitions results in confusion of counting and calculations. At any rate in this thesis, the EN1991-2 [25] definition of heavy vehicle, in which the minimum GVW is 100 kN, is accepted and will be applied in the simulations. This decision will be justified in Section 5.3.5. Since SRTC measurements are based on the truck definition and because truck weight is not measured, where possible, the analysed parameters are modified using the corresponding WIM measurements. In the following sections, the term of "truck" is used for any vehicle with the weight over 35 kN and the term of "heavy vehicle" is used for trucks over 100 kN.

5.3 Swiss Traffic flow

5.3.1 Hourly Truck Traffic Variations

Based on the measurement of Swiss Road Traffic Census (SRTC) the number of vehicles passing during a day can be estimated. SRTC measurement distinguishes six categories of vehicles which are [81]:

- Motorcycles: motorcycles, tricycles, scooters (excluding motorcycles)
- Passenger cars: passenger cars with trailers, minibuses
- Cars, Bus coaches (buses), buses (including bus routes)
- Car Delivery: light automobiles (also with trailer) for transport of goods and whose GVW not exceeding 35 kN, and very large passenger cars, minibuses
- Trucks: motor vehicles used to transport heavy cargo and a GVW exceeding 35 kN, without a trailer or semi-trailer

- Road trains and articulated vehicles: heavy motor vehicles used to transport goods and whose GVW exceeds 35 kN with trailer and semitrailer.

Two last categories with GVW over 35 kN are considered as trucks. The Hourly Truck Traffic Variations (HTTV) in holidays in comparison with weekdays is reported by Maddah et al. [54] for different highway locations. Generally, the most passage of trucks is during the day and it is decreasing sharply during the night. Truck drivers are not allowed to drive on Sundays and holidays except with an especial permission and they tend to not work on Saturdays. Therefore, the truck traffic in weekdays is noticeably more than holidays, which allows us simulating truck traffic on weekdays only, and neglecting the truck circulation on weekends and holidays.

The Average Weekday Truck Traffic (AWTT) is different in each station. In order to find appropriate HTTV for simulations, the variations are normalized by dividing them by the corresponding AWTT for all stations. Figure 5.2 represents the normalized daily truck traffic on weekdays; the average variations of stations is also Shown in Figure 5.2, which helps to find a simplified pattern of HTTV as a percentage of AWTT. The same pattern is applicable for heavy vehicle traffic assuming the Hourly Heavy Vehicle Traffic Variations (HHVTV) is similar to HTTV.

The preliminary fatigue analysis of bridges, Chapter 3, shows the HTTV with two peaks in compare with a flat variation in 10 hours gives slightly greater damage sum for bridges with longer span. It tempts to put forward higher peaks for the proposed pattern; however, considering future traffic growth, the maximum capacity of roadways is limited. As a result, the future trend of HTTV will be flatter than current one, and the proposed pattern remains conservative.

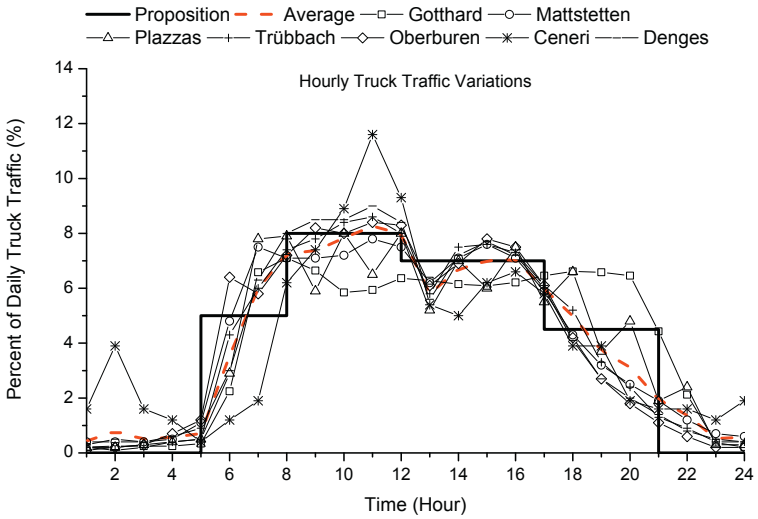

Figure 5.2: Normalized Hourly Truck Traffic Variations (HTTV) of the stations on weekdays and the proposed pattern

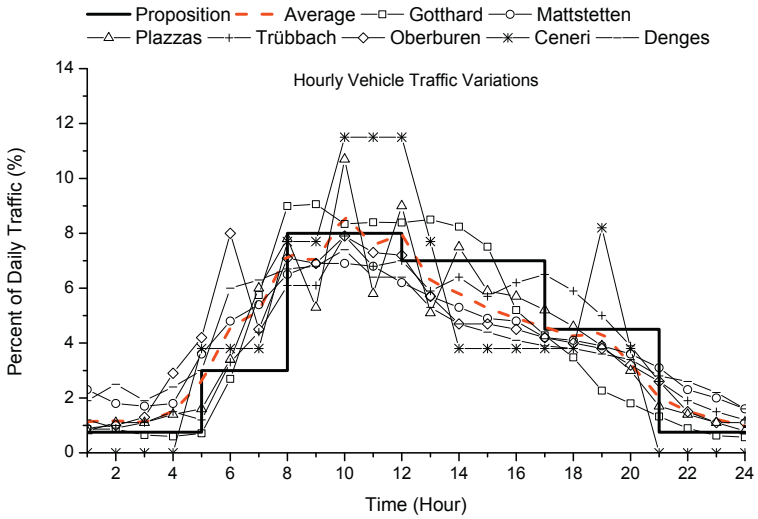

Figure 5.3: Normalized Hourly Traffic Variations (HTV) of stations on weekdays and the proposed pattern

5.3.2 Hourly Traffic Variations

Both SRT and SRTC [81] can be used for determining Hourly Traffic Variations (HTV). For the sake of integrity with the other sections the SRTC of 2005 has been applied. In reference [54], the HTV on weekdays in comparison with weekend and holidays is reported for the same measurement stations.

Similar to the Hourly Truck Traffic Variations (HTTV), it is possible to find the normalized Hourly Traffic Variations (HTV) by dividing the variations by corresponding Annual Average Weekdays Traffic (AAWT) for all stations. Figure 5.3 represents the normalized HTV on weekdays. In addition, the average variations of stations is shown in Figure 5.3 which facilitates finding a simplified pattern of HTV. The area under the normalized HTV curves is the AAWT which kept the same for the proposed HTV pattern as well.

Unlike the truck traffic, the Annual Average Daily Traffic (AADT) is almost equal to the Annual Average Weekday Traffic (AAWT) at the different stations, as given in Table 5.1. Whereas it is

Table 5.1: Comparison of AADT with AAWT and calculation of the annual weekday traffic ratio

Station	AAWT (Vehicle / Day)	AADT	Ratio (AAWT × 254 / AADT × 365)
Götthard	15009	16069	0.65
Mattstetten	75323	73637	0.71
Plazzas	13982	14768	0.66
Trübbach	31481	31120	0.7
Oberbüren	50940	48489	0.73
Ceneri	11513	10750	0.75
Denges	84946	80591	0.73
Average Ratio			0.7

decided to perform the simulations on weekdays only, the annual traffic on weekdays should be distinguished. The number of weekdays is 254 in the year 2005. In Table 5.1, the annual weekdays traffic as a ratio of the annual traffic for each station is calculated . Table 5.1 shows, averagely, 70 percent of the annual traffic is circulating on weekdays.

5.3.3 Proportion of trucks in the traffic stream

The light-weight traffic has little effect in the fatigue damage calculation because its weight causes very low internal forces which are expected to be below the fatigue cut-off limit. Nevertheless, it determines the distance between trucks.

The Hourly Variations of Heavy Vehicles Proportion in Traffic (HVHVPT) is a function of HTV, HHVTV, and the average proportion of heavy vehicles in traffic (P_{HV}). In Section 5.3.2 and in Section 5.3.1, the normalized pattern of HTV as a ratio of AAWT and normalized pattern of HHVTV as a ratio of AWHVT (assumed to be similar to the normalized pattern of HTTV) are determined. However, the average proportion of heavy vehicles in the traffic (P_{HV}) still needs to be determined.

The average proportion of trucks in traffic (P_T) as well as the average proportion of heavy vehicles in traffic (P_{HV}) are given in Table 5.2 for the different WIM stations from 2005 to 2009. Generally, P_T as well as P_{HV} are varying considerably depending on the location. The Götthard station has the highest and Denges has the lowest proportions. At any rate, the simulations can be done once with P_{HV} = 7.0% and again with P_{HV} = 17.5%, which are the average and the maximum measured P_{HV}. Since the simulations will be done for weekdays only, the average proportion of heavy vehicles in traffic on weekdays ($P_{HV,W}$) should be calculated by dividing P_{HV} by 0.7. To put is simply, the $P_{HV,W}$ can be considered as 25 and 10 percent (as the average and the maximum values) for the simulations. It is now possible to find HVHVPT on weekdays as shown in Figure 5.4; the HVHVPT curves of different stations are also printed for comparison purpose.

Table 5.2: The average proportion of trucks and heavy vehicles in traffic (P_T and P_{HV})

Year	Denges	Mattstetten	Oberbüren	Schafisheim	Ceneri	Götthard	Trübbach
Average Proportion of Trucks in the Traffic P_T (%)							
2005	4	9.1	7.9	–	11.1	18.3	7.1
2006	4	9.7	7.9	10.9	11.1	19.8	7.1
2007	4	9.2	8	9.7	10	18.4	7.3
2009	3.8	9	7.1	9.4	9.4	16.9	–
Average Proportion of Heavy Vehicles in the Traffic P_{HV} (%)							
2005	2.7	6.7	5.2		9.1	16	4.8
2006	2.7	6.8	5.4	7.6	9.1	17.3	4.7
2007	2.7	6.7	5.6	6.7	8.3	16	4.8
2009	2.6	6.5	5	6.6	7.7	14	

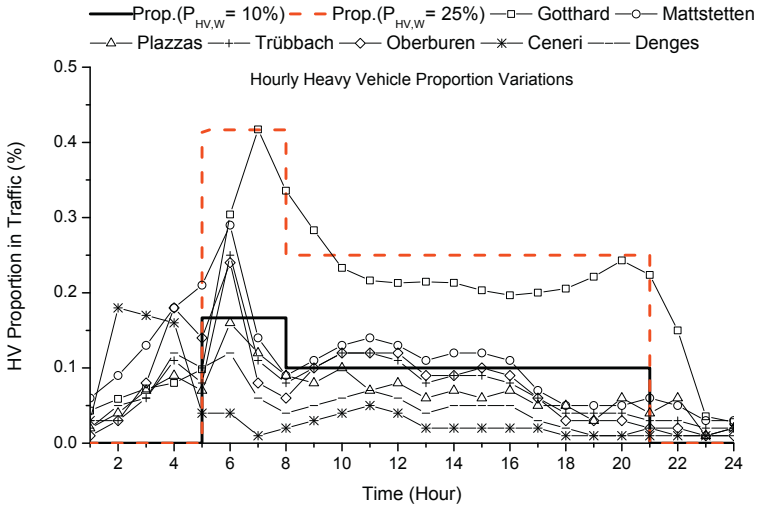

Figure 5.4: Hourly Variations of Heavy Vehicles Proportion in Traffic (HVHVPT) of stations on weekdays and the proposed pattern

5.3.4 Truck traffic distribution per lane

Among different WIM measurements in Switzerland on 2005, the fast lane measurement on Trübbach, Ceneri and Oberbüren is available. Whereas the WIM measurement of Mattstetten is available for only 60 days in the year 2005 (due to device changes), it is excluded here. Besides, the stations of Götthard and Plaza have only two lanes in different directions, and in Denges, there was no measurement facility installed on the fast lanes.

The Average Daily Truck Traffic (ADTT) as well as Average Daily Heavy Vehicle Traffic (ADHVT) in each lane are given in Table 5.3, and the traffic in fast lane as a ratio of traffic in slow lane is calculated. The station of Ceneri has the maximum fast lane truck and heavy vehicle traffic ratio which is mostly because it has three lanes in the direction of Götthard. The third lane

Table 5.3: Fast lane truck and heavy vehicle traffic for some Swiss WIM stations

Station	Average Daily Truck Traffic				Fast Lane / Slow Lane	
	Slow Lane 1	Fast Lane 1	Slow Lane 2	Fast Lane 2	Ratio 1	Ratio 2
Denges	1708	-	-	1503	-	-
Oberbüren	1828	183	145	1675	10.0%	8.7%
Ceneri	1683	283	186	1989	16.8%	9.3%
Götthard	1414	-	-	1530	-	-
Trübbach	1067	55	59	1029	5.2%	5.7%
Plaza	544	-	-	521	-	-
	Average Daily Heavy Vehicle Traffic				Fast Lane / Slow Lane	
Denges	1078	-	-	1026	-	-
Oberbüren	1217	22	26	1197	1.8%	2.1%
Ceneri	1402	196	55	1708	14.0%	3.2%
Götthard	1349	-	-	1217	-	-
Trübbach	736	11	21	709	1.5%	3.0%
Plaza	381	-	-	382		

allows heavy vehicles to circulate in the second lane without perturbing the passage of light vehicles. The SIA261 [79] does not give any value for the fast lane traffic, but the EN1991-2 [25] proposes to take into account 10 percent of slow lane heavy vehicle traffic for the fast lane, which is lower than the maximum measured value in Ceneri with 14 percent of fast lane heavy vehicle traffic ratio. The simulations can be performed with the two following ratios: 10 percent and 20 percent, to compare the ratio effect on fatigue damage sum. It is important to note that the traffic distribution in the lanes can be completely different in special conditions, e.g. where a bridge is close to an interchange; however, these conditions will not be considered in the current study.

5.3.5 Gross Vehicle Weight (GVW)

The GVW distributions are obtained from WIM measurements for different stations. The detailed GVW distribution of each station is reported by Maddah et al. [54]. Figure 5.5 summarizes the GVW distribution of stations in 2005. In Figure 5.5, two main types of GVW distribution curves can be identified: fist, international i.e. Ceneri and Götthard; second, national i.e. Denges, Mattstetten. Therefore, it can be proposed to apply Götthard as an international and Mattstetten as a national GVW distribution for simulations.

In Figure 5.5 from right to left as the GVW decreases, the GVW distribution curves soar up remarkably from 60 kN. This is due to either vast amount of over-weighted cars or of light trucks. In any case, it clears up the light trucks and overweighed cars are mixed up in this domain. To prevent confusion in counting, and because the light trucks (or over weighted cars) are not causing significant fatigue damages to bridges, the heavy vehicles with the minimum

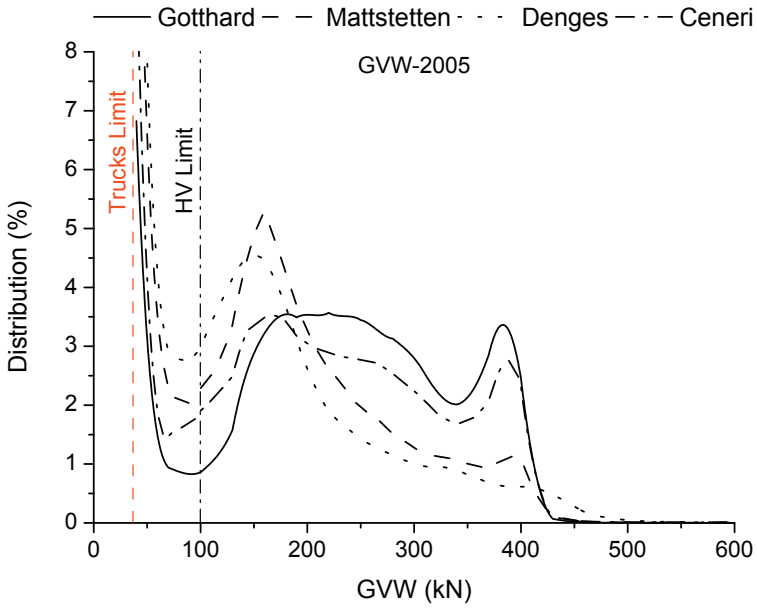

Figure 5.5: GVW distribution of some WIM stations measured in 2005

weight of 100 kN will be used in the simulations (as mentioned before) which is in accordance with the definition of the EN1991-2 [25]. Though average GVW is not given in the SIA codes, by replacing annual number of trucks with the same number of heavy vehicles, the average GVW of trucks slightly increases. Nevertheless, average GVW for the traffic simulations are given and it can be adapted by the partial damage equivalence factor, λ_2.

5.4 European Traffic flow

The simulation parameters proposed in the current thesis are based on the traffic measurements in Switzerland. However, some values for fatigue design of bridges given in the SIA codes [79, 80] (e.g. annual truck traffic) originate from the EN1993-2 [27]; therefore, the current section resume the WIM measurements constituting the basis of the European codes.

The basis for preparation of the traffic loads model in the EN1993-2 [27] has been developed in parallel at various locations in Europe. The available records of European traffic were mainly the results of large measurements campaign performed between 1977 and 1988 on several roads in Europe [73]. Recorded daily truck traffic flows in slows lane were varying between 1000 and 8000 trucks on highways and between 600 to 1500 trucks on main roads. Table 5.4 gives samples of traffic flows per lane recorded at different European stations which comprise different types of roads (e.g. highway and roadway). The Annual Average Daily Traffic (AADT) as well as Average Daily Truck Traffic (ADTT) is significantly varying station by station.

The maximum truck traffic flow was recorded in 1980 in Germany (Limburger Bahn) with 8600 trucks per day per slow lane [73]. Such a traffic flow results in annual truck traffic of about 3'140'000 (per slow lane) that is more than 50% higher than the corresponding design value in the Eurocode. The annual truck traffic per slow lane at the Auxerre station, in 1986, was about 960'000 (2630×365) which is less than the corresponding design value for highways given in the Eurocode.

In Figure 5.6, the accumulated distribution of GVW and axle loads are given, where n_{30} is the number of vehicles with GVW over 30 kN and similarly n_{10} is the number of axles with load

Table 5.4: Traffic flows per lane at some European stations (adopted from [76] and [73])

Station	Lane	Year	AADT	ADTT
Brohltal (D)	Slow	1984	11126	4793
Garonor (F)	Slow	1984	-	3686
Auxerre (F)	Slow	1986	8158	2630
Auxerre (F)	Fast	1986	1664	153
Forth (GB)	Slow	1978	5097	1250
Doxey (GB)	Slow + Fast	1985	(34500)	(14500)
Fiano R. (I)	Slow	1987	(8500)	(4000)
Piacenza (I)	Slow	1987	(8500)	(5000)
Sasso M. (I)	Slow	1987	(7500)	(3500)

* The numbers in parentheses are estimated.

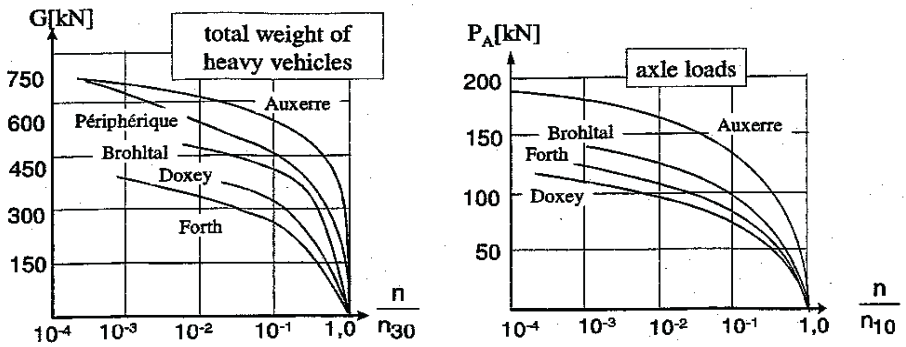

Figure 5.6: Accumulated distribution of GVW and axle load at various European stations [76]

over 10 kN. Figure 5.6 sets out the Auxerre traffic, though does not exhibit the largest GVW and axle loads, has the highest frequency of large GVW and axle loads; this is particularly due to the high frequency of heavy trucks in the traffic.

Eventually, the data from the Auxerre traffic were selected as a basis for the development of the Eurocode traffic load model [27] because of the following reasons:

- the proportion of trucks in traffic is 32% in slow lane and 10% in fast lane and in relation to other stations is rather high,
- the portion of loaded trucks from all trucks is 66% and hence exemplify the trend for an improved transport management,
- data were fully recorded for a large time period for both slow lane and fast lane in a 4-lane highway.

It must be finally mentioned that European traffics exist, which are more aggressive than the Auxerre traffic; nevertheless, such traffics are not very significant since they depend on local situations and are hard to be generalized to Swiss traffic.

5.5 Future traffic trend

The approximation of future traffic trend over 100 years is not within the scope of the current study. Consequently, the traffic given in the code will be applied for the simulations. However, the given values of codes are compared here with a very simplified estimation of future traffic trend assuming the traffic grows linearly with the same rate as the past traffic trend.

The traffic development has been determined in Switzerland from 1990 on Rapp Trans AG [72]. For instance, the Annual Average Daily Traffic (AADT) and the Annual Average Weekday Traffic (AAWT) has been increased by 30.2 and 39.9 percent respectively from 1990 to 2009. But, this measurement method does not give any information about the trucks traffic development.

Generally, the capacity of highways is limited and, in fact, the traffic volume will stabilize at a certain level. The theoretical capacity [39] of a highway with two lanes in each direction is about 4120 (veh./hour/dir.) in the ideal conditions: e.g. 120-km/h base free flow speed, 3.6-m-wide lanes and level terrain. The maximum measured traffic corresponds to Denges with ADTT of 42'000 (veh./dir.), which theoretically takes about 10 hours to pass with the maximum theoretical capacity of the highway. However, the daily traffic flow is generally less than the sum of the theoretical hourly capacity due to either lower demand in certain hours or congested traffic conditions.

The truck traffic trend is calculated using the available WIM measurements. Two stations of Götthard and Mattstetten started working in 1994, and the measurement data of Mattstetten is available since 1995. The quality of measurements in Mattstetten had been very low because of a technical installation problem, unlike the Götthard station which had more reliable results. However, the file format of these measurements is unknown to the author and it is decided to apply the more recent measurements starting from 2003 when six more WIM stations were installed.

The two most important aspects of traffic trend are: the Average Daily Truck and Heavy Vehicle Traffic (ADTT, ADHVT), and the Average Gross Weight of Trucks and Heavy Vehicles (AGWT and AGWHV). These two aspects are studied separately in the following sections.

5.5.1 Average Daily Truck and Heavy Vehicle Traffic

The Average Daily Truck Traffic (ADTT) and the Average Daily Heavy Vehicle Traffic (ADHVT) are reported by Maddah et al. [54] for the available WIM measurement stations between 2003 and 2009. ADTT and ADHVT are based on traffic on both directions, and where applicable, in both lanes. In order to find the development index, the traffic of each station is divided by its value in the year 2003 as a base point. The obtained value for annual development index of ADTT and ADHVT are 0.35% and 0.40% respectively.

The ADTT based on the SIA261 [79] is 2'000'000 per direction for highways, which gives the ADTT of 5480 per direction. Assuming a linear growth over 100 years (as the design life), the ADTT in 50 years is the average value. The ADTT will thus increase by $50 \times 0.35\% = 17.5\%$. The maximum measured ADTT corresponds to Mattstetten with 3540 trucks per direction, which will probably increase up to $3540 \times 1.175 = 4160$ after 50 years, and it is still lower than the ADTT given by the SIA261 [79] (5480 veh./dir.).

In addition, the annual number of heavy vehicles based on the EN1991-2 [25] is 2'000'000 per slow lane per year. Assuming 10 percent of the slow lane traffic passing on the fast lane, the ADHVT of the EN1991-2 [25] is 6027 (veh./dir.). Similar to the ADTT, the ADHVT will increase by $50 \times 0.40\% = 20.0\%$. The maximum measured ADHVT corresponds to Mattstetten with 2520 (veh./dir.), which will increase up to $2520 \times 1.20 = 3024$ after 50 years, and it is lower than the half of the ADHVT given by the EN1991-2 [25].

5.5.2 Average Gross Weight of Trucks and Heavy Vehicles

Another important aspect of the traffic trend is Average Gross Weight of Trucks and Heavy Vehicles (AGWT and AGWHV). Since the damage accumulation using miner rule depends on the slope of the S-N curve, the EN1993-2 [27] proposes to calculate the AGWT and AGWHV with the power of 5 as given by Equation 3.7. The annual development index of AGWT and AGWHV are defined as 0.078% and 0.027 % respectively [54].

The SIA263 [80] does not give AGWT directly, but it applies three types of trucks with various weights and different contributions, load model D076(40) [84], where AGWT of these three trucks is 314 kN (see Appendix A.1). Assuming a linear growth over 100 years (as the design life) AGWT in 50 years is the average value. The AGWT will thus increase by $50 \times 0.078\% = 3.9\%$. The maximum measured AGWT corresponds to Götthard with $Q_m = 303$ kN, which will grow up to $303 \times 1.04 = 315.1$ kN in 50 years, and it is slightly higher than AGWT given by the SIA code (314 kN).

Furthermore, AGWHV based on the [27] is 480 kN. Similar to AGWT, AGWHV will increase by $50 \times 0.027\% = 1.4\%$. The maximum measured AGWHV corresponds to Götthard with $Q_m = 313$ kN, which will grow up to $313 \times 1.01 = 316$ kN in 50 years, which is it about 20 percent lower than the AGWHV given by the EN1993-2 [27].

5.6 Heavy vehicles properties

Traffic simulations will be performed by WinQSIM program which was initially developed by Meystre and Hirt [59]. This program is adapted for the purpose of fatigue analysis in order to perform the flow traffic simulations and extract cycles from bridge responses. For the vehicles classification, the same rules will apply, except the minimum GVW of heavy vehicles will be 100 kN, specifically, vehicles with the GVW below 100 kN will also be considered as cars. Besides, the vehicle type 23 is added in the vehicle classes. More description of this program and the detailed specifications of the heavy vehicles, including geometry, axle load and weight, are provided in Appendix B.

The schematic geometry of different heavy vehicles classes as well as their contributions in the traffic of Götthard (2009) and Mattstetten (2009) are shown in Table 5.5. The other heavy vehicle properties like GVW, geometry, axles weight distribution, etc. are updated based on the traffic of Götthard and Mattstetten 2009. The measured as well as the applied statistical distributions for GVW, the axles weight and the distances between axles of each vehicle class for both station of Götthard (2009) and Mattstetten (2009) are reported by Maddah et al. [54]. For more explanation regarding the heavy vehicles properties and the assumptions of WinQSIM program see Appendix B.

Table 5.5: Heavy vehicles geometry and contributions

Type	Geometry	Contributions (%)	
		Götthard	Mattstetten
11		9.93	16.02
12		3.90	4.73
22		0.57	3.21
23		0.37	0.81
111		0.56	3.11
1111r		3.69	18.75
112r		5.41	2.45
1211r	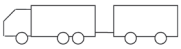	2.71	4.76
122		6.13	1.10
1112r		0.42	0.47
112a		11.44	22.06
113a		54.64	22.29
123a		0.23	0.25

5.7 Summary

Truck traffic simulations over bridges need to be based on realistic parameters. The main goal of the current chapter is to propose the appropriate parameters for a free flow traffic condition with the aim of study on fatigue assessment of bridges.

The current traffic flow parameters as well as the future traffic development are estimated based on the measurement records. Besides in this study, to prevent confusion in the counting of over-weighted cars as trucks (with GVW over 35 kN), it is decided to define heavy vehicles with GVW over 100 kN. Where possible, the traffic simulation parameters for both definitions of trucks and heavy vehicles are separately determined. In addition, it is decided to perform the traffic simulations for weekdays only, since the truck traffic on weekend and holidays is negligible in comparison with weekdays.

The main parameters studied of the traffic flow are: Hourly Heavy Vehicle Traffic Variations (HHVTV), Hourly Traffic Variations (HTV), Hourly Variations of Heavy Vehicles Proportion in Traffic (HVHVPT), proportion of heavy vehicles in traffic (P_{HV}), heavy vehicle traffic dis-

tribution by lane, and GVW distribution. Each traffic parameter is obtained from one of the mentioned measurement methods and, where relevant, compared with the corresponding values in the code. The Hourly Heavy Vehicle Traffic Variations (HHVTV) is given for weekdays at different stations, and then the average of the normalized variations is proposed to be used for simulations. Similarly, the normalized Hourly Traffic Variations (HTV) is proposed based on the average of the corresponding normalized hourly variations at different stations. The HVHVPT is not constant during a day, and in fact, it is a function of three parameters: HHVTV, HTV and P_{HV}. A maximum and an average value for P_{HV}, i.e. 25% and 10% in weekdays, are proposed based on the measured values at the same stations. The heavy vehicle traffic distribution by lane is also determined based on WIM measurements for the stations where the second lane exist, and its maximum and its average values, 20% and 10% respectively, are proposed for traffic simulations. Besides, the GVW distribution is presented for the different stations and two main distributions for national (Mattstetten) and international (Götthard) traffic are chosen to be used for the final traffic simulations.

Two main aspects of future traffic development are studied: Average Gross Weight of Heavy Vehicles (AGWHV) and Average Daily Heavy Vehicle Traffic (ADHVT). Then, based on the traffic trend, the future traffic development is compared with the values given in the Codes. Assuming a linear grow of AGWHV and ADHVT, it is found that both SIA codes and Eurocodes gives conservative values for Average Gross Weight of Heavy Vehicles (AGWHV) and Average Daily Heavy Vehicle Traffic (ADHVT) .

6 Final traffic simulations

In the current chapter, all important parameters as previously determined are summarized and their variation range fixed. Then, detailed results of damage equivalence factors are presented for various cases separately, both for single lane and double lane traffics. Propositions of modifications for damage equivalence factors from Chapter 4 are here assessed by comparing λ and λ_{max} obtained from the different traffic conditions. In addition, validity of damage equivalence factors for special bridge cases, as well as particular fatigue resistance curves, are also studied.

6.1 Final simulations parameters

Based on the analytical studies performed in Chapter 4, the damage equivalence factors, λ_1 and λ_{max}, were found to mainly be function of fatigue equivalent length (L_λ); L_λ equals the area under the influence line divided by stress range due to passage of unit load on the bridge. In reality, the fatigue equivalent length represents the influence of three parameters: bridge static system, detail location and bridge span length. In order to investigate the accuracy of such representation, the following bridge types and detail locations are considered:

- single-span bridges, mid span moment (1SS-MM);
- two-span continuous bridges with equal spans length, second support negative moment (2CS-2SM), second support reaction (2CS-2SR), and mid-span moment (2CS-MSM);
- three-span continuous bridges with equal spans length, mid-bridge moment (3CS-MM), second support moment (3CS-2SM), first support reaction (3CS-1SR) and second support reaction (3CS-2SR).

The span length of the bridges ranges from 1 m to 200 m, including: 1, 2, 3, 4, 5, 7, 10, 15, 20, 30, 50, 100, 200 m. The examples of influence line shape as well as corresponding fatigue equivalent lengths are presented in Figure 4.14.

Table 6.1: Matrix of parameters composing different simulated traffic conditions

Single lane traffic condition						
Abbreviation	Traffic	Type	N_{obs} ($\times 10^3$)	Q_m (kN)	P_{HV} (%)	DAF
G25HW	Götthard	highway	2000	313	25	1.4
M25HW	Mattstetten	highway	2000	282	25	1.4
G25MR	Götthard	main road	500	313	25	1.4
G10HW	Götthard	highway	2000	313	10	1.4
G25HWDAF	Götthard	highway	2000	313	25	Var.
G25MRDAF	Götthard	main road	500	313	25	Var.
Double lane traffic conditions (Götthard, P_{HV} = 25%)						
Abbreviation	Direction	Type	N_{obs} ($\times 10^3$)	N_2 ($\times 10^3$)	Bridge section	DAF
UD10020	unidirectional	highway	2000	400	box	1.4
UD10010	unidirectional	highway	2000	200	box	1.4
UD10020IG	unidirectional	highway	2000	400	2I-Girder	1.4
BD100100	bidirectional	highway	2000	2000	box	1.4
BD10020	bidirectional	highway	2000	400	box	1.4
BD100100MR	bidirectional	main road	500	500	box	1.4
UD10020DAF	unidirectional	highway	2000	400	box	Var.
BD100100DAF	bidirectional	highway	2000	2000	box	Var.
BD100100MRDAF	bidirectional	main road	500	500	box	Var.

The λ_2-factor adapts the traffic volume passing over a bridge. The average gross weight, Q_m, and the annual number of trucks in slow lane, N_{obs}, are the parameters that represent the traffic volume. As proposed in Chapter 5, the statistical parameters of actual traffic are based on Weigh-In-Motion (WIM) measurements from stations of Götthard (as an international station) and Mattstetten (as a national station) of Switzerland in 2009. The average gross vehicle weight of Götthard is 313 kN and Mattstetten is 282 kN. For comparison purpose, the simulations are done for the maximum and average of annual proportion of heavy vehicle in traffic (P_{HV}) on weekdays which are respectively 25% and 10% percent in Switzerland. In addition, two traffic conditions are simulated: highways and main roads. The annual number of simulated trucks per slow lane (N_{obs}) is 2'000'000 for the highways, and it is 500'000 for the main roads. The composition of different traffic conditions are summarized in Table 6.1. All simulations are executed for one year, then to obtain the cycles spectrum for the whole design life (assumed to be 100 years), the number of cycles are multiplied to 100.

The λ_4-factor is intended for multi-lane traffic conditions; some modifications to λ_4 are proposed in order to take into account the effect of crossing and overtaking on bridges. For double lane traffic, the same bridge static systems and detail location are chosen. The traffic simulation parameters as well as calculation of damage equivalence factors are similar to the single lane traffic. Six double lane traffic conditions are studied, as summarized in Table 6.1 (three cases for the bidirectional traffic and three cases for the unidirectional traffic). The heavy vehicle properties of double lane traffic simulations are based on the Götthard WIM measurements in 2009. Also, the annual proportion of heavy vehicles in traffic is always 25 percent in double lane traffic conditions.

In the case of unidirectional traffic, slow lane always has highway traffic with 2'000'000 annual heavy vehicles, and the fast lane traffic in one case is 10 percent (UD10010) and in another case is 20 percent (UD10020) of the slow lane traffic. The main objective of the double lane simulation is to study the effect of heavy vehicles which are crossing (or overtaking) on the bridge. The determination of actual frequencies of these situations is not part of this study.

The transverse distribution of load has the key role on interaction with loading on other lanes. In the case of box section, the most unfavourable case, there is no transverse distribution, and it is acceptable to assume that the box section is uniformly charged regardless of axles transverse position. In order to study the cross section effect, simulations for a double I-Girder Bridge where the transverse distribution factor for slow lane traffic is 1 and for the fast lane is 0.4 (UD10020IG) are also performed. For the latter case, the traffic condition is unidirectional with 2'000'000 heavy vehicles on the slow lane and 400'000 heavy vehicles on the fast lane.

The bidirectional traffic conditions comprise main road with 500'000 annual heavy vehicles traffic (BD100100MR) and highway with 2'000'000 annual heavy vehicles (BD100100) in each direction. In order the compare the bidirectional with unidirectional traffic condition, a special bidirectional traffic condition is considered; in this case the one direction has highway traffic with 2'000'000 annual heavy vehicles and the other direction traffic is 20 percent (BD10020).

The traffic simulations are performed statically and, for most traffic simulations, a constant dynamic amplification factor equal to 1.4 is applied to each vehicle weight to conservatively obtain the dynamic bridge response. For some traffic simulations, however, a variable dynamic amplification factor is considered based on the total weight of traffic on bridge at each moment [51, 59], as illustrated in Figure 2.15. For these cases, when the total weight on the bridge is lower than 300 kN, the dynamic factor is 1.4; when the total weight of traffic on the bridge is more than 1500 kN the dynamic factor is 1.0; for the total weights in between, the dynamic factor decreases linearly between 1.4 and 1.0.

The fatigue resistance curve of steel is considered, as defined in EN 1993-1-9 (2005), with slope of 3 for cycles with stress ranges higher than constant amplitude fatigue limit (CAFL), and slope of 5 for cycles lower than CAFL; furthermore, cycles lower than cut-off limit are dismissed. In addition, two particular S-N curves for shear resistance and shear studs are considered. The results of damage equivalence factors for these two particular S-N curves are provided in Section 6.4.

6.2 Damage equivalence factor for single lane traffic

The final simulations are performed for the single lane traffic conditions and the damage equivalence factors are determined for the different bridge cases as mentioned in the previous section. First, the results of final simulations are compared with the damage equivalence factors, λ and λ_{max} from the EN1993-2 [27]. To this end, the simulation results of the main road traffic with 25 percent annual proportion of heavy vehicle traffic (G25MRDAF) and

variable DAF are chosen. The damage equivalence factor for the other traffic conditions are reported in Appendix C.1. Figure 6.1 shows the λ-factor obtained for different bridge static systems. The corresponding damage equivalence factors of the EN1993-2 [27] are also shown in Figure 6.1. Since the average gross weight of heavy vehicles on station Götthard (2009) is 313 kN, partial equivalent factor, $\lambda_2 = 313/480$, is increased to get the damage equivalence factor, λ, of the code. Figure 6.1 confirms the conclusions drawn in Chapter 3 that the damage equivalence factor obtained for both mid-span and support sections are above the curve of the code, expressing that the code can be non-conservative for some bridge cases.

It should be noted that the Eurocode damage equivalence factor is adapted in term of average gross vehicle weight (Q_m) to be in accordance with the simulated traffic conditions. In reality, the practical engineers are not able to precisely modify λ_2 because they can hardly estimate the value of Q_m, especially for the design cases. The intended value for Q_m in the EN1993-2 [27] is 480 kN, which is based on the maximum measured value in Europe (Auxerre). The maximum Q_m in Switzerland corresponds to Götthard with $Q_m = 313$ kN. Even considering the annual average increase rate of 0.027%, the EN1993-2 [27] still gives a conservative value for Q_m, which provides more safety margin. However, the latter point is true providing the engineers do not apply λ_2 for adapting Q_m based on measurements, for example in the case of an existing bridge. Assuming that the SIA codes aim to increase the design Q_m up to the same level as given in the Eurocode ($Q_m = 480kN$), then the simulation results for the Götthard traffic should increase by the factor of $\lambda_2 = 480/313$ in order to provide the same safety level as Eurocode.

The λ_{max}-factor is also determined for the different bridge cases under the same traffic condition (G25MRDAF), and it is represented in Figure 6.2. The maximum stress range, $max(\Delta\sigma)$, for calculation of maximum damage equivalence factor, λ_{max}, is the value with the stress ranges above it produce less than 1% of total damage. The λ_{max}-factor obtained

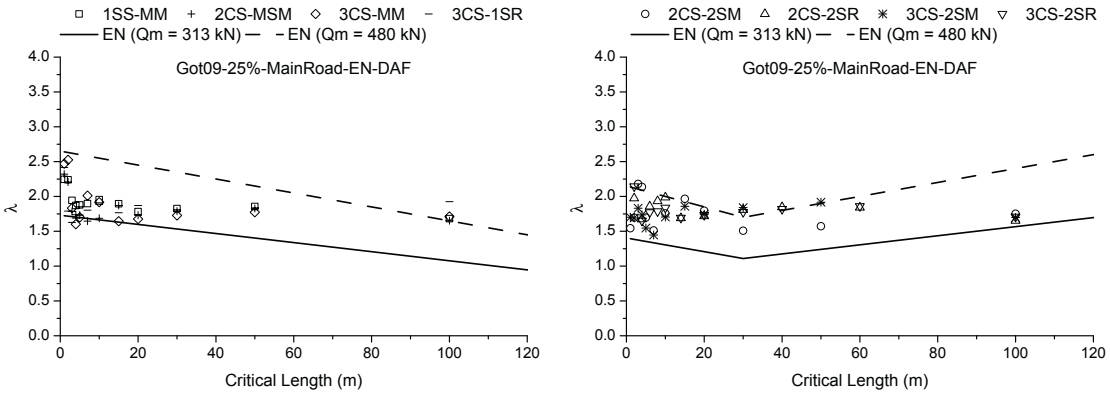

(a) Mid-span sections

(b) Support sections

Figure 6.1: Eurocode-base λ obtained for Götthard main road traffic with $P_{HV} = 25\%$ and variable DAF in comparison with the code

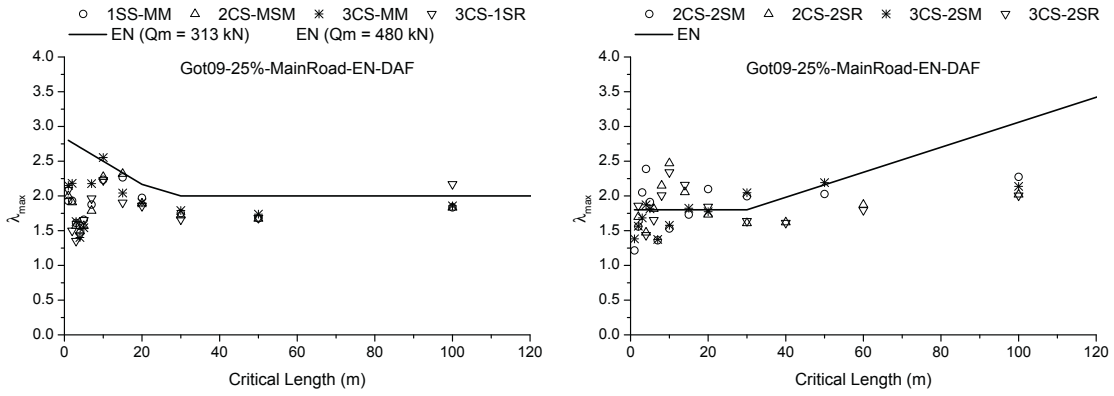

(a) Mid-span sections (b) Support sections

Figure 6.2: Eurocode-base λ_{max} obtained for Götthard main road traffic with P_{HV} = 25% and variable DAF in comparison with the code

for different cases are also greater than the curve of the Eurocode, indicating the factor λ_{max}, same as λ, given by the Eurocode is maybe non-conservative for some cases.

In addition to the Eurocode, the damage equivalence factors, λ and λ_{max}, based on the SIA263 [80] are obtained for the case of highway traffic with 25 percent annual proportion of heavy vehicle traffic (G25HWDAF); the result of other traffic simulations are provided in Appendix C.1. Figure 6.3 illustrates the λ and λ_{max} curves for the different bridge cases in comparison with the SIA code curves [80] for highways; the best nonlinear fitting curve corresponding to the results of λ and λ_{max} are also plotted. The code curve, which is based on the 70 years of design life, increased by the partial damage equivalence factor, $\lambda_3 = (100/70)^{1/5}$, since simulations results corresponds to 100 years. The coefficient of determination (R^2) for λ and λ_{max} are

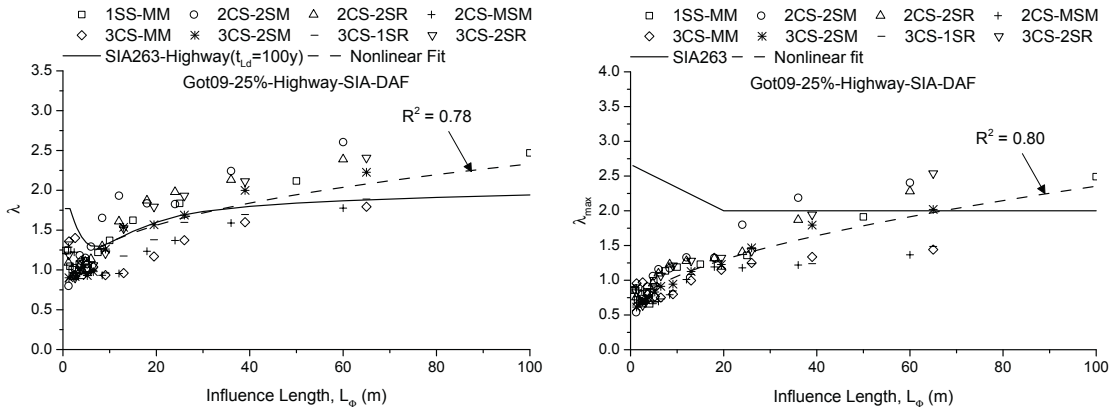

(a) λ (b) λ_{max}

Figure 6.3: SIA-base λ and λ_{max} obtained for Götthard highway traffic with P_{HV} = 25% and variable DAF in comparison with the code

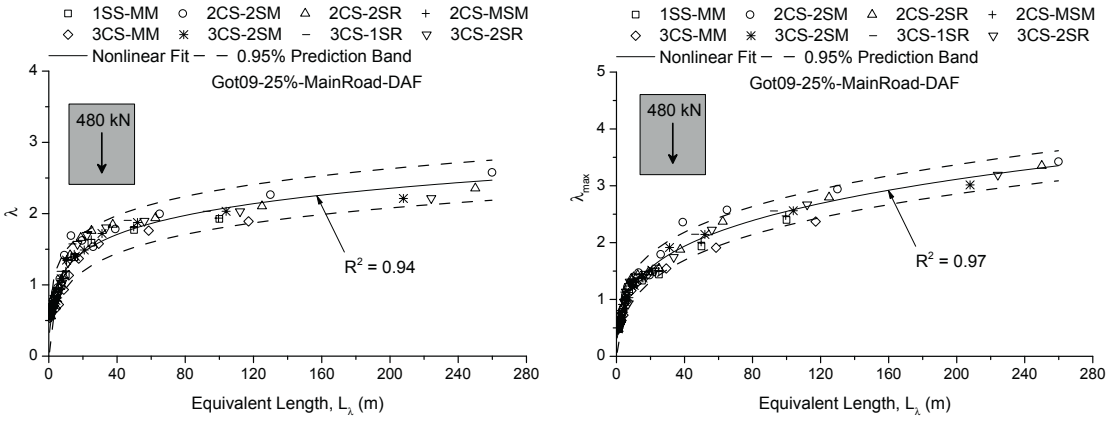

(a) λ (b) λ_{max}

Figure 6.4: λ and λ_{max} based on the proposed method obtained for Götthard highway traffic with P_{HV} = 25% and variable DAF

determined 0.78 and 0.80 retrospectively; obviously, R^2 corresponding to the current code curve is much lower than the best fitting curve. Figure 6.3 confirms the main conclusions made in Chapter 3, and it shows both λ and λ_{max} obtained for the different bridge cases are scattered and in some cases the curve of the code is below the obtained values, expressing that the safety margin of the SIA code depends upon the span length and bridge static system, and in some cases, it is non-conservative.

The same simulations are used to determine the damage equivalence factor, λ, as well as λ_{max}, by the new method proposed in Chapter 4 for different bridge cases, as illustrated in Figure 6.4. The proposed curve is based on the 500'000 passages of heavy vehicle per slow lane with average gross weight of 313 kN and design life of 100 years. It worthy of note that the λ value is presented in Figure C.24a, thus the λ_5 is also included in the damage equivalence factors. Nevertheless, λ_5 is only applicable for the case of mid-support moment of two-span continuous bridge (λ_5 = 1.15) and for the other cases it is equal to 1.

The curves obtained for the different static systems show a clear trend with a narrow dispersion band (R^2 corresponding to λ and λ_{max} obtained 0.95 and 0.98 respectively), well represented by the proposed curves. The range of equivalent length on the abscissa in Figure 6.4 is extended up to 280 m, since in some bridge cases the equivalent length can be long. The damage equivalence factors, λ and λ_{max}, based on the proposed method for the other traffic conditions are also given in Appendix C.2.

Dividing the damage equivalence factor, λ, by the λ_2-factor (Equation 3.6), the λ_1-factor for the different single lane traffic can be calculated. Similar to the Eurocode [27], the base value of average gross weight, Q_0, is taken as 480 kN and the base value of annual heavy vehicle traffic, N_{obs}, is taken as 500'000 for calculation of λ_2. Figure 6.5 demonstrates λ_1 obtained for the different traffic conditions for mid-span moment of simple span bridges as well as second

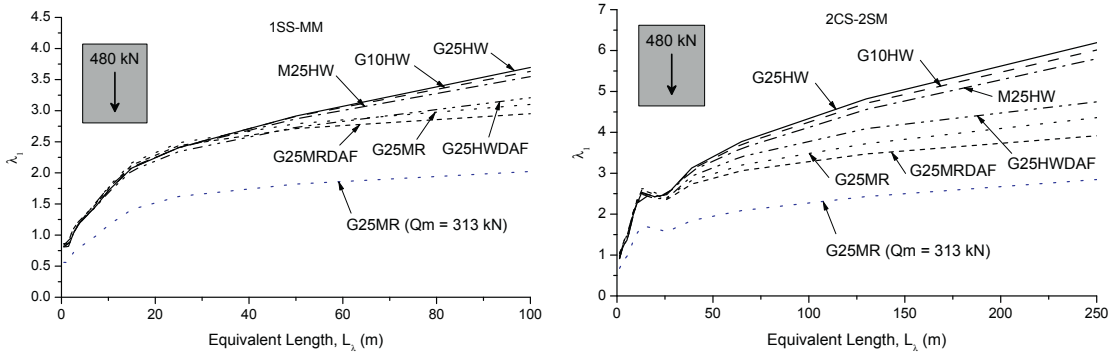

(a) Mid-span moment of simple span bridge

(b) Second support moment of two-span continuous bridge

Figure 6.5: λ_1 based on proposed method for different single lane traffic conditions

support moment of two-span bridges. For comparison, a curve of λ (before dividing it by λ_2) is also plotted on the same figures for the case of main road traffic (G25MR). In Figure 6.5, there is a slight difference between different traffic conditions with a constant DAF, except in the case of main road traffic condition (G25MR). Such a difference shows that the average gross vehicle weight can properly be adapted with λ_2; however, the annual number of heavy vehicle cannot be adapted with λ_2. This can be explained by the fact that the probability of having several heavy vehicles together on a bridge depends on the total annual number of heavy vehicles in traffic. Obviously, this difference is more pronounced for bridges with longer equivalent length for the same reason. In Figure 6.5, as the equivalent length increases, the damage equivalence factors obtained for traffic cases with variable DAF are growing at a smaller pace compared to the same traffic cases with constant DAF, which shows that the effect of simultaneity is mitigated for longer bridge lengths due to reduction of DAF (increasing length correlates with increased total load on bridge). However, the difference between the

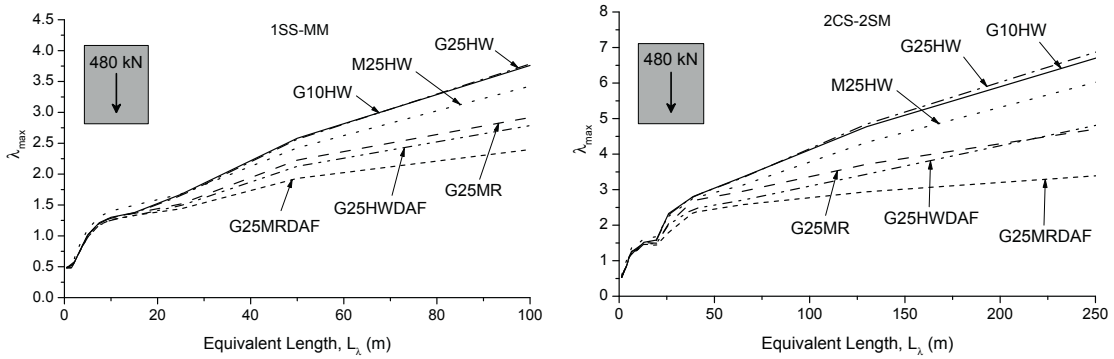

(a) Mid-span moment of simple span bridge

(b) Second support moment of two-span continuous bridge

Figure 6.6: λ_{max} based on proposed method for different single lane traffic conditions

λ_1-factor resulting from the highway traffic (G25HWDAF) and main road traffic (G25MRDAF) confirm that the annual number of heavy vehicle in traffic is indispensable and cannot be properly addressed by λ_2.

In addition, the maximum damage equivalence factor, λ_{max}, for different single lane traffic conditions is illustrated in Figure 6.6 for mid-span moment of simple span bridges as well as second support moment of two-span bridges. Among the simulation cases with constant DAF, the λ_{max} values obtained for the traffic condition with main road traffic (G25MR) is lower than the other cases. Generally, it is believed that λ_{max} is independent from annual number of heavy vehicles (N_{obs}) because the ordinate of CAFL is the only determinant parameter. However, the maximum stress range (i.e. 1%-damage-threshold) increases with simultaneous presence of heavy vehicles on bridges, which is dependent of annual number of heavy vehicles (N_{obs}). Considering variable DAF, the λ_{max}-factors are reduced for both traffic cases of main road (G25MRDAF) and highway (G25HWDAF). Nevertheless, the difference between λ_{max}-factors obtained for the main road and highway traffic remains tangible. To address this issue, λ_{max} can be differentiated and given for the relevant annual heavy vehicle traffic volumes.

6.3 Damage equivalence factor for double lane traffic

The λ_4-factor for each bridge static system based on the method proposed in Section 4.3 is calculated. The λ_4-factor for the case of bidirectional highway traffic (BD100100) as well as unidirectional highway traffic with 20 percent fast lane traffic (UD10020) are illustrated in Figure 6.7. The corresponding λ_4 from the codes (the Eurocodes or the SIA codes) as well as λ_4 obtained from Equation 4.25 are also plotted. The effect of crossing and overtaking in the case of unidirectional and bidirectional traffic, as shown in Figure 6.7, depends on the traffic condition (annual number of heavy vehicles in each lane) and bridge static system, and it is more pronounced than the effect of traffic volume as considered in the codes.

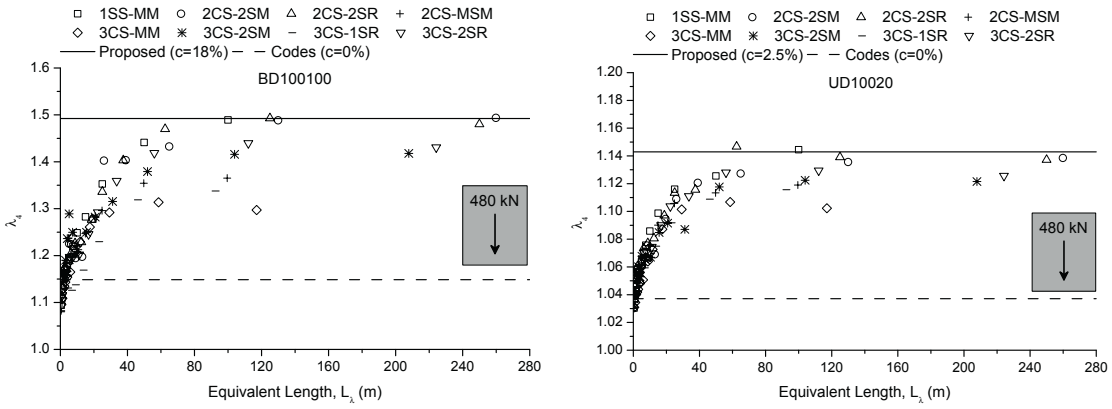

(a) bidirectional traffic, BD100100

(b) unidirectional traffic, UD10020

Figure 6.7: λ_4 based on the proposed method for two traffic conditions

By trial and error, it is found that the simulation results can be conservatively represented assuming: c = 18% for bidirectional highway traffic condition (BD100100) and c = 2.5% for unidirectional highway traffic condition (UD10020). The crossing ratios for other traffic conditions are also shown in the corresponding graphs of Appendix C.2.

The λ_4-factor for different double lane traffic conditions are compared in Figure 6.8 for two cases of mid-span moment of simple span bridges (1SS-MM) and second support moment of two-span continuous bridge (2CS-2SM). In Figure 6.8, comparing two double lane cases of BD10020 and UD10020, in which the traffic volumes within each lanes are similar and the traffic direction of their second lane are opposite, it can be concluded that the traffic direction has no effect in damage equivalence factors.

The curves obtained for UD10020IG case in Figure 6.8 in comparison with UD10020, shows the overtaking effect is mostly important for the box cross section, where the second lane and the first lane transverse load distributions are assumed to be equal; therefore, the overtaking effect upon damage equivalence factors can be neglected for I-Girder bridges.

In Figure 6.8, the λ_4-factors obtained for the cases with variable DAF are lower than the similar cases with constant DAF. This is because the DAF generally reduces with the total load on the bridges and the multiple presence of heavy vehicles causes increasing the total load on the bridges. The reduction of DAF due to multiple presence of heavy vehicles is in contrast to the effect of simultaneity that results in increasing λ_4-factors. Figure 6.8 shows that reduction of DAF can diminish the simultaneity effect, but this reduction is so limited that it can not completely eliminate the simultaneity effect on damage equivalence factors.

The λ_4-factor for other double lane traffic conditions are reported in Appendix C.2 based on the proposed method. The principal parameters that have influence on λ_4 are: the traffic volume on each lane, fatigue equivalent length, bridge-vehicle dynamic amplification and influence line types. The partial damage equivalence factors, λ_4, obtained for the different

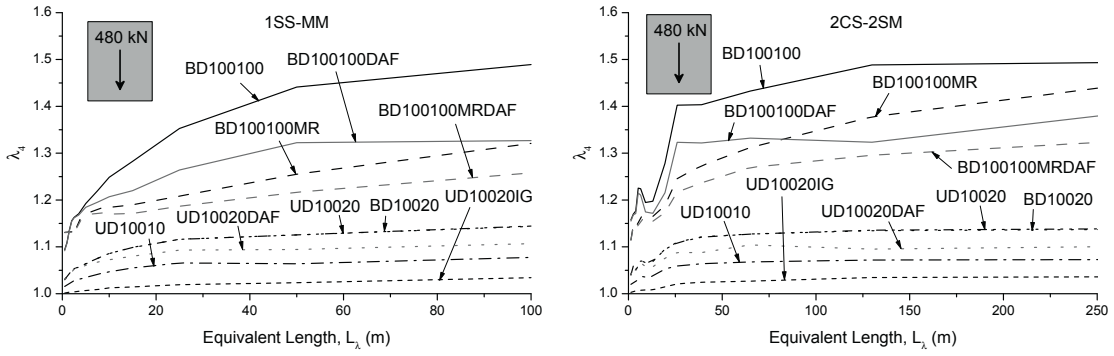

(a) Mid-span moment of simple span bridge

(b) Second support moment of two-span continuous bridge

Figure 6.8: λ_4 based on the proposed method for different double lane traffic conditions

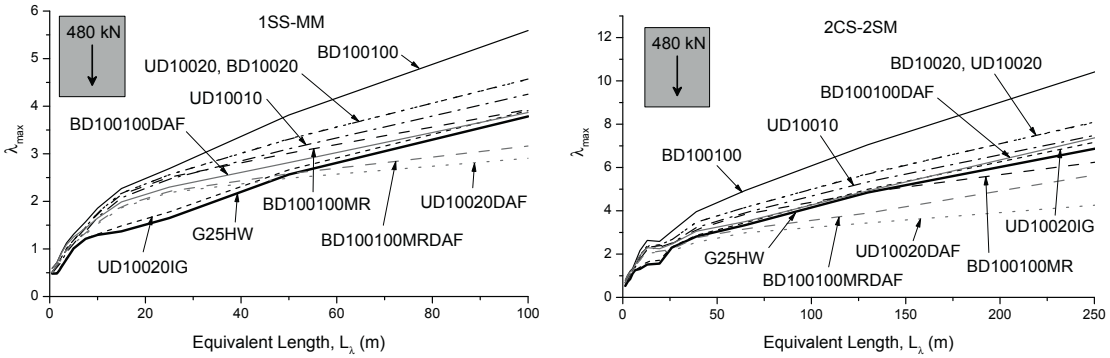

(a) Mid-span moment of simple span bridge

(b) Second support moment of two-span continuous bridge

Figure 6.9: λ_{max} based on proposed method for different double lane traffic conditions

influence lines are slightly scattered in some double lane traffic conditions. Since the current study is limited to modifications of damage equivalence factors, then the accuracy of the λ_4-factors cannot be improved more. Nevertheless, the proposed crossing ratios for the difference traffic conditions and influence line types provide an acceptable safe design.

The maximum damage equivalence factor, λ_{max} for the different double lane traffic conditions are determined. The resulting λ_{max} are shown in Figure 6.9 for two cases of mid-span moment of simple span bridge (1SS-MM) and second support moment of two-span continuous bridge (2CS-2SM); a single lane λ_{max} corresponding to the Götthard highway traffic with 25% of heavy vehicle ratio is also plotted for comparison (G25HW). It can be observed that λ_{max} resulting from different traffic conditions are varying significantly. This can be explained by the fact that the probability of crossing and overtaking on the bridges and consequently the maximum stress range (i.e. 1%-damage-threshold) are highly dependent of the given double lane traffic condition. Also, the comparison of double lane to single lane λ_{max}-factors

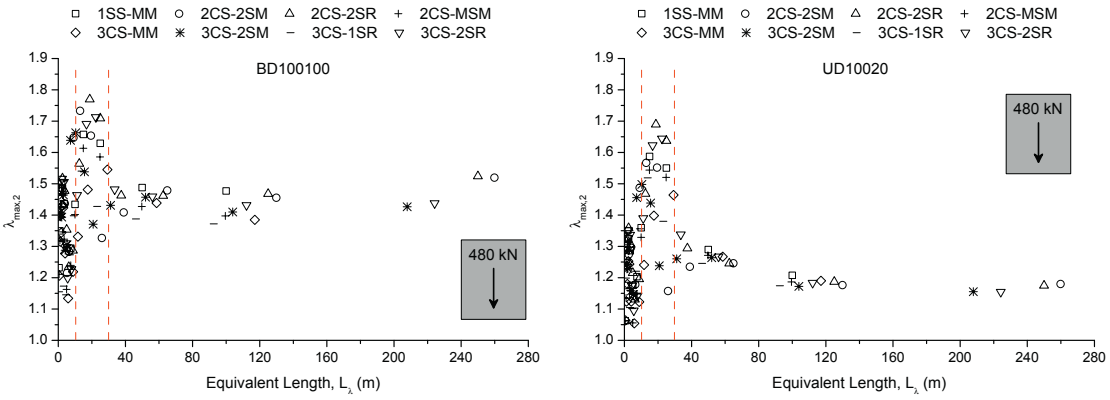

(a) bidirectional traffic, BD100100

(b) unidirectional traffic, UD10020

Figure 6.10: $\lambda_{max,2}$ based on the proposed method for two traffic conditions

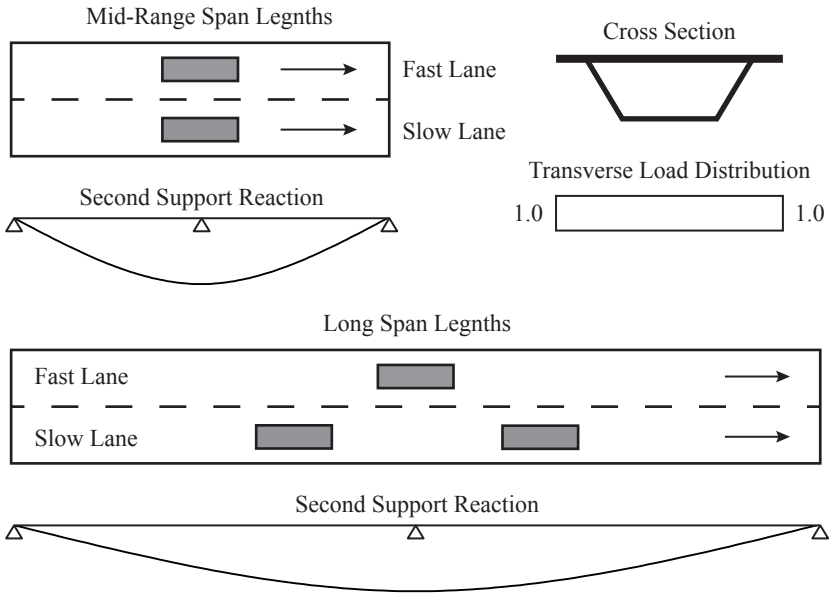

Figure 6.11: Schematic view of two overtaking cases

emphasises the importance of crossing and overtaking effect. However, it can be observed (in Fig. 6.9) that the influence of crossing and overtaking is almost negligible for I-girder cross section.

By dividing the λ_{max} corresponding to double lane traffic by the λ_{max} corresponding to single lane traffic (G25HW), the effect of the second lane traffic on λ_{max} can be determined ($\lambda_{max,2}$). For two double lane cases of BD10020 and UD10020, $\lambda_{max,2}$ is presented in Figure 6.10 for the different bridge cases. One can notice the effect of the second lane traffic on λ_{max} can increase it up to 80%. Also, the $\lambda_{max,2}$ does not steadily grow with the fatigue equivalent length and its maximum value occurs in the range of 10 m to 30 m. This can be explained by an example, as shown in Figure 6.11. For bridges with mid-range span lengths and box section, a side-by-side passage of two similar heavy vehicles on the bridge causes a stress range up to double of the stress range due to passage of the heavy vehicle on the first lane. Such a probability is the main cause that the λ_{max} for double lane traffic is about 1.8 times larger than λ_{max} for single lane traffic. In the case of bridges with long span lengths, however, the effect of the second heavy vehicle (following vehicles) on λ_{max} is already included. In this case, the presence of the third heavy vehicle may increase the stress range up to one-third of the stress range due to the heavy vehicles on the first lane (see Fig. 6.11). In addition, the probability of presence on a bridge of three heavy vehicles with all a large GVW is rather low.

6.4 Damage equivalence factor for special cases

Up to this point, the fatigue resistance curve for steel details under direct stress ranges has been applied in determination of damage equivalence factors. However, this curve cannot be

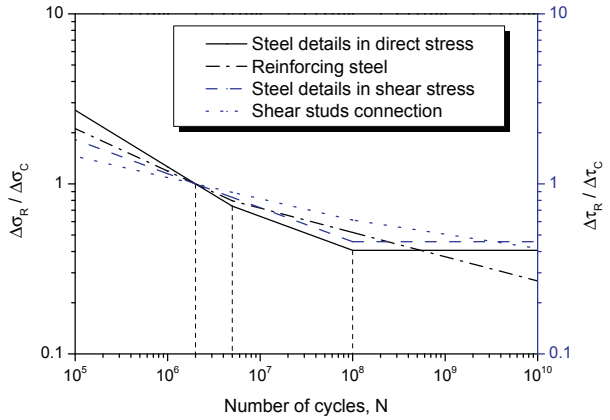

Figure 6.12: Samples of S-N curves for different details

applied for all cases, for instance details under shear stresses, shear studs or reinforcing steels. In order to evaluate the effect of S-N curve on damage equivalence factors, three additional fatigue strength curves are considered, as shown in Figure 6.12. The fatigue strength curves for details under shear stress have a single slope of 5, and a cut-off limit at 10^8 cycles. As for shear studs, the S-N curve slope is 8 and there is no CAFL or cut-off limit. The fatigue resistance curve of reinforcing steels (concrete rebars) has slope of 4 for cycles above CAFL at 5×10^6 cycles and it has slope of 7 for below CAFL.

In addition to fatigue strength curve, the damage equivalence factor for some special bridge influence lines are studied here, including: two-span continuous bridges with equal spans length, mid-span shear (2CS-MSS), 3/4 span length shear (2CS-34SS), and 3/4 span length moment (2CS-34SM). The Götthard highway traffic with 25 percent heavy vehicle proportion in traffic (G25HW) is chosen to perform these simulations. Damage equivalence factors for those three bridge influence lines are determined by applying each fatigue strength curves. Note that the three influence lines might not, in reality, correspond to a detail with every fatigue

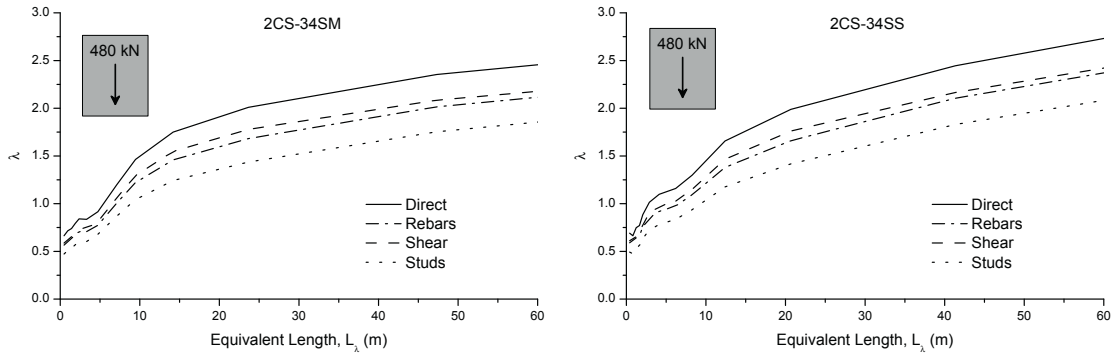

(a) Two-span continuous bridge, 3/4 span length moment

(b) Two-span continuous bridge, 3/4 span length shear

Figure 6.13: λ obtained for different fatigue strength curves

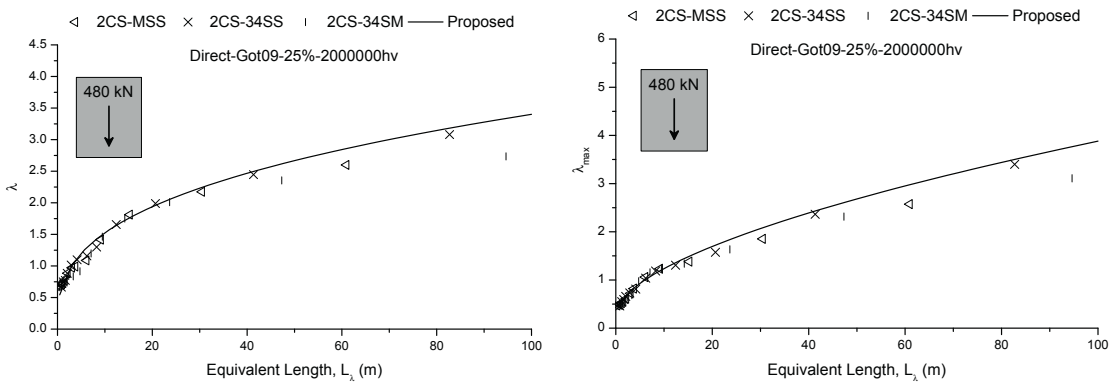

(a) λ (b) λ_{max}

Figure 6.14: λ and λ_{max} for special bridge influence lines

strength curve; nevertheless, for all mentioned influence lines, the damage equivalence factor are calculated by applying those four fatigue strength curves for comparison.

The damage equivalence factors applying the different fatigue strength curves are illustrated in Figure 6.13 obtained for 3/4 span length moment and for shear of two-span continuous bridges. Figure 6.13 shows that the damage equivalence factors obtained by applying the four S-N curves are proportional for both bridge influence lines at different equivalent lengths. Thus, a constant factor can be taken into account to adapt the effect of fatigue strength curves on the damage equivalence factor. Considering the damage equivalence factors obtained by applying fatigue strength curves for direct stress range, shear stress ranges, shear studs and reinforcing steels, the ratios of $\lambda_{direct}/\lambda_{shear}$, $\lambda_{direct}/\lambda_{studs}$ and $\lambda_{direct}/\lambda_{rebars}$ equal to respectively 1.13, 1.40 and 1.17 can be proposed.

The damage equivalence factors, λ and λ_{max}, for the special bridge influence lines are illustrated in Figure 6.14; the proposed λ and λ_{max} for the same traffic conditions are also plotted in the corresponding figures. The applied fatigue resistance curve is direct stress range (with slope 3 then 5 with cut-off limit). Figure 6.14 justifies that the proposed method for damage equivalence factors, as well as the proposed curves, can be safely applied for shear bridge responses.

6.5 Summary

In the current chapter, the damage equivalence factors for several cases are calculated to study the effect of different parameters. The main parameters assumed to have an effect on damage equivalence factors are first defined and their range of variation is determined.

To verify the accuracy of the proposed fatigue load model and fatigue equivalent length, several bridge static systems and detail locations are studied. The proposed fatigue load model and

fatigue equivalent length could improve the situation by reducing the dispersion of the results. The coefficient of determination (R^2) for the best fitting curve of the SIA code is equal to 0.8 and it grows to 0.95 for λ-factors. Also, R^2 for λ_{max}-factors raises from 0.82 to 0.97. Therefore, the proposed fatigue load model and fatigue equivalent length are defined properly.

The single lane traffic conditions parameters includes: annual heavy vehicle traffic, average gross vehicle weight (or gross vehicle weight distribution), proportion of heavy vehicle in traffic, and model of dynamic amplification factor. Among these parameters, annual heavy vehicle traffic, average gross vehicle and model of dynamic amplification factor are dominant and proportion of heavy vehicle in traffic has a minor effect. The partial damage equivalence factor, λ_2, takes into account the "traffic volume" effect of N_{obs} and Q_m; however, the effect of simultaneous passage of heavy vehicles on bridge increase as N_{obs} increases. Whereas the λ_2-factor is based on vehicle-by-vehicle passage of vehicles, the effect of having several trucks in the same lane is neglected. Considering a variable DAF which is more realistic than constant DAF, permits reducing the simultaneity effect, consequently the damage equivalence factors decrease as well. However, the difference between the λ-factors obtained for highway and roadway traffic even after applying variable DAF remains tangible. To address this issue, as it is done in the SIA code, the curves of damage equivalence factor for certain annual heavy vehicle traffic volumes (e.g. highway, main road) can be provided. Still, λ_2 can be used for modification of "traffic volume" when interpolating between two given curves.

The main parameters studied in double lane traffic simulations are annual number of traffic in each lane, traffic direction, transverse load distribution and model of DAF. The simulations results confirm that the traffic direction has no effect on the damage equivalence factors value, but the annual number of trucks in each lane, transverse load distribution and model of DAF are indispensable parameters. The partial damage equivalence factor of the codes, λ_4, sums up the effect of "traffic volume" of each lane, neglecting the effect of crossing and overtaking. The proposed equation for double lane traffic, which can take into account the effect of crossing and overtaking on bridge, can improve the accuracy of λ_4 to a certain degree as given for the simulated traffic conditions in the current chapter. The traffic simulations show that the reduction of DAF as a function of total load on bridge marginally decreases the effect of crossing and overtaking, however this decrease does not allow neglecting the crossing and overtaking effect.

The effect of crossing and overtaking on λ_{max} is also investigated. The results show that λ_{max} resulting from the double lane traffic conditions can be up to 80% higher than the λ_{max} obtained from the single lane condition. It is also found that the maximum ratio ($\lambda_{max,2}$) occurs for the bridges with equivalent length ranging from 10 m to 30 m. In addition, it is found that the influence of double lane traffic on λ_{max} in the case of bridges with I-girder cross-sections can be neglected.

The effect of fatigue strength curves on damage equivalence factors as well as special bridge cases are also studied in this chapter. The special bridge cases include the shear response

of bridges and the moment response at 3/4-span length of bridges. The resulting damage equivalence factor obtained from the simulations justifies that the same damage equivalent length and fatigue load model can be applied for these cases. To study effect of fatigue strength curves on damage equivalence factors, two additional S-N curves are studied: details under shear stresses and shear studs. The curves obtained for the different fatigue strength curves are proportional, which allow us to propose a constant value for taking into account the change from the basic S-N curves family (double slope S-N curve with a cut-off limit).

7 Conclusions and Future work

In this chapter, the conclusions of the works described herein are given, followed by some recommended areas of future studies.

7.1 Conclusions

Conclusions are arranged in accordance with the objectives from Section 1.3 and the most important ones are written in bold characters. The first objective was to model single lane and double lane traffic conditions on bridges for determining internal forces and damage sum for various traffic conditions. The second objective was to evaluate the SIA code as well as the Eurocode fatigue design rules for various traffic conditions and bridge types, by comparing the damage equivalence factors of the codes with the results obtained from the traffic simulations. For these two objectives, the following conclusions are drawn:

- **The definition of fatigue equivalent length, based on both Eurocode and SIA code is limited, and it does not allow treating all bridge static systems and detail locations.**
- Monte-Carlo traffic simulations for one year provides representative sampling that leads to stable results for determining damage equivalence factors.
- The hourly traffic distribution scenarios may have some effects on damage equivalence factors, but one generic realistic scenario is sufficient for the traffic simulations.
- The effect of having several trucks on bridges either in the same lane or in several lanes is important and it should be taken into account.
- Both Eurocodes and SIA codes neglect the effect of simultaneity, which may result in larger values of λ and λ_{max} than the values given by codes for some bridge cases, especially for long-span bridges.
- The damage equivalence factors, λ and λ_{max}, obtained for different bridge influence

lines, based on both Eurocodes and SIA codes hypothesis, are widespread; thus attributing one value to all influence lines does not give a uniform safety level.

Regarding the work presented herein for clarifying the rules for the determination of the fatigue equivalent length in order to have a unique method based on the influence line, resulting wider range of validity of damage equivalence factor (Objective 3) and for defining a proper fatigue load model in order to have a coherent fatigue verification for any influence line (Objective 4), the following conclusions are drawn:

- For vehicle-by-vehicle traffic simulations and assuming one repetition on a given influence line, the equivalent force range for very short span lengths can be obtained by damage summation from each axle response, and for very long span lengths, the damage summation from gross vehicle weight response bears the equivalent force range. For mid-span lengths, an *equivalent vehicle* can be defined to representative of entire heavy vehicle traffic for calculation of the equivalent force range.
- **The fatigue equivalent length can be proposed as the area under the influence line divided by the difference between the maximum and minimum values of the influence line.**
- **The fatigue load model does not need to represent a real truck or to be similar; it can be advantageous proposed as a single axle weighting 480 kN.**
- **A new partial damage equivalence factor, λ_5, should be defined (as defined in Eq. 4.15) for taking into account the effect of repetition in the influence line.**
- **The λ_4-factor based on the SIA code as well as the Eurocode can be further developed in order to account for the effect of crossing and overtaking on bridge (Eq. 4.25 and 4.28).**
- For concrete decks, the new proposition is applied to calculate fatigue equivalent length for several negative moments at cantilever support of bridge's deck with span length ranging from 5 to 80 m. The obtained fatigue equivalent lengths are in line with expectations and demonstrate the general validity of the proposed method.
- When effect of variation in the transverse location of vehicles is essential for calculation of damage sum, the fatigue equivalent length corresponding to every transverse location should be determined, then λ_1 can be calculated with Equation 4.32.

Regarding the work presented herein for determining the damage equivalence factors based on the proposed modifications and for different traffic conditions as well as bridge types (Objective 5) and for quantifying the effect of more than one lane traffic and traffic direction in damage equivalence factor (Objective 6), the following conclusions are drawn:

- **The different traffic conditions for free-flow traffic simulations can be represented by the following main parameters: Hourly Heavy Vehicle Traffic Variations (HHVTV), Hourly Traffic Variations (HTV), Hourly Variations of Heavy Vehicles Proportion in Traffic (HVHVPT), proportion of heavy vehicles in traffic (P_{HV}), heavy vehicle traffic distribution by lane, and GVW distribution.**

- The use of heavy vehicles definition, for which the minimum GVW is 100 kN, is better as compared to trucks with minimum GVW of 35 kN, since it prevents confusion in the counting of over-weighted cars as trucks.

- Evolution of Average Gross Weight of Heavy Vehicles (AGWHV) and Average Daily Heavy Vehicle Traffic (ADHVT) for different WIM stations in Switzerland between the years 2003 to 2009 show that the corresponding values in the Eurocodes and SIA codes are safe and to some degree conservative assuming linear growth of these parameters for 100 years.

- For six simulated single-lane traffic conditions, the proposed fatigue equivalent length and fatigue load model significantly reduce the dispersion of damage equivalence factors obtained for the different influence lines (R^2 for the best fitting curve based on the SIA code was between 0.80~0.82 which could be raised to 0.96~0.98). This also applies to the special bridge cases where the shear response of bridge elements is considered.

- The resulting maximum damage equivalence factors confirm the dispersion of λ_{max} obtained for different influence lines; this dispersion considerably decreases when the proposed fatigue load model and fatigue equivalent length are applied.

- The traffic simulation results obtained for different traffic conditions show that the annual heavy vehicle traffic and average gross vehicle are the dominant parameters in determining damage equivalence factors; proportion of heavy vehicles in traffic has a minor effect in the studied range ($10\% \leq P_{HV} \leq 25\%$).

- **The single lane traffic simulation results pointed out that the partial damage equivalence factor for "traffic volume", λ_2, cannot properly account for the effect of simultaneous passage of heavy vehicles on a bridge since the effect of simultaneous passage of heavy vehicles on the bridge increases as N_{obs} increases. Some curves with certain traffic volumes (e.g. highway, main road) should be given in the codes.**

- The double lane traffic simulations confirm that the traffic direction (bidirectional versus unidirectional) has no effect on the damage equivalence factors, but the annual number of heavy vehicles in each lane and transverse load distribution are indispensable parameters.

- The proposed equations for double lane traffic (Eq. 4.25 and 4.28) which take into account the effect of crossing and overtaking on bridges, can increase the accuracy and safety level of λ_4.

- The crossing and overtaking effect may increase up to 80% the value of the maximum damage equivalence factor, λ_{max}, for bridges with box cross-sections, while for bridges with I-girder cross sections, this effect is negligible.
- **The damage equivalence factors obtained for the S-N curves corresponding to steel details under shear stress and shear studs connections are proportional to the damage equivalence factors determined for steel details under direct stress. This allows for a constant factor for adapting the computed values to other S-N curves.**
- For both single lane and double lane traffic conditions, considering a reduction of DAF as a function of total load on bridge allows deceasing the damage equivalence factors, λ and λ_{max}, especially for bridges with long fatigue equivalence lengths, however this decease is not enough to neglect the simultaneity effect.

7.2 Future work

Based on the work presented and the conclusions drawn, the following main future work items are recommended:

- A new traffic simulation software will be needed for future traffic simulations. In the current study, the WinQSIM software is upgraded and used for all traffic simulations. Main limitations of this software are: modelling traffic with a constant vehicle speed, modelling traffic with a steady traffic flow condition (always free-flow or always congested), lack of overtaking or lane change within the length of bridge (results from the constant speed), lack or proper modelling of truck traffic and driver behaviour.
- For maximum damage equivalence factor, the "allowable" percentage of cycles exceeding the CAFL or the corresponding damage percentage must be precised. In the current study, the maximum stress range assumed is the one that contributed to less than 1% of total damage. However, the corresponding damage percentage could for example be determined with a probabilistic fracture mechanics approach in which the variation of parameters like initial crack size, stress range spectrum and stress coefficient factors are taken into account.
- Further studies would be of interest to extend the results of the current study to the details subjected to multi-axial fatigue loads. The details which are subjected to proportional (in-phase) multi-axial loading might be treated similarly to the details with uni-axial loads using the Von-Mises criteria. However, when non-proportional loadings are involved, the fact that the principal stress direction may rotate during the load cycle results in a difficult evaluation of the fatigue safety and it is not known if a λ approach can be used.
- More work on the fatigue of concrete rebars is necessary. In the current study, the damage equivalence factor corresponds to typical fatigue resistance curve of concrete

rebars is determined and compared with the steel details. However, the stress ranges in rebars highly depend on the cracking state of the concrete, which results in non-linear stress-strain behaviour. This must be considered with other concrete-related parameters (creep, prestressing, ...) for proper fatigue assessment of concrete rebars.

- A comprehensive study of dynamic amplification factor (DAF) regarding fatigue limit state needs to be done. The dynamic amplification factor in this study is based on the research carried out by Ludescher and Brühwiler [51]; however, the main focus of that research is the dynamic amplification related to ultimate limit state. The accuracy of the proposed DAF for different bridge static systems and detail locations as well as various vehicle loading situations, especially when the multiple presence of heavy vehicles is an issue, needs further validation.

Bibliography

[1] AASHTO. *Standard specification for Highway Bridge*. American Association of State Highway and Transportation Officials, 1992.

[2] AASHTO. *LRFD bridge design specifications*. American Association of State Highway and Transportation Officials, 1998.

[3] C. Amzallag, J. P. Gerey, J. L. Robert, and J. Bahuaud. Standardization of the rainflow counting method for fatigue analysis. *International Journal of Fatigue*, 16(4):287–293, Jun 1994.

[4] R. J. Anthes. Modified rainflow counting keeping the load sequence. *International Journal of Fatigue*, 19(7):529–535, Aug 1997.

[5] AUSTROADS. *Bridge Design Code*. Australia's national road authority, 1992.

[6] Bächtold & Moor AG Ingenieure Planer. *Auswertung der WIM-Messdaten des Jahres 2005*. ASTRA - Erhebung Strassenverkehr, 2009.

[7] S.F. Bailey. *Basic principles and load models for the structural safety evaluation of existing road bridges*. PhD thesis, École Polytechnique FÉdÉrale de Lausanne - EPFL, Lausanne, Switzerland, 1996.

[8] A. Bassetti and S. F. Bailey. *Lastfaktoren für Eigenlast und Auflast zur Beurteilung der Tragsicherheit bestehender Strassenbrücken*. Mandat de recherche OFROU 86/94, Union des professionels suisses de la route (VSS 530), Zurich, 1998.

[9] R. Bez. *Modélisation des charges dues au traffic routier*. PhD thesis, EPFL, Lausanne, 1989.

[10] R. Bez, S. Bailey, and V. Haesler. *Modèles de charge actualisés pour l'évaluation de la sécurité structurale de ponts-routes existants*. Mandat de recherche OFROU 90/90, Union des professionels suisses de la route (VSS 515), Zurich, 1995.

[11] S.P. Brady, E.J. O'Brien, and A. Znidarie. Effect of vehicle velocity on the dynamic amplification of a vehicle crossing a simply supported bridge. *Journal of Bridge Engineering*, 11 (2):241 – 249, 2006.

[12] J. H. Bulloch. The influence of mean stress or r-ratio on the fatigue crack threshold characteristics of steels - a review. *International Journal of Pressure Vessels and Piping*, 47 (3):263–292, 1991.

[13] J.-A. Calgaro, M. Tschumi, and H. Gulvanessian. *Designer's guide to Eurocode 1: Actions on bridges - EN 1991-2, EN 1991-1-1, -1-3 to -1-7 and EN 1990 ANNEX A2*. Thomas Telford, London, UK, 2010.

[14] R. Cantieni. Dynamic load testing of highway bridges. *International Association for Bridge and Structural Engineering*, 8(3):57 – 72, 1984.

[15] C.C. Caprani, A. Gonzalez, P.H. Rattigan, and E.J. OBrien. Assessment dynamic ratio for traffic loading on highway bridges. *Structure and Infrastructure Engineering: Maintenance, Management, Life-Cycle Design and Performance*, 8(3):295 – 304, 2012.

[16] T.H.T. Chan and C. O'Connor. Vehicle model for highway bridge impact. *Journal of Structural Engineering*, 116(7):1772 – 1793, 1990.

[17] P. Chotickai and M. D. Bowman. Truck models for improved fatigue life predictions of steel bridges. *Journal of Bridge Engineering*, 11(1):71–80, Jan-Feb 2006.

[18] COST323. *Weigh-in-Motion of Road Vehicles - Final report of the COST 323 Action (WIM-LOAD) COST 323 (1993-1998)*. LCPC, 2002.

[19] C. Crespo-Minguillon and J. R. Casas. A comprehensive traffic load model for bridge safety checking. *Structural Safety*, 19(4):339–359, 1997.

[20] L. Deng and C.S. Cai. Development of dynamic impact factor for performance evaluation of existing multi-girder concrete bridges. *Engineering Structures*, 32(1):21 – 31, 2010.

[21] O. Ditlevsen. Traffic loads on large bridges modeled as white-noise fields. *Journal of Engineering Mechanics-ASCE*, 120(4):681–694, Apr 1994.

[22] N. E. Dowling, C. A. Calhoun, and A. Arcari. Mean stress effects in stress-life fatigue and the walker equation. *Fatigue & Fracture of Engineering Materials & Structures*, 32(3): 163–179, 2009.

[23] S. D. Downing and D. F. Socie. Simple rainflow counting algorithms. *International Journal of Fatigue*, 4(1):31–40, 1982.

[24] ECCS. *Recommendations for the fatigue design of steel structures*. European Convention for Constructional Steelwork - ECCS, first edition edition, 1985.

[25] EN1991-2. *Eurocode 1 - Actions On Structures - Part 2: Traffic Loads On Bridges*. European Committee for Standardization, Brussels, 2002.

[26] EN1993-1-9. *Eurcode 3: Design of steel structural - Part 1-9: Fatigue*. European Committee for Standardization, Brussels, 2005.

[27] EN1993-2. *Eurocode 3 - Design of steel structures - Part 2: Steel Bridges*. European Committee for Standardization, Brussels, 2006.

[28] B. Enright. *Simulation of traffic loading on highway bridges*. PhD thesis, College of Engineering, Mathematical and Physical Sciences of University College Dublin, 2010.

[29] A. Fatemi and L. Yang. Cumulative fatigue damage and life prediction theories: a survey of the state of the art for homogeneous materials. *International Journal of Fatigue*, 20(1): 9–34, Jan 1998.

[30] J. W. Fisher, A. Nussbaumer, P. B. Keating, and B. T. Yen. Resistance of welded details under variable amplitude long-life fatigue loading. Technical Report 354, National Cooperative Highway Research - NCHRP, 1993.

[31] M. Ghosn and F. Moses. Markov renewal model for maximum bridge loading. *Journal of Engineering Mechanics*, 111(9):1093–1104, 1985.

[32] G. Glinka and J. C. P. Kam. Rainflow counting algorithm for very long stress histories. *International Journal of Fatigue*, 9(4):223–228, Oct 1987.

[33] J.-F. Gorse. Le calcul des effets produits par plusieurs voies de trafic routier sur un pont. le logiciel TRAFMULTI. *Bulletin de Liaison des Laboratoires des Ponts et Chaussees*, 164: 54–63, 1989.

[34] T. Gurney. *Cumulative damage of welded joints*. CRC Press, Washington, D.C., 2006.

[35] E. Haibach. The influence of cyclic material properties on fatigue life prediction by amplitude transformation. *International Journal of Fatigue*, 1(1):7–16, 1979.

[36] E. Haibach. Review of fatigue assessment procedures for welded aluminium structures. *International Journal of Fatigue*, 25(12):1359–1378, 2003.

[37] S. Haldimann-Sturm and A. Nussbaumer. *Charges de trafic CFF et évaluation à la fatigue*. Rapport du groupe de travail ad-hoc à la commision SIA 261, ICOM/EPFL, 2006.

[38] Z. Hashin and A. Rotem. A cumulative damage theory of fatigue failure. *Materials Science and Engineering*, 34(2):147–160, 1978.

[39] HCM2000. *Highway Capacity Manual*. Trasnportation Research Board, National Reseach Council, Washington DC, 2000.

[40] E.-S. Hwang and A.S. Nowak. Simulation of dynamic load for bridges. *Journal of Structural Engineering*, 117(5):1413 – 1434, 1991.

[41] D. Imhof, S. Bailey, and M. A. Hirt. *Modèle de charge (trafic 40t) pour l'évaluation des ponts-routes à deux voies avec trafic bidirectionnel*. Mandat de recherche OFROU 81/99, Union des professionels suisses de la route (VSS 556), Zurich, 2001.

[42] A. K. Khosrovaneh and N. E. Dowling. Fatigue loading history reconstruction based on the rainflow technique. *International Journal of Fatigue*, 12(2):99–106, Mar 1990.

[43] D. P. Kihl and Sh. Sarkani. Mean stress effects in fatigue of welded steel joints. *Probabilistic Engineering Mechanics*, 14(1-2):97–104, 1999.

[44] P. Kunz and M. A. Hirt. Grundlagen und Annahmen für den Nachweis der ermüdungssicherheit in den Tragwerksnormen des SIA. Technical Report D076, Schweizerischer Ingenieur - ud Architekten-Verein (SIA), 1991.

[45] J. A. Laman and A. S. Nowak. Fatigue-load models for girder bridges. *Journal of Structural Engineering-ASCE*, 122(7):726–733, Jul 1996.

[46] R.D. Larrabee. *Modeling extreme vehicle loads on highway bridges*. Department of Civil Engineering, MIT, Cambridge, 1978.

[47] S.S. Law and X.Q. Zhu. Bridge dynamic responses due to road surface roughness and braking of vehicle. *Journal of Sound and Vibration*, 282(3-5):805 – 830, 2005.

[48] H.-H. Lee, J.-C. Jeonl, K.-S. Kyung, and T. Mori. Influence of moving vehicle on fatigue of steel girder bridge. *Steel Structures*, 6:269 – 278, 2006.

[49] Yung-Li Lee, Jwo Pan, Richard Hathaway, and Mark Barkey. *Fatigue Testing and Analysis*. Materials & Mechanical. Butterworth-Heinemann, 2004.

[50] H. H. E. Leipholz. On the modified S-N curve for metal fatigue prediction and its experimental-verification. *Engineering Fracture Mechanics*, 23(3):495–505, 1986.

[51] H. Ludescher and E. Brühwiler. Vergrösserungsfaktoren für die wirkung von strassenverkehr auf bestehende brücken, mandat de recherche OFROU 89/98. Technical Report 571, Union des professionnels suisses de la route (VSS), 2004.

[52] H. Ludescher and E. Brühwiler. Dynamic amplification of traffic loads on road bridges. *Structural Engineering International - IABSE*, 19(2):190 – 197, 2009.

[53] G. Macchi, E.F. Radogna, G. Magenes, and A.L. Materazzi. Analisis probabilistica della sicurezza a fatica dei ponti. *Giomali de1 Genio Civile*, 4:151–187, 1989.

[54] N. Maddah, A. Nussbaumer, and T. Meystre. Traffic simulation parameters based on Switzerland measurements. Technical Report EPFL-169876, Ecole polytechnique fédérale de Lausanne - ICOM, 2012.

[55] S. S. Manson and G. R. Halford. Practical implementation of the double linear damage rule and damage curve approach for treating cumulative fatigue damage. *International Journal of Fracture*, 17(2):169–192, 1981.

[56] S. S. Manson and G. R. Halford. Re-examination of cumulative fatigue damage analysis - an engineering perspective. *Engineering Fracture Mechanics*, 25(5-6):539–571, 1986.

[57] A. D. May. *Traffic Flow Fundamentals*. Prentice-Hall, New Jersey, 1990.

[58] C. H. McInnes and P. A. Meehan. Equivalence of four-point and three-point rainflow cycle counting algorithms. *International Journal of Fatigue*, 30(3):547–559, Mar 2008.

[59] T. Meystre and M. A. Hirt. *Evaluation de ponts routiers existants avec un modèle de charges de trafic actualisé*. Mandat de recherche AGB2002/005, Office Fédéral des Routes, OFROU, Publication VSS 594, Bern, 2006.

[60] T. J. Miao and T. H. T. Chan. Bridge live load models from WIM data. *Engineering Structures*, 24(8):1071–1084, 2002.

[61] C. Miki, Y. Goto, H. Yoshida, and T. Mori. Computer simulation studies on the fatigue load and fatigue design of highway bridges. *Proc. of JSCE Structural Eng./Earthquake Eng*, 2(1):37–46, 1985.

[62] M. A. Miner. Cumulative damage in fatigue. *Journal of Applied Mechanics-Transactions of the Asme*, 12(3):A159–A164, 1945.

[63] H. Moghimi and H.R. Ronagh. Impact factors for a composite steel bridge using non-linear dynamic simulation. *International Journal of Impact Engineering*, 35(11):1228 – 1243, 2008.

[64] T. Mori, H.-H. Lee, and K.-S. Kyung. Fatigue life estimation parameter for short and medium span steel highway girder bridges. *Engineering Structures*, 29(10):2762–2774, 2007.

[65] A. S. Nowak. Live load model for highway bridges. *Structural Safety*, 13(1-2):53–66, 1993.

[66] A. Nussbaumer, L. Borges, and L. Davaine. *Fatigue design of steel and composite structures*. ECCS - European Convention for Constructional Steelwork, France, 2011.

[67] E. J. O'Brien and C.C. Caprani. Headway modelling for traffic load assessment of short to medium span bridges. *The Structural Engineer*, 83(16):33–36, 2005.

[68] E. J. O'Brien and B. Enright. Modeling same-direction two-lane traffic for bridge loading. *Structural Safety*, 33(4-5):296 – 304, 2011.

[69] A. O'Connor and E. J. O'Brien. Traffic load modelling and factors influencing the accuracy of predicted extremes. *Canadian Journal of Civil Engineering*, 32(1):270–278, Feb 2005.

[70] C. O'Connor and R. W. Pritchard. Impact studies on small composite girder bridge. *Journal of Structural Engineering*, 111(3):641 – 653, 1985.

[71] OHBD. *Ontario Highway Bridge design code*. Ministry of Transportation, 1983.

[72] Rapp Trans AG. *Entwicklungsindizes des Schweizerischen Strassenverkehrs Fortschreibung 1995 - 2009*. Bundesamt für Strassen ASTRA, Zürich, 2010.

[73] L. Sanpaolesi and P. Croce. *Handbook 4: Design of bridges - Guide to basis of bridge design related to Eurocodes supplemented by practical examples*. JRC Scientific and Technical Reports, 2005.

[74] C. G. Schilling. Stress cycles for fatigue design of steel bridges. *Journal of Structural Engineering-ASCE*, 110(6):1222–1234, 1984.

[75] C. G. Schilling, K. H. Klippstein, J. M. Barsom, and G. T. Blake. Fatigue of welded steel bridge members under variable-amplitude loadings. Technical Report 188, National Cooperative Highway Research - NCHRB, 1978.

[76] G. Sedlacek, G. Merzenich, and M. Paschen. *Background document to EN 1991 - Part 2: Traffic loads for road bridges - and consequences for the design*. JRC Scientific and Technical Reports, 2008.

[77] SETRA. *Ponts metalliques et mixtes - Resistance a la fatigue - Guide de conception de justifications*. Service d'Études Techniques des Routes et Autoroutes, France, 1996.

[78] SIA260. *Basis of Structural Design*. Swiss Society of Engineers and Architects, Zurich, 2004.

[79] SIA261. *Actions on Structures*. Swiss Society of Engineers and Architects, Zurich, 2003.

[80] SIA263. *Steel Construction*. Swiss Society of Engineers and Architects, Zurich, 2003.

[81] Sigmaplan. *Comptage suisse de la circulation routière 2005*. Office fédéral des routes (OFROU), Office fédéral de la statistique (OFS), Neuchatel, 2006.

[82] B. Sivakumar, M. Ghosn, and F. Moses. *Protocols for collecting and using traffic data in bridge design*. NCHRP, Washington, D.C., 2011.

[83] I. F. C. Smith, C.A Castiglioni, and P.B. Keating. An analysis of fatigue recommendations considering new data. In *IABSE Proceedings P-137/89*, pages 97–108, 1989.

[84] M. Thomann and J.-F. Wavre. *Pont sur l'Aar a Felsenau, rapport de mandat No. IC667-6*. ICOM-EPFL, Lausanne, 2002.

[85] C.C. Tung. Random response of highway bridges to vehicle loads. *Journal of the Engineering Mechanics Division*, 93(5):79–94, 1967.

[86] S. J. Wang and M. W. Dixon. A new criterion for positive mean stress fatigue design. *Journal of Mechanical Design*, 119(1):135–137, Mar 1997.

[87] T.L. Wang, M. Shahawz, and D.Z. Huang. Dynamic response of highway trucks due to road surface roughness. *Journal of Cornpurrs and Structures*, 49(6):1055 – 1067, 1993.

[88] A. Wöhler. Über die versuche zur ermittlung der festigkeit von achsen, welche in den werksttätten der niederschlesisch-märkischen eisenbahn zu frankfurt a.d.o. angestellt sind. *Z. f. Bauwesen 13*, pages 233–258, 1863.

A Evaluation of the codes background

A.1 Comparison of the SIA λ-factor with the three truck types

In this section of the appendix, the results of the background evaluation of the SIA codes is presented. Herein, the simulations on which the code values are based are redone with the same assumptions. The traffic load model expressed with three truck types (3TT), as shown in Fig. 3.5, is passing one-by-one on the bridges. The GVW frequency and average GVW (Q_m) for these three truck types are given in Table A.1.

The geometry of the SIA fatigue load model (Q_{fat}) [79], which is in accordance with damage equivalence factors, includes two axles with distance a 1.2 m, each weighting 270 kN and in total 540 kN. In addition, the influence length (L_Φ) is taken as the dynamic factor length according to the SIA261 [79]. The λ-factors are determined, for different traffic volumes, with a dynamic amplification factor 1.2 (on the 3TT).

The fatigue resistance curve of steel is considered with slope of 3 for cycles with stress range higher than constant amplitude fatigue limit (CAFL), and slope of 5 for cycles lower than CAFL, also cycles lower than cut-off limit are dismissed. The total damage sum is calculated for 70 years of traffic assuming a stationary process.

Based on the above-mentioned simplified assumptions, the damage equivalence factors are obtained for the different bridges static systems. Figures A.1 to A.4 illustrate the damage equivalence factors for bridges with different traffics and are compared with the curves given in the SIA263 [80]. One can notice that the code curves represent:

- for λ_1, an average for short to medium spans lengths and upper bound for long spans lengths,
- for λ_{max}, an upper bound.

Appendix A. Evaluation of the codes background

Table A.1: GVW frequency for three truck types of SIA code

C1 (38%)		C2 (50%)		C3 (12%)		C1	C2	C3
Weight (kN)	Frequency (%)	Weight (kN)	Frequency (%)	Weight (kN)	Frequency (%)	$n_i \times {Q_i}^5$	$n_i \times {Q_i}^5$	$n_i \times {Q_i}^5$
14.3	0	14.3	0	14.3	0	0.00E+00	0.00E+00	0.00E+00
42.9	0.035	42.9	0.006	42.9	0.016	1.92E+06	1.73E+05	9.72E+05
71.4	0.048	71.4	0.022	71.4	0.068	3.39E+07	8.18E+06	5.31E+07
100.0	0.101	100.0	0.011	100.0	0.034	3.84E+08	2.20E+07	1.43E+08
128.6	0.157	128.6	0.01	128.6	0.009	2.10E+09	7.03E+07	1.33E+08
157.1	0.172	157.1	0.018	157.1	0.025	6.26E+09	3.45E+08	1.01E+09
185.7	0.187	185.7	0.093	185.7	0.083	1.57E+10	4.11E+09	7.70E+09
214.3	0.109	214.3	0.114	214.3	0.145	1.87E+10	1.03E+10	2.75E+10
242.9	0.086	242.9	0.11	242.9	0.11	2.76E+10	1.86E+10	3.90E+10
271.4	0.031	271.4	0.077	271.4	0.065	1.74E+10	2.27E+10	4.02E+10
300.0	0.01	300.0	0.076	300.0	0.063	9.23E+09	3.69E+10	6.43E+10
328.6	0.015	328.6	0.089	328.6	0.057	2.18E+10	6.82E+10	9.17E+10
357.1	0.013	357.1	0.075	357.1	0.053	2.87E+10	8.72E+10	1.29E+11
385.7	0.013	385.7	0.125	385.7	0.124	4.22E+10	2.13E+11	4.45E+11
414.3	0.01	414.3	0.121	414.3	0.109	4.64E+10	2.95E+11	5.59E+11
442.9	0.006	442.9	0.045	442.9	0.031	3.88E+10	1.53E+11	2.22E+11
471.4	0.003	471.4	0.007	471.4	0	2.65E+10	3.26E+10	0.00E+00
500.0	0.002	500.0	0	500.0	0.006	2.38E+10	0.00E+00	7.88E+10
528.6	0	528.6	0	528.6	0.002	0.00E+00	0.00E+00	3.47E+10
557.1	0.002	557.1	0	557.1	0	4.08E+10	0.00E+00	0.00E+00
585.7	0	585.7	0.001	585.7	0	0.00E+00	1.38E+10	0.00E+00
Sum						3.66E+11	9.56E+11	1.73E+12
Q_m						314.0 (kN)		

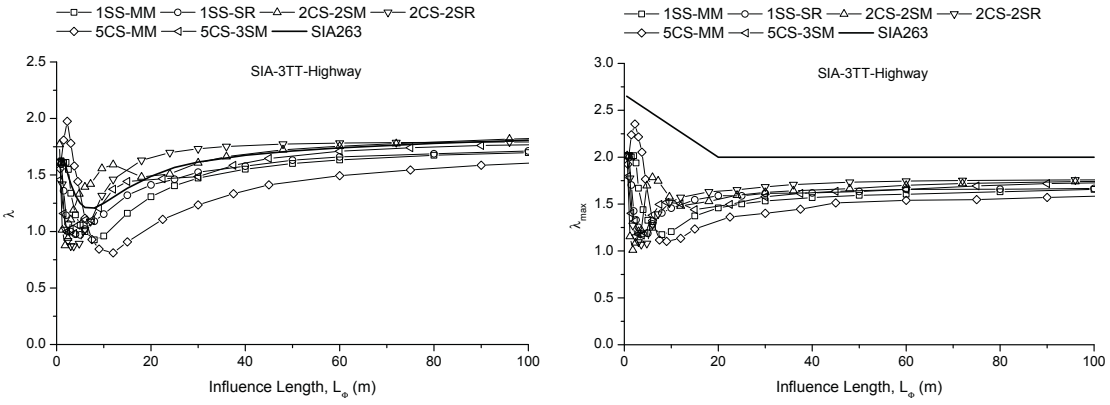

(a) λ (b) λ_{max}

Figure A.1: λ and λ_{max} obtained from 3TT for highway traffic in comparison with SIA263

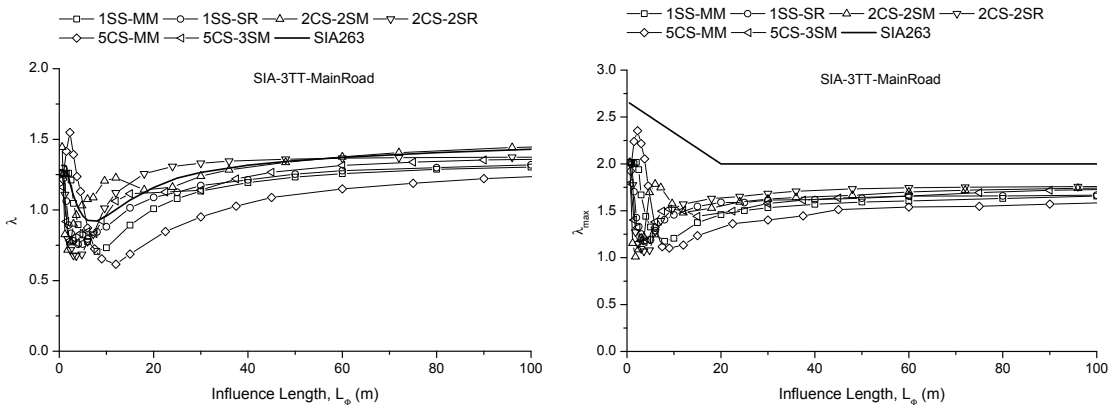

(a) λ (b) λ_{max}

Figure A.2: λ and λ_{max} obtained from 3TT for main road traffic in comparison with SIA263

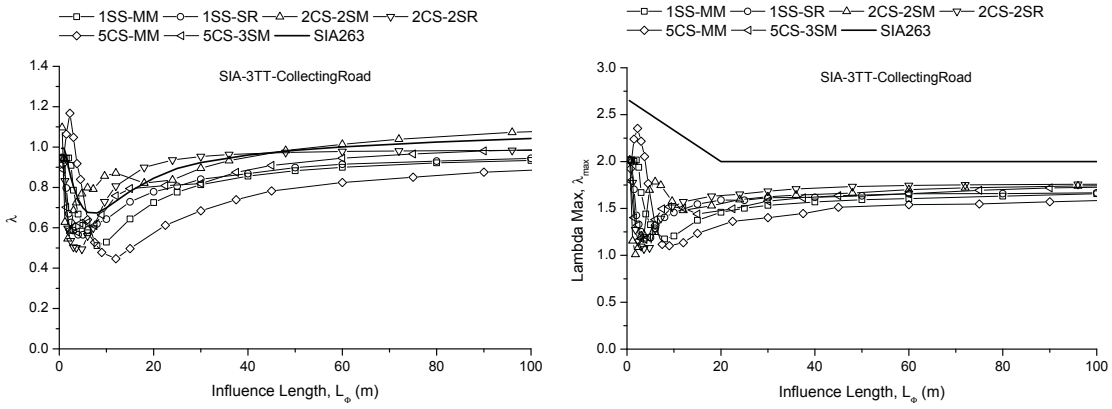

(a) λ (b) λ_{max}

Figure A.3: λ and λ_{max} obtained from 3TT for collecting road traffic in comparison with SIA263

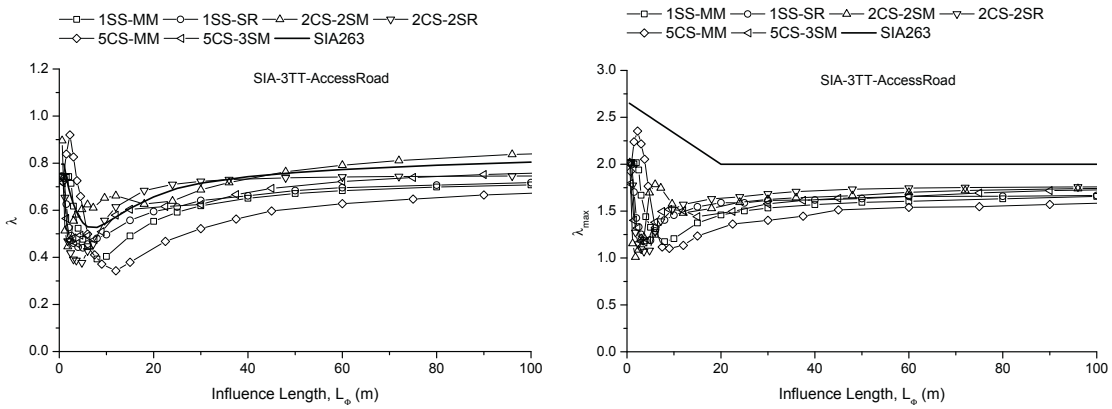

(a) λ (b) λ_{max}

Figure A.4: λ and λ_{max} obtained from 3TT for access road traffic in comparison with SIA263

A.2 Evaluation of the Eurocode λ-factor with FLM4

In this, the damage equivalence factors obtained from the Eurocode FLM4 [25] are compared with the damage equivalence factors given by the EN1993-2 [27]. To this end, the five lorries intended for Fatigue Load Model 4 (as shown in Table 3.1) are applied as a real traffic load model for determining damage equivalence factor, λ. The five lorries of Fatigue Load Model 4 as well as Fatigue Load Model 3 include identic dynamic load amplification appropriate for pavements of good quality, hence it does not needed to consider any dynamic amplification factor.

The Fatigue Load Model 3 consists of 4 axles, as shown in Figure 3.7, where the weight of each axle is 120 kN. For bridges with total length more than 40 m, a second set of axles in the same lane should be taken into account. The distance between axles of the second set is similar to the first set, whereas the weight of each axle is equal to 36 kN (instead of 120 kN). The minimum distance between two vehicles measured from centre to centre of vehicles is at least 40 m.

The fatigue resistance curve of steel is considered in the same way as explained in the previous section. The total damage sum is calculated for 100 years of traffic with 500'000 trucks per year per slow lane. Based on the above-mentioned assumptions, the damage equivalence factors are obtained for the different bridges static systems. Figures A.5 to A.7 illustrate the damage equivalence factors for bridges with different traffics and are compared with the curves given in the EN1993-2 [27]. The curves of the code are multiplied to λ_2 (see Eq. 3.6) based on the corresponding average GVW of traffic, as indicated in the captions.

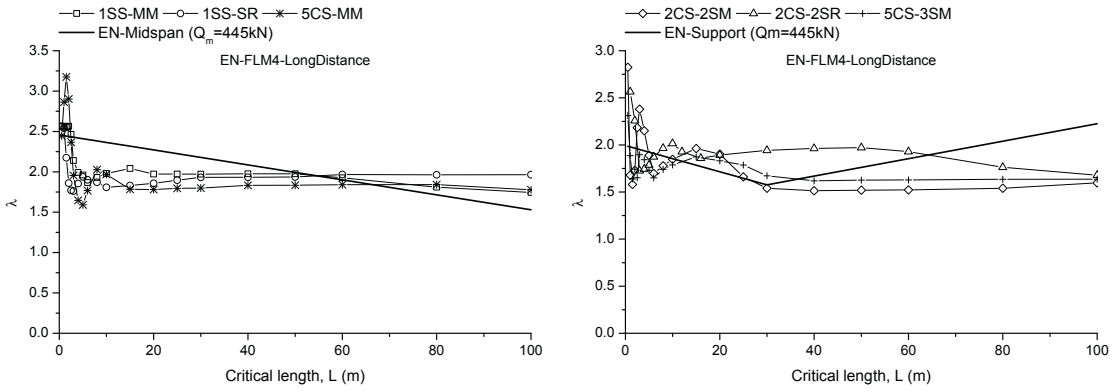

(a) At support (b) At mid span

Figure A.5: Comparison of λ with FLM4 for long distance traffic

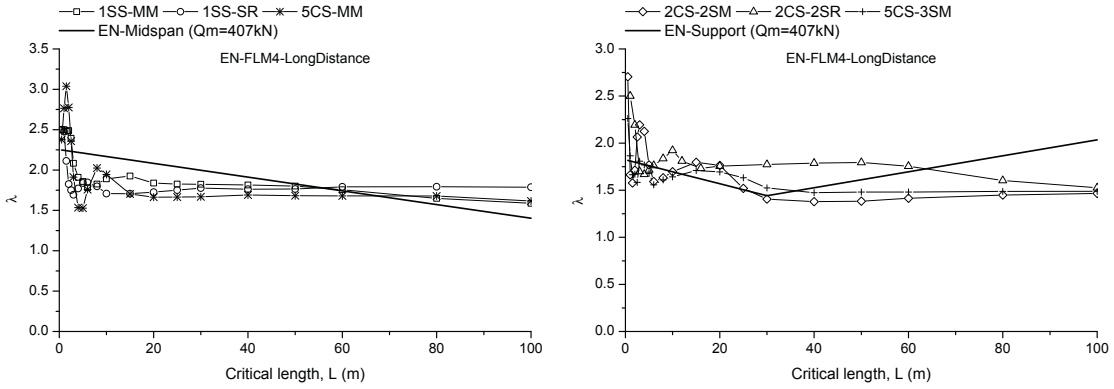

(a) At support (b) At mid span

Figure A.6: Comparison of λ with FLM4 for medium distance traffic

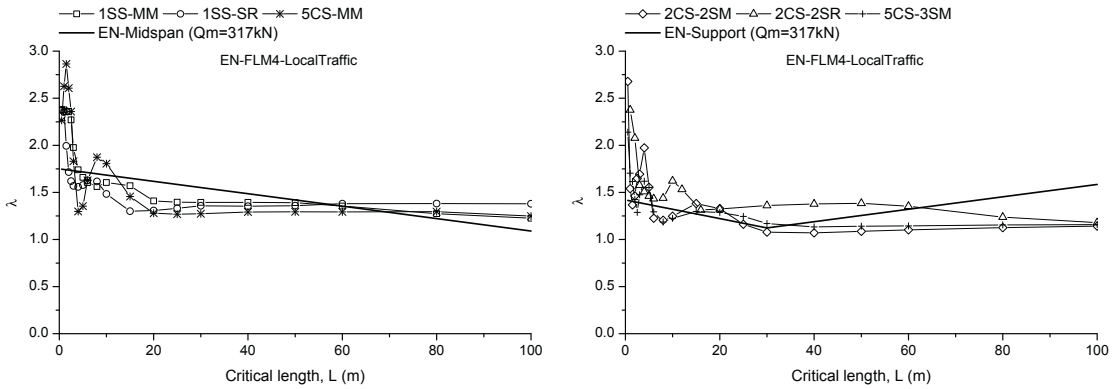

(a) At support (b) At mid span

Figure A.7: Comparison of λ with FLM4 for local traffic

B Traffic simulation methodology

B.1 WinQSIM program

The WinQSIM program, written in the programming language C#, is based on the probabilistic traffic model developed by Bailey [7]. This program was originally developed for determining extreme load event statistics for the reliability analysis of bridges with respect to static strength. Its development is further discussed by Meystre and Hirt [59]. The required inputs include: a probabilistic traffic model, the number of traffic lanes and the travel direction for each traffic lane, influence lines for each traffic lane, percentages of the total traffic and trucks in each traffic lane, as well as the traffic volume (V) and speed (s).

The probabilistic traffic model is defined by a number of truck types (determined by the user), along with distributions for the GVWs, axle weights, and spacing for each truck type. The traffic modelling consists of a Monte-Carlo simulation method, where parameters for each successive truck are chosen and the vehicle positions are shifted in a stepwise manner. At each step of the analysis, the local load effect or stress is recorded. The Rainflow cycle counting method is then used to obtain a load effect or stress range histogram at the end of the analysis.

Both congested and free-flow conditions can be modelled, thought only free-flow mode is used in this thesis. The distance between vehicles for free-moving traffic condition is given by a shifted exponential probability distribution [7]. The probability density function (PDF) for this distribution is as follows:

$$f_D(D) = \frac{V}{3600 \cdot s} \exp\left(-\frac{V}{3600 \cdot s} \cdot (d - 5.5)\right) \tag{B.1}$$

where V is the traffic volume in vehicles per hour, s is the traffic speed in m/s, and d is the distance between vehicles in m. This approach assumes full independence of the spacing between subsequent vehicles. "Light" traffic (cars) can be included in the analysis. The stress ranges due to cars are assumed to be negligible. Thus, the main effect of cars is to influence the spacing between the trucks. Figure B.1 shows a screenshot from the WinQSIM program.

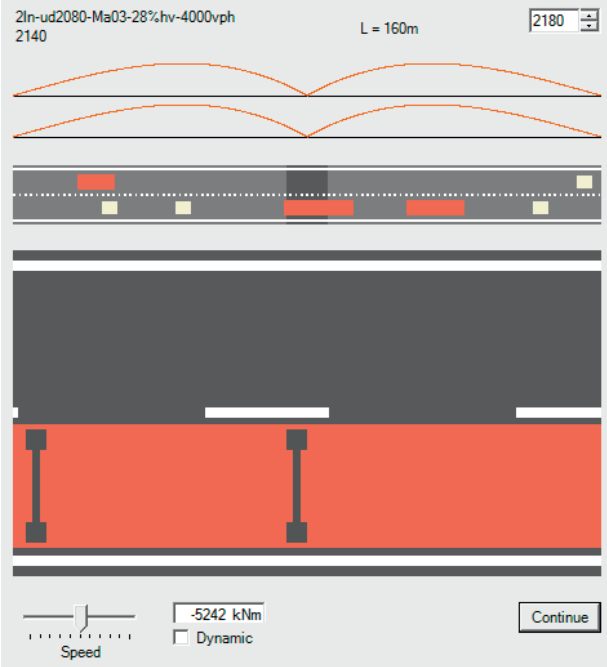

Figure B.1: A screenshot from the WinQSIM program

The vehicle speed, s, is set to 22 m/s (80 km/h) in all simulations. WinQSIM is not able to model traffic flow with variable speed. Thus, it does not model overtaking or lane changes within the bridge length.

B.2 FDABridge program

The FDABridge program is also developed based on Microsoft C#. It aims to perform cycle counting and damage accumulation in order to calculate fatigue equivalence factor for a given S-N curve family, fatigue load model and bridge influence line, see screenshots in Figure B.2. The FDABridge can either take a real traffic stress range histogram or WinQSIM output file as input, or it can perform vehicle-by-vehicle traffic simulation applying a given WIM raw data (truck traffic record) or a set of determined vehicles.

The damage equivalence factor, λ, is then obtained by shifting the S-N curve vertically until the cumulative damage index based on Miner's sum equals 1.0 for the real traffic cycles spectrum. λ is then calculated by dividing the force range (or, equivalently, stress range) at 2×10^6 cycles for this S-N curve by the force range due to the passage of the fatigue load model.

B.3 Analysis of traffic and inputs of traffic models

The truck databases used to construct the probabilistic traffic models are based on the Swiss WIM measurements. Specifically, for the initial traffic simulations the database from Mattstet-

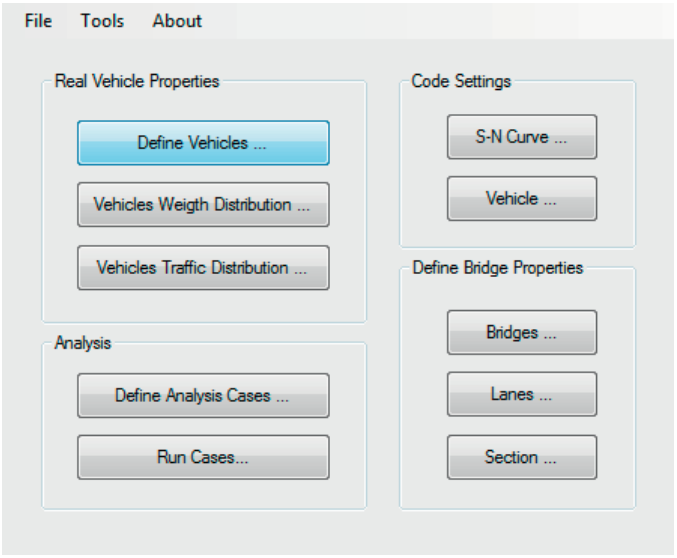

(a) Main menu

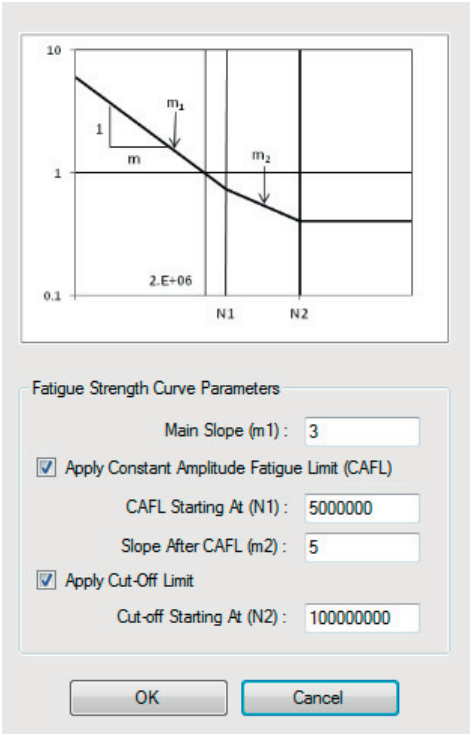

(b) S-N curve definition dialog box

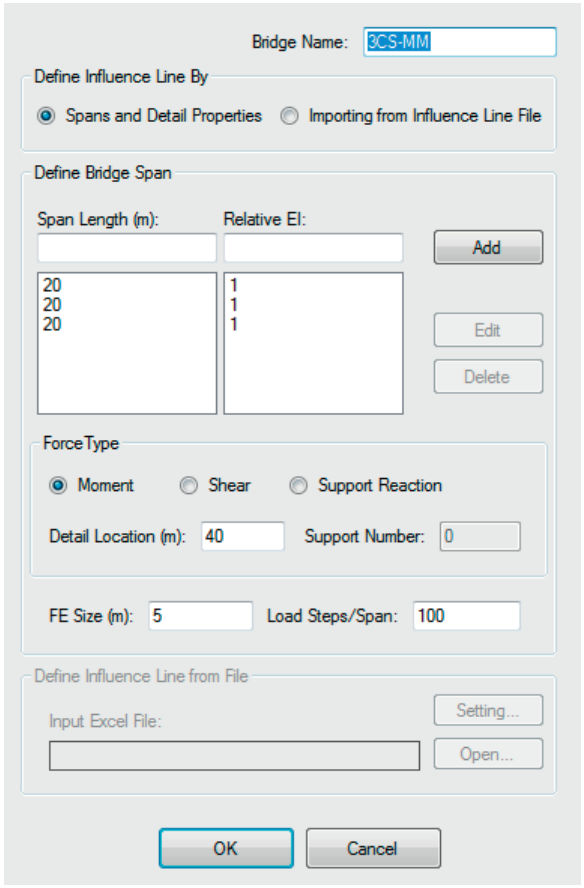

(c) Bridge definition dialog box

Figure B.2: Three screenshots from the FDABridge program

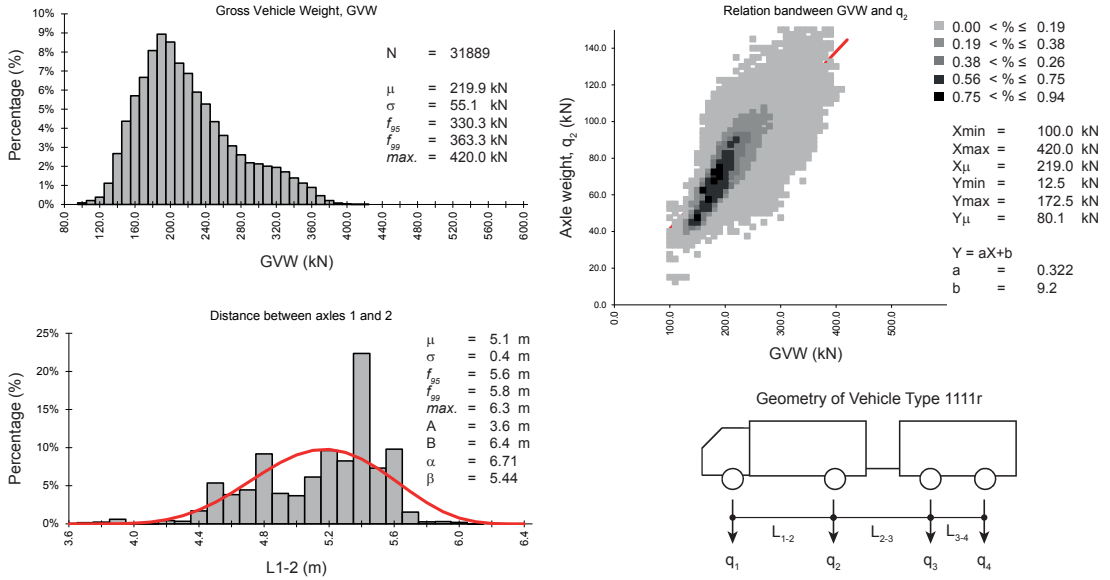

Figure B.3: Sample of statistical analysis of data from Götthard traffic database

ten traffic in 2003, and for final traffic simulations, Götthard traffic in 2009 as well as Mattstetten traffic in 2009 are used to model the real traffic.

The WIM database only includes truck traffic with GVW over 35 kN. The traffic for Mattstetten traffic in 2003 includes 2'289'927 trucks. The Mattstetten and Götthard traffic in 2009 include 2'515'171 and 1'037'141 trucks respectively, of which 71% and 85% are heavy vehicles with GVW over 100 kN.

The WIM database includes axle weight and spacing data for each measured truck. To define the probabilistic traffic model, the trucks are categorized into 13 truck types. The percentage of contribution for each truck type is given in Table B.1 for the three traffic simulation cases. These categories are the same as the ones defined by Meystre and Hirt [59] except for the Type-23 which is added in the current study for the final traffic simulations.

The ranges for each axle weight and spacing are defined, so that trucks could be slotted into one of these truck types. From all heavy vehicles of Mattstetten and Götthard traffic, respectively, 2.9% and 6.7% remained unclassified. Figure B.3 shows samples of axle weight and spacing data for truck Type 1111r, along with the fitting of Beta distributions to this data for the probabilistic traffic model.

Table B.2 show the input values for defining the geometry of the different truck types for Mattstetten traffic in 2003. The Foreside (distance from forehead of vehicle to the first axle or to the first axle of first axles group), and backside (distance from the last axle or the first axle of last axles group to the back of the vehicle) and axles spacing within a group are deterministic parameters. However, the distance between axles or group of axles (the base point for an axles group is the location of the first axle) is defined with Beta distribution function; the shape

parameter of the distribution is also given in Table B.2 for each truck type. The truck traffic geometry for Götthard and Mattstetten traffic in 2009 are respectively shown in Tables B.3 and B.4.

The axles load repartition for each vehicle type is defined as a linear function of GVW. For the case of truck type 113a, as an example, axles load repartition of the most loaded axles group can be calculated as $q_3 = a_3 \times GVW + b_3$, then the second axle load q_2 can be determined as $a_2 \times (GVW - q_3) + b_2$, and the last axle can be obtained as $q_1 = GVW + q_2 - q_3$. For the group of axles (tandem or tridem), load ratio between two or three axles which compose the group is fixed. The input parameters used for defining the axles load are provided in Table B.5 for Mattstetten traffic in 2003. Also, the truck axles load repartition for Götthard and Mattstetten traffic in 2009 are respectively shown in Tables B.6 to B.7.

The bimodal Beta distribution is used to define the trucks GVW of trucks for the Mattstetten traffic in 2003. The GVW distribution often has two peaks because of loaded and empty trucks, and bimodal Beta distribution allows modelling these two peaks. For each truck type

Table B.1: Heavy vehicles geometry and contribution percentages composing the three simulation traffics

Type	Geometry	Contributions (%)		
		Götthard 2009	Mattstetten 2009	Mattstetten 2003
11		9.93	16.02	30.35
12		3.90	4.73	6.21
22		0.57	3.21	4.39
23		0.37	0.81	N/A
111		0.56	3.11	4.71
1111r		3.69	18.75	18.47
112r		5.41	2.45	2.60
1211r	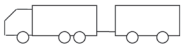	2.71	4.76	2.60
122		6.13	1.10	0.78
1112r		0.42	0.47	0.71
112a		11.44	22.06	16.37
113a		54.64	22.29	11.59
123a		0.23	0.25	1.21

of Mattstetten traffic in 2003, the input shape-parameters of two Beta distributions as well as the contribution percentage of the second Beta distribution in the total are shown in Table B.8.

For the Götthard and Mattstetten traffic in 2009, the GVW distributions of heavy vehicles are directly used as input. The GVW distribution of each truck type is shown in Figures B.4 to B.15. In addition, Figure B.17 shows the GVW distribution of all truck types measured in Götthard and Mattstetten station in 2009.

Table B.2: Geometry of trucks defined based on the Mattstetten traffic in 2003

Type	Foreside	Backside	Axles spacing within group(s)	Parameter	Beta distribution			
					A	B	α	β
	(m)	(m)	(m)		(m)	(m)		
11	1.5	2.5		L_{1-2}	3.6	7.2	2.97	3.09
12	1.5	3.3	1.3	L_{1-2}	3.6	7.2	2.33	2.78
22	1.5	2.3	1.5, 1.3	L_{1-2}	3.5	7.9	2.1	6.95
111	1.5	2.5	-	L_{1-2}	3.2	4.5	2.96	4.04
				L_{2-3}	3.6	8.6	1.47	1
1111r	1.5	1	-	L_{1-2}	3.6	6.4	6.09	3.48
				L_{2-3}	3.6	7.2	9.09	5.13
				L_{3-4}	3.6	6.4	7.04	5.54
112r	1.5	3.6	1.1	L_{1-2}	4.5	6.4	1.99	2.15
				L_{2-3}	3.6	8.6	9.93	2.49
1211r	1.5	1	1.3	L_{1-2}	3.6	6.4	6.59	7.31
				L_{2-3}	4.9	7.7	6.21	4.89
				L_{3-4}	3.6	6.4	4.96	4.16
122	1.5	3.3	1.3, 1.3	L_{1-2}	3.6	6.4	1.58	1.69
				L_{2-3}	4.9	9.9	6.44	4.67
1112r	1.5	2.3	1.3	L_{1-2}	3.6	6.4	3.18	3.2
				L_{2-3}	3.6	6.4	3.05	3.18
				L_{3-4}	3.6	6.4	4.08	5.47
112a	1.5	3.3	1.3	L_{1-2}	3.2	4.5	4.24	4.64
				L_{2-3}	3.6	8.6	4.62	2.54
113a	1.5	4.6	1.3	L_{1-2}	3.2	4.5	3.83	4.02
				L_{2-3}	3.6	8.6	9.68	10.87
123a	1.5	4.6	1.3, 1.3	L_{1-2}	2.4	3.6	1.71	1.57
				L_{2-3}	4.9	9.9	5.64	6.09

Table B.3: Geometry of trucks defined based on the Götthard traffic in 2009

Type	Foreside	Backside	Axles spacing within group(s)	Parameter	Beta distribution			
					A	B	α	β
	(m)	(m)	(m)		(m)	(m)		
11	1.5	2.5	-	L_{1-2}	3.6	7.2	4.48	2.90
12	1.5	3.4	1.4	L_{1-2}	3.6	7.2	2.54	1.51
22	1.5	2.4	1.8, 1.4	L_{1-2}	3.8	8.2	2.09	9.88
23	1.5	3.8	1.8, 1.4	L_{1-2}	2.4	8.2	6.27	23.77
111	1.5	2.5	-	L_{1-2}	3.2	4.5	6.25	10.39
				L_{2-3}	3.6	8.6	4.76	2.87
1111r	1.5	1	-	L_{1-2}	3.6	6.4	6.71	5.44
				L_{2-3}	3.6	7.2	9.35	5.69
				L_{3-4}	3.6	6.4	11.34	10.33
112r	1.5	3.8	1.3	L_{1-2}	4.5	6.4	6.61	6.23
				L_{2-3}	3.6	8.6	34.44	9.62
1211r	1.5	1	1.4	L_{1-2}	3.6	6.4	13.33	21.03
				L_{2-3}	5.0	7.8	11.84	12.07
				L_{3-4}	3.6	6.4	7.19	7.35
122	1.5	3.6	1.4, 1.6	L_{1-2}	3.6	6.4	6.26	6.31
				L_{2-3}	5.0	10.0	28.04	21.35
1112r	1.5	2.3	1.3	L_{1-2}	3.6	6.4	5.76	7.43
				L_{2-3}	3.6	6.4	2.49	4.35
				L_{3-4}	3.6	6.4	3.16	4.57
112a	1.5	3.3	1.3	L_{1-2}	3.2	4.5	7.15	10.80
				L_{2-3}	3.6	8.6	11.05	5.60
113a	1.5	4.6	1.3	L_{1-2}	3.2	4.5	8.58	12.99
				L_{2-3}	2.4	8.6	30.86	27.55
123a	1.5	4.7	1.3, 1.3	L_{1-2}	2.4	3.6	1.42	2.56
				L_{2-3}	4.9	9.9	7.06	9.06

Table B.4: Geometry of trucks defined based on the Mattstetten traffic in 2009

Type	Foreside	Backside	Axles spacing within group(s)	Parameter	Beta distribution			
					A	B	α	β
	(m)	(m)	(m)		(m)	(m)		
11	1.5	2.5	-	L_{1-2}	3.6	7.2	4.52	4.42
12	1.5	3.4	1.4	L_{1-2}	3.6	7.2	1.59	1.86
22	1.5	2.4	1.8, 1.4	L_{1-2}	3.8	8.2	2.61	9.23
23	1.5	3.8	1.8, 1.4	L_{1-2}	2.4	8.2	6.37	20.49
111	1.5	2.5	-	L_{1-2}	3.2	4.5	8.71	15.53
				L_{2-3}	3.6	8.6	5.17	2.65
1111r	1.5	1	-	L_{1-2}	3.6	6.4	8.28	6.09
				L_{2-3}	3.6	7.2	13.59	8.84
				L_{3-4}	3.6	6.4	13.14	12.03
112r	1.5	3.8	1.3	L_{1-2}	4.5	6.4	4.06	4.63
				L_{2-3}	3.6	8.6	17.88	5.12
1211r	1.5	1	1.4	L_{1-2}	3.6	6.4	11.14	16.29
				L_{2-3}	5.0	7.8	11.11	10.90
				L_{3-4}	3.6	6.4	8.71	8.25
122	1.5	3.5	1.4, 1.5	L_{1-2}	3.6	6.4	3.34	4.53
				L_{2-3}	5.0	10.0	10.33	7.48
1112r	1.5	2.3	1.3	L_{1-2}	3.6	6.4	2.60	4.10
				L_{2-3}	3.6	6.4	3.91	4.89
				L_{3-4}	3.6	6.4	2.39	4.77
112a	1.5	3.4	1.4	L_{1-2}	3.2	4.5	8.29	13.44
				L_{2-3}	3.6	8.6	8.82	4.85
113a	1.5	4.6	1.3	L_{1-2}	3.2	4.5	7.61	11.94
				L_{2-3}	2.4	8.6	17.04	15.30
123a	1.5	4.8	1.3, 1.4	L_{1-2}	2.4	3.6	1.94	1.66
				L_{2-3}	4.9	9.9	4.33	5.03

Table B.5: Axle load relation defined based on the Mattstetten traffic in 2003

Type	Ordinate Parameter	Abscissa Parameter	Axle load ratio within group(s)	a	b
11	q_2	GVW		0.701	-15
12	q_2	GVW	0.67-0.33	0.803	-27
22	q_2	GVW	0.5-0.50,0.50-0.50	0.728	-36
111	q_2	$GVW - q_3$	-	0.579	-5
	q_3	GVW		0.317	2
1111r	q_2	GVW	-	0.336	4
	q_3	$GVW - q_2$		0.438	-17
	q_4	$GVW - q_2 - q_3$		0.677	-28
112r	q_2	GVW	0.50-0.50	0.321	7
	q_3	$GVW - q_2$		0.791	-28
1211r	q_2	GVW	0.67-0.33	0.407	6
	q_3	$GVW - q_2$		0.437	-18
	q_4	$GVW - q_2 - q_3$		0.671	-28
122	q_2	GVW	0.67-0.33, 0.50-0.50)	0.403	12
	q_3	$GVW - q_2$		0.902	-49
1112r	q_2	GVW	0.50-0.50	0.282	3
	q_3	$GVW - q_2$		0.331	-13
	q_4	$GVW - q_2 - q_3$		0.839	-40
112a	q_2	$GVW - q_3$	0.50-0.50	0.796	-33
	q_3	GVW		0.574	-35
113a	q_2	$GVW - q_3$	0.33-0.34-0.33	0.81	-35
	q_3	GVW		0.656	-46
123a	q_2	$GVW - q_3$	0.67-0.33, 0.33-0.34-0.33	0.865	-38
	q_3	GVW		0.661	-56

Table B.6: Axle load relation defined based on the Götthard traffic in 2009

Type	Ordinate Parameter	Abscissa Parameter	Axle load ratio within group(s)	a	b
11	q_2	GVW	-	0.76	-22.6
12	q_2	GVW	0.65-0.35	0.805	-27
22	q_2	GVW	0.5-0.50, 0.50-0.50	0.711	-42.1
23	q_2	GVW	0.5-0.50, 0.30-0.35-0.35	0.711	-46.5
111	q_2	$GVW - q_3$	-	0.784	-34.7
	q_3	GVW		0.443	-20.9
1111r	q_2	GVW	-	0.322	9.2
	q_3	$GVW - q_2$		0.458	-21.6
	q_4	$GVW - q_2 - q_3$		0.722	-32.8
112r	q_2	GVW	0.50-0.50	0.321	10.3
	q_3	$GVW - q_2$		0.823	-34.1
1211r	q_2	GVW	0.67-0.33	0.422	0.8
	q_3	$GVW - q_2$		0.434	-19.2
	q_4	$GVW - q_2 - q_3$		0.751	-37.2
122	q_2	GVW	0.67-0.33, 0.50-0.50	0.448	-5.5
	q_3	$GVW - q_2$		0.875	-44
1112r	q_2	GVW	0.50-0.50	0.249	11.9
	q_3	$GVW - q_2$		0.320	-11.1
	q_4	$GVW - q_2 - q_3$		0.889	-48.4
112a	q_2	$GVW - q_3$	0.50-0.50	0.831	-40.7
	q_3	GVW		0.574	-38.1
113a	q_2	$GVW - q_3$	0.33-0.34-0.33	0.827	-40.9
	q_3	GVW		0.698	-58.2
123a	q_2	$GVW - q_3$	0.36-0.64, 0.33-0.34-0.33	0.893	-44.5
	q_3	GVW		0.648	-57.9

Table B.7: Axle load relation defined based on the Mattstetten traffic in 2009

Type	Ordinate Parameter	Abscissa Parameter	Axle load ratio within group(s)	a	b
11	q_2	GVW	-	0.755	-23.9
12	q_2	GVW	0.60-0.40	0.786	-23.0
22	q_2	GVW	0.5-0.50, 0.50-0.50	0.704	-36.6
23	q_2	GVW	0.5-0.50, 0.30-0.35-0.35	0.788	-45.4
111	q_2	$GVW - q_3$	-	0.747	-28.4
	q_3	GVW		0.398	-12.3
1111r	q_2	GVW	-	0.326	5.5
	q_3	$GVW - q_2$		0.437	-18.2
	q_4	$GVW - q_2 - q_3$		0.628	-23.9
112r	q_2	GVW	0.50-0.50	0.288	13.9
	q_3	$GVW - q_2$		0.784	-27.4
1211r	q_2	GVW	0.50-0.50	0.389	11.1
	q_3	$GVW - q_2$		0.429	-17.1
	q_4	$GVW - q_2 - q_3$		0.680	-28.9
122	q_2	GVW	0.60-0.40, 0.50-0.50	0.448	-0.7
	q_3	$GVW - q_2$		0.852	-40.5
1112r	q_2	GVW	0.50-0.50	0.268	5.1
	q_3	$GVW - q_2$		0.314	-12.6
	q_4	$GVW - q_2 - q_3$		0.853	-42.2
112a	q_2	$GVW - q_3$	0.50-0.50	0.796	-34.6
	q_3	GVW		0.560	-33.3
113a	q_2	$GVW - q_3$	0.33-0.34-0.33	0.812	-37.3
	q_3	GVW		0.685	-53.1
123a	q_2	$GVW - q_3$	0.45-0.55, 0.33-0.34-0.33	0.822	-42.1
	q_3	GVW		0.654	-58.2

Table B.8: GVW distribution of trucks defined based on the Mattstetten traffic in 2003

Type	Contribution of second Beta distribution (%)	First Beta distribution				Second Beta distribution			
		A_1 (kN)	B_1 (kN)	α_1	β_1	A_2 (kN)	B_2 (kN)	α_2	β_2
11	33.20	35	265	6.9	16.5	80	300	10	20
12	80.20	45	390	13.7	11.5	35	400	6.5	11.2
22	43.70	35	455	24.8	12.9	70	600	5.7	29.4
111	75.00	40	355	12.5	86.8	95	600	3.3	18.2
1111r	91.40	55	460	33.1	14.6	65	600	4.9	14.5
112r	56.60	110	600	22.3	41.5	45	465	10	20
1211r	52.90	35	600	27.1	20	35	600	9.8	17
122	27.40	70	600	9.9	24	95	565	9.9	9.5
1112r	44.40	35	575	8.5	23.6	65	550	9.9	8.4
112a	40.70	40	510	10	24.8	65	600	10	14.6
113a	44.30	80	600	3.8	13.2	35	580	20.2	14.1
123a	52.50	80	555	8.8	23.8	80	580	5.9	4.9

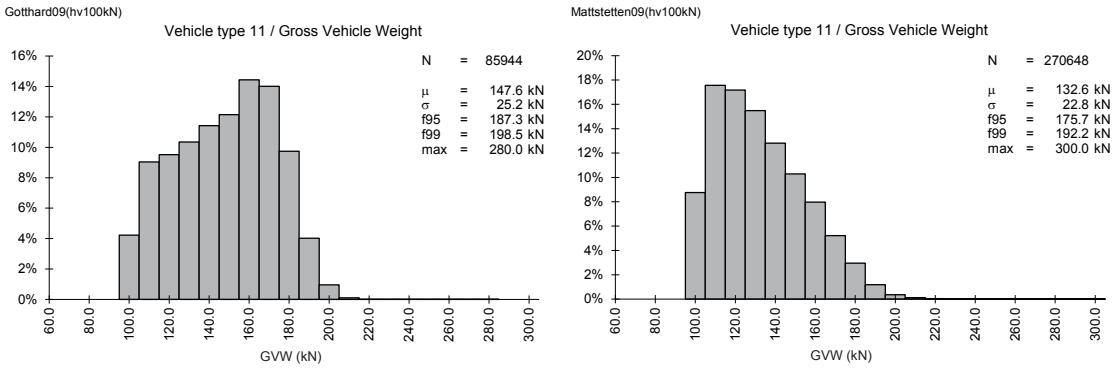

(a) Götthard 2009 (b) Mattstetten 2009

Figure B.4: Frequency of GVW for truck Type 11

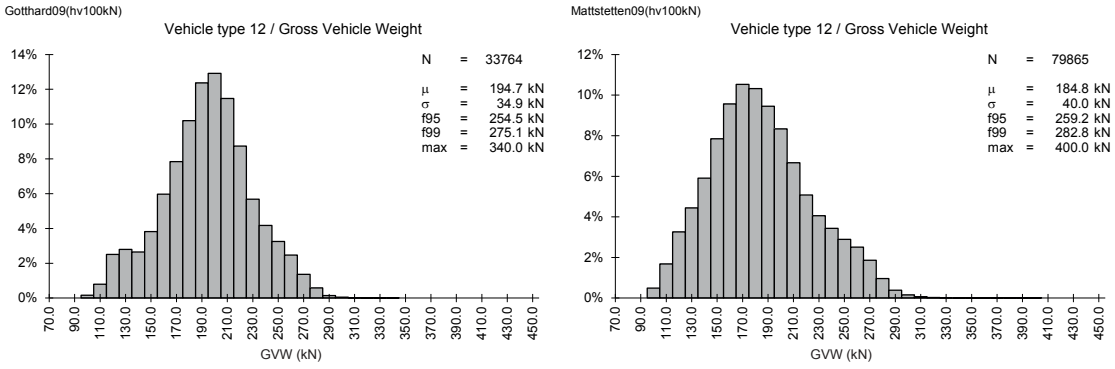

(a) Götthard 2009 (b) Mattstetten 2009

Figure B.5: Frequency of GVW for truck Type 12

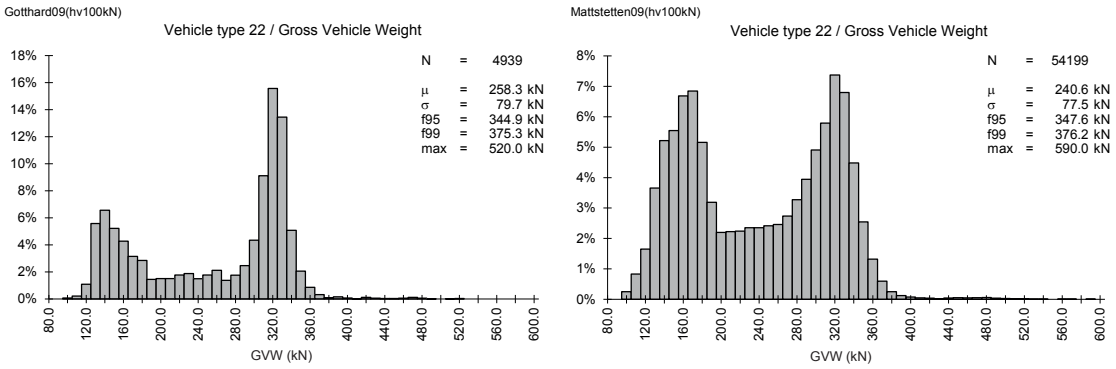

(a) Götthard 2009 (b) Mattstetten 2009

Figure B.6: Frequency of GVW for truck Type 22

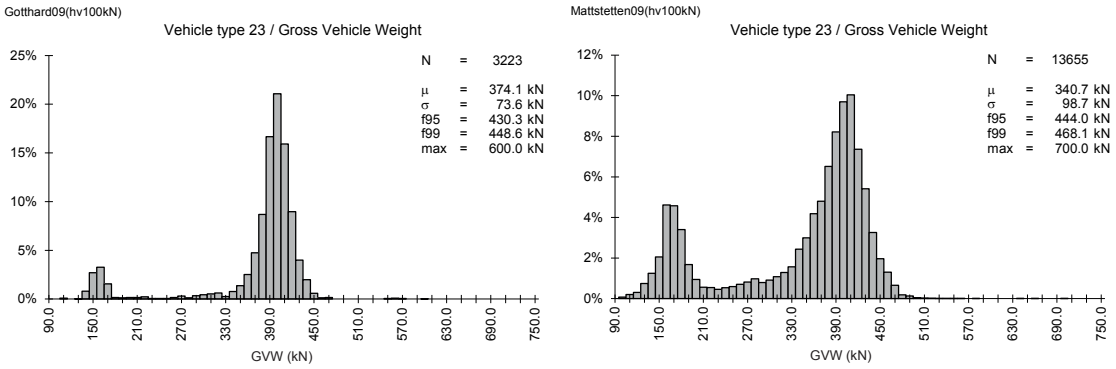

(a) Götthard 2009 (b) Mattstetten 2009

Figure B.7: Frequency of GVW for truck Type 23

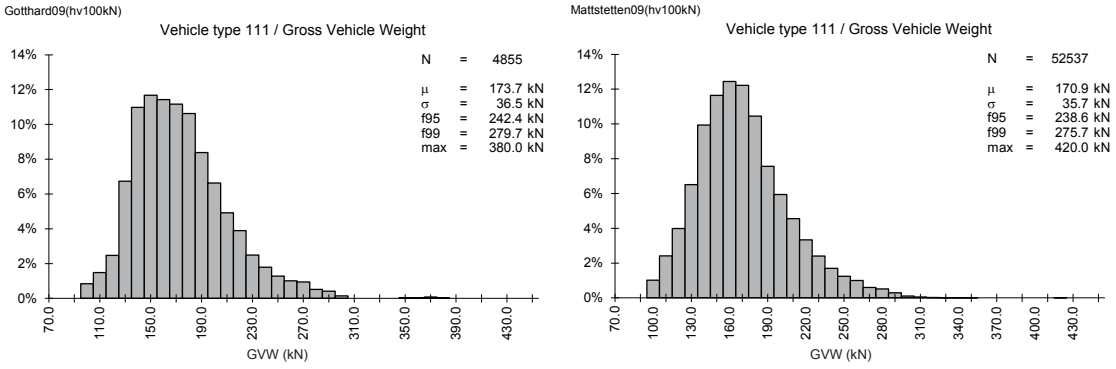

(a) Götthard 2009 (b) Mattstetten 2009

Figure B.8: Frequency of GVW for truck Type 111

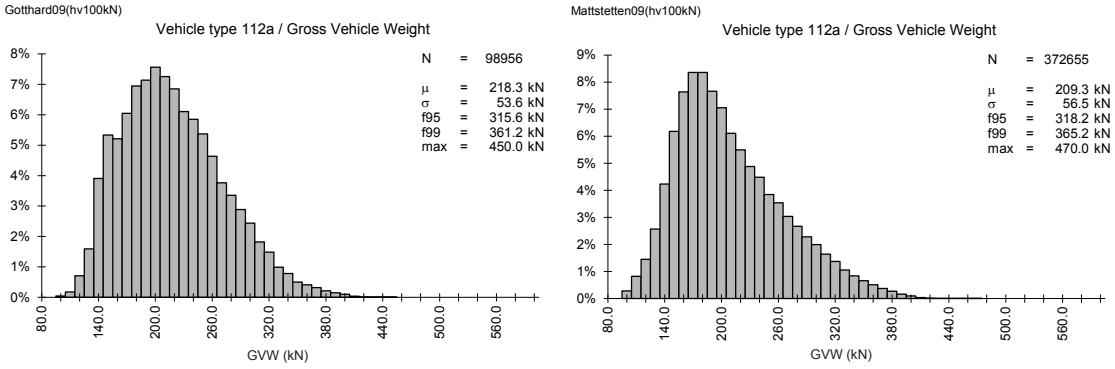

(a) Götthard 2009 (b) Mattstetten 2009

Figure B.9: Frequency of GVW for truck Type 112a

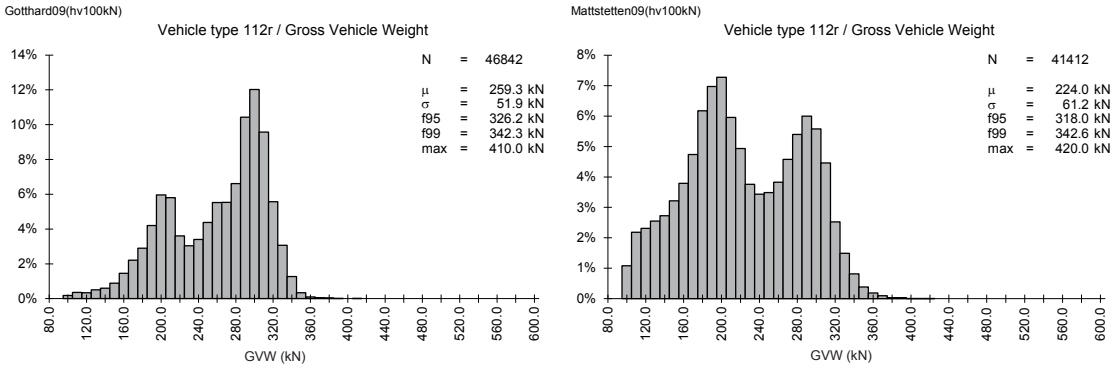

(a) Götthard 2009 (b) Mattstetten 2009

Figure B.10: Frequency of GVW for truck Type 112r

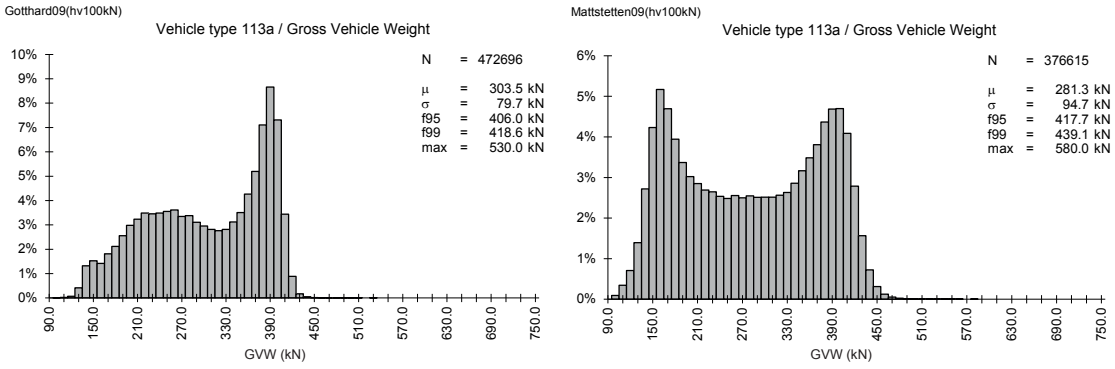

(a) Götthard 2009 (b) Mattstetten 2009

Figure B.11: Frequency of GVW for truck Type 113a

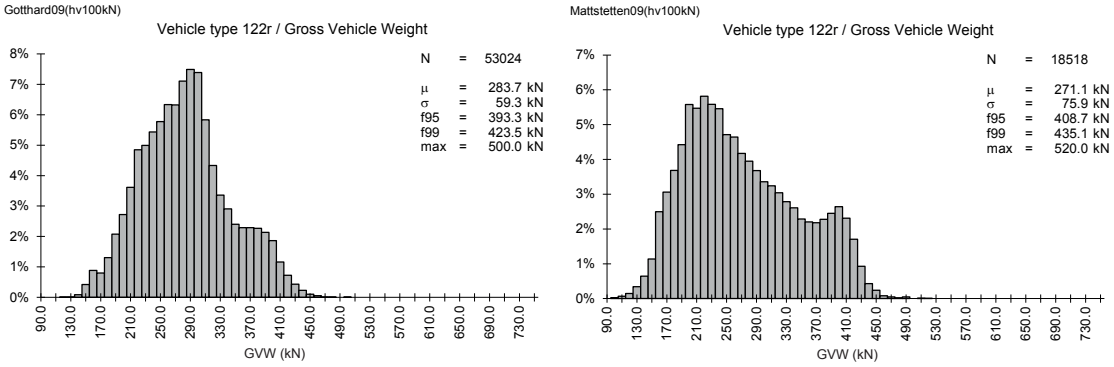

(a) Götthard 2009 (b) Mattstetten 2009

Figure B.12: Frequency of GVW for truck Type 122r

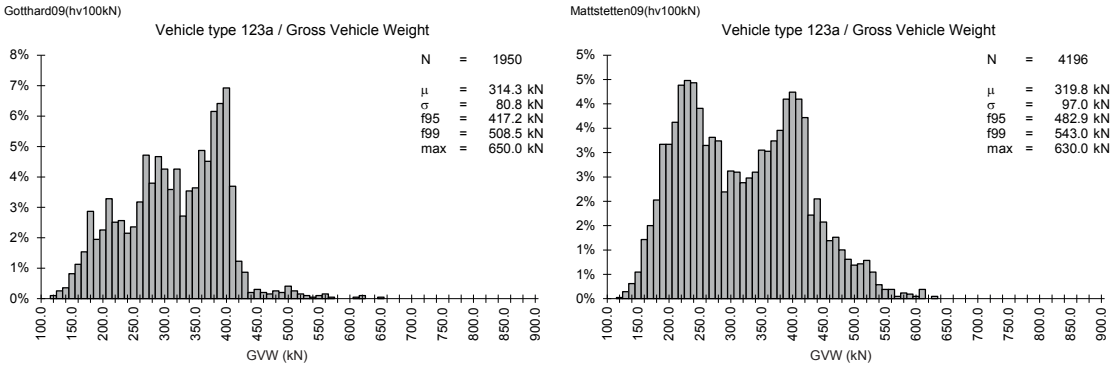

(a) Götthard 2009 (b) Mattstetten 2009

Figure B.13: Frequency of GVW for truck Type 123a

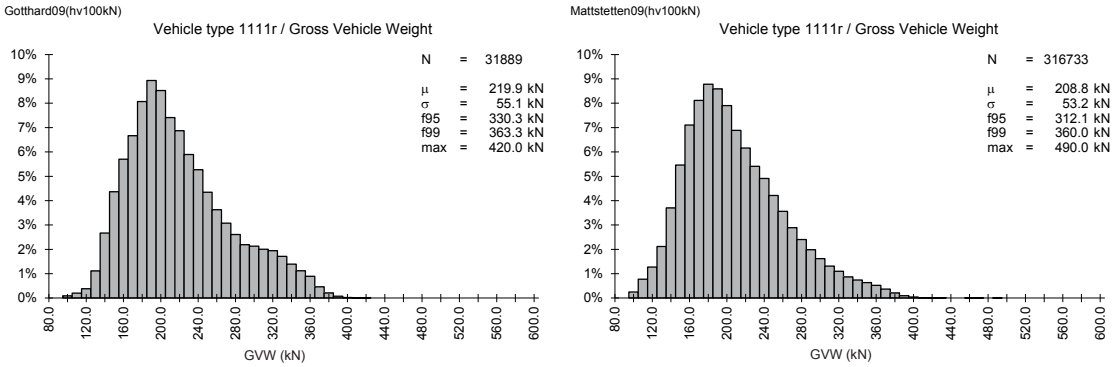

(a) Götthard 2009 (b) Mattstetten 2009

Figure B.14: Frequency of GVW for truck Type 1111r

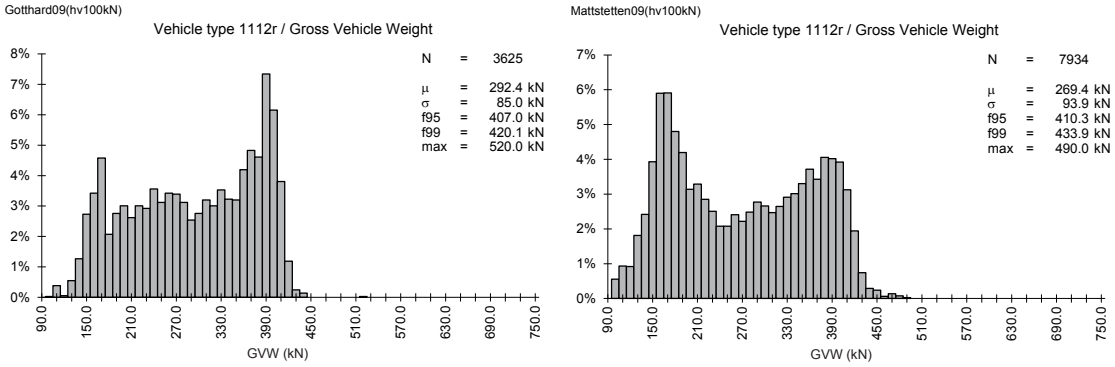

(a) Götthard 2009 (b) Mattstetten 2009

Figure B.15: Frequency of GVW for truck Type 1111r

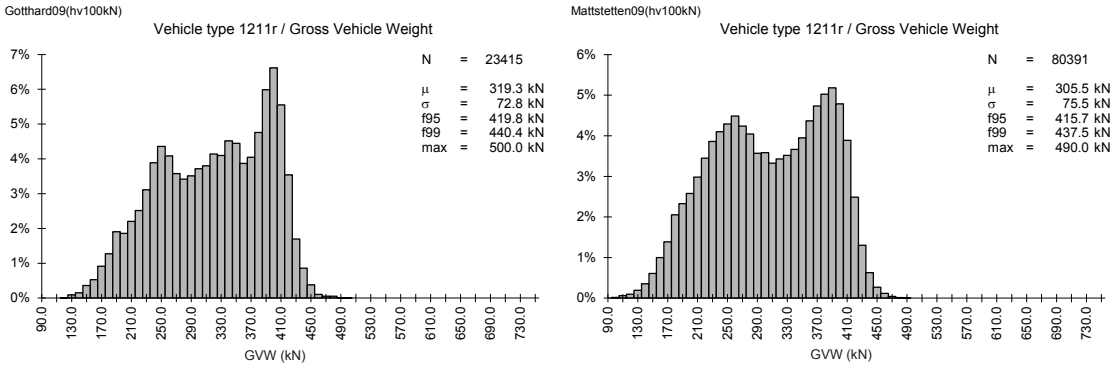

(a) Götthard 2009 (b) Mattstetten 2009

Figure B.16: Frequency of GVW for truck Type 1211r

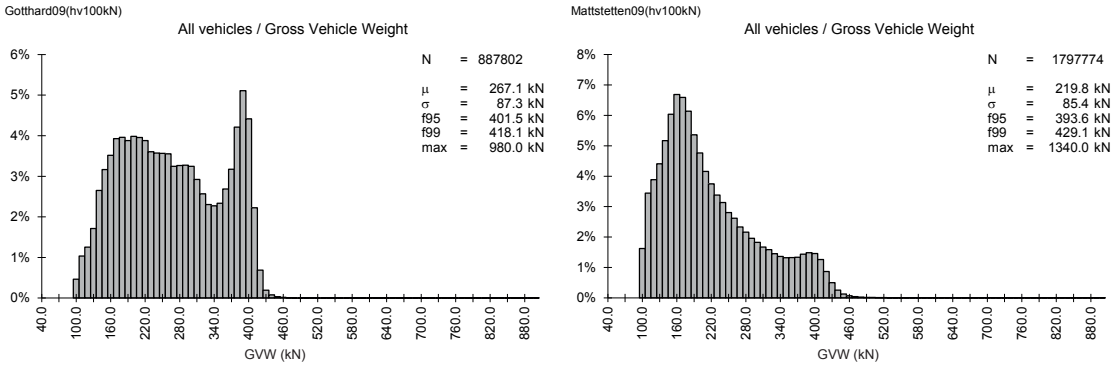

(a) Götthard 2009 (b) Mattstetten 2009

Figure B.17: Frequency of GVW for all truck types

C Final traffic simulations results

C.1 Damage equivalence factors based on the codes

In the current section, the results of the final simulations are compared with the damage equivalence factors, λ and λ_{max}, from the SIA263 [80] and EN1993-2 [27]. The fatigue load model and the critical span length based on the SIA codes and the Eurocodes are described, respectively, in Sections 3.1.1 and 3.1.2. In addition, the traffic simulation cases and the bridge cases for final traffic simulations are explained in Chapter 6.

Figures C.1 to C.6 shows the resulting λ and λ_{max} based on the SIA code parameters for the six traffic conditions, along with the curves of the SIA code. Since the basis service life of the SIA code is 70 years and the λ-factors from the simulations are obtained for 100 years of traffic, the λ_1-factors of the code are increased by $\lambda_3 = (100/70)^{(1/5)}$ in order to be comparable with the λ-factors from the traffic simulations. If a service life of 70 years is required then the values in the graphs should be multiplied using Equation 3.8. The best fitting nonlinear curve is also plotted on the same figures to assess the dispersion of the damage equivalence factors for the different bridge cases.

The resulting damage equivalence factors based on the Eurocode are shown in Figures C.7 to C.18. The corresponding λ and λ_{max} based on the Eurocode[27] are also plotted in the same figures. The average gross weight of heavy vehicles (Q_m) as well as annual number of heavy vehicles (N_{obs}) are adapted by λ_2 according to the values corresponding to the traffic simulations. Specifically, the value of Q_m for Götthard and Mattstetten heavy vehicle traffic in 2009 is 313 kN and 282 kN respectively. Also N_{obs} depends on traffic condition and it is 2'000'000 and 500'000 per year respectively for highways and main roads traffic. In addition, the Eurocode λ for Q_m = 480 kN is also plotted in the same figures. For all figures of the current section the calculation of maximum damage equivalence factor, λ_{max}, the maximum stress range is the value that the superior stress ranges produce less than 1% of total damage (it also applies to the figures corresponding to the SIA code).

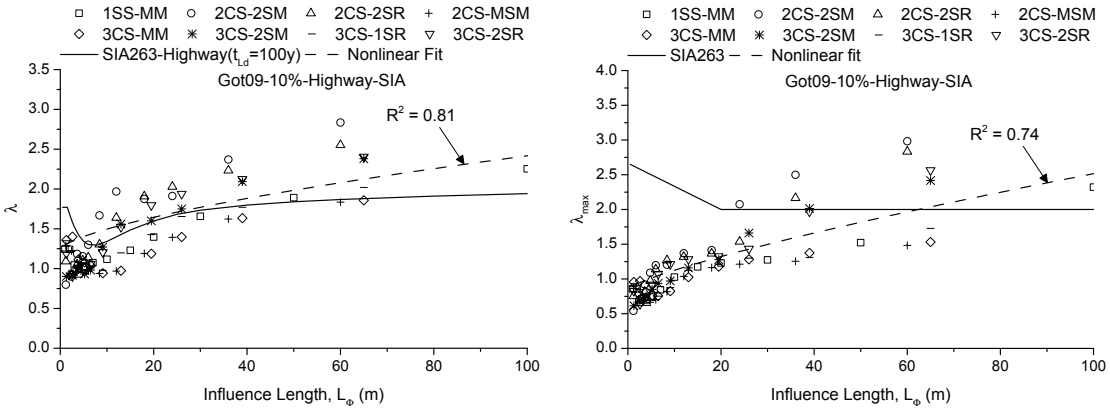

(a) λ (b) λ_{max}

Figure C.1: SIA-base damage equivalence factors for G10HW traffic

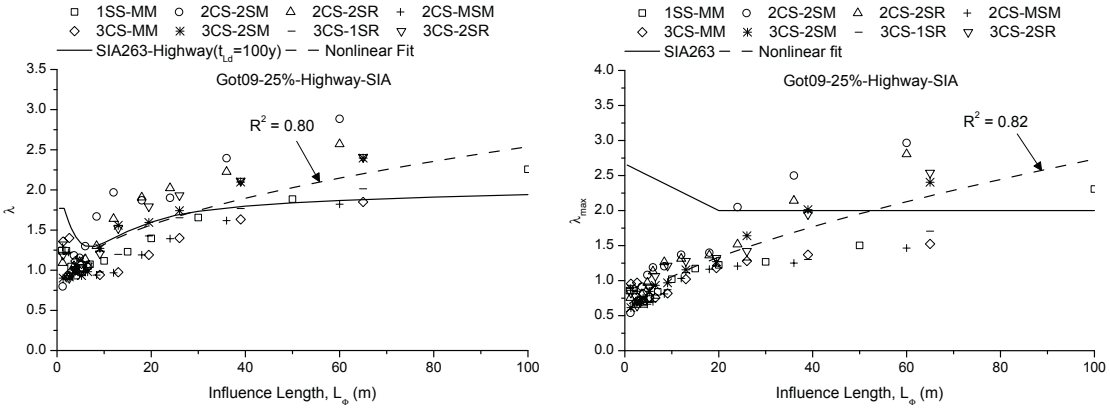

(a) λ (b) λ_{max}

Figure C.2: SIA-base damage equivalence factors for G25HW traffic

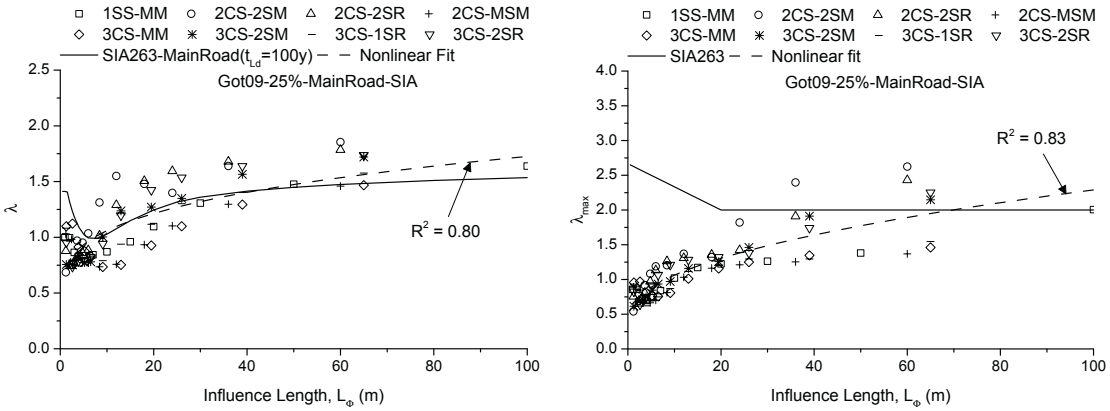

(a) λ (b) λ_{max}

Figure C.3: SIA-base damage equivalence factors for G25MR traffic

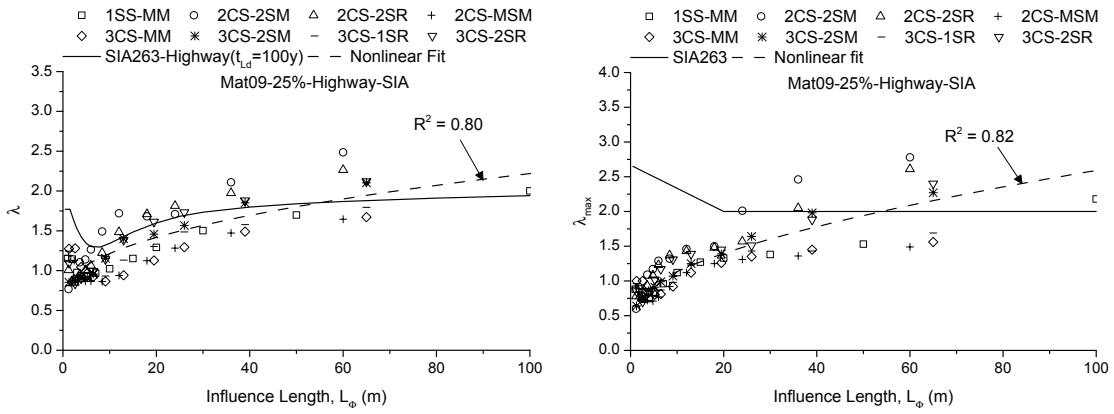

(a) λ (b) λ_{max}

Figure C.4: SIA-base damage equivalence factors for M25HW traffic

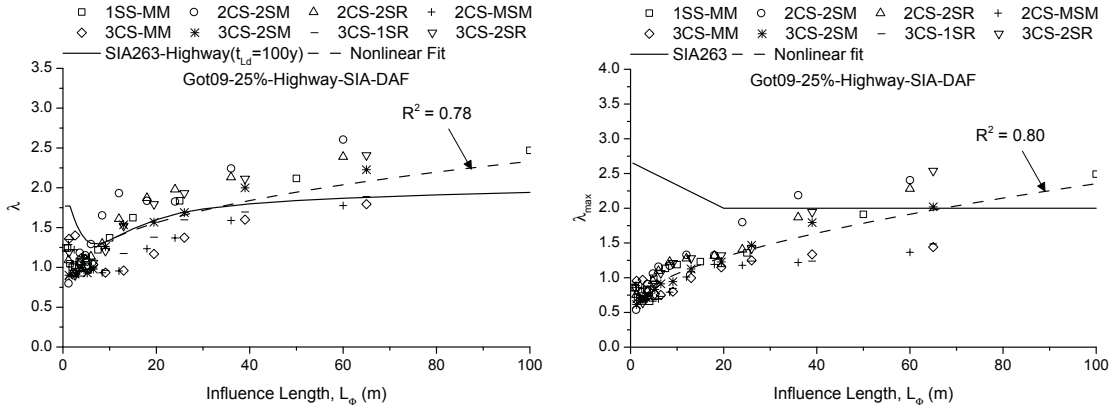

(a) λ (b) λ_{max}

Figure C.5: SIA-base damage equivalence factors for G25HWDAF traffic

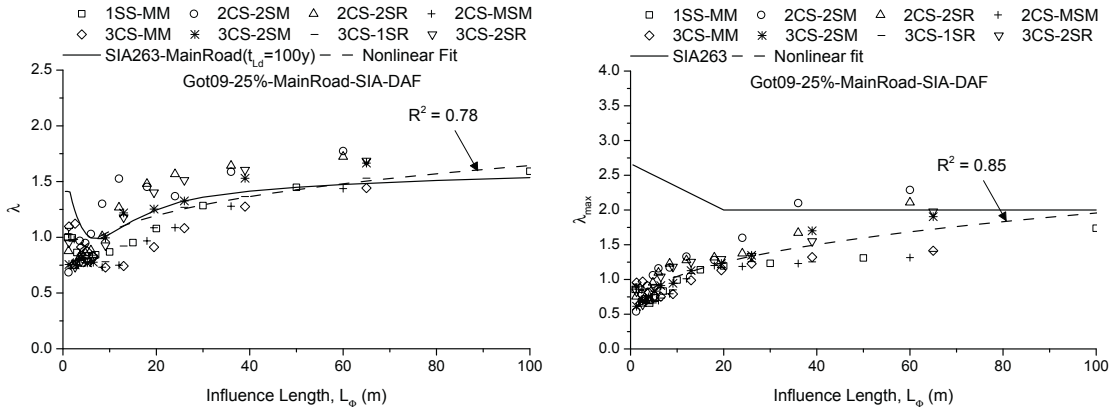

(a) λ (b) λ_{max}

Figure C.6: SIA-base damage equivalence factors for G25MRDAF traffic

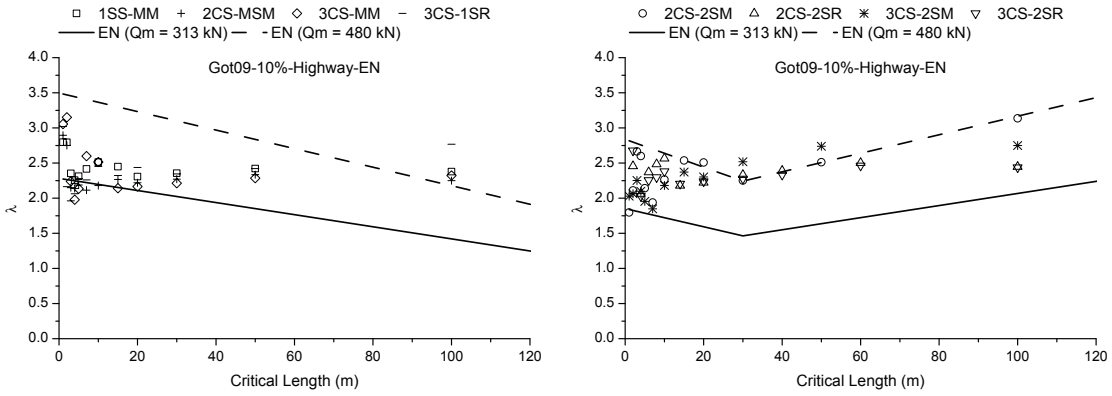

(a) Mid-span sections (b) Support sections

Figure C.7: Eurocode-base λ for G10HW traffic

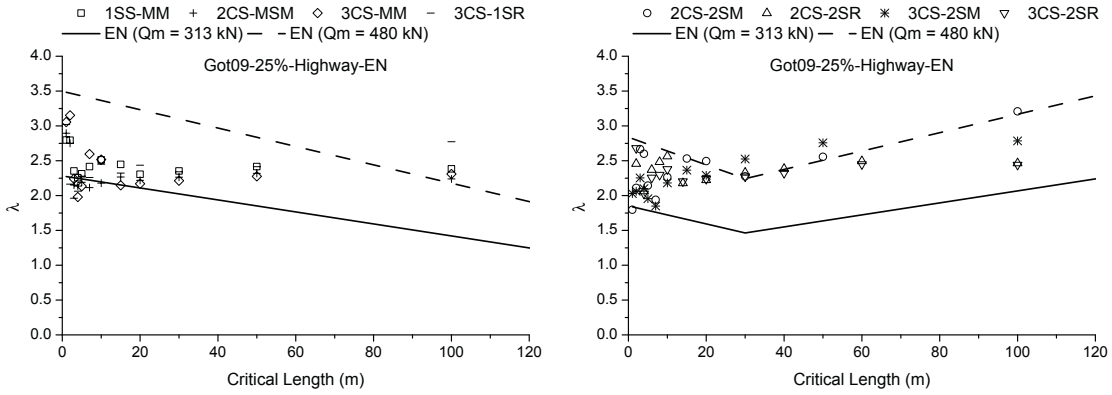

(a) Mid-span sections (b) Support sections

Figure C.8: Eurocode-base λ for G25HW traffic

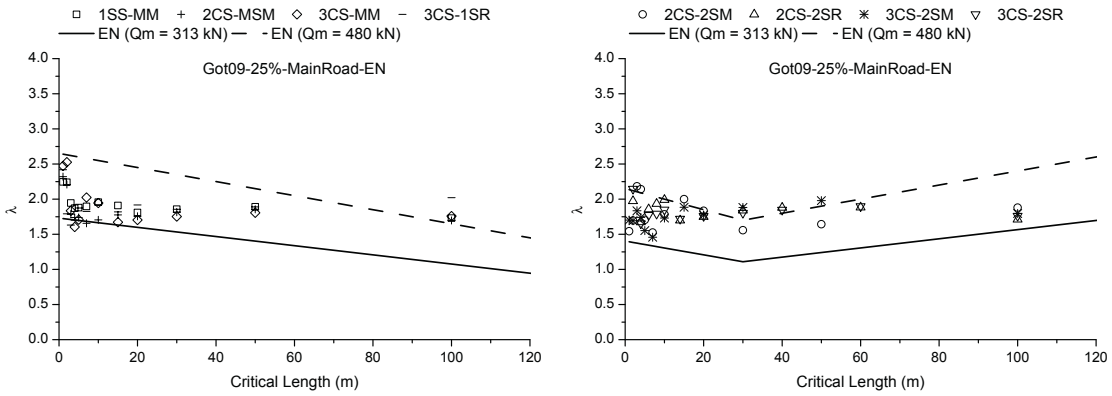

(a) Mid-span sections (b) Support sections

Figure C.9: Eurocode-base λ for G25MR traffic

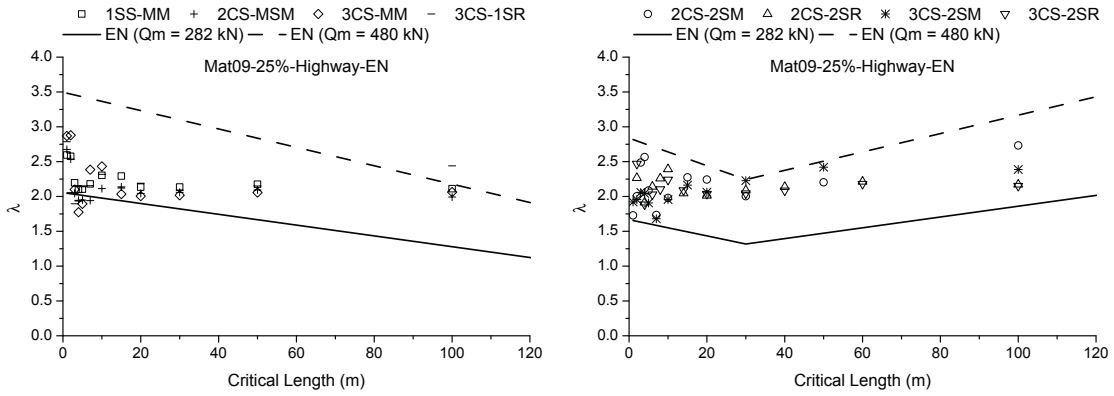

(a) Mid-span sections (b) Support sections

Figure C.10: Eurocode-base λ for M25HW traffic

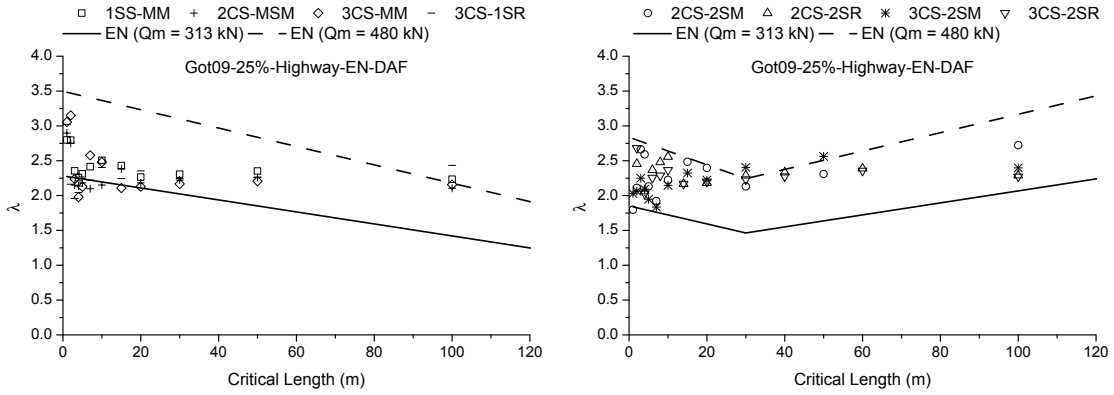

(a) Mid-span sections (b) Support sections

Figure C.11: Eurocode-base λ for G25HWDAF traffic

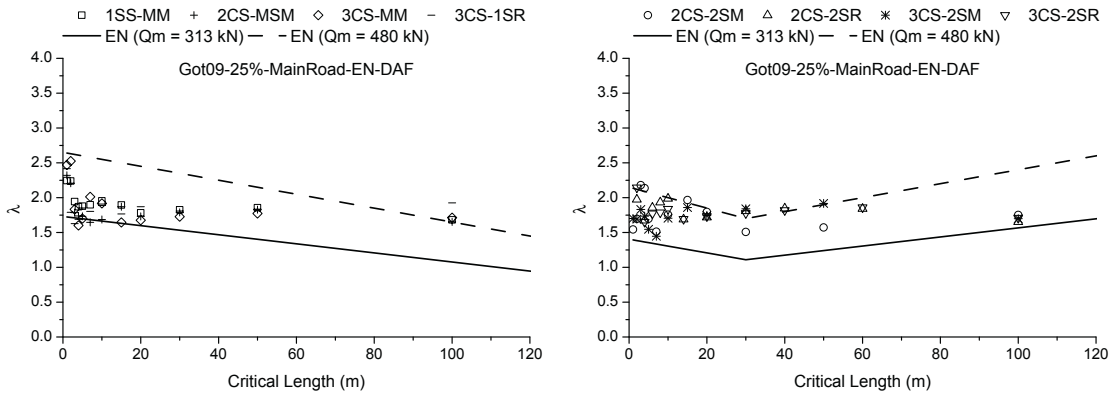

(a) Mid-span sections (b) Support sections

Figure C.12: Eurocode-base λ for G25MRDAF traffic

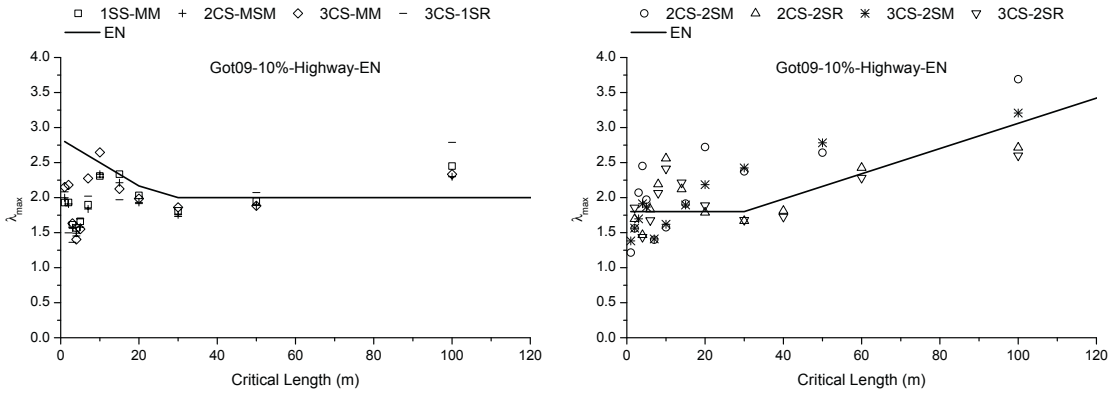

(a) Mid-span sections (b) Support sections

Figure C.13: Eurocode-base λ_{max} for G10HW traffic

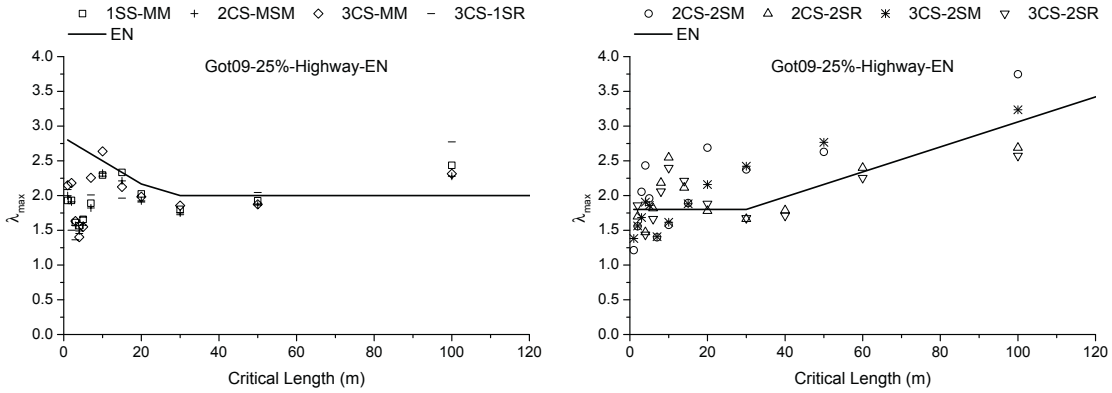

(a) Mid-span sections (b) Support sections

Figure C.14: Eurocode-base λ_{max} for G25HW traffic

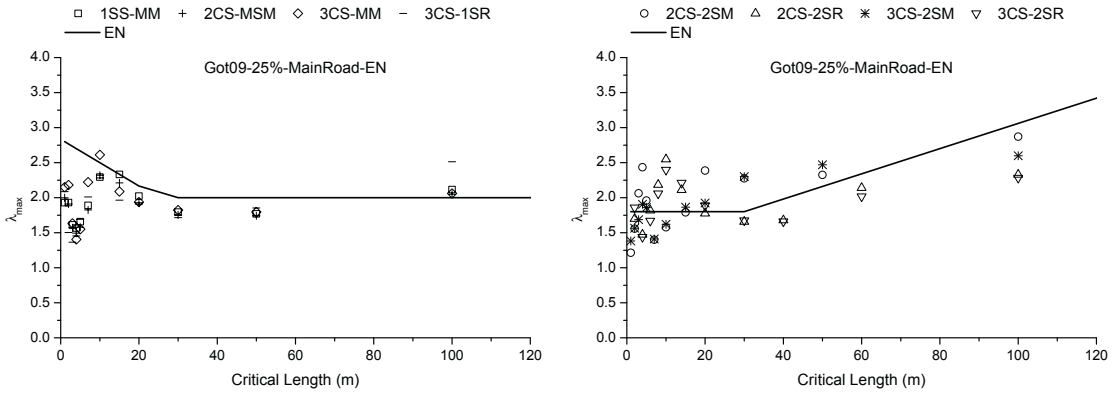

(a) Mid-span sections (b) Support sections

Figure C.15: Eurocode-base λ_{max} for G25MR traffic

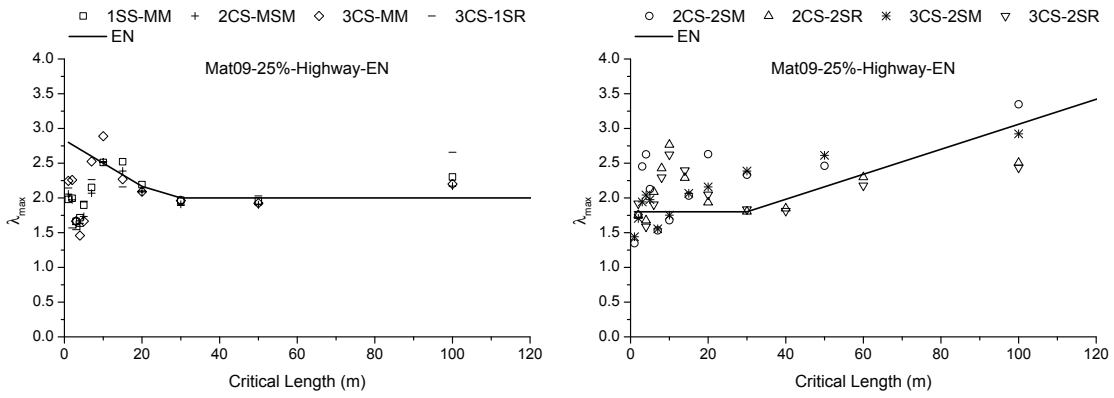

(a) Mid-span sections (b) Support sections

Figure C.16: Eurocode-base λ_{max} for M25HW traffic

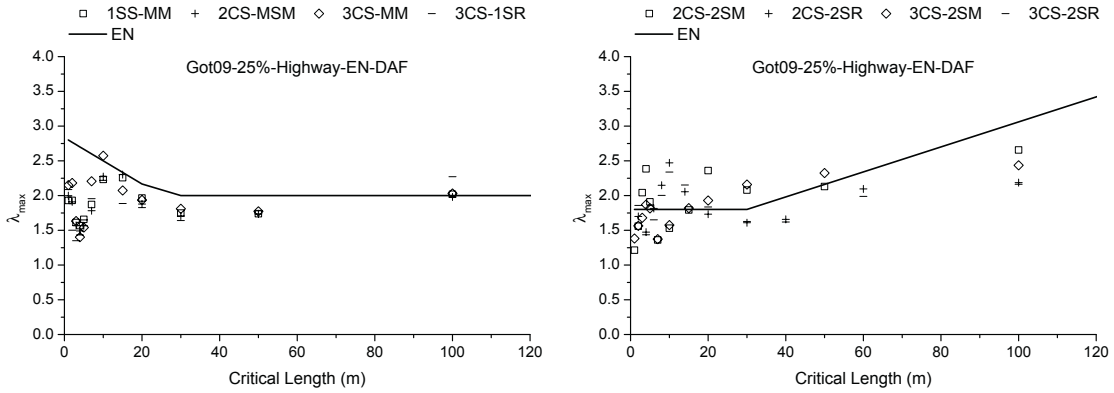

(a) Mid-span sections (b) Support sections

Figure C.17: Eurocode-base λ_{max} for G25HWDAF traffic

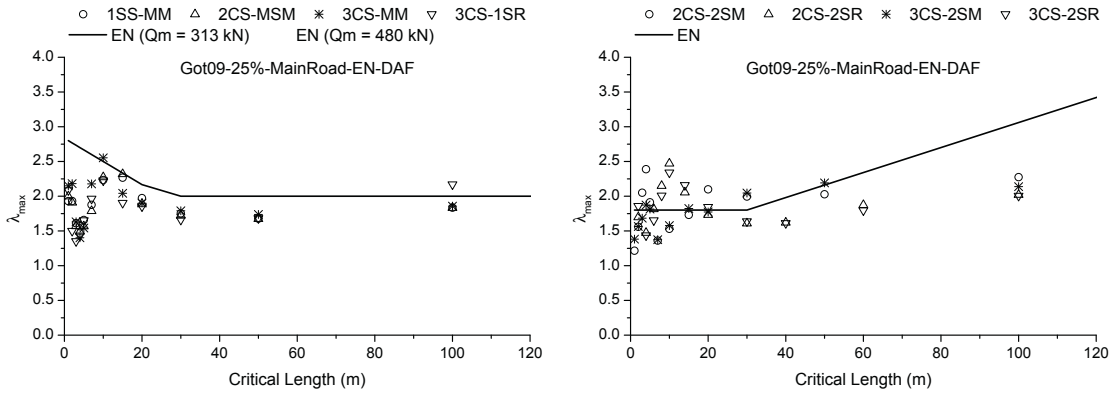

(a) Mid-span sections (b) Support sections

Figure C.18: Eurocode-base λ_{max} for G25MRDAF traffic

C.2 Damage equivalence factors based on the proposed method

In this section, the results of the final simulations based on the proposed method are illustrated. The fatigue load model includes a single axle with weight of 480 kN, and the fatigue equivalent length for a given influence line is equal to the absolute sum of area under the influence line divided by the maximum and minimum values on the influence line. The traffic simulations cases and the bridge cases for the final traffic simulations are explained in Chapter 6. Note that the results are given for 100 years of service life.

The resulting damage equivalence factors, λ and λ_{max}, are shown in Figures C.19 to C.24 for single lane traffic conditions; the best fitting curve corresponding to each traffic condition as well as the 95% prediction band are also plotted. It must be noted that the λ value presented comprises λ_5, though λ_5 is about 1.0 for all cases except for the case of mid-support moment of two-span continuous bridge ($\lambda_5 = 1.15$). For all figures of the current section the calculation of maximum damage equivalence factor, λ_{max}, the maximum stress range is the value that the superior stress ranges produce less than 1% of total damage.

Figures C.25 to C.33 shows λ and λ_{max} obtained for the different double lane traffic conditions, along with the best fitting curve and 95% prediction band. The description of double lane traffic cases are provided in Chapter 6.

In addition, the partial damage equivalence factors, λ_4, resulting from the traffic simulations are shown in Figures C.34 to C.42. The corresponding λ_4 from the codes (Eurocode or SIA code) as well as λ_4 obtained from Equation 4.25 are also plotted. By trial and error, the crossing ratio c is estimated for each traffic condition and plotted in the corresponding figures.

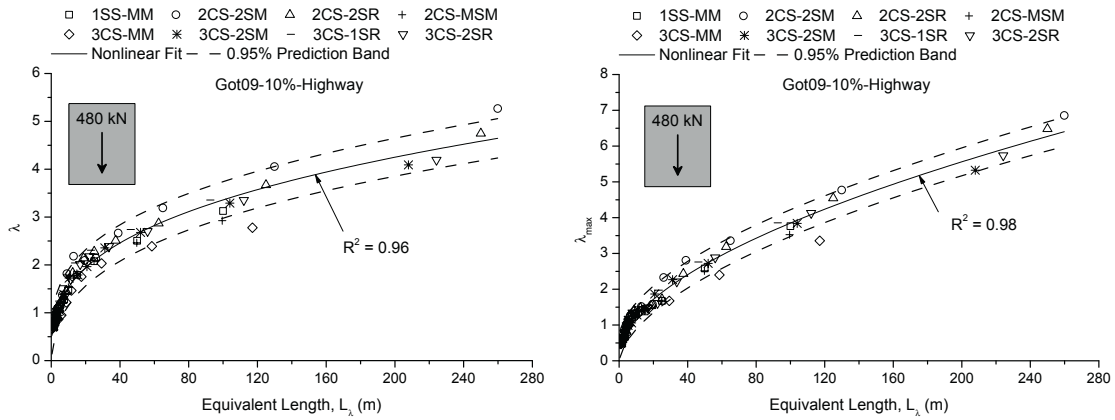

(a) λ (b) λ_{max}

Figure C.19: λ and λ_{max} based on the proposed method obtained for G10HW traffic

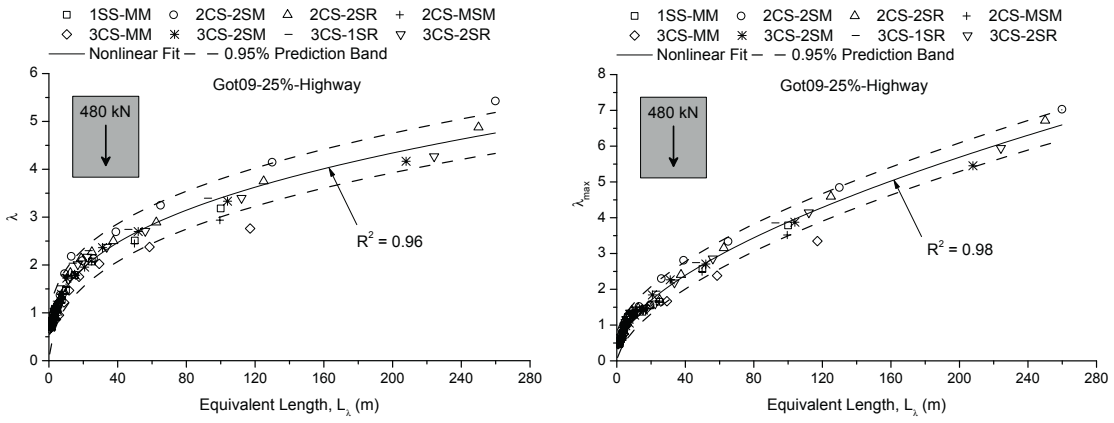

(a) λ (b) λ_{max}

Figure C.20: λ and λ_{max} based on the proposed method obtained for G25HW traffic

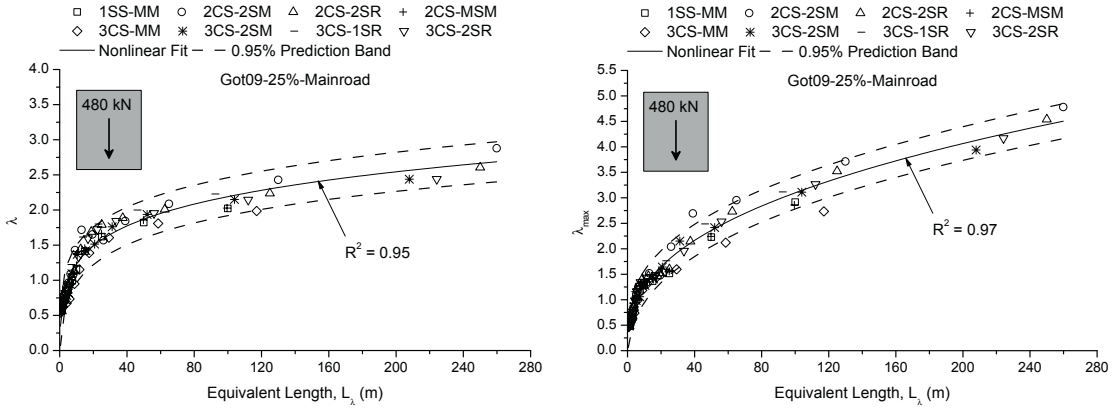

(a) λ (b) λ_{max}

Figure C.21: λ and λ_{max} based on the proposed method obtained for G25MR traffic

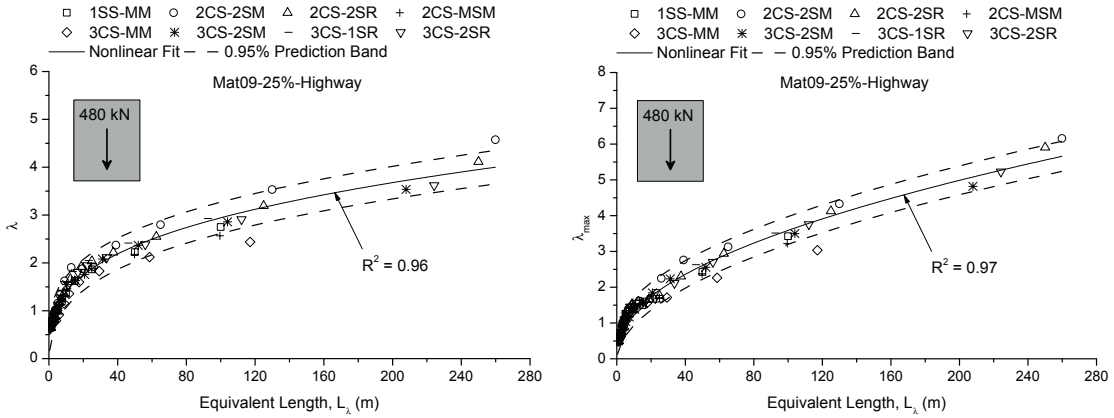

(a) λ (b) λ_{max}

Figure C.22: λ and λ_{max} based on the proposed method obtained for M25HW traffic

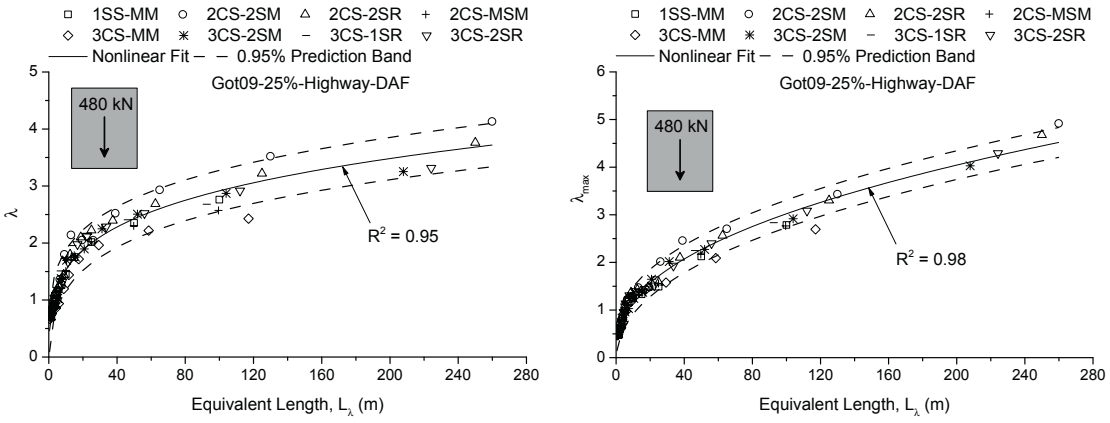

(a) λ (b) λ_{max}

Figure C.23: λ and λ_{max} based on the proposed method obtained for G25HWDAF traffic

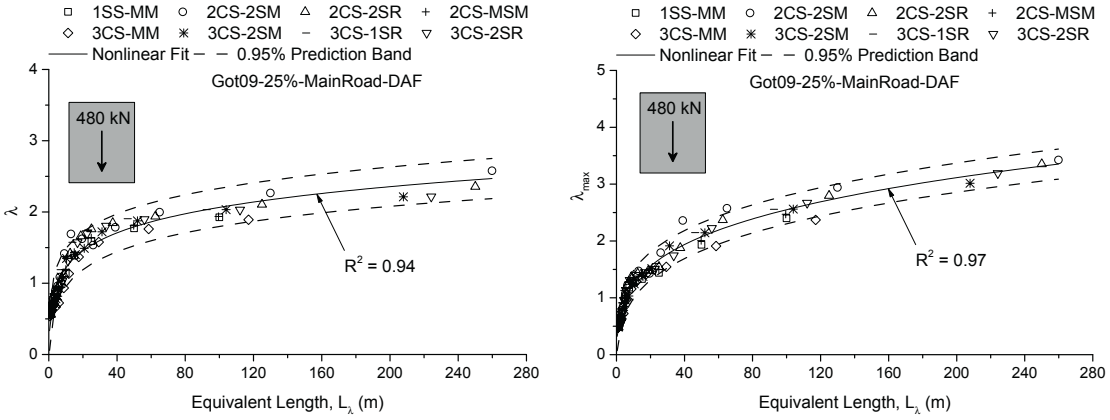

(a) λ (b) λ_{max}

Figure C.24: λ and λ_{max} based on the proposed method obtained for G25MRDAF traffic

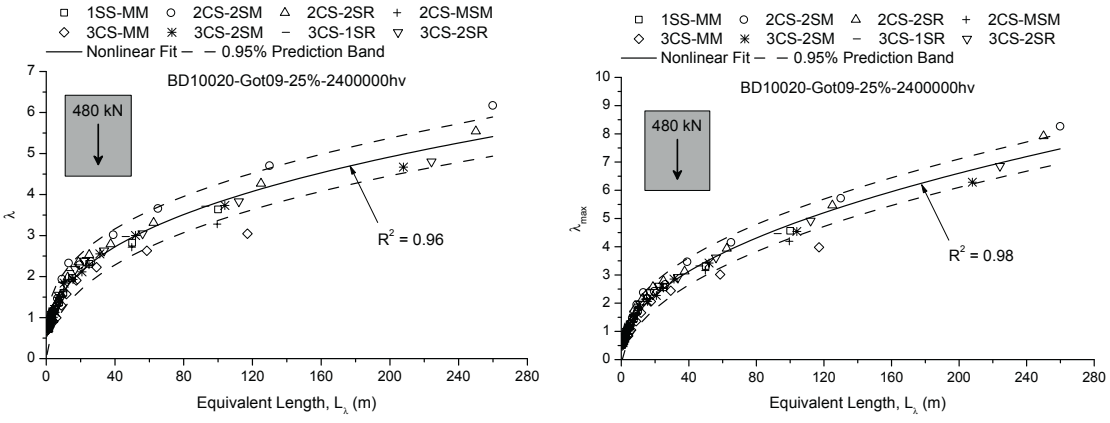

(a) λ (b) λ_{max}

Figure C.25: λ and λ_{max} based on the proposed method obtained for BD10020 traffic

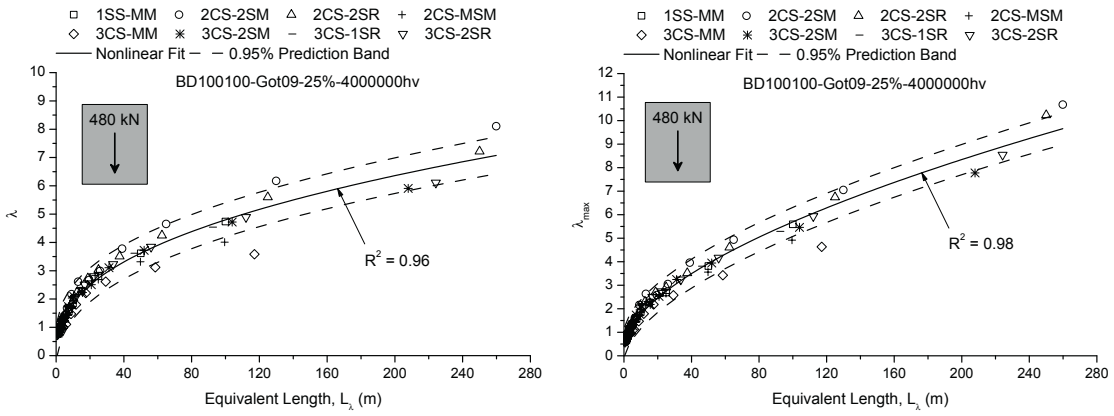

(a) λ (b) λ_{max}

Figure C.26: λ and λ_{max} based on the proposed method obtained for BD100100 traffic

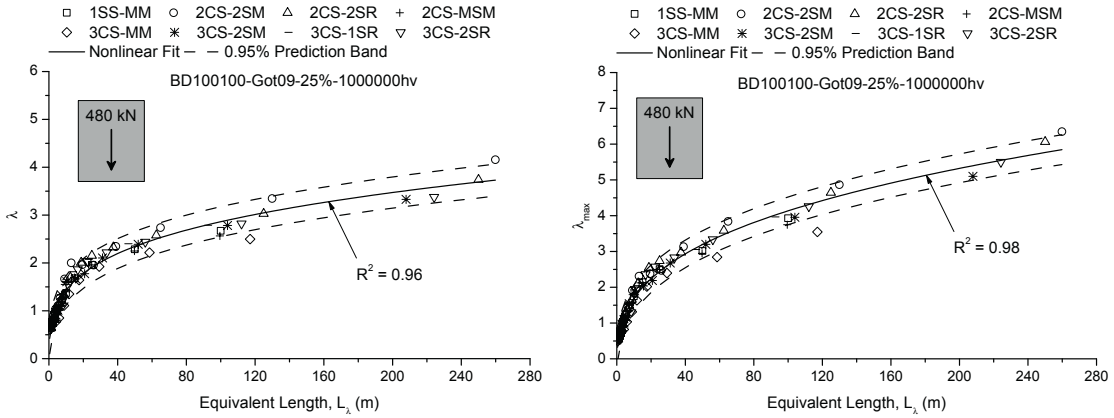

(a) λ (b) λ_{max}

Figure C.27: λ and λ_{max} based on the proposed method obtained for BD100100MR traffic

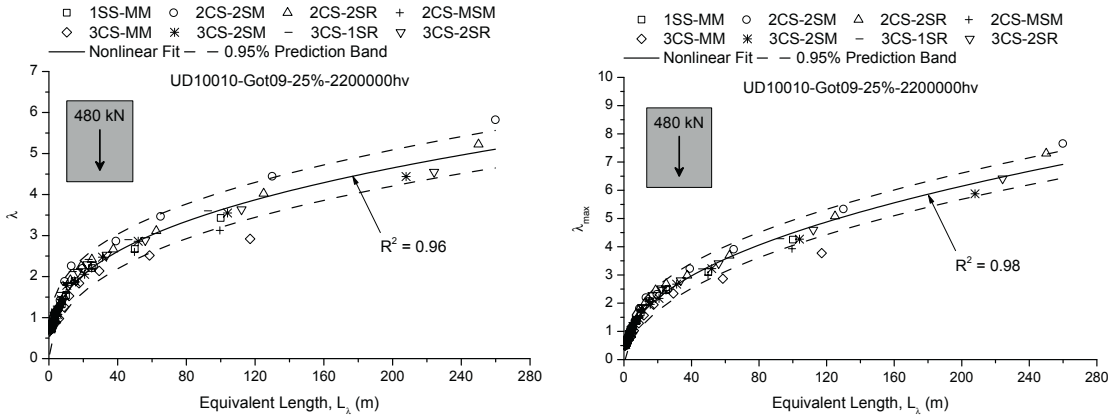

(a) λ (b) λ_{max}

Figure C.28: λ and λ_{max} based on the proposed method obtained for UD10010 traffic

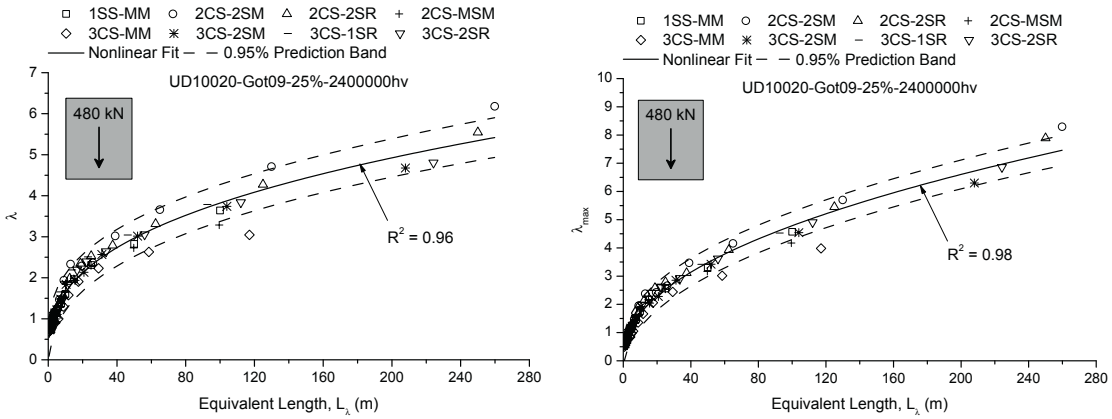

(a) λ (b) λ_{max}

Figure C.29: λ and λ_{max} based on the proposed method obtained for UD10020 traffic

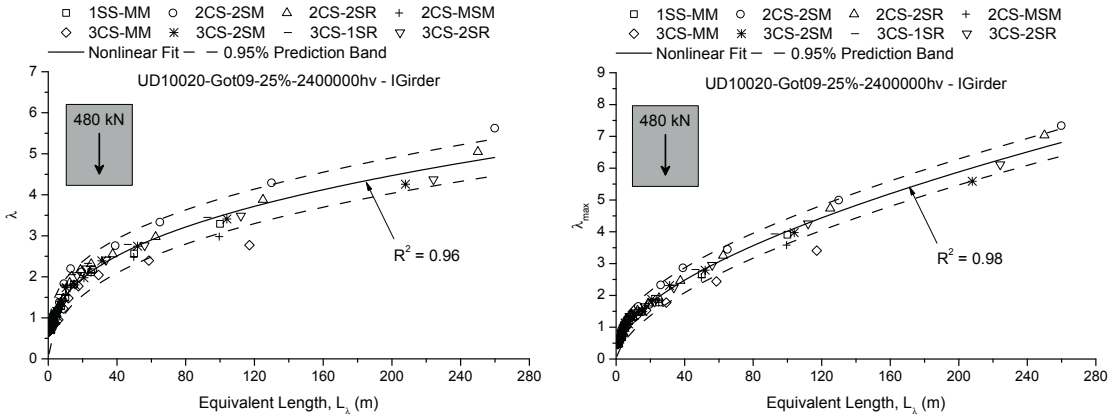

(a) λ (b) λ_{max}

Figure C.30: λ and λ_{max} based on the proposed method obtained for UD10020IG traffic

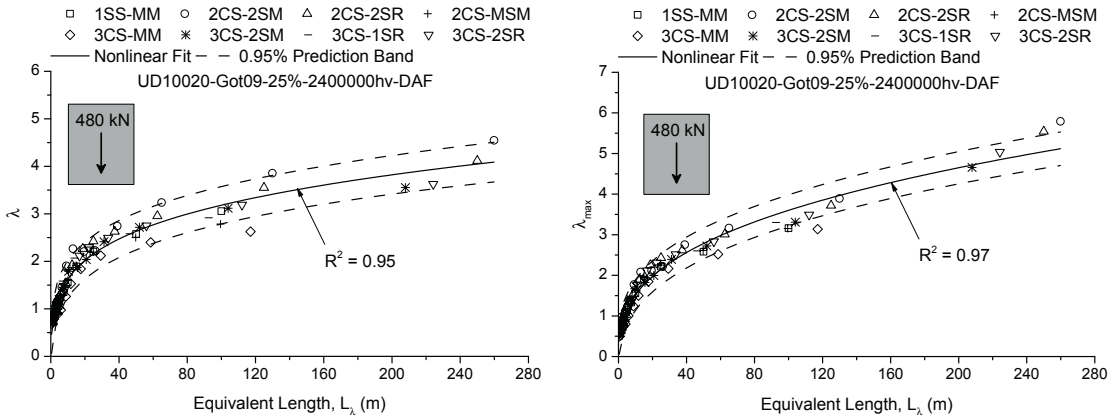

(a) λ (b) λ_{max}

Figure C.31: λ and λ_{max} based on the proposed method obtained for UD10020DAF traffic

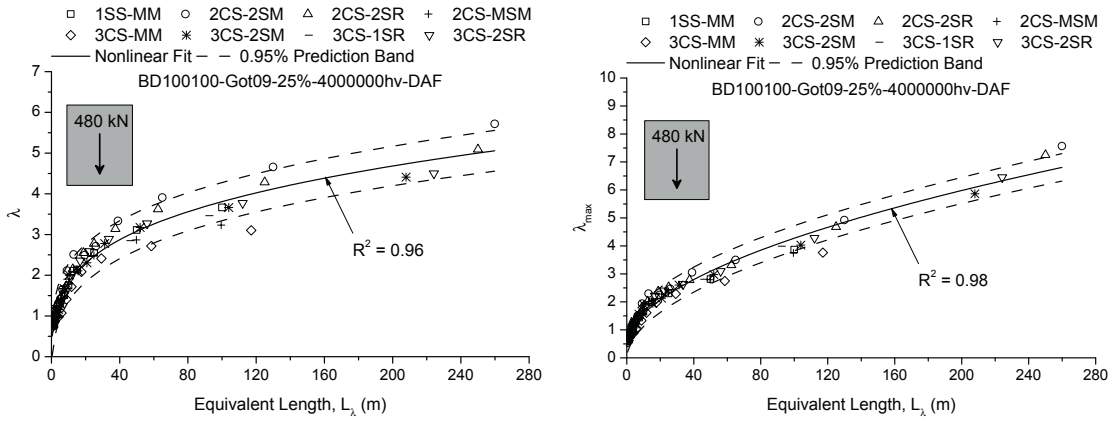

(a) λ (b) λ_{max}

Figure C.32: λ and λ_{max} based on the proposed method obtained for BD100100DAF traffic

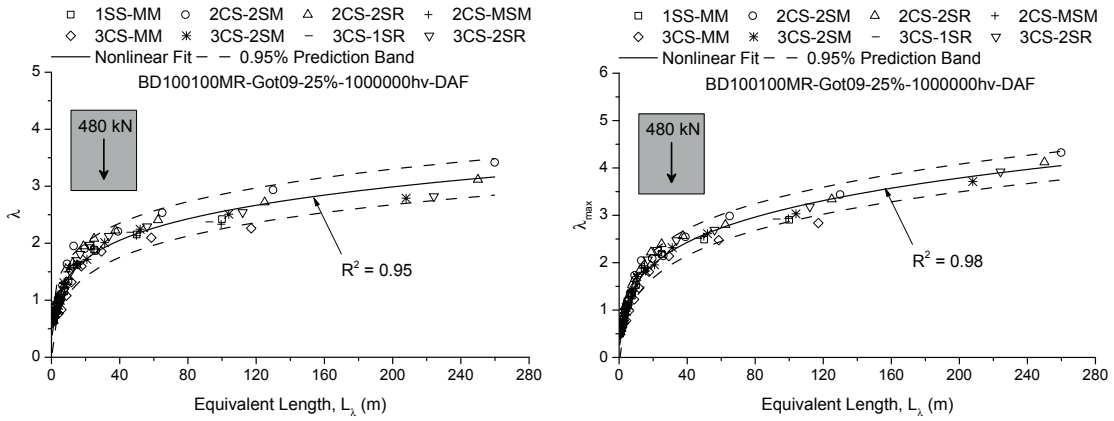

(a) λ (b) λ_{max}

Figure C.33: λ and λ_{max} based on the proposed method obtained for BD100100MRDAF traffic

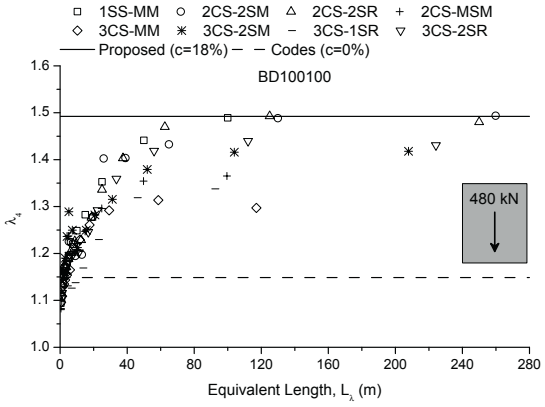

Figure C.34: λ_4 based on the proposed method for BD100100 traffic

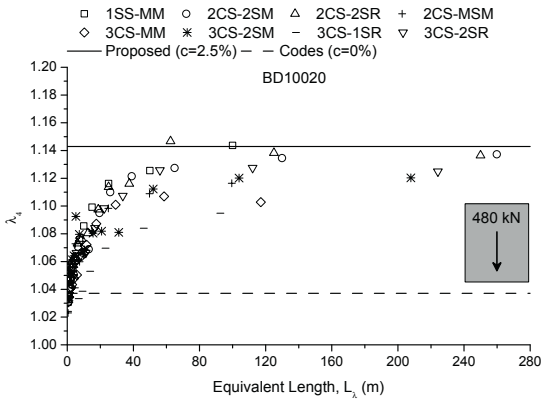

Figure C.35: λ_4 based on the proposed method for BD10020 traffic

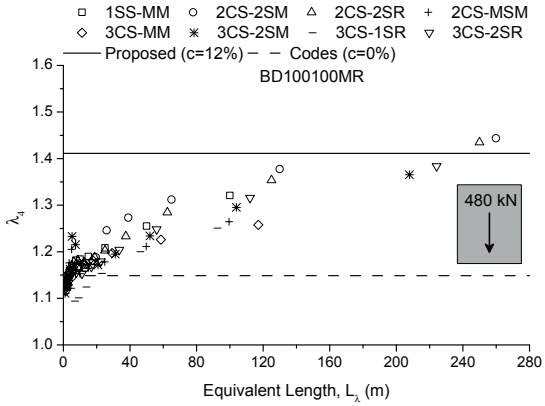

Figure C.36: λ_4 based on the proposed method for BD100100MR traffic

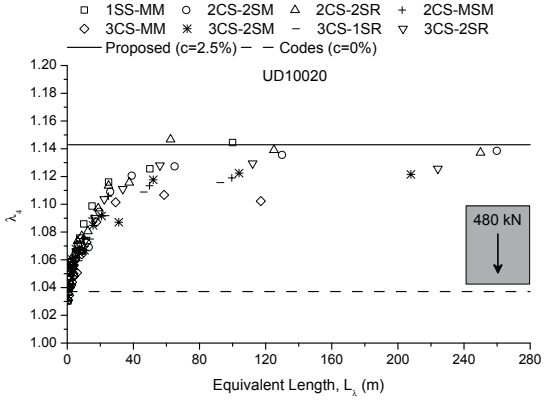

Figure C.37: λ_4 based on the proposed method for UD10020 traffic

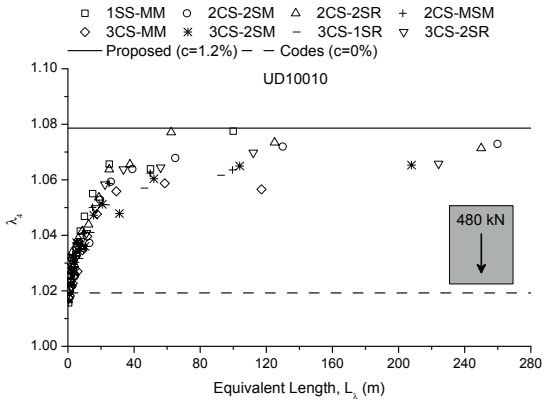

Figure C.38: λ_4 based on the proposed method for UD10010 traffic

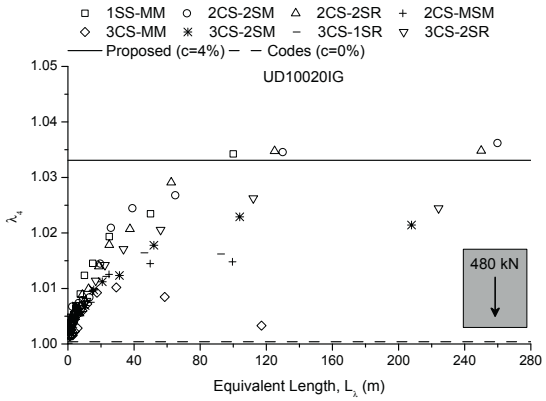

Figure C.39: λ_4 based on the proposed method for UD10020IG traffic

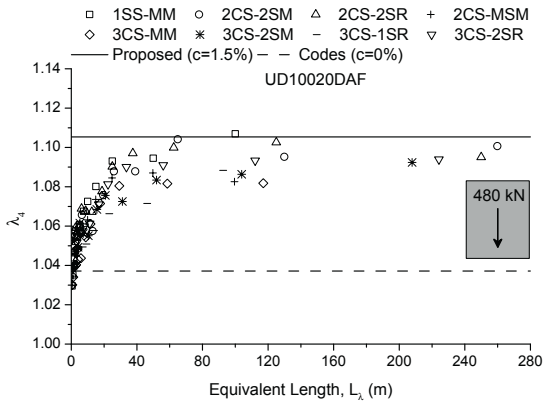

Figure C.40: λ_4 based on the proposed method for UD10020DAF traffic

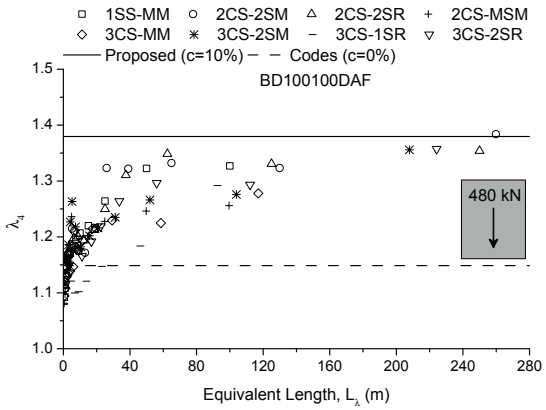

Figure C.41: λ_4 based on the proposed method for BD100100DAF traffic

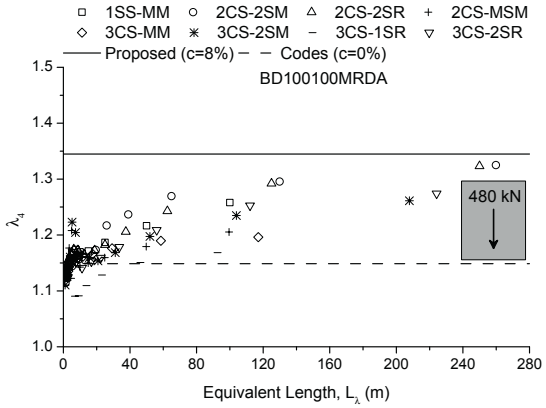

Figure C.42: λ_4 based on the proposed method for BD100100MRDAF traffic

Nariman Maddah

Current position	Doctoral assistant, EPFL, Steel Structure Laboratory (ICOM)
Office	GC B3 465 Telephone: +41 21 6932430
Address	EPFL ENAC IIC ICOM, Station 18, CH-1015 Lausanne, Switzerland
Email	nariman.maddah@gmail.com

Education

Nov. 2008 – Oct. 2012 (Expected)	Ph.D., civil engineering, Swiss Federal Institute of Technology (EPFL) Advisor: professor A. Nussbaumer, Focus: structural engineering • Thesis on fatigue life assessment of bridges under actual traffic loads • Expertise of project to strengthen Gstaad and Flendruz viaducts, Suisse
Sep. 2004 – Mar. 2007	M.Sc., civil eng., Iran University of Science and Technology (IUST), Tehran, Iran Advisor: professor G. Ghodrati Amiri, Focus: earthquake engineering • Thesis on seismic analysis of rectangular underground structures
Sep. 1999 – Sep. 2004	B.Sc., civil eng., Islamic Azad University, Central Tehran Branch, Tehran, Iran

Work Experiences

Apr. 2006 – Oct. 2008	Project engineer (full-time), Faradid Consulting Engineering (FCE), Tehran, Iran
Tasks	Management of projects for structural group, design and calculation of structures
Main projects	• Design of Shariaty underground station (a novel construction method), Iran • Retrofitting of Zayanderood steel bridge (steel trusses) of Isfahan, Iran
Nov. 2004 – Mar. 2006	Structural engineer (part-time), Faradid Consulting Engineering (FCE), Iran
Tasks	Structural modelling, calculation and preparation of reports and drawings
Main projects	• Seismic hazard analysis of Omid2 Tower, Tehran, Iran • Design of Hamidabad-Shoosh bridge (precast I-beam), Iran • Structural design of industrial buildings of Glass Filament Production Co., Iran • Structural design for track tire test, Rubber Industry of Barez, Kerman, Iran • Reinforcement of six concrete box-culverts, Iran

Research Projects

Dec. 2011 – Dec 2012	Fatigue evaluation of shear studs for steel-concrete composite road bridges
Sep. 2011 – Dec 2012	Stress in girders measurements under real traffic on Venoge Bridge, Vaud, Suisse
Jan. 2011 – Apr. 2011	Estimation of remaining fatigue life for slab's rebars of Bergbachviadukt, Suisse
Dec. 2010 – Oct. 2011	Proposing modifications to fatigue design rules of the SIA codes (SIA260, SIA261 and SIA263)

Languages

English	Fluent (C2), with TOEFL IBT certificate (score 89)
French	Intermediate (B1/B2), certificate from Language centre of EPFL
Persian	Fluent, mother tongue

Personal Information

Gender	Male	Birth date:	07.09.1981
Marital status	Married	Nationality:	Iranian
Membership	International Association for Bridge and Structural Engineering (IABSE)		

Publications

Journals and conferences

- S. Walbridge, N. Maddah, V. Fischer and A. Nussbaumer. Effect of Simultaneous Vehicle Crossings on Fatigue Correction Factors for North American Roadway Bridges. ASCE Journal of Bridge Engineering, (accepted 12.11.2012).
- N. Maddah and A. Nussbaumer. Analytical Approach for Improving Damage Equivalence Factors. Journal of Engineering Structures, (submitted 01.11.2012).
- N. Maddah and A. Nussbaumer. Fatigue Evaluation of Roadway Bridges under Actual Load Model. The 6th International Conference on Bridge Maintenance, Safety and Management (IABMAS 2012), July 8-12, 2012.
- N. Maddah and A. Nussbaumer. Evaluation of damage equivalent factor for roadway bridges. Proceedings of the 35th International Symposium of IABSE, London, UK, 2011.
- N. Maddah, A. Nussbaumer and Th. Meystre. Fatigue life assessment of road bridges with actual traffic loads: Traffic Simulation Parameters Based on Switzerland Measurements. École Polytechnique Fédérale de Lausanne, ICOM-169876, Dec. 2011.
- H.R. Razeghi, G. Ghodrati Amiri, N. Maddah. Seismic deformation of rectangular underground structures. Civil Engineering Infrastructures Journal (Submitted in November 2011).
- N. Maddah and A. Nussbaumer. Evaluation du facteur de correction en fatigue des ponts routiers sous charges de trafic actualisées. Presented at: Journée SIA, Olten, November 2010. Zurich: SIA, D0234, 2010.
- G. Ghodrati Amiri, N. Maddah and B. Mohebi. Effective parameters on seismic design of rectangular underground structures. Proceedings of the 2008 Seismic Engineering International Conference (MERCEA'08), Reggio Calabria, Italy, July 8-11, 2008.
- G. Ghodrati Amiri, B. Mohebi and N. Maddah. Optimization of damage index in RC structures using genetic algorithm. Proceedings of the 14th World Conference on Earthquake Engineering, Beijing, China, Oct. 12-17, 2008.

Personal Skills

Design of structures	• Design of structures including: bridges, buildings and underground structures • Application of Swiss codes (SIA) and Eurocodes for design of structures
Reinforcement of existing structures	• Control of existing structures e.g. bridges and buildings for upgraded loads • Design of reinforcement system for existing structures
FE modelling	• Advanced user in structural modelling with SCIA engineering, SAP2000
Programming skills	• Three years programming experience with MS visual C# and Excel VB